University of Alberta

Artificial Neural Networks for Modelling Ground-Level Ozone

by

Diane Su

A thesis submitted to the Faculty of Graduate Studies and Research in partial fulfillment of the requirements for the degree of Master of Science

in

Environmental Engineering

Department of Civil and Environmental Engineering

Edmonton, Alberta

Fall 2004

Library and Archives Canada

Published Heritage Branch

395 Wellington Street
Ottawa ON K1A 0N4
Canada

Bibliothèque et Archives Canada

Direction du Patrimoine de l'édition

395, rue Wellington
Ottawa ON K1A 0N4
Canada

Your file Votre référence
ISBN: 0-612-95860-4
Our file Notre référence
ISBN: 0-612-95860-4

The author has granted a non-exclusive license allowing the Library and Archives Canada to reproduce, loan, distribute or sell copies of this thesis in microform, paper or electronic formats.

L'auteur a accordé une licence non exclusive permettant à la Bibliothèque et Archives Canada de reproduire, prêter, distribuer ou vendre des copies de cette thèse sous la forme de microfiche/film, de reproduction sur papier ou sur format électronique.

The author retains ownership of the copyright in this thesis. Neither the thesis nor substantial extracts from it may be printed or otherwise reproduced without the author's permission.

L'auteur conserve la propriété du droit d'auteur qui protège cette thèse. Ni la thèse ni des extraits substantiels de celle-ci ne doivent être imprimés ou aturement reproduits sans son autorisation.

In compliance with the Canadian Privacy Act some supporting forms may have been removed from this thesis.

Conformément à la loi canadienne sur la protection de la vie privée, quelques formulaires secondaires ont été enlevés de cette thèse.

While these forms may be included in the document page count, their removal does not represent any loss of content from the thesis.

Bien que ces formulaires aient inclus dans la pagination, il n'y aura aucun contenu manquant.

Canada

Acknowledgement

First and foremost, many heartfelt thanks to Dr. Mohamed Gamal El-Din for providing me with the opportunity to work on this project. His guidance and counsel throughout the course of this project, on ANN-related matters and otherwise, have contributed immensely to the success of this project and my motivation to complete it.

Thank you to Dr. Ahmed Idriss and Alberta Environment, and Mr. Brian Wiens and Environment Canada for providing the project funding. These gentlemen also enriched the learning experience in this project by kindly providing lessons on air dispersion modelling and meteorology.

Thanks also to Kevin McCullum, who provided the data used to develop the models, and Dr. Ahmed Gamal El-Din, a voice of reason who generously shared his technical expertise with a stranger.

To the many new friends, including faculty, students, and support staff, who have made the completion of this degree an enjoyable experience— thank you! A huge thank you to Katie Clarke, who provided a fresh perspective on the program and many hours of laughter.

Finally, I would like to acknowledge the support and encouragement of my family, who nurtured my curiosity and instilled in me the value of an education, and the many friends who have made, and continue to make, this journey worthwhile. They have shaped the person I am, and are the reasons I have made it this far in life. Especially, I would like to thank Rob, my buddy in life and my quiet inspiration.

TABLE OF CONTENTS

1.0 GENERAL INTRODUCTION 1

References 2

2.0 A REVIEW OF OZONE CHEMISTRY AND HEALTH EFFECTS 5

2.1 Introduction 5

2.2 Ozone Chemistry 5

2.2.1 Processes contributing to the formation and presence of ground-level ozone 5

2.2.2 Sources of ozone precursor compounds and ozone sinks 6

2.2.3 Effects of meteorology and atmospheric physical processes 8

2.3 Ozone Health Effects 9

2.3.1 Criteria and considerations in review of health literature 9

2.3.2 Summary of results from Canadian epidemiological studies 10

2.4 Regulatory Control Strategies 11

2.4.1 Current standards and guidelines 11

2.4.2 Ozone control measures 13

2.5 Discussion: The Consequences of Ground-level Ozone to Current Lifestyles in Canada 13

2.6 Conclusions 16

2.7 References 17

3.0 REVIEW OF THE APPLICATION OF ANNs TO OZONE MODELLING 21

3.1 Introduction 21

3.2 Air Pollution Modelling Techniques 21

3.3 Artificial Neural Networks— Background 24

3.3.1 History of ANNs 24

3.3.2 Neural Network Architectures 25

3.3.3 Neural Network Learning 27

3.3.4 ANN Capabilities and Model Design Considerations 30

3.4 Application of ANNs to Model Ground Level Ozone 32

3.4.1 Model Inputs 33

3.4.2 Data Quality 37

3.4.3 Network Architecture 40
3.4.4 Performance Evaluation 41
3.5 Conclusions 43
3.6 References 44
4.0 HISTORICAL OZONE DATA PATTERNS AND TRENDS IN EDMONTON AND CALGARY 50
4.1 Introduction 50
4.2 Background 51
4.3 Ozone Chemistry 52
4.4 Methods 52
4.4.1 Monitoring Data 52
4.4.2 Statistical Analysis 53
4.5 Results and Discussion 54
4.5.1 Edmonton East Data Trends 54
4.5.2 Calgary East Data 64
4.5.3 Artificial Neural Networks Brief Description 73
4.5.4 Time Series Models Brief Description 74
4.5.5 Implications of Pollutant Data Trends for the ANN and Time Series Models 76
4.6 Conclusion 78
4.7 References 79
5.0 EDMONTON EAST OZONE ANN MODELS 82
5.1 Introduction 82
5.2 Background 85
5.3 Methodology 85
5.3.1 Evaluation of network performance 95
5.4 Results and Discussion 98
5.5 Conclusions 136
5.6 References 137
6.0 CALGARY EAST OZONE MODELS 141
6.1 Introduction 141
6.2 Background 141

6.3 Methodology 144
6.4 Results and Discussion 147
6.5 Conclusions 173
6.6 References 173
7.0 GENERAL DISCUSSION AND CONCLUSIONS 178
References 190
APPENDIX A: CONNECTION WEIGHTS OF EDMONTON EAST MODELS 194
APPENDIX B: CONNECTION WEIGHTS OF CALGARY EAST MODELS 205

LIST OF TABLES

Table 2-1	Examples of human activities that are major contributors to urban levels of ozone precursor compounds	8
Table 4-1	Statistical parameters for pollutants monitored at the Edmonton East and Calgary East stations, summer months of 1999-2002 (in ppm)	53
Table 5-1	Values assigned to temporal variables in Edmonton East ozone models.	89
Table 5-2	Wind direction sectors.	90
Table 5-3	Settings for activation function combination testing	92
Table 5-4	Parameters available for input to the Edmonton East virtual monitor model.	93
Table 5-5	Edmonton East basic statistics for available inputs.	99
Table 5-6	Activation function test results.	100
Table 5-7	Changes to R^2 with addition of inputs to core input set (R^2 for core input set = 0.73)	101
Table 5-8	Summary of network features for best Edmonton East ANN models	134
Table 5-9	Summary of performance statistics for best Edmonton East ANN models.	135
Table 6-1	Calgary East basic statistics of available inputs.	147
Table 6-2	Summary of network features for best Calgary East ANN models.	172
Table 6-3	Summary of performance statistics for best Calgary East ANN models.	172
Table 7-1	Comparison of virtual monitor models to models reported in the literature	182
Table 7-2	Comparison of forecast models to models reported in the literature.	183
Table 7-3	Summary of literature models.	185
Table A- 1	First layer of virtual monitor model.	195
Table A- 2	Second layer of virtual monitor model.	196
Table A- 3	First layer of virtual monitor model with time series.	197
Table A- 4	Second layer of virtual monitor model with time series	198
Table A- 5	First layer of one hour forecast model.	199

Table A- 6 Second layer of one hour forecast model.....199
Table A- 7 First layer of one hour forecast model with time series.....200
Table A- 8 Second layer of one hour forecast model with time series.....200
Table A- 9 First layer of two hour forecast model.....201
Table A- 10 Second layer of two hour forecast model.....202
Table A- 11 First layer of two hour forecast model with time series.....203
Table A- 12 Second layer of two hour forecast model with time series.....204
Table B- 1 First layer of virtual monitor model.....206
Table B- 2 Second layer of virtual monitor model.....207
Table B- 3 First layer of virtual monitor model with time series.....208
Table B- 4 Second layer of virtual monitor model with time series.....209
Table B- 5 First layer of one hour forecast model.....209
Table B- 6 Second layer of one hour forecast model.....209
Table B- 7 First layer of one hour forecast model with time series.....210
Table B- 8 Second layer of one hour forecast model with time series.....210

LIST OF FIGURES

Figure 2-1 Tropospheric ozone balance in the absence of polluting human activities. 6

Figure 2-2 Ozone production in the presence of VOCs. 7

Figure 3-1 Schematic of a three-layer multilayer perceptron artificial neural network 25

Figure 3-2 Activation functions used in ANNs: (a) logistic; (b) linear; (c) hyperbolic tangent; (d) hyperbolic tangent(1.5x); (e) sine; (f) symmetric logistic; (g) Gaussian; and (h) Gaussian complement. 28

Figure 3-3 Learning algorithms, ANN functions, and network types. 31

Figure 4-1 Edmonton East typical hourly average ozone concentrations. Data from May 2001. 54

Figure 4-2. Edmonton East 1999-2002 diurnal hourly average concentration trends for: (a) ozone; (b) nitric oxide; (c) nitrogen dioxide; (d) sulphur dioxide; and (e) total hydrocarbons 56

Figure 4-3. Edmonton 1999- 2002 day of the week trends in hourly average concentrations for: (a) ozone; (b) nitric oxide; (c) nitrogen dioxide; (d) sulphur dioxide; and (e) total hydrocarbons. 59

Figure 4-4. Edmonton 1999-2000 monthly patterns of average hourly concentrations for: (a) ozone; (b) nitric oxide; (c) nitrogen dioxide; (d) sulphur dioxide; and (e) total hydrocarbons. 61

Figure 4-5 Calgary East typical hourly average ozone concentrations. Data for May 2001. 64

Figure 4-6 Calgary East diurnal hourly average concentration trends for: (a) ozone; (b) nitric oxide; (c) nitrogen dioxide; (d) sulphur dioxide; and (e) total hydrocarbons. 66

Figure 4-7 Calgary East day of the week variation in hourly average concentrations for: (a) ozone; (b) nitric oxide; (c) nitrogen dioxide; (d) sulphur dioxide; and (e) total hydrocarbons. 68

Figure 4-8 Calgary East monthly patterns of average hourly concentrations for: (a) ozone; (b) nitric oxide; (c) nitrogen dioxide; (d) sulphur dioxide; and (e) total hydrocarbons....71
Figure 5-1. VOC contribution to ground-level ozone formation....83
Figure 5-2 Typical Edmonton East ozone data (July 2002)....99
Figure 5-3 Relative contribution factors of the Edmonton East model using the best inputs, 4 hidden layer neurons, 1000 training epochs, logistic hidden and output layer activation functions....101
Figure 5-4 Edmonton East virtual monitor effects of ozone time series, fixed network architecture of 7 hidden layer neurons and 1000 training epochs....105
Figure 5-5 Edmonton East virtual monitor surface plot of network architecture testing....106
Figure 5-6 Edmonton East virtual monitor model results for July 2002 production set data, $R^2 = 0.87$....107
Figure 5-7 Edmonton East virtual monitor scatter plot of agreement between observed and modelled ozone concentrations....107
Figure 5-8 Edmonton East virtual monitor model residuals analysis: variance with time for 2002 production data....108
Figure 5-9 Edmonton East virtual monitor model residuals analysis: variance with modelled ozone concentration....109
Figure 5-10 Edmonton East virtual monitor effects of adding previous hours' ozone concentrations as input with optimized network structure for each case....110
Figure 5-11 Edmonton East virtual monitor modelled ozone concentration variation with temporal parameters: (a) month; and (b) day of the week....112
Figure 5-12 Edmonton East virtual monitor modelled ozone concentration variation with pollutant concentrations: (a) NO; (b) NO_2; (c) SO_2; and (d) THC....113

Figure 5-13 Edmonton East virtual monitor modelled ozone concentration variation with meteorological parameters: (a) opacity; (b) relative humidity; (c) temperature; (d) wind direction; and (e) wind speed..... 117
Figure 5-14 Comparison of relative contribution factors for daylight only data and 24 hour data. 119
Figure 5-15 Edmonton East virtual monitor model with time series effects included: surface plot of architecture determination. 121
Figure 5-16 Edmonton East virtual monitor model with ozone time series: performance for July 2002 production data, $R^2 = 0.94$..... 121
Figure 5-17 Edmonton East virtual monitor model with ozone time series: comparison of actual to modelled ozone concentrations. 122
Figure 5-18 Edmonton East virtual monitor model with time series: variance of residuals with time for 2002 production set data. 122
Figure 5-19 Edmonton East virtual monitor model with time series: variance of residuals with modelled ozone concentration. 123
Figure 5-20 Edmonton East virtual monitor comparison of relative contribution factors for model with and without ozone time series effects. 124
Figure 5-21 Edmonton East one hour in advance forecast model surface plot of architecture determination..... 124
Figure 5-22 Edmonton East one hour forecast model performance for July 2002 production set data, $R^2 = 0.89$. 125
Figure 5-23 Edmonton East one hour forecast model comparison of actual and modelled ozone concentrations..... 126
Figure 5-24 Edmonton East one hour forecast model residuals analysis: variance with time for 2002 production set data. 126
Figure 5-25 Edmonton East one hour forecast model scatter plot of residuals: variation with modelled ozone concentration. 127
Figure 5-26 Edmonton East one hour in advance forecast with ozone time series effects: model performance for July 2002 production set data, $R^2 = 0.90$..... 128
Figure 5-27 Edmonton East two hours in advance forecast model surface plot..... 129

Figure 5-28 Edmonton East two hours in advance forecast model performance for July 2002 production set data, $R^2 = 0.75$. 129
Figure 5-29 Edmonton East two hours in advance forecast model comparison of actual to modelled ozone concentration. 130
Figure 5-30 Edmonton East two hours in advance forecast model residuals variance with time. 131
Figure 5-31 Edmonton East two hours in advance forecast model residuals variance with modelled ozone concentration. 131
Figure 5-32 Edmonton East two hours in advance forecast with ozone time series: model performance on July 2002 production set data, $R^2 = 0.78$ 132
Figure 5-33 Edmonton East forecast model effects of increased prediction window and inclusion of time series inputs. 133
Figure 6-1 Schematic of a three layer perceptron network. 143
Figure 6-2 Calgary East typical hourly average ozone concentration data for May 2001 148
Figure 6-3 Calgary East function analysis results, average of three settings. 149
Figure 6-4 Calgary East virtual monitor model surface plot of architecture analysis. 150
Figure 6-5 Calgary East virtual monitor model performance on May 2001 production set data, $R^2 = 0.85$. 151
Figure 6-6 Calgary East virtual monitor model comparison of actual and modelled ozone concentrations. 152
Figure 6-7 Calgary East virtual monitor model residuals analysis: variation with modelled ozone concentration 152
Figure 6-8 Calgary East virtual monitor model residuals variation with time 153
Figure 6-9 Calgary East comparison of input parameter relative importance for ozone modelling using 24-hour and daylight only data. 155
Figure 6-10 Calgary East variation of virtual monitor modelled ozone concentration with month. 156

Figure 6-11 Calgary East sensitivity of virtual monitor modelled ozone concentration to pollutant concentrations: (a) NO; (b) NO_2; (c) SO_2; and (d) THC. 156
Figure 6-12 Calgary East sensitivity of virtual monitor modelled ozone concentration to meteorological parameters. 158
Figure 6-13 Calgary East virtual monitor model surface plot of network architecture evaluation when ozone concentration at t-1 included as input. 160
Figure 6-14 Calgary East virtual monitor model with ozone time series performance for May 2001 production set data, $R^2 = 0.92$. 160
Figure 6-15 Calgary East virtual monitor model with ozone time series: comparison of actual to modelled ozone concentration for production set data. 161
Figure 6-16 Calgary East virtual monitor model with ozone time series residuals analysis: variation with modelled ozone concentration for production set data. 162
Figure 6-17 Calgary East virtual monitor model with ozone time series residuals analysis: variance with time for 2001 production set data. 162
Figure 6-18 Calgary East virtual monitor model ozone time series effects 164
Figure 6-19 Calgary East one hour forecast surface plot of network architecture evaluation. 164
Figure 6-20 Calgary East one hour forecast model performance for May 2001 production set data, $R^2 = 0.86$. 165
Figure 6-21 Calgary East one hour forecast model comparison of actual to modelled ozone concentration for production set data. 165
Figure 6-22 Calgary East one hour forecast model residuals analysis: variance with modelled ozone concentration for production set data. 166
Figure 6-23 Calgary East one hour forecast model residuals analysis: variance with time for 2001 production set data. 166
Figure 6-24 Calgary East one hour forecast with ozone time series surface plot of network architecture evaluation 167

Figure 6-25 Calgary East one hour forecast with ozone time series performance for May 2001 production set data, $R^2 = 0.87$ 168
Figure 6-26 Calgary East one hour forecast with ozone time series comparison of actual to modelled ozone concentration for production set data. 169
Figure 6-27 Calgary East one hour forecast model with ozone time series residuals variance with modelled ozone concentration for production set data. 169
Figure 6-28 Calgary East one hour forecast model with ozone time series residuals analysis: variance with time for 2001 production set data. 170
Figure 6-29 Calgary East forecast model effects of increasing prediction window and adding previous hours' ozone concentrations. 171

NOMENCLATURE

Symbols

a_i ..... activation level of neuron 'i'

a_t ..... a random drawing from a fixed distribution at time t

B ..... backshift operator

b ..... delay parameter

d_1 ..... Wilmott index of agreement

d_2 ..... Wilmott index of agreement (conservative form)

F_i ..... activation function of neuron 'i'

f_i ..... output function of neuron 'i'

i ..... subscript denoting layer or neuron in the neural network

j ..... subscript denoting layer in the neural network

N_j ..... summed weighted input to the neuron in layer 'j'

n ..... number of data patterns

o_i ..... output of neuron 'i'

p ..... order of a stochastic model

q ..... order of a stochastic model

r ..... Pearson's product-moment correlation coefficient

R^2 ..... coefficient of multiple determination

t ..... time

w_{ij} ..... weight of the connection between neuron in layer i and neuron in layer j

X ..... input series

x ..... actual value of output variable

$\bar{x}$ ..... mean of all actual output values

$\bar{x}_{25}$ ..... average of the 25 highest observed values

Y ..... output series

y ..... modelled output value

$\bar{y}_{25}$ ..... average of the 25 predicted values corresponding to 25 highest observed values

z_t ..... process generating a time series

Greek Alphabet Symbols

ϕ .....auto-regressive operator of a stochastic model

N .....noise process, stochastic model component

θ .....moving average operator of a stochastic model

σ_a^2 .....variance of a sequence of random variables a

σ_y.....standard deviation of pollutant dispersion in the y direction

σ_z.....standard deviation of pollutant dispersion in the z direction

υ.....impulse response (transfer) function

ψ .....linear filter function

Abbreviations

AAQG .....Ambient Air Quality Guideline

AE_{max}.....maximum absolute error

AE_{min} .....minimum absolute error

ANN .....artificial neural network

ARBF .....adaptive radial basis function

ARMA.....auto-regressive moving average

ART.....adaptive resonance theory

AUG.....neuron indicating data records from month of August

CASA .....Clean Air Strategic Alliance

CCME .....Canadian Council of Ministers of the Environment

CEPA.....Canadian Environmental Protection Act

CH_4.....methane concentration

CO.....carbon monoxide concentration

CO_2.....carbon dioxide concentration

DAY.....day of the week

DEV.....wind direction deviation

EPEA.....Environmental Protection and Enhancement Act

FB .....fractional bias

FPAC.....federal/provincial advisory committee

FRI .....neuron indicating data records from Fridays

HO_2 ..... hydrogen dioxide

HO_x ..... oxides of hydrogen

HOUR ..... hour of the day

JUL ..... neuron indicating data records from month of July

JUN ..... neuron indicating data record from month of June

MAE ..... mean absolute error

MAY ..... neuron indicating data records from month of May

MIX ..... mixing height

MLP ..... multilayer perceptron

MON ..... neuron indicating data records from Mondays

MSE ..... mean squared error

MTH ..... month

NARSTO ..... North American Research Strategy for Tropospheric Ozone Synthesis Team

NMHC ..... non-methane hydrocarbons concentration

NN ..... neural network

NO ..... nitric oxide concentration

NO_2 ..... nitrogen dioxide concentration

NO_x ..... concentration of oxides of nitrogen

O_2 ..... oxygen molecule

O_3 ..... ground level ozone molecule or concentration

OH ..... hydroxyl radical

OPA ..... opacity

ppm ..... parts per million by volume

RBF ..... radial basis function

RH ..... relative humidity

SAT ..... neuron indicating data records from Saturdays

SECT ..... wind direction sector

SEP ..... neuron indicating data records from month of September

SO_2 ..... sulphur dioxide concentration

SOM ..... self-organizing map

SUN ..... neuron indicating data records from Sundays

SS ..... sum of the squares

tanh.....hyperbolic tangent function

TEMP .....temperature

THC.....total hydrocarbons concentration

THU.....neuron indicating data records from Thursdays

TUE .....neuron indicating data records from Tuesdays

USEPA .....Unites States Environmental Protection Agency

VOC.....volatile organic compound

WDR.....wind direction

WED.....neuron indicating data records from Wednesdays

WGAQOG .....Working Group on Air Quality Objectives and Guidelines

WSP.....wind speed

1.0 GENERAL INTRODUCTION

In recent years, air quality, particularly in urban areas where population and vehicle traffic are concentrated, has become a major public concern. Ground-level ozone is a secondary photochemical pollutant that has been identified as a target for regulatory control and an indicator of poor air quality. Exposure to ground-level ozone has been implicated in numerous epidemiology studies for causing or aggravating a host of respiratory illnesses (Bates et al. 1990; Burnett et al. 1998; Last et al. 1998; Lipfert and Hammerstrom 1992; McDonnell et al. 1998; Thurston et al. 1997) and damaging vegetation (Bates 1991).

In the urban environment, ozone is formed mainly from anthropogenic activities that emit its precursor compounds, oxides of nitrogen (NO_x) and volatile organic compounds (VOCs). The populations of Edmonton and Calgary have rapidly bloomed recently. This potentially impacts ground-level ozone in two ways. First, concentrations of the precursor compounds for ozone will rise with the increase in vehicular traffic and commuting distances, potentially resulting in increased ozone formation (Keating 1997). Second, with the larger population, there is greater probability for widespread harm as a larger number of individuals are exposed to ground-level ozone. Regulatory standards for ozone have recognized this growing public concern. The Canada-Wide Standards for ground-level ozone are currently set for a 2010 target of 0.065 ppm, averaged over 8 hours (CCME 2000). The Alberta Ambient Air Quality Guidelines are set at an hourly average concentration of 0.082 ppm (EPEA 1992).

The chemistry of ozone is nonlinear and complex, limiting the success of more traditional mechanistic modelling approaches for describing atmospheric processes. This has initiated the search for an accurate modelling tool that regulatory agencies can use to model and forecast urban ground-level ozone concentrations. Artificial neural networks (ANNs) are a modelling approach that is especially suited to nonlinear, complex, and poorly understood processes. Neural networks consist of individual processing elements ("neurons") configured and inter-connected in one or more layers (Flood and Kartam 1997). The combination of the functions used in the neurons, the magnitudes and signs of the connections between neurons, and the structure of the network describe and are dependant

on the process being modelled. Although artificial neural networks have been available since the 1940's, their "black box" nature has limited their popularity (Jain et al 1996). Recently, they have been applied successfully to numerous areas, including stock market analyses, speech pattern recognition, and cloud characterization. ANNs have also experienced a popularity resurgence in the atmospheric sciences, with applications in modelling and forecasting pollutant levels in both urban and rural settings.

In this project, the potential use of ANNs as a modelling approach for ground-level ozone concentrations in Edmonton and Calgary is assessed. The objective of this research is to generate valuable tools for the modelling and prediction of ground-level ozone in these cities. These tools would increase the availability of air quality information to the public, providing an alternate source of air quality information when existing ambient air monitors are down for maintenance and repair work. Successful ANN models would enable regulatory agencies to evaluate proposed pollution reduction strategies and determine the effectiveness of existing efforts. They would provide the public with advance warning of extreme ozone or poor air quality events, allowing measures to be taken to avoid exposure. Four models each for Calgary and Edmonton are constructed using a systematic approach. For each city, a "virtual monitor" model is developed to model ground-level ozone behaviour. The virtual monitor processes real-time pollutant and meteorological data to generate a corresponding ozone concentration. A forecast model is constructed to predict ozone concentrations, with the largest prediction window possible that does not compromise prediction performance. The forecast model uses the currently available pollutant and meteorological data to predict the ozone concentration at a future hour. The last two models are variants of the virtual monitor and forecast models that incorporate ozone time series effects.

References

Bates, D. 1991. The effects of ozone on plants and humans. In the Air & Waste Management Association Tropospheric Ozone and the Environment 3; Papers from an International Conference, Air & Waste Management Association, Pennsylvania, held March 19-22, 1990 in Los Angeles, CA, 15-22.

Bates, D.V., Baker-Anderson, M. and Sizto, R. 1990. Asthma attack periodicity: a study of hospital emergency visits in Vancouver. Environmental Research, 51: 51-70.

Burnett, R.T., Cakmak, S. and Brook, J.R. 1998. The effect of the urban ambient air pollution mix on daily mortality rates in 11 Canadian cities. Canadian Journal of Public Health, 89(3): 152-156.

CCME— Canadian Council of Ministers of the Environment. 2000. Canada-Wide Standards for Particulate Matter (PM) and Ozone. CCME Council of Ministers, Quebec City, PQ. Accessed via the Internet at http://www.ccme.ca/assets/pdf/pmozone_standard_e.pdf on July 10, 2003.

EPEA— Environmental Protection and Enhancement Act. 1992. Alberta Ambient Air Quality Guidelines. Alberta Queen's Printer, Edmonton, AB. Accessed via the Internet at http://www3.gov.ab.ca/env/protenf/approvals/factsheets/ABAmbientAirQuality.pdf on July 10, 2003.

Flood, I., and Kartam, N. (1997). "Systems." Artificial Neural Networks for Civil Engineers : Fundamentals and Applications, J. H. Garrett, ed., The Society, New York, NY, 19-43.

Jain, A. K., Mao, J, and Mohiuddin, K.M. 1996. Artificial neural networks: a tutorial. Computer, 29: 31-44.

Keating, M. and the Canadian Global Change Program. 1997. Canada and the State of the Planet; the social, economic and environmental trends that are shaping our lives. Oxford University Press, Toronto, ON.

Last, J., Trouton, K. and Pengelly, D. 1998. Taking Our Breath Away: The Health Effects of Air Pollution and Climate Change. David Suzuki Foundation, Vancouver, BC.

Lipfert, F.W. and Hammerstrom, T. 1992. Temporal patterns in air pollution and hospital admissions. Environmental Research, 59: 374-399.

McDonnell, W.F., Abbey, D.E., Nishino, N. and Lebowitz, M.D. 1999. Long-term ambient ozone concentration and the incidence of asthma in non-smoking adults: the AHSMOG study. Environmental Research, Section A, 80: 110-121.

Thurston, G.D., Lippmann, M., Scott, M.B. and Fine, J.M. 1997. Summertime haze air pollution and children with asthma. American Journal of Respiratory and Critical Care Medicine, 155: 655-660.

2.0 A REVIEW OF OZONE CHEMISTRY AND HEALTH EFFECTS

2.1 Introduction

Ground-level ozone is a secondary pollutant that has recently gained notoriety for its detrimental effects on public health. Although its presence in the stratosphere as the ozone layer is desirable, ozone in the lower troposphere has been linked to vegetation injury, materials damage, and respiratory illness. It is of special concern in urban environments, where sources of precursor compounds are concentrated. This paper summarizes the current understanding of ozone chemistry, the reported health effects, regulatory control efforts, and their consequences to the existing urban lifestyle in Canada.

2.2 Ozone Chemistry

The ozone that is associated with health effects is present in the lower troposphere at ground level. Its presence is attributable to a combination of reactions between the oxides of nitrogen (NO_x) and volatile organic compounds (VOCs) of human and natural origin, transport from the stratosphere and other locations, and numerous other chemical reactions and atmospheric dispersion and transport mechanisms (CEPA/FPAC WGAQOG 1999; McElroy 2002).

2.2.1 Processes contributing to the formation and presence of ground-level ozone

Ozone occurs naturally at background levels free of human emissions. These levels depend on the location, temperature, wind speed and direction, vertical motion, and season of the year. Background ozone can originate in the stratosphere and from reactions between naturally occurring methane and VOCs with NO_x (Jacobson 1999; Potter and Coleman 2003; USEPA 1996). In atmospheres free of human influences, ozone exists in a dynamic equilibrium, with no net formation or destruction occurring (USEPA 1996). The process is described schematically in Figure 2-1. In the presence of ultraviolet energy, the nitrogen dioxide (NO_2) molecule is broken down to form nitric oxide (NO) and an oxygen atom. The oxygen atom combines with oxygen in air (O_2) to form the ozone molecule (O_3). The

ozone molecule is subsequently consumed through reaction with NO to re-form NO_2, and the cycle continues.

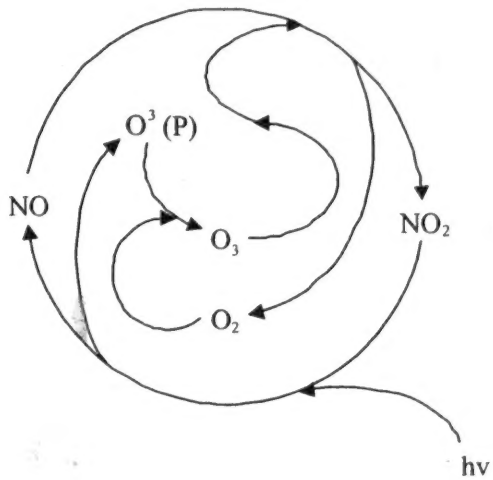

Figure 2-1 Tropospheric ozone balance in the absence of polluting human activities.

Based on reactions in USEPA (1996).

When VOCs are present (either anthropogenic or natural), NO reacts with the VOCs to produce NO_2, without consuming the ozone molecule. Since ozone participation in the formation of NO_2 is not required, there is a net production of ozone. (USEPA 1996) VOCs may also react with hydroxyl radicals (OH) in the atmosphere to produce ozone. The reaction process is described in Figure 2-2. VOCs and NO_x concentrate in urban areas. In these areas, anthropogenic emissions are the dominant sources of ozone precursor compounds.

2.2.2 Sources of ozone precursor compounds and ozone sinks

Sources of NO_x and VOC ozone precursor compounds are both human and natural. NO_x are formed in combustion processes from nitrogen present in the fuel source. The human activities mainly responsible for NO_x emissions are transportation, stationary source fuel combustion, industrial processes, and solid waste disposal (Potter and Coleman 2003; USEPA 1996). Natural sources of NO_x include lightning strikes, soils, wildfires,

stratospheric intrusion, and evaporation over large bodies of water (USEPA 1996). VOCs are naturally emitted in large quantities from deciduous vegetation and conifers. Evaporative and combustion processes are anthropogenic sources of VOCs. The sources of these ozone precursors are listed in Table 2-1. Ozone formation is expected to increase with the ratio of VOCs to NO_x.

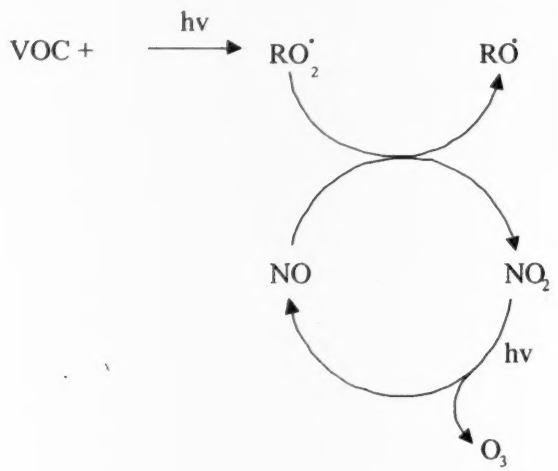

Figure 2-2 Ozone production in the presence of VOCs.
(USEPA 1996)

Major natural sinks for ozone are chemical reactions in the gaseous or aqueous phase and deposition (CEPA/FPAC WGAQOG 1999; Heinsohn and Kabel 1999). The chemical reactions that destroy ozone in the atmosphere include the HO_x (= OH + HO_2) (CEPA/FPAC WGAQOG 1999; Jacobson 1999; Potter and Coleman 2003) and NO_x (CEPA/FPAC WGAQOG 1999; Jacobson 1999) catalytic ozone destruction cycles. Reactions with unsaturated hydrocarbons also consume ozone (CEPA/FPAC WGAQOG 1999).

Table 2-1 Examples of human activities that are major contributors to urban levels of ozone precursor compounds.

Adapted from USEPA (1996).

Category	NO_x Sources	VOC Sources
Transportation	• Gasoline/diesel powered motor vehicles • Aircraft • Railcars • Vessels • Off-highway vehicles	• Vehicles
Stationary sources	• Electric utilities • Industrial and commercial/institutional boilers • Industrial furnaces • Space heaters	• Electric utilities • Industrial boilers and furnaces
Industrial processes	• Petroleum refining • Paper production • Glass production • Steel production • Cement production • Chemical production	• Solvent use • Petroleum product storage and transfer (fugitive emissions) • Chemical manufacturing
Solid waste disposal	• Incineration • Open waste burning	• Waste disposal and recycling
Miscellaneous	• Forest slash burning • Agricultural burning • Coal refuse burning • Structure fires	

2.2.3 Effects of meteorology and atmospheric physical processes

Several meteorological parameters affect the ozone balance in the atmosphere. Ultraviolet radiation, wind speed, and temperature influence the chemical reactions that occur in the atmosphere (USEPA 1996). In addition, surface scavenging and atmospheric mixing and transport processes can alter the ozone balance (USEPA 1996). Regional terrain also influences the dispersion of atmospheric pollutants. Ultraviolet radiation is required as an energy source to power the photochemical reactions in ozone formation. The amount of ultraviolet radiation in any given location is a function of the season, cloud cover, and atmospheric conditions. Temperature affects reaction kinetics and influences atmospheric mixing through convection currents. Wind speeds also affect atmospheric mixing through pressure gradients. The prime meteorological conditions for ozone formation and

accumulation are high pressure, temperature, and solar radiation, and light surface winds (Jacobson 1999).

2.3 Ozone Health Effects

Ozone has been linked to vegetation and crop injury (Bates 1991), materials damage (USEPA 1996), and health effects in animals, in addition to adverse effects in human beings. This section focuses on the key discoveries in recent (1990 or later) Canadian epidemiology studies.

2.3.1 Criteria and considerations in review of health literature

Determining the credibility of the reported associations between ozone exposure and adverse health effects necessitates understanding the traits requisite to good epidemiological studies. Epidemiological studies have some advantages over animal toxicology and controlled laboratory studies. They yield results for humans directly, eliminating the need to extrapolate results from animals to humans. This can reduce the uncertainty in the effect estimate, since physiological and anatomical traits of the human respiratory system (the system most often associated with ozone and air pollution exposure) are distinct from animal surrogates. In addition, unlike human clinical studies, epidemiological studies deal with real exposure levels and conditions. In clinical studies with human volunteers, ethical considerations prohibit the administration of doses that may inflict serious harm on the subject. Laboratory experiments are also limited to healthy volunteers, precluding the assessment of impacts to the most sensitive individuals of the population. Conversely, numerous confounding variables such as lifestyle, diet, and genetics make establishing cause-effect relationships in epidemiological studies difficult. These confounding factors are more easily controlled in animal toxicology studies, allowing cause and effect relationships to be determined. However, when epidemiology studies are well designed and executed, and multiple researchers repeatedly arrive at the same results, these studies constitute a convincing argument warranting further investigation of and concern about the relationships between ozone exposure and adverse health.

Craun et al. (1996) list the traits of a good epidemiological study. In addition to having an adequate sample size to provide statistical power, an epidemiological study should be free of or minimize random and systematic errors. The associations should be clear and lead to easily identifiable effects that occur after the exposure, and should be biologically conceivable. In addition, differences in sensitivities of sub-groups in the study population and seasonal fluctuations in ozone concentrations should be accounted for in studies (Bates et al. 1990).

2.3.2 *Summary of results from Canadian epidemiological studies*

Bates et al. (1990) studied emergency room attendance records at nine acute care hospitals in the Vancouver region. The emergency department records were evaluated with their corresponding air pollution data. They subdivided the study data according to the age of the patient, and accounted for seasonal fluctuations in their data. They found no associations between summer respiratory illness and ozone concentrations. They did find an increase in asthma attendance in the fall for the 15-60 years age group. The authors propose that ozone exposure increases airway sensitivity to other factors, such as pollen, house dust, infectious agents, and sulphur dioxide (SO_2).

Delfino et al. (1997) found positive associations between summer ambient ozone concentrations and hospital emergency room visits in Montreal, Quebec. Their study concluded that the elderly were most susceptible to adverse health effects from ozone exposure. The reasons the authors provided for the increased sensitivity of this age group was their greater likelihood of having pre-existing pulmonary diseases and lower respiratory tract infections. Delfino et al. also suggested the associations found were underestimated since they focussed only on respiratory illnesses.

Lipfert and Hammerstrom (1992) studied pollution and weather relationships with daily admissions to 79 acute care hospitals in Southern Ontario over a 6-year study period. They found a small but statistically significant association between ozone concentrations and respiratory admissions for the months of July and August.

Burnett et al. (1998) studied associations between ambient levels of gaseous air pollutants and daily deaths for non-accidental causes in 11 Canadian cities over 11 years. They determined that ozone exposure increased the risk of death by 1.8% ($p<0.01$). The data were pre-filtered to remove city-specific mortality trends due to population increases, seasonal, weekly, and daily fluctuations, and variations attributable to short-term epidemics. They found the risks from ozone were low for Calgary, Edmonton, and Winnipeg in the years studied. When a multi-pollutant model was used to evaluate a mixture of pollutants, the relative risk for ozone was higher than in the single pollutant model. The authors speculated that this increase implicates ozone as a promoter of the effects of other air pollutants and may not be toxic on its own.

Last et al. (1998) report that in Ontario, a 99 $\mu g/m^3$ ambient ozone concentration increases average hospital respiratory admissions by 4.5% compared to no ozone exposure. They also associate this concentration with a 1.35% increase in premature mortality. The effects associated with low level ozone exposure in healthy people include chest pain, pulmonary congestion, nausea, and cough. They identify asthmatics (5%-8% of all Canadians), children, the elderly, and those suffering from heart and lung diseases as those most vulnerable to the effects of ozone exposure.

2.4 Regulatory Control Strategies

A number of regulatory control strategies are used internationally to manage ozone levels in urban areas. Some of the management strategies include ambient air quality standards and guidelines, source emission limits, and controlled operation of major sources of precursor compounds.

2.4.1 Current standards and guidelines

In Canada, the federal government sets National Ambient Air Quality Objectives (NAAQO) to protect human health, vegetation, animals and materials. The current NAAQO is set at 82 ppb for a one hour average concentration. The NAAQO for ozone was set in 1976 as

part of the 1973 Clean Air Act, and was upheld under the Canadian Environmental Protection Act in 1989. (NARSTO 2000.)

More recently, Canada Wide Standards (CWSs) were developed, setting a 2010 target ozone level of 65 ppb averaged over 8 hours (CCME 2000). The Health Objectives Working Group, a committee composed of federal and provincial representatives, has recommended the daily one hour maximum reference level be set at 15 ppb, based on the lowest ambient concentration resulting in statistically significant health responses (Sandhu 1999).

In Alberta, the current one hour average Ambient Air Quality Guideline (AAQG) for ozone is also set at 82 ppb (160 $\mu g/m^3$) (EPEA 1992). Alberta Environment is the regulatory body responsible for monitoring ozone via a network of continuous air quality stations. For the final quarter of 2001, the average hourly concentration measured for ground level ozone was 10.3 ppb (20.1 $\mu g/m^3$) for Edmonton, and 10.7 ppb (20.9 $\mu g/m^3$) for Calgary (Alberta Environment 2001). These values were the averages of three monitors in each city.

The USEPA sets primary standards to protect public health and secondary standards to protect public welfare. The existing ozone maximum one hour average, set at 120 ppb (234 $\mu g/m^3$), is in the process of being replaced with a new 8 hour average limit of 80 ppb (156 $\mu g/m^3$) (USEPA 1997). Compliance with the new standard is based on the three year average of the annual 4th highest daily maximum 8 hour concentration. The objective of this type of standard is to prevent long exposure periods.

Directive 2002/3/EC governs ozone levels in the European Union, targeting a maximum daily 8 hour mean ozone concentration of 120 $\mu g/m^3$ (61 ppb) for 2010 (European Parliament and the Council of the European Union 2002). In addition, the maximum allowed number of days exceeding the directive per year is 25 days, averaged over 3 years.

2.4.2 *Ozone control measures*

A variety of ozone control and management strategies are in place internationally. Control strategies seek to limit emissions of ozone precursor compounds while management strategies tend to focus on minimizing exposure. Examples of management strategies include the Canadian air quality advisory programs (Cannon and Lord 2000), the "Ozone Alert Days" in Houston that were implemented in response to their USEPA non-attainment area designation (Prybutok et al. 2000), and the ozone alarm system in Seoul, South Korea (Sohn et al. 2000).

Several mechanisms of ozone control are used world-wide, with varying degrees of economic and social impact. In Athens, Greece, Leicester, U.K., and Houston, U.S., traffic management systems have been implemented to control vehicular emissions (Greig et al. 2000; Prybutok et al. 2000). Similarly, Santiago, Chile restricts vehicle circulation and shuts down principal emission sources during high PM_{10} episodes (Jorquera et al. 1998). In addition to these measures, areas that fail to meet regulated ozone levels face strict penalties. In the U.S., the USEPA can penalize non-attainment areas with sanctions and restrictions that impede industrial and commercial development, greater vehicle inspection requirements, and loss of federal funding (Prybutok et al. 2000).

2.5 Discussion: The Consequences of Ground-level Ozone to Current Lifestyles in Canada

Besides the Canadian studies, ozone exposure has been associated with increased mortality and morbidity in numerous other epidemiological studies (Dockery et al. 1993; McDonnell et al. 1999; and Thurston et al. 1997). A major problem with many epidemiological studies is the lack of control for confounding factors and a lack of measurement of actual exposures. These include differences within the population under study, as well as the location and characteristics of the study site. Potential confounding factors within the individuals participating in the study include differences in personal exposure levels, time spent and level of activity in different microenvironments, smoking, diet, gender, and genetic predisposition to disease. Study sites also differ in local industrial activity that could influence the chemical

composition and physical characteristics of ambient pollutants, meteorological and topographical characteristics that affect pollutant dispersion and accumulation, and pollution monitoring site distribution. Failure to adequately control these confounding factors could significantly contribute to the error in effects estimates.

In addition, many studies rely on death certificates or hospital admission records that are subject to illness classification errors or misdiagnoses (Bates et al. 1990; Dockery et al. 1993). Studies that rely on personal diaries for physical health information are prone to the sensitivities of the individual study participant. Each individual has a different level of tolerance for pain and discomfort, possibly resulting in different ratings for the same conditions. The ideal study would use a combination of different evaluation tools, including animal toxicology, epidemiological, and controlled laboratory studies, to develop a cause-effect relationship, but funding limitations result in deviations from the ideal.

Lagged and additive, synergistic, cumulative or antagonistic effects that depend on the particular cocktail of pollutants at a given location could also invalidate study results. It is possible for certain pollutants to weaken an individual's respiratory system, making the individual more susceptible to other substances later on that could produce effects not linked to the initial exposure. This would make it difficult to trace effects back to the original pollutant from short term epidemiological studies, or to identify non-acute effects attributable to the original pollutant. The epidemiological studies also attempt to relate health effects to ozone concentrations measured within various timeframes. Although popular measures include mean and daily maximum concentrations, there is no universal standard. Difficulty arises in establishing whether long-term low levels or peaks have a greater effect on human health. The use of average ozone concentrations over an extended period of time could also mask the effects of infrequent concentration excursions.

All the epidemiological studies use air monitoring data to establish personal exposure. This is potentially the greatest weakness of these studies, because monitoring station data are not equivalent to actual personal exposures. Monitors are generally placed in areas where high pollutant levels are likely to occur, so that violations can be detected. When data from multiple air monitors are employed, the methodology individual researchers use to determine

the concentration at a specific location will affect the accuracy of the personal exposure estimates used in their analysis. The amount of time individuals spend outdoors will also affect their personal exposure. However, the actual atmospheric pollutant exposures of study participants are likely to be lower than the levels detected at air monitoring stations, as people spend limited time outdoors. The mainly positive associations found in the epidemiological studies would be further strengthened if actual personal exposures were used in place of monitoring station data. Lipfert and Hammerstrom (1992) also report that indoor air pollutants best approximate outdoor levels in the summertime, when windows are open. This means that summer ambient monitoring data may then be a better indication of personal exposure to ambient pollutants than winter monitoring data. After the typically long, cold Canadian winters, Canadians are also likely to spend a greater portion of their summer days outdoors appreciating the warmer weather and longer daylight hours.

Despite the challenges facing epidemiologists, the consistency of the associations found between adverse health effects and ozone exposure at a variety of locations, in both laboratory and actual conditions, is cause for concern. It is unlikely that all locations would be subject to the same confounding factors, and in response to a better understanding of the science, more recent epidemiological studies show an awareness of confounding factors and attempt to control them. Some researchers include results of sensitivity analyses to show the robustness of the observed associations. Although environmental epidemiology studies notoriously result in relative risk estimates in the low range close to 1, at least one study found a strong association greater than 2 (McDonnell et al. 1998). Some studies were also conducted on healthy or "typical" participants, while the elderly, asthmatics, children, and individuals with already compromised immune systems are most sensitive to adverse health effects from ozone exposure. The issue of whether these effects are due to long term low level exposure or occasional exceedances of ambient guidelines is relevant from a public health perspective only for determining the format of ozone standards and control measures. The repeated observations of ozone pollution induced adverse health effects in epidemiological studies, supported by toxicological and clinical evidence, potentially represent an unacceptable public health risk and suggest benefits from reduced ambient ozone levels. The concern with urban air quality issues is reflected in the extensive control and management strategies world-wide.

Canadians face unique challenges in managing urban air quality issues. Canada's population, especially in urban centres, is increasing. As cities expand, commuting distances and times and the number of vehicles on roadways are also increasing, resulting in increased total emissions of ozone precursors. Public transportation access is also limited in newer suburbs, increasing the need for personal vehicle use. Developments in engine combustion efficiency and the gains associated with cleaner burner fuels and exhaust scrubbing units are offset by increases in urban traffic and industrial expansions accommodating the growing consumer market. Canada's large land mass results in greater distances between urban centres, increasing fuel use for inter-city travel and delivery of goods. The economy here is heavily dependant on the exploitation of raw resources that must be transported to markets. Canada's climate of cold winters with little daylight also results in greater fuel and power consumption to meet heating and lighting requirements.

All these factors require consideration when developing and implementing ozone and air pollution management strategies. Strict, regimental control of ozone levels may inhibit economic growth, but may also open doors for innovative solutions in industrial process improvements and alternate clean fuel technologies, as well as lower health care costs. In addition, Canadians must be willing to change current behaviours and lifestyles in exchange for improved air quality and health, and actively support ozone control and management policies. Regulatory agencies are faced with the difficult task of assessing the epidemiological and scientific evidence about ground-level ozone in urban areas, in order to balance the nation's economic prosperity with the quality of life.

2.6 Conclusions

Ozone chemistry is nonlinear, complex, and difficult to model. The amount and types of species present in the atmosphere, regional terrain, and meteorology and atmospheric physical processes all influence the ozone balance, and are challenging to represent with the current scientific knowledge. The epidemiology studies of ozone health effects are subject to problems in controlling confounding factors. Regardless, recent epidemiological studies indicate ozone as a cause or promoter of adverse health effects, prompting responses from

regulatory agencies to control or manage ozone levels. Regulatory strategies vary internationally, and include early warning systems for high ozone events, traffic management, and financial penalties. Ozone is of particular concern in urban areas, where sources of precursors and the numbers of human receptors are concentrated. Canadians face unique challenges to ozone control and management, borne out of Canadian climate considerations, the country's large land mass, current lifestyles, expanding urban populations, industrial development, and transportation trends. Solutions to the ozone problem must consider these issues to achieve balance between economic prosperity and quality of life.

2.7 References

Alberta Environment. 2001. Quarterly Air Quality Reports. Accessed via the Internet at http://www3.gov.ab.ca/env/air/airqual/quart.html on May 15, 2003.

Bates, D. 1991. The effects of ozone on plants and humans. In the Air & Waste Management Association Tropospheric Ozone and the Environment 3; Papers from an International Conference. Air & Waste Management Association, Pennsylvania, held March 19-22, 1990 in Los Angeles, CA.

Bates, D.V., Baker-Anderson, M. and Sizto, R. 1990. Asthma attack periodicity: a study of hospital emergency visits in Vancouver. Environmental Research, 51: 51-70.

Burnett, R.T., Cakmak, S. and Brook, J.R. 1998. The effect of the urban ambient air pollution mix on daily mortality rates in 11 Canadian cities. Canadian Journal of Public Health, 89(3): 152-156.

Cannon, A. J., and Lord, E. R. 2000. Forecasting summertime surface-level ozone concentrations in the Lower Fraser Valley of British Columbia: an ensemble neural network approach. Journal of the Air & Waste Management Association, 50: 322-339.

CCME— Canadian Council of Ministers of the Environment. 2000. Canada-Wide Standards for Particulate Matter (PM) and Ozone. CCME, Quebec City, PQ. Accessed via the Internet at http://www.ccme.ca/assets/pdf/pmozone_standard_e.pdf on July 10, 2003.

CEPA/FPAC WGAQOG— Canadian Environmental Protection Act Federal/Provincial Working Group on Air Quality Objectives and Guidelines. 1999. National Ambient Air Quality Objectives for Ground-Level Ozone Science Assessment Document, Catalogue No. En42-17/702-1999E. Health Canada and Environment Canada, Downsview, ON and Ottawa, ON.

Craun, G.F., Calderonon, R.L. and Frost, F.J. 1996. An introduction to epidemiology. Journal of the American Water Works Association, September: 54-65.

Delfino, R.J., Murphy-Moulton, A.M., Burnett, R.T., Brook, J.R., and Becklake, M.R. 1997. Effects of air pollution on emergency room visits for respiratory illnesses in Montreal, Quebec. American Journal of Respiratory and Critical Care Medicine, 155: 568-576.

Dockery, D.W., Pope, C.A., Xu, X., Spengler, J.D., Ware, J.H., Fay, M.E., Ferris, B.G. and Speizer, F.E. 1993. An association between air pollution and mortality in six U.S. cities. The New England Journal of Medicine, 329: 1753-1759.

EPEA— Environmental Protection and Enhancement Act. 1992. Table 1— Alberta Ambient Air Quality Guidelines. Alberta Queen's Printer, Edmonton, AB. Accessed via the Internet at http://www3.gov.ab.ca/env/protenf/approvals/factsheets/ABAmbientAirQuality.pdf on May 15, 2003.

European Parliament and the Council of the European Union. 2002. Directive 2002/3/EC of the European Parliament and of the Council of 12 February 2002 Relating to Ozone in Ambient Air. Accessed via the Internet at http://europa.eu.int/eur-lex/pri/en/oj/dat/2002/l_067/l_06720020309en00140030.pdf on July 31, 2003.

Greig, A.J., Cawley, G., Dorling, S., Eben, K., Fiala, A.J., Karppinen, A., Keder, J., Kolehmainen, M., Kukkonen, K., Libero, B., Macoun, J., Niranjan, M., Nucifora, A., Nunnari, A., Palus, M., Pelikan, E., Ruuskanen, J., and Schlink, U. 2000. Air pollution episodes: modelling tools for improved smog management (APPETISE). In Proceedings of the Eighth International Conference on Air Pollution. New Hall, Cambridge University, UK, 89-98.

Heinsohn, R. J., and Kabel, R. L. 1999. Sources and Control of Air Pollution. Prentice-Hall, Inc., Upper Saddle River, NJ.

Jacobson, M. Z. 1999. Fundamentals of Atmospheric Modeling. Cambridge University Press, Cambridge, UK and New York, NY.

Jorquera, H., Perez, R., Cipriano, A., Espejo, A., Letelier, M. V., and Acuna, G. 1998. Forecasting ozone daily maximum levels at Santiago, Chile. Atmospheric Environment, 32(20): 3415-3424.

Last, J., Trouton, K. and Pengelly, D. 1998. Taking Our Breath Away: The Health Effects of Air Pollution and Climate Change. David Suzuki Foundation, Vancouver, BC.

Lipfert, F.W. and Hammerstrom, T. 1992. Temporal patterns in air pollution and hospital admissions. Environmental Research, 59: 374-399.

McDonnell, W.F., Abbey, D.E., Nishino, N. and Lebowitz, M.D. 1999. Long-term ambient ozone concentration and the incidence of asthma in non-smoking adults: the AHSMOG study. Environmental Research, Section A, 80: 110-121.

McElroy, M. B. 2002. The Atmospheric Environment: Effects of Human Activity. Princeton University Press, Princeton and Oxford.

NARSTO--North American Research Strategy for Tropospheric Ozone Synthesis Team. 2000. An Assessment of Tropospheric Ozone Pollution: A North American Perspective. Accessed via the Internet at http://www.cgenv.com/Narsto on May 15, 2003.

Potter, T. D., and Colman, B. R. 2003. Handbook of Weather, Climate, and Water: Chemistry, Hydrology, and Societal Impacts. John Wiley and Sons, Inc., Hoboken, NJ.

Prybutok, V. R., Yi, J., and Mitchell, D. 2000. Comparison of neural network models with ARIMA and regression models for prediction of Houston's daily maximum ozone concentrations. European Journal of Operational Research, 122(1): 31-40.

Sandhu, H. S. 1999. Ground-Level Ozone in Alberta. Alberta Environmental Protection, Edmonton, AB.

Sohn, S. H., Oh, S. C., Jo, B. W., and Yeo, Y. K. 2000. Prediction of ozone formation based on neural network. Journal of Environmental Engineering, 126(8): 688-696.

Thurston, G.D., Lippmann, M., Scott, M.B. and Fine, J.M. 1997. Summertime haze air pollution and children with asthma. American Journal of Respiratory and Critical Care Medicine, 155: 655-660.

USEPA— United States Environmental Protection Agency. 1996. Air Quality Criteria for Ozone and Related Photochemical Oxidants-Volume I, II & III, EPA/600/P-93/004aF. Office of Research and Development, Washington, DC.

USEPA--United States Environmental Protection Agency. 1997. National Ambient Air Quality Standards (NAAQS). Accessed via the Internet at http://www.epa.gov/airs/criteria.html on May 15, 2003.

3.0 REVIEW OF THE APPLICATION OF ANNs TO OZONE MODELLING

3.1 Introduction

In the atmospheric environment, the formation and destruction of pollutants is a complex and dynamic process, receiving input from both anthropogenic and natural sources. Added to this complexity are the physical processes responsible for the accumulation, distribution, dispersion, and deposition of reactants and products alike. In urban settings, human habits and industrial activity tend to concentrate these compounds, creating a threat to public health. Not surprisingly, regulatory agencies, atmospheric scientists, and environmental engineers are quick to embrace innovative tools that allow them to forecast the occurrence of high pollution scenarios that may compromise human health. One such innovation is the artificial neural network (ANN), a modelling tool that harnesses the exponentially increasing computing power of the modern era. This chapter describes the components of an ANN, identifies the issues that challenge users of this modelling approach, and reviews the literature pertaining to their use for modelling ground level ozone concentrations.

3.2 Air Pollution Modelling Techniques

There are many ways to classify air pollution models. In one approach, Ojha et al. (2002) divide forecast models into four basic types. Depending on the desired complexity, models may marry elements of the following categories:

- *Trend models*. Trend models are developed with observations of the phenomenon modelled. These models usually require expert advice from specialists in the field to achieve forecasting success.
- *Historical/statistical models*. These models combine statistical knowledge of the local meteorology with measured pollutant data to generate predictions. Historical models rely on the principle that history has a tendency to repeat itself.
- *Causal models*. Causal models require identification of variables related to the formation of the pollutant being forecasted. These variables are combined with

dispersion and transport processes, atmospheric chemistry, and deposition characteristics of the area (terrain data) to formulate a mathematical relationship.

- *Physical models*. Physical models attempt to simulate the physical processes that a pollutant may undergo in the atmosphere. Potential processes include transport and dispersion. These smaller scale models are generally constructed to represent the meteorological and ambient conditions in the actual domain under consideration (Collett and Oduyemi 1997).

In the air pollution field, scientists and researchers use models to: assess air emission scenarios, forecast and quantify environmental impacts of existing or new developments, assess the potential effects of accidental releases, optimize facility operations, and determine compliance with regulatory standards and objectives (Collett and Oduyemi 1997). However, no single technique exists that is universally applicable (Angle and Sakiyama 1991).

Air pollution turbulent diffusion has traditionally been numerically simulated using two techniques: the Eulerian approach and the Lagrangian approach. The difference between these approaches is the frame of reference. In Eulerian type models, the reference system is fixed in one location, similar to what a fixed monitoring station would experience as it samples air flowing past the monitor. In the Lagrangian approach, the motion of a particle of air in the atmosphere is followed (Seinfeld 1986; Zannetti 1990).

The conservation of mass principle in a volume element of air is the basis for Eulerian models. The system is considered turbulent, with each parameter made up of an average component and a variable component. Terms in the mass balance represent physical and chemical processes, including advection, turbulent and molecular diffusion, and source/sink effects (Zannetti 1990). This equation is solved on a temporally and spatially discretized mesh. The model's resolution is then dependent on how the mesh is partitioned. Although a detailed mesh requires extensive computational resources, it produces a wealth of transport data at all points on the mesh (Zannetti 1990).

The Lagrangian approach uses statistics to describe the behaviour of fluid particles in the flow stream (Hanna et al. 1982; Seinfeld 1986; Weil 1988). The approach assumes a constant

wind velocity and homogeneous and instantaneous mixing (Zannetti 1990). It applies when no chemical reactions occur and an adequate understanding of the system turbulence is available to evaluate the probability density function (Seinfeld 1986).

A Gaussian distribution of the pollutant in the crosswind and vertical directions is assumed in a common dispersion plume model. This model incorporates several other simplifying assumptions (Angle and Sakiyama 1991; Collett and Oduyemi 1997; Hanna et al. 1982; and Turner 1994):

- Pollutant dispersion is dependent on the source emission rate.
- The system concentration does not change with time.
- Meteorological conditions do not vary spatially or with time.
- The source emission is a point source, and unchanging with space and time. Release and sampling times are long compared to the time required for the pollutant to travel from source to receptor.
- The pollutant is conservative.
- The system terrain is flat and homogeneous.
- The plume is symmetrical with a straight line trajectory.

The standard deviation of the pollutant dispersion in the y and z directions (σ_y and σ_z) is dependent on local turbulence, the stability of the atmosphere, and the distance travelled. The most popular method for determining σ_y and σ_z is based on the Pasquill stability classes, and is semi-empirical (Hanna et al. 1982). The main advantage of the Gaussian plume dispersion model is its ease of use (Collett and Oduyemi 1997).

Other common approaches to atmospheric modelling are based on statistical principles and probability theory. Semi-empirical relationships are derived from measured data, applying scientific knowledge of physical and chemical processes to establish cause and effect relationships at the source (Collet and Oduyemi 1997; Zannetti 1990). Statistical (or stochastic) models usually use online data to generate real-time, short-term forecasts to increase the efficiency of process operations. Some techniques in the literature are the Box-Jenkins method, regression analysis, and time series methods.

An alternative modelling approach is receptor modelling, in which observed ambient concentrations are traced to potential sources (Zannetti 1990). These statistical models are location specific, and are independent of dispersion or physical behaviours of the pollutants in the atmosphere.

Regulatory agencies, particularly the United States Environmental Protection Agency (USEPA) have participated in developing several atmospheric dispersion models that are accepted by Alberta Environment for regulatory applications (Idriss 2003). However, these models are imperfect, due to incomplete knowledge about the dynamic chemical and physical processes in the atmosphere. This is particularly true for secondary compounds like ozone that are formed and removed through complex and nonlinear processes. These considerations, coupled with the ready availability of high speed parallel processing technology, have paved the way for application of ANNs to air pollution modelling.

3.3 Artificial Neural Networks— Background

3.3.1 History of ANNs

McCulloch and Pitts first developed ANNs in the 1940s (Jain et al. 1996). They fashioned the ANN on the human brain, mimicking the brain's pattern recognition, processing, and problem solving abilities (Jain et al. 1996). Since that time, their popularity has waxed and waned with new developments and criticisms. In the 1980s, interest in ANN research was renewed with Rumelhart et al.'s (1986) reinvention of the backpropagation learning algorithm for the multilayer perceptron ANN (Henseler 1995; Jain et al. 1996). Recently, they have experienced renewed popularity in the atmospheric sciences, due to their ability to handle complex, nonlinear processes.

3.3.2 *Neural Network Architectures*

There are six basic types of ANNs, described in detail in numerous texts (see Hudson and Postma 1995). The most common of these is the multilayer perceptron (MLP). This network consists of an input layer, one or more hidden layers, and an output layer, all made up of neurons. These neurons form the basic processing unit of the ANN. A schematic of a simple MLP structure is shown in Figure 3-1.

Neurons in the input layer are the first interface between the external world and the network, receiving input data. They transmit the information to neurons in the hidden layer (hidden because they have no contact with the external world), where the signals are processed and passed to neurons in the output layer. The neurons in the output layer are responsible for communicating the network results to the external world.

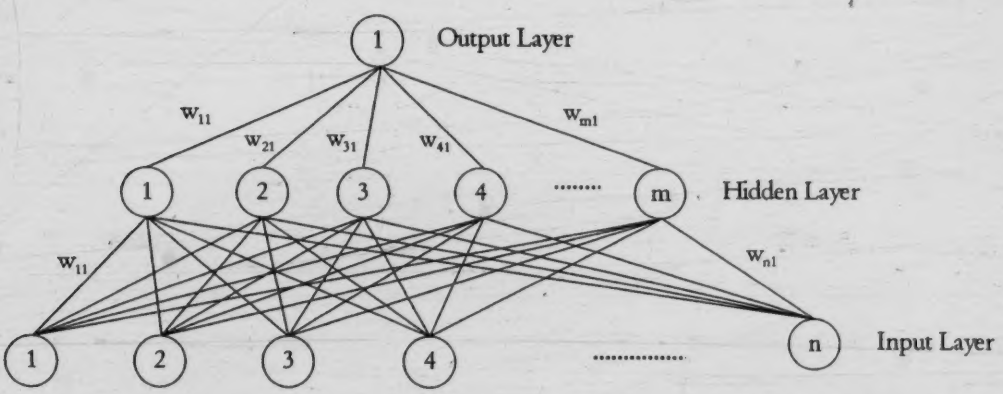

Figure 3-1 Schematic of a three-layer multilayer perceptron artificial neural network

Adapted from Plochl 2001.

The number of neurons in the input layer is equal to the number of input variables, with each neuron representing a single input variable. Input values are generally normalized, by dividing the value of each data point by the maximum value for that variable, so that no single variable dominates the network. In the simplest networks, only one output parameter is modelled, so that the output layer contains a single neuron. Multiple variables may be modelled with a single network. However, this increases the complexity of the network and

makes the interactions between neurons more difficult to interpret. In the ANN literature for ground-level ozone, the number of neurons in the hidden layer is typically established through a trial and error process to determine the number that produces an acceptable network performance. Recently, El-Din and Smith (2002) proposed a systematic approach for determining the most efficient network structure. Although they applied the systematic approach to a wastewater system, it may be applied to develop a network for any process.

The neurons in each layer of the network may be connected only to neurons in subsequent layers (feedforward) or to all other neurons in the network (fully connected) (Flood and Kartam 1997). These connections are weighted to reflect the strength and effect of the preceding neuron in layer i on the neuron under consideration in layer j (Garrett et al. 1997). If the weight value is positive, the connection is considered excitatory. Excitatory connections indicate that the neuron in layer i encourages activation of the neuron in layer j. If the weight is negative, the connection is inhibitory (the neuron in layer i suppresses the activity of the neuron in layer j), while a neutral connection weight represents an inactive connection. The connections between neurons in the ANN are analogous to the system of dendrites and axons that form the communication highways between neurons in the human brain (Jain et al. 1996).

The net input to a neuron is determined as the sum of all outputs from neurons in the preceding layer multiplied by their connection weights. This is represented mathematically by the equation (Garrett et al. 1997):

$$N_j = \sum_i o_i w_{ij} \quad \text{.....Equation 3-1}$$

where

N_j = summed weighted input to the neuron in layer j

o_i = output of neuron in layer i

w_{ij} = weight of the connection between neuron in layer i and neuron in layer j

An activation function is applied to the summed weighted input to the neuron to determine the neuron's level of activation:

$$a_i = F_i(N_j) \quad \text{.....Equation 3-2}$$

where

a_i = level of activation of neuron i

F_i = activation function of neuron i

The activation level of a function is subsequently used to determine the neuron's output value using the equation:

$$o_i = f_i(a_i) \quad \text{.....Equation 3-3}$$

where

o_i = output from neuron i

f_i = output function of neuron i

a_i = level of activation of neuron i

Examples of activation and output functions that may be used (F_i and f_i) are depicted in Figure 3-2. The functions used most often are the sigmoid (logistic), linear, and hyperbolic tangent functions.

3.3.3 Neural Network Learning

Training an ANN involves allowing the network to learn the relationships between a set of input parameters and an output variable. This requires an ample and representative historical database of input and output parameters. A learning rule dictates how a network responds to training data. There are four fundamental types of learning rules: error correction, Hebbian, Boltzmann, and competitive learning (Jain et al. 1996).

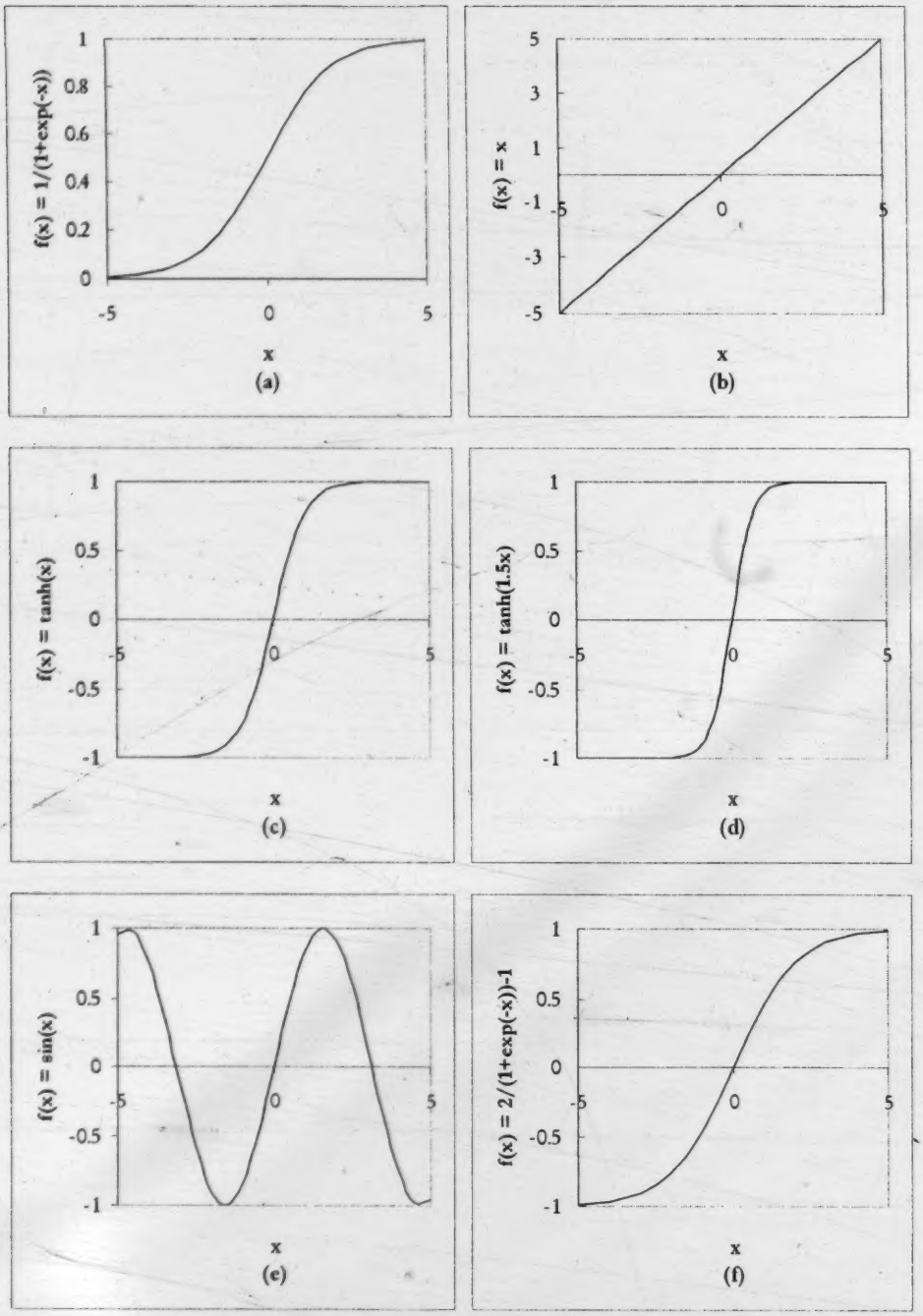

Figure 3-2 Activation functions used in ANNs: (a) logistic; (b) linear; (c) hyperbolic tangent; (d) hyperbolic tangent(1.5x); (e) sine; (f) symmetric logistic; (g) Gaussian; and (h) Gaussian complement.

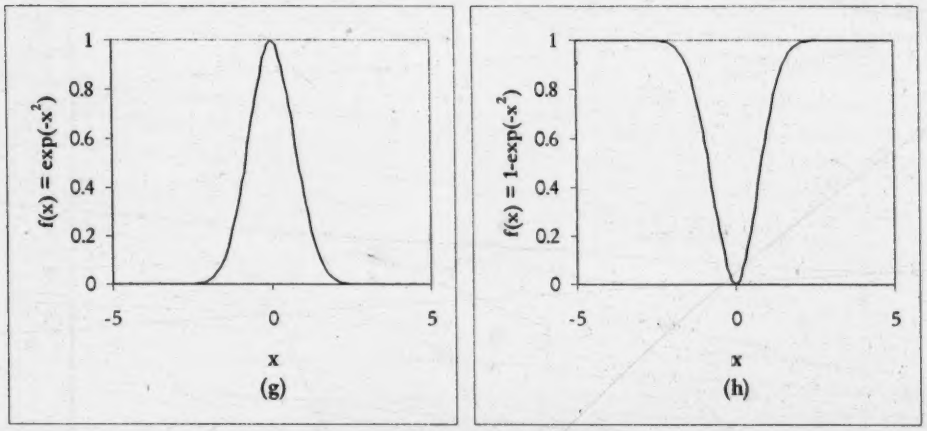

Figure 3 2 cont'd. **Activation functions used in ANNs: (a) logistic; (b) linear; (c) hyperbolic tangent; (d) hyperbolic tangent(1.5x); (e) sine; (f) symmetric logistic; (g) Gaussian; and (h) Gaussian complement.**

The most commonly used learning rule in MLP networks is the Generalized Delta Rule or backpropagation, a form of error correction. Initially, random weight values are assigned to the neuron connections. As data records are introduced to the network, the connection weights are adjusted to minimize the error between the network prediction and actual measured values of the output variable. The process is repeated until an acceptable error is achieved or a specified number of iterations are met. This type of learning, in which actual values of the output variable are presented to the network, is termed "supervised" learning. In unsupervised learning, the network is allowed to develop its own conclusions about correlations underlying structures and categories present in the training data, without any output variable information.

The fundamental principle underlying Hebbian learning is that when a neuron A repeatedly participates in stimulating a second neuron B, A's efficiency in firing B is increased (Garrett et al. 1997). In Boltzmann learning, thermodynamic and statistical principles are applied to adjust the neuron connection weights, resulting in a network state that satisfies the desired probability distribution (Henseler 1995). Competitive learning is used when the data are to be categorized or clustered based on similarities in the input data (Henseler 1995). These learning algorithms are described in greater detail in the references.

The data available for developing an ANN model are usually divided into two or three subsets. The first set is used for training the network, the second set for testing, and the last set for validation. Where only two subsets are created, the validation set is omitted. Each data subset should be representative of the entire data set, including all events the network may encounter and is expected to recognize during actual use. The data sets used for training the network must be pre-processed to remove noise, measurement errors, and non-random unexplained variances so the ANN can learn the true relationships between input and output variables (Comrie 1997; Gardner and Dorling 2001). Pre-processing can also attempt to identify the input variables most critical to output variable prediction.

During training, the number of presentations of the data to the ANN is limited to avoid overtraining. Overtraining results in the network memorizing the data patterns, including noise, instead of the underlying relationships. A classic symptom of overtraining is an acceptable error during the training phase of the model development, but unacceptably large errors when the model is applied to an independent set of data. In the training phase of model development, the data may be presented to the ANN in rotation, in which each data pattern or record is presented to the ANN in the order in which it appears in the training set. Connection weights are adjusted after each data pattern. An alternative approach, termed "batch", may be used, in which all data patterns in the training set are presented to the ANN. Predictions are generated for each pattern before the connection weights are adjusted. Each cycle through the training set is called an "epoch". The batch approach is more computationally efficient than the rotation approach.

3.3.4 ANN Capabilities and Model Design Considerations

ANNs are commonly used for scientific and engineering tasks such as pattern classification, categorization/clustering, function approximation, forecasting, optimization, and control (Jain et al. 1996). The design considerations for application of ANNs to accomplish these tasks include (Jain et al. 1996; Hudson and Postma 1995):

- The network's ability (or lack of ability) to learn.
- The network's ability to generalize and adapt to data never before encountered.

- Input and output data types (i.e., Boolean or continuous, single or multiple).
- System stability.
- Dimensionality and number of neurons in each layer.
- Selection of a learning algorithm.
- Selection of activation and output functions.
- Scalability of the developed network to real life application.
- Execution and learning speed.

The applications of the various types of networks and their associated learning algorithms are illustrated in Figure 3-3. The remainder of this chapter deals with the application of ANNs to model ground level ozone and includes a review of the current literature.

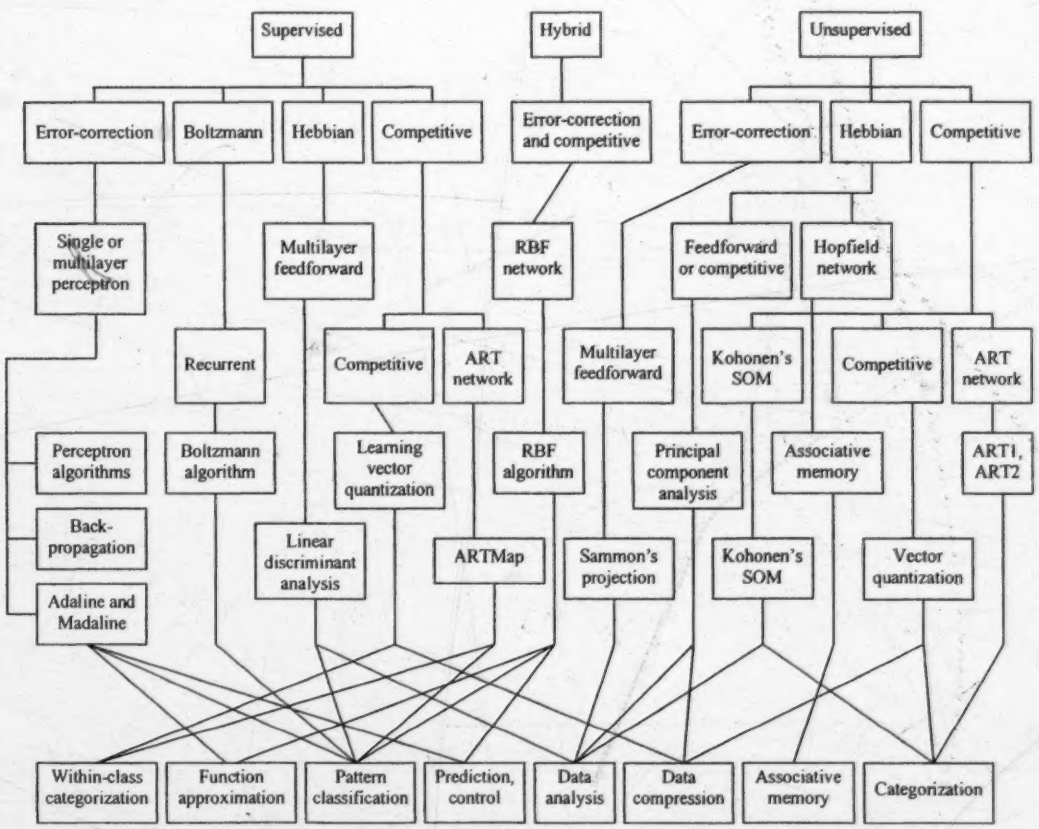

Figure 3-3 Learning algorithms, ANN functions, and network types.
Adapted from Jain et al. 1996.

3.4 Application of ANNs to Model Ground Level Ozone

Ground level ozone, as a secondary pollutant formed through complex and non-linear reactions between primary pollutant compounds, is well suited for application of ANNs. This realization has spurred widespread research into the success of ANN application to ozone modelling and the limitations of its use. Research efforts extend into the international arena, where several multi-national studies are underway to determine how ANNs can best be used for environmental data processing and atmospheric modelling. Burrascano (2001/2002) reports an Italian government project applying neural networks to environmental management problems, including air and electromagnetic pollution and water resources management. Greig et al. (2000) describe the efforts of a consortium from nine different institutions across Europe investigating the relative merits of the tools available for modelling air pollution episodes, and in particular the use of ANNs.

Gardner and Dorling (2001) had a unique application for ANNs, using the ANN to determine the effects of weather parameters on ozone concentrations. Their intent was to quantify these effects so they could be removed when measuring the success of emission control programs. They built ANN models for Cliffside Park, NJ, Washington, DC, Decatur, GA, Miami, FL, Chicago, IL, and Los Angeles, CA, using data from 1984 to 1995. Inputs to the model were surface temperature, specific humidity, ceiling height, opaque cloud cover, wind speed, modelled global solar radiation data, and the sine and cosine functions of the Julian day of the year. These inputs were selected to allow comparison of their ANN results with a previous study. Like many others, Gardner and Dorling's results indicated that the ANN approach improved prediction performance at all sites except Chicago.

The flurry of recent interest in ANNs for modelling ground level ozone has brought to light several issues, associated with the approach, that still require resolution. In particular, the ANN model development remains largely subjective, requiring the user to exercise a certain level of expertise and skill with regards to the process modelled.

3.4.1 Model Inputs

One area where this subjectivity has generated a motley of approaches is in the selection of inputs for the models. Ground level ozone concentrations are dependent on a combination of meteorological conditions and concentration of precursor compounds (McElroy 2002; Jacobson 1999; Potter and Coleman 2003; Sandhu 1999; and Seinfeld 1986). In several papers, researchers choose to focus on only one of these two aspects, limiting the success of the models. In addition, these approaches do not take full advantage of the ANN's ability to handle complex data. Comrie (1997) forecast daily maximum one hour ozone concentrations in several American cities, using data from May through to September for the years 1991 to 1995. For parsimony, the author used only four meteorological inputs to the model: daily maximum temperature, average daily dewpoint temperature, average daily wind speed, and daily total sunshine. The previous day's maximum ozone concentration was also used as an additional input parameter for some "lagged" forecast models for comparison. The historical data were randomly partitioned into training and validation data sets. The neural network architectures were not optimized for this work. These considerations may have contributed to Comrie's conclusion that the performance of the neural networks was only marginally better than multiple regression models.

Another example of an ANN model with a limited number of inputs comes from Jorquera et al. in 1998. Jorquera et al. modelled daily maximum hourly ozone concentrations in Santiago, Chile using the previous day's ozone concentration and maximum temperature, and the forecast day's maximum temperature. To simulate the error associated with forecasted temperatures, they added a Gaussian noise term to the actual maximum temperatures on the forecast day. The performance of the ANN model was compared to time series and fuzzy models. They concluded that the fuzzy model performed best, with the lowest number of false positives for all the validation data sets, but noted that the models could be improved with concentrations of ozone precursors as input.

Nunnari et al. (1998) focused only on concentrations of air pollutants for their ozone model. They predicted ambient ozone concentrations in Sicily one hour in advance using ANNs, fuzzy neural networks, and autoregressive models. The ANN model used previous hours'

ozone, nitrogen dioxide (NO_2), NO_x, and non-methane hydrocarbon (NMHC) concentrations for input. They found that the ANN was the most accurate predictor out of the three modelling approaches.

Although models using a limited number of input variables can provide information about the effects of the specific inputs on ozone concentrations, influences from other parameters potentially important to ozone formation lack representation in the models. Comparing these types of models to other statistical or time series approaches is essentially a spurious comparison, because the approaches have different strengths and limitations. To reduce the number of inputs to the ANN model so that the number of inputs are equal to those used in these other approaches robs the ANN approach of its full information processing capabilities. For a true valuation of each approach's forecasting potential, each model should be optimized before the comparison is made. This would allow the strengths of each technique to be fully showcased.

It is also critical to examine the current scientific knowledge of the process, even if incomplete, for clues about the variables that may be relevant to the process. In situations where the data required to adequately train the ANN are unavailable or insufficient, it may be necessary to investigate alternate modelling methods, although Kao and Huang (2000) report that the ANN approach performed better than time series models for a limited data situation Taiwan. In this case, Kao and Huang collected ozone concentrations at three monitoring stations to develop an ozone forecast model. Their model used only concentration data from the 24 hours prior to the forecast hour as input. The selection of the preceding 24 hours was also arbitrary in this instance, highlighting the fact that when time series inputs are used in models, no method has been consistently applied in the literature to select a suitable time window to include.

A possible solution for selecting a suitable time window is to build and optimize a series of ANN models incorporating an increasing number of previous hours' concentrations as inputs. This simple approach will help to determine whether increments in the input time window correspond to performance gains. Hadjiiski and Hopke (2000) applied a similar method, using volatile organic compound (VOC), nitric oxide (NO), and NO_2

concentrations, temperature, and radiant energy data to predict ambient ozone concentrations in Texas up to 5 hours in advance. The authors evaluated the effectiveness of increasing the number of concentrations from previous hours into their model, concluding that the most efficient model included only ozone concentrations from the previous two hours. However, they did not attempt to repeat the optimization of their model with the additional inputs. It would be expected that, with a change in the number of input variables (due to the addition of previous hours' concentrations), the optimum network structure would also change. In addition, Hadjiiski used modelled concentrations rather than actual concentrations for the previous hours, which could increase the error in their forecasts.

When a sufficient data history is readily available, the next question posed to the model developer is: what inputs are relevant to the process and should be included as input? Since ANNs are typically applied when mechanistic models are inadequate due to a lack of knowledge about the process modelled, this question is difficult to answer. One approach investigated in the literature is the method Garson proposed in 1991. In Garson's paper, an equation is developed to partition connection weights of a trained network back to the input variables. This allows less important variables to be removed from the input variable set. Abdul-Wahab (2001), Abdul-Wahab and Al-Alawi (2002), and Elkamel et al. (2001) applied the Garson method to analyze the relative importance of the inputs to their models. Although all three studies were completed in Kuwait (the first two studies in the Khaldiya residential area and the third in the Shuaiba industrial area), the relative importance of the input parameters varied among the three studies. In all three studies, pollutant concentration and meteorological data were obtained from a mobile monitor. Inputs to the Abdul-Wahab and the Abdul-Wahab and Al-Alawi studies were identical except that NO_x was included in addition to NO and NO_2 concentrations in one of the studies. Both models were considered successful predictors of ozone concentration, with coefficients of multiple determination greater than 0.86. However, the Garson method produced very different results in the relative importance of the inputs. In the Abdul-Wahab (2001) paper, the order of importance of the input variables was solar energy, wind direction, carbon dioxide (CO_2), relative humidity (RH), NO_x, NO_2, temperature, wind speed, NO, NMHC, and methane (CH_4). The remaining variables were unimportant to the model. This list compares poorly

to the Abdul-Wahab and Al-Alawi paper (2002), for the same residential area, in which the order of importance of inputs was: NO, sulphur dioxide (SO_2), RH, NMHC, NO_2, CH_4, temperature, CO_2, dust, CO, radiation, wind speed, and wind direction. These results suggest that the Garson method lacks robustness. The Elkamel et al. (2001) study also found CO to be an important input variable. This is contrary to studies by other authors (e.g., Jacobson 1999 and Ruiz-Suarez et al. 1995), who report CO as a relatively inert compound in the urban atmosphere. Although CO may be an indicator of wind drift, this parameter was already explicitly represented in the Elkamel study. Other than the Garson approach, there is a conspicuous lack of a widely accepted methodology for determining the relative importance of inputs to ANN models.

The majority of authors use ambient monitoring data to develop ANN models. This is not surprising, as in most cases, the data are readily available and encompass a broad spectrum of both meteorological and pollutant parameters. A strategy for incorporating these data then becomes an issue, with authors required to choose data from numerous monitors within a geographical area and establish an appropriate averaging time for the measured parameters. Some authors incorporate data from a network of stations to model the overall maximum ozone in the region. Cobourn et al. (2000) combined meteorological data from seven different monitoring stations, from a mixture of urban, rural, and suburban sites near Louisville, Kentucky. They modelled the peak ozone concentration for the entire region. The ANN model inputs included dew point temperature, cloud cover, and wind speed, all averaged over late morning and early afternoon hours, hourly temperature, daily precipitation, and the number of overnight calms. This may become confusing for the ANN, since relationships between ozone concentrations and local wind direction, wind speed, and pollutant sources are potentially obfuscated. There is also potentially great spatial and temporal variability in meteorological parameters, like wind speed and wind direction. Averaging of these variables results in a loss in information that may be relevant in identifying particular sources or conditions that may be strongly associated with ozone events. In addition, emission sources and dispersion characteristics may be different in urban and rural sites. These differences are lost when the information from all stations is combined in one model.

Guardani et al. (1999) attempt to consider wind behaviour when choosing the stations to include in their ANN. They employed ANNs to determine the relationship between variables measured at the core of the Sao Paulo Metropolitan Area in Brazil and afternoon ozone concentrations at a monitoring station downwind of the city centre. Data from June to December 1996 for CO, NMHC, NO, NO_2, wind speed, and wind direction at the city core station (averaged for the hours from 8:00 to 11:00), and radiation and temperature from downwind stations (averaged from 12:00 to 17:00) were used to predict the average ozone concentration between 12:00 and 17:00 at the downwind stations. Guardani et al. found good agreement between neural network predictions and observed ozone concentrations. They suggest a more detailed and systematic study in the future on a larger data set. This method may work well in regions where winds are predominantly from one direction. In areas where winds are highly variable, an alternate approach may be to develop individual models for each monitoring station and evaluating the results from all models to establish the peak ozone concentration in the region. This method would allow the ANNs to determine influences form local area effects.

The selection of an averaging time should be based on consideration of the formats of governing regulations and guidelines, and the available monitoring data. Smaller averaging times would limit the loss of information about the variables' behaviours. However, the volume of data would increase, resulting in increased calculation requirements and processing time. Hourly averages are the most popular choice, and allow the determination of compliance with most standards.

3.4.2 Data Quality

Associated with the availability of historical data is consideration of how well the data represent the process. For the ANN to be able to learn and recognize ozone events, and to properly evaluate the network's predictive abilities, each of the training, test, and production data sets must also be representative of the data set as a whole. The ANN relies on the training data to learn the features and relationships of the modelled process, so it is imperative that this data set contains all the possible scenarios that may occur, to build the ANN's experience with these situations. Since the model is judged based on its performance

on the test or validation data, it is important that these are representative of the historical data, so the ANN's performance is not biased up or down. Sohn et al. (2000) forecast ozone up to 24 hours in advance in Seoul, Korea. They chose a MLP ANN with a fixed hidden layer consisting of 50 neurons, trained with a scaled conjugate gradient algorithm. The ANN model inputs were previous hours' concentrations of ozone, NO_2, CO, and SO_2, temperature, wind speed, sunlight, and humidity, totalling 30 variables. Sohn et al. had limited historical data with which to train the ANN, the training set containing only 31 patterns. They found the ANN generally performed well, but speculated that an interval of poor prediction performance was attributable to a failure to account for precipitation falling during that interval.

Cannon and Lord (2000) circumvent this issue with the use of re-sampling techniques and multiple networks. They predicted daily maximum hourly average ozone concentrations from May through September for the Lower Fraser Valley in British Columbia. Cannon and Lord applied a bootstrap aggregation method, creating multiple training data sets through re-sampling from the historical database, and training several ANNs with the training sets. According to the authors, approximately 37% of the training cases are excluded from the bagged sets of data using this method, but the final aggregate model is more stable and the model selection efficiency is improved. Cannon and Lord also applied a histogram equalization process to increase the frequency of extreme events in the training data set, seeing improved ANN performance with these models.

Since ozone is related to hot, sunny days, Cannon and Lord (2000), along with other researchers (e.g., Comrie 1997) chose to use forecast values of meteorological inputs such as daily maximum temperature in their models. These forecast values inherently contain some element of noise, and are dependant on the skill of the meteorologist. To decrease the reliance on human judgement, Balaguer Ballester et al. (2002) attempted "true" forecasting of ozone, using previous hours' inputs (ozone at t-24 to t-1, other inputs of wind speed, wind direction, temperature, pressure, solar irradiance, relative humidity, NO, and NO_2 at time t-24) to predict ozone at time t. The predicted ozone concentration at time t, along with the other inputs (ozone at t-1 to t-22, others at t-22), were then used to predict ozone concentration at t+1, and so on until a forecast for ozone concentration at t+24 was created.

Hadjiiski and Hopke (2000) used the same approach to generate ozone concentration predictions up to 5 hours in advance, except that the inputs to their model were VOC, NO, NO_2, temperature, and radiant energy at time t. As the authors observed, the use of ANN predicted concentrations to forecast the next ozone concentration term in the time series tends to allow errors to accumulate, so that the larger the prediction window, the greater the error. In evaluating model performance and use in forecasting then, a minimum acceptable performance needs to be established by the user to ensure an acceptable level of quality of the forecast values.

A related issue is the procedure used to divide the historical data into training, test, and production data sets. Some authors choose a random process of assigning data patterns to a data subset. With this method, and especially with a small historical database, the possibility of one of the subsets being unrepresentative is large. Other authors choose to divide the data sets according to year. The disadvantage with this procedure is the possibility that all scenarios may not occur in any given year, and an atypical year may bias the network performance as discussed earlier. If a year of relatively low ozone concentrations were used as the test set, the ANN performance would be artificially elevated. The opposite would be true if the test year contained unusually high ozone concentrations or the training set contained only low ozone years. Seasonal fluctuations in ozone concentration are also a consideration. An ANN to forecast the daily maximum hourly ozone concentrations in Houston was developed by Prybutok et al. (2000) using data collected from a number of USEPA monitoring stations in the area. NO_2, NO, CO_2, and NO_x concentrations, wind speed, and wind direction (all averaged for the hours between 6:00 and 9:00 a.m.), an index for working or holiday day, the ozone concentration at 9:00 a.m., and the actual maximum daily temperature formed the inputs to the model. The data from June through September 1994 were used for training the ANN, while data from the first two weeks of October were reserved for testing the network performance. While this method of data division may work well in places like Houston, it would be inappropriate for Alberta, where there are seasonal effects to consider and large ranges in daily hours of sunlight. In Alberta, October ozone concentrations would be considerably lower than in May or June, resulting in a prediction performance that is biased upwards if the October data were used to evaluate the network performance.

Annual changes in meteorology also require consideration. This is one of the reasons an ANN model requires periodic re-training, to ensure medium term fluctuations in meteorology are accounted for. Melas et al. (2000) developed an ANN model using hourly average pollutant concentrations and meteorology for Athens, from 1987 to 1990. However, the test set of data was obtained from 1995, a span of five years from the training data. This may be the reason for the authors' finding that the ANN exhibited only marginal performance improvement when compared to regression models in the literature, Cobourn et al. (2000), in their paper discussed above, also noted large differences from year to year ANN performance. They attributed the ANN's poor performance in 1998 to unusual meteorology in that year.

Soja and Soja (1999) used a simple neural network (2-2-1 architecture) to predict ozone indices in rural Austria, using only daily maximum temperature and sunshine duration for input. The historical data were collected from May to September, and spanned the years 1993-1996. Data for the first three years were used to train the network, while the 1996 data were reserved for testing the models. They found that the ANN models did not always outperform optimized regression models. However, this may also be attributable to the simplicity of the ANN structure and the small number of inputs used in their model.

3.4.3 Network Architecture

The selection of an ANN structure is still predominantly ad hoc or arbitrary in nature. Most authors choose to fix the network architecture. Despite the proposal of a systematic approach by El-Din and Smith (2002), some authors continue to adopt trial and error methods to determine the network type, number of layers, number of neurons within each layer, and training epochs. Generally, the tested ranges of each feature are arbitrarily selected. However, there are indications of interest in applying a systematic approach for the atmospheric sciences, with several authors using a quasi-systematic methodology to develop their models. Yi and Prybtok (1996) used ANNs to predict daily maximum ozone concentrations in an industrial area of Dallas-Fort Worth. NO_2, NO, CO_2, and NO_x concentrations, a variable representing a holiday or working day, ozone concentration at 9:00

a.m. of the forecast day, average wind speed and direction between 6:00 and 9:00 of the forecast day, and the maximum daily temperature on the forecast day formed the inputs to the model. The network features, including various combinations of the number of hidden layers, number of hidden layer neurons, and transfer functions were evaluated in over 50 experiments.

In the United Kingdom, Spellman (1999) used ANNs to predict daily one hour maximum surface ozone concentrations at five monitoring stations, using surface meteorological variables (maximum temperature, hours of sunshine) and the previous day's ozone concentration for inputs. To determine the optimum network architecture, Spellman used a trial and error approach, although details of the specific protocol employed were not provided.

In spite of the lack of an established methodology for optimizing the ANN structure, the flexibility in building the ANN, with a vast array of options for connection styles, activation functions, and training algorithms, etc., is also one of the desirable characteristics of the ANN modelling approach. The assortment of potential architectures makes ANNs amenable to modelling a variety of processes. This is illustrated in Wang et al. (2003), who approached the modelling of ozone for Hong Kong with an atypical radial basis function (RBF) network and an adaptive radial basis function (ARBF) network that combined the RBF with statistical characterization of ozone concentrations. They used data collected at three monitoring stations to train and test the ARBF network. The variables input to the model, selected based on the statistical analysis, were concentrations of ozone, NO_2, and NO_x, wind speed, temperature, and solar radiation. Wang et al. found the ARBF successfully predicted daily maximum ozone concentrations at the three stations.

3.4.4 Performance Evaluation

The statistical parameters used to evaluate the ANN model performance are widely variable from paper to paper. Currently, there appears to be no consensus on the best statistical parameter to use, resulting in a large array of options in the literature. This makes comparisons of different studies difficult. Some authors provide no statistical indicators at

all, purely using graphics to represent their results. This is the technique employed by Konovalov (2001), who used a neural network based model to study the sensitivity of ambient ozone concentrations to concentrations of various precursor compounds. The ANN model was built with an extensive data bank, collected over 15 years. Konovalov concluded that ANN models are good tools for determining ozone sensitivity to precursor compounds. The use of graphical illustrations to qualitatively evaluate the network performance is undoubtedly an information rich technique. Plots of ANN predictions with actual ozone concentrations can highlight deviations from the observed ozone trends and systematic under- or over-prediction of extreme values. However, statistical indicators such as the coefficient of multiple determination, Wilmott's indices of agreement, and bias also provide specific, quantitative information about the ANN performance and facilitate comparison of the ANN performance with other studies.

Schlink et al. (2003) attempted to compare time series and statistical modelling approaches to ANN models for a number of European cities. To allow comparisons between the different models, they chose several performance indicators that were calculated for all models. This approach of providing an array of performance indicators is more comprehensive, because each statistical parameter is an indication of a different aspect of the model performance. For example, the commonly used coefficient of multiple determination provides a general indication of how much of the variability in the output is explained by the model inputs, while the bias detects any systematic deviations from the desired output that may not be apparent from parameters such as the mean absolute error. Based on this type of approach, Schlink et al. determined that the preferred modelling technique was dependant on the scenario modelled, the available data, and the modelling objectives. However, they suggest that ANNs provide a good compromise.

Finally, practicality considerations are necessary when assessing the value and usability of an air quality model. Narasimhan et al. (2000) developed several ANN models for ozone in Tulsa, Oklahoma. The first model used 8 inputs: NO, NO_2, temperature, radiation, relative humidity, wind speeds at two heights, and barometric pressure. This model was used to determine the sensitivity of ozone concentrations to changes in the input variables. A second ANN model was built incorporating concentrations of ozone from the previous

three days. A third ANN model included modelled upper air data (vertical temperature profile, vertical relative humidity profile, mixing depth, vertical wind speed, and a four layer lifting index). They recommend further development of their models to include soil temperature, soil moisture, wind direction, and rainfall data. However, these types of inputs may not be readily available in Alberta, with the same frequencies as the ambient monitoring data. Any ANN models developed for a region must draw their inputs from the available pool of information in the region. Although a limited number of inputs may be non-ideal, a model requiring inputs that are difficult or costly to obtain would have limited usefulness. Therefore, the need for completeness of the model must be tempered with practicality considerations.

Like traditional models, the ANN requires quality historical data, and due to its "black box" nature, provides limited information about the modelled process. Currently, no method is available for analyzing the ANN structure to generate descriptive functions of the modelled process. This has slowed widespread acceptance of ANNs for atmospheric modelling. Despite these challenges, ANNs are an attractive alternative to traditional mechanistic models, as the large number of papers in the literature attests. The advantages they offer include the ability to learn nonlinear patterns in the data, flexibility in model structuring, and the ability to efficiently use available computing power, resulting in time and cost savings.

3.5 Conclusions

A variety of approaches are available for atmospheric modelling. ANNs are particularly well suited to modelling ground-level ozone due to their ability to handle complex, poorly understood, nonlinear processes and the flexibility in their design. However, this flexibility also generates challenges associated with developing a consistent methodology for choosing appropriate inputs, evaluating the quality of historical data, and selecting an efficient network structure. In addition, these challenges must be balanced with usability considerations, scientific knowledge, and available funds.

3.6 References

Abdul-Wahab, S.A. 2001. IER photochemical smog evaluation and forecasting of short-term ozone pollution levels with artificial neural networks. Process Safety and Environmental Protections: Transactions of the Institution of Chemical Engineers, Part B, 79(2): 117-128.

Abdul-Wahab, S.A. and Al-Alawi, S.M. 2002. Assessment and prediction of tropospheric ozone concentration levels using artificial neural networks. Environmental Modelling & Software, 17: 219-228.

Angle, R.P. and Sakiyama, S.K. 1991. Plume Dispersion in Alberta. Alberta Environment, Edmonton, AB.

Balaguer Ballester, E., Camps i Valls, G., Carrasco-Rodriguez, J.L., Soria Olivas, E., and del Valle-Tascon, S. 2002. Effective 1-day ahead prediction of hourly surface ozone concentrations in eastern Spain using linear models and neural networks. Ecological Modelling, 156: 27-41.

Burrascano, P. 2001/2002. Neural networks for environmental data processing: a research project of relevant national interest for the Italian Government. International Journal of Applied Electromagnetics and Mechanics, 13: 3-11.

Cannon, A.J. and Lord, E.R. 2000. Forecasting summertime surface-level ozone concentrations in the Lower Fraser Valley of British Columbia: an ensemble neural network approach. Journal of the Air & Waste Management Association, 50: 322-339.

Cobourn, W.G., Dolcine, L., French, M., and Hubbard, M.C. 2000. A comparison of nonlinear regression and neural network models for ground-level ozone forecasting. Journal of the Air & Waste Management Association, 50: 1999-2009.

Collett, R.S. and Oduyemi, K. 1997. Air quality modelling: a technical review of mathematical approaches. Meteorological Applications, 4: 235-246.

Comrie, A.C. 1997. Comparing neural networks and regression models for ozone forecasting. Journal of the Air & Waste Management Association, 47: 653-663.

El-Din, A. and Smith, D.W. 2002. A neural model to predict the wastewater inflow incorporating rainfall events. Water Research, 36: 1115-1126.

Elkamel, A., Abdul-Wahab, S., Bouhamra, W., and Alper, E. 2001. Measurement and prediction of ozone levels around a heavily industrialized area: a neural network approach. Advances in Environmental Research, 5: 47-59.

Flood, I. and Kartam, N. 1997. Systems. In Artificial Neural Networks for Civil Engineers: Fundamentals and Applications, N. Kartam, I. Flood, and J.H. Garrett Jr., eds. American Society of Civil Engineers, New York, NY.

Gardner, M. and Dorling, S. 2001. Artificial neural network-derived trends in daily maximum surface ozone concentrations. Journal of the Air & Waste Management Association, 51: 1202-1210.

Garrett, J.H., Jr., Gunaratman, D.J. and Ivezic, N. 1997. Introduction. In Artificial Neural Networks for Civil Engineers: Fundamentals and Applications, N. Kartam, I. Flood, and J.H. Garrett, Jr. Eds. American Society of Civil Engineers, New York, NY.

Garson, G.D. 1991. Interpreting neural-network connection weights. AI Expert, 4: 47-51.

Greig, A.J., Cawley, G., Dorling, S., Eben, K., Fiala, A.J., Karppinen, A., Keder, J., Kolehmainen, M., Kukkonen, K., Libero, B., Macoun, J., Niranjan, M., Nucifora, A., Nunnari, A., Palus, M., Pelikan, E., Ruuskanen, J., and Schlink, U. 2000. Air pollution episodes: modelling tools for improved smog management (APPETISE). In Proceedings of

the Eight International Conference on Air Pollution, New Hall, Cambridge University, UK, 89-98.

Guardani, R., Nascimento, C.A.O., Guardani, M.L.G., Martins, M.H.R.B., and Romano, J. 1999. Study of atmospheric ozone formation by means of a neural network-based model. Journal of the Air & Waste Management Association, 49: 316-323.

Hadjiiski, L. and Hopke, P. Application of artificial neural networks to modeling and prediction of ambient ozone concentrations. 2000. Journal of the Air & Waste Management Association, 50: 894-901.

Hanna, S.R., Briggs, G.A., and Hosker, R.P. 1982. Handbook on Atmospheric Diffusion, Prepared for the Office of Health and Environmental Research, Office of Energy Research, U.S. Department of Energy. Technical Information Center, U.S. Department of Energy, Oak Ridge, TN.

Henseler, J. 1995. Backpropagation. Artificial Neural Networks: An Introduction to ANN Theory and Practice, P.J. Braspenning, F. Thuijsman, and A.J.M.M. Weijters, eds. Springer, Berlin and New York, NY, 37-66.

Hudson, P. T. W., and Postma, E. O. 1995. Choosing and using a neural net. Artificial Neural Networks : An Introduction to ANN Theory and Practice, P.J. Braspenning, F. Thuijsman, and A.J.M.M. Weijters, eds. Springer, Berlin and New York, NY, 273-287.

Idriss, A. 2003. Air Quality Model Guideline. Alberta Environment, Edmonton, AB.

Jacobson, M. Z. 1999. Fundamentals of Atmospheric Modeling. Cambridge University Press, Cambridge, UK and New York, NY.

Jain, A.K., Mao, J., and Mohiuddin, K.M. 1996. Artificial neural networks: a tutorial. Computer, 29: 31-44.

Jorquera, H., Perez, R., Cipriano, A., Espejo, A., Letelier, M.V., and Acuna, G. 1998. Forecasting ozone daily maximum levels at Santiago, Chile. Atmospheric Environment, 32(20): 3415-3424.

Kao, J., and Huang, S. 2000. Forecasts using neural network versus Box-Jenkins methodology for ambient air quality monitoring data. Journal of the Air & Waste Management Association, 50: 219-226.

Konovalov, I.B. 2002. Application of neural networks for studying nonlinear relationships between ozone and its precursors. Journal of Geophysical Research, 107(D11): ACH8-1-ACH8-14.

McElroy, M. B. 2002. The Atmospheric Environment: Effects of Human Activity. Princeton University Press, Princeton and Oxford.

Melas, D., Kioutsioukis, I., and Ziomas, C. 2000. Neural network model for predicting peak photochemical pollutant levels. Journal of the Air & Waste Management Association, 50: 495-501.

Narasimhan, R., Keller, J., Subramaniam, G., Raasch, E., Croley, B., Duncan, K., and Potter, W.T. 2000. Ozone modeling using neural networks. Journal of Applied Meteorology, 39: 291-296.

Nunnari, G., Nucifora, A.F.M., and Randieri, C. 1998. The application of neural techniques to the modelling of time-series of atmospheric pollution data. Ecological Modelling, 111: 187-205.

Ojha, S., Coutinho, J., and Kumar, A. 2002. Developing systems to forecast ozone and particulate matter levels. Environmental Progress, 21(2): J7-J12.

Plochl, M. 2001. Neural network approach for modelling ammonia emission after manure application on the field. Atmospheric Environment, 35:5833-5841.

Potter, T. D. and Colman, B. R. 2003. Handbook of Weather, Climate, and Water: Chemistry, Hydrology, and Societal Impacts. John Wiley and Sons, Inc., Hoboken, NJ.

Prybutok, V.R., Yi, J., and Mitchell, D. 2000. Comparison of neural network models with ARIMA and regression models for prediction of Houston's daily maximum ozone concentrations. European Journal of Operational Research, 122: 31-40.

Ruiz-Suarez, J.C., Mayora-Ibarra, O.A., Torres-Jimenez, J., and Ruiz-Suarez, L.G. 1995. Short-term ozone forecasting by artificial neural networks. Advances in Engineering Software, 23: 143-149.

Rumelhart, D.E., McClelland, J.L., and the PDP Research Group. 1986. Parallel Distributed Processing: Explorations in the Microstructure of Cognition, vol. 2. M.I.T. Press, Cambridge, MA.

Sandhu, H. S. 1999. Ground-Level Ozone in Alberta. Alberta Environmental Protection, Edmonton, AB.

Schlink, U., Dorling, S., Pelikan, E., Nunnari, G., Cawley, G., Junninen, H., Greig, A., Foxall, R., Eben, K., Chatterton, T., Vondracek, J., Richter, M., Dostal, M., Bertucco, L., Kolehmainen, M., and Doyle, M. 2003. A rigorous inter-comparison of ground-level ozone predictions. Atmospheric Environment, 37: 3237-3253.

Seinfeld, J.H. 1986. Atmospheric Chemistry and Physics of Air Pollution. Wiley, New York, NY.

Sohn, S.H., Oh, S.C., Jo, B.W., and Yeo, Y. 2000. Prediction of ozone formation based on neural network. Journal of Environmental Engineering, 126(8): 688-696.

Soja, G. and Soja, A. 1999. Ozone indices based on simple meteorological parameters: potentials and limitations of regression and neural network models. Atmospheric Environment, 33: 4299-4307.

Spellman, G. 1999. An application of artificial neural networks to the prediction of surface ozone concentrations in the United Kingdom. Applied Geography, 19: 123-136.

Turner, D.B. 1994. Workbook of Atmospheric Dispersion Estimates: An Introduction to Dispersion Modeling. Lewis Publishers, Boca Raton, FL.

Wang, W., Lu, W., Wang, X., and Leung, A.Y.T. 2003. Prediction of maximum daily ozone level using combined neural network and statistical characteristics. Environment International, 29: 555-562.

Weil, J.C. 1988. Dispersion in the convective boundary layer. Lectures on Air Pollution Modeling, A. Venkatram, J.C. Wyngaard, and American Meteorological Society, eds. American Meteorological Society, Boston, MA.

Yi, J. and Prybutok, V.R. 1996. A neural network model forecasting for prediction of daily maximum ozone concentration in an industrialized urban area. Environmental Pollution, 92(3): 349-357.

Zannetti, P. 1990. Air Pollution Modeling: Theories, Computations Methods, and Available Software. Computational Mechanics Publications and Van Nostrand Reinhold, Southampton, Boston, MA, and New York, NY.

4.0 HISTORICAL OZONE DATA PATTERNS AND TRENDS IN EDMONTON AND CALGARY[1]

4.1 Introduction

Ozone is an invisible, gaseous compound present in the stratospheric and lower tropospheric layers of the atmosphere. In recent years, ozone has come to the forefront of public awareness as a pollutant that may cause or aggravate existing respiratory illnesses. Although its presence in the atmosphere has been acknowledged since the 1800s, only recently have numerous epidemiological studies intimated the role it plays in respiratory illnesses (Bates et al. 1990, Burnett et al. 1998, Lipfert and Hammerstrom 1992, McDonnell et al. 1999, Thurston et al. 1997). Ozone is also implicated in vegetation injury and materials damage (Bates 1991, USEPA 1996).

In Canada, ozone air quality objectives were first established in 1971. Today, regulators continue to set guidelines for ground-level ozone to protect human health and welfare. The current Canada-Wide Standard reflects increasing public concern, with a target of 0.065 ppm (127 $\mu g/m^3$), averaged over 8 hours, for 2010. In Alberta, the one hour average Ambient Air Quality Guideline (AAQG) for ozone is 0.082 ppm (160 $\mu g/m^3$). To ensure compliance with guideline levels, Alberta Environment has established an air monitoring network throughout the province.

The potential adverse public health effects associated with ground-level ozone give rise to the need for an effective method of predicting ground-level ozone concentrations. Such a model would enable regulatory bodies to forewarn the public of impending elevated ozone events. However, ozone is a secondary photochemical pollutant with complex and non-linear chemistry. This complexity has challenged the widespread application of the traditional

---

[1] A version of this chapter has been presented and will be submitted to the Journal of Environmental Engineering and Science. Su, D., Gamal El-Din, A., Idriss, A., Gamal El-Din, M., and Wiens, B. 2004. Investigation of historical data patterns for ozone and related compounds in Edmonton and Calgary and their application to modelling ground-level ozone. In Proceedings of the Cold Regions Engineering & Construction Conference May 16-19, 2004, Edmonton, AB.

mechanistic Gaussian-based dispersion models to ozone. In this report, we discuss the potential of employing "black-box" models, such as Artificial Neural Networks (ANNs) and time series models, for predicting ground-level ozone concentrations. The historical trends of ozone and its precursors obtained from Alberta's Edmonton East and Calgary East stations will be evaluated. Also discussed is how to structure ANN and time series models to include these historical trends.

4.2 Background

Edmonton, the capital of Alberta, Canada, is a city of just under a million people, with 9,532 square kilometres of land area around the North Saskatchewan River valley. Major industrial areas are located in the northwest, northeast, and southeast quadrants of the city. Typical industries in the region include petroleum refineries, power plants, and chemical manufacturing facilities. Alberta Environment monitoring stations are located in the east, northwest, and central districts of the city. Pollutants relevant to ozone formation monitored at the Edmonton East station include nitric oxide (NO), nitrogen dioxide (NO_2), sulphur dioxide (SO_2), total hydrocarbons (THC), and ozone (O_3). The Edmonton East station data were selected for analysis of historical trends because in the period of this study, winds at this station blow predominantly from the southwest. Using data from this downwind station ensures representative urban data. In addition, ozone levels are typically highest downwind of urban areas, and it is the high concentrations that are of most from a public health and regulatory compliance standpoint.

The city of Calgary is located on 5,083 square kilometres along the Bow River approximately 300 km directly south of Edmonton. Its population is just under a million. Major industries in the region include agriculture, oil and gas, and manufacturing facilities. Alberta Environment has three monitoring stations in the east, northwest and central areas of the city. With the same considerations listed above for the Edmonton East station, data for the Calgary East station are analyzed in this paper. Pollutants monitored at the Calgary East station include NO, NO_2, SO_2, THC, and O_3.

4.3 Ozone Chemistry

Ground-level ozone is a secondary pollutant formed through reactions involving volatile organic compounds (VOCs) and oxides of nitrogen (NO_x). VOCs involved in ozone formation are emitted from evaporative and combustion processes, and consist of two to twelve carbons atoms. The major categories of VOC sources are transportation and industrial processes. The major categories of human activity responsible for NO_x emissions are transportation, stationary source fuel combustion, industrial processes, solid waste disposal, and other miscellaneous sources (USEPA 1996). Ozone and its precursors also interact with other pollutants like SO_2 in the atmosphere. As well, meteorological factors like sunlight, windspeed, atmospheric stability, and temperature play a major role in ozone formation (CEPA/FPAC WGAQOG 1999). The meteorological and climate conditions in Alberta, with warm, short summer seasons, and extended cold winters, make this region distinct from its neighbours in the south and east, resulting in unique behaviours in air pollutant trends (Sandhu 1999). This analysis is confined to the historical trends of pollutants affecting ozone concentrations, since these are the likely targets for regulatory control.

4.4 Methods

4.4.1 Monitoring Data

Pollutant data from the Edmonton and Calgary East stations are collected on a continuous basis and reported as an hourly average concentration in the publicly available Clean Air Strategic Alliance (CASA) Data Warehouse (http://www.casadata.org). NO and NO_2 concentrations are determined with chemiluminescence. O_3 is measured with an ultraviolet light process, while SO_2 concentration is determined using pulsed fluorescence. THC is measured with a hydrogen flame ionization detector. These methods are described in detail on the CASA website (http://www.casadata.org/airquality/cont_mon.asp). All hourly average concentrations are preprocessed to remove erroneous data and are reported in ppm. This paper considers data collected from 1999 to 2002, for the months from May to September inclusive. Ozone seasonal trends are well established (Sandhu 1999), so only the photochemically significant summer season is relevant for the purposes of predicting high

ozone episodes. The pollutants evaluated in this paper were selected based on a literature review carried out to determine important contributors to ozone formation, and taking into consideration the availability of historical monitoring data.

4.4.2 Statistical Analysis

The mean, minimum, maximum, 95th percentile values, and standard deviation of the measurements for each pollutant were calculated from the monitoring station hourly averaged data and tabulated in Table 4-1. The data were manipulated with a VisualBasic macro to determine average and maximum hourly, weekly, and monthly trends for the data period. All values were calculated using data from the entire 1999-2002 history. For example, the average ozone concentration at 14:00 was calculated as the average of all 14:00 readings in the data period, regardless of day of the week or season. Blank entries were excluded from all computations. The number of hours in which average hourly concentrations exceeded the 0.082 ppm AAQG for O_3 was also counted.

Table 4-1 Statistical parameters for pollutants monitored at the Edmonton East and Calgary East stations, summer months of 1999-2002 (in ppm).

Pollutant	Mean	Standard Deviation	Minimum	Maximum	95th Percentile
Edmonton East					
NO	0.008	0.014	0	0.166	0.032
NO_2	0.013	0.009	0	0.068	0.031
SO_2	0.002	0.003	0	0.061	0.007
THC	2.4	0.9	1.5	25	3.4
O_3	0.026	0.016	0	0.101	0.053
Calgary East					
NO	0.021	0.03	0	0.502	0.078
NO_2	0.019	0.017	0.001	0.086	0.037
SO_2	0.002	0.002	0	0.028	0.006
THC	2.1	0.2	1.7	5.6	2.5
O_3	0.021	0.015	0	0.069	0.046

4.5 Results and Discussion

4.5.1 Edmonton East Data Trends

Ozone. A sample of typical Edmonton East data for ozone is depicted in Figure 4-1. In general, ground-level ozone concentrations in Edmonton are well below the AAQG value in the study period, with an average hourly concentration of 0.026 ppm and a 95th percentile value of 0.056 ppm. Ozone values have a definite relationship with the hour of the day, reflecting the importance of photochemical reactions for ozone formation. Figure 4-2a shows the historically observed, diurnal ozone trends. The ozone peak occurs between 15:00 and 16:00. The daily ozone minimum tends to occur at 6:00.

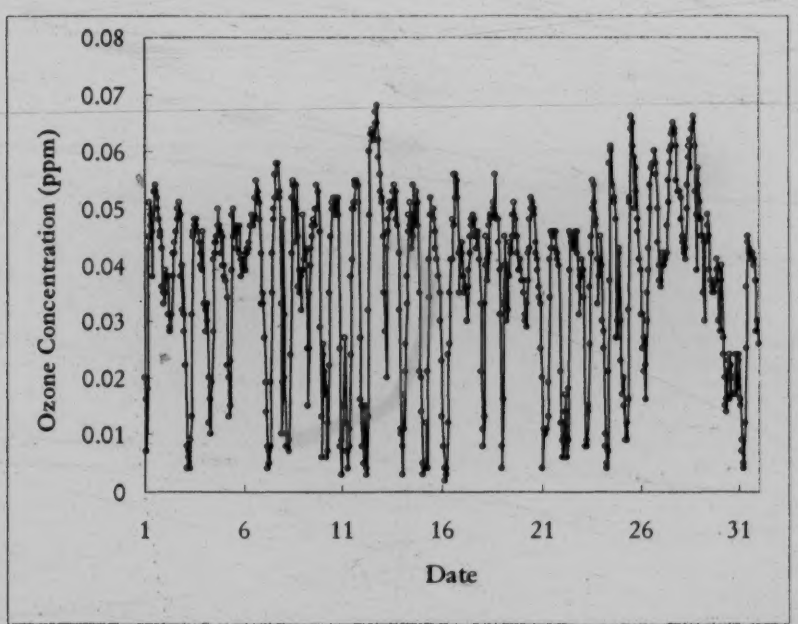

Figure 4-1 Edmonton East typical hourly average ozone concentrations. Data from May 2001.

For all the years analyzed, slightly lower ozone values occur during the beginning of the week, on either Monday or Tuesday. As the week progresses, average hourly ozone values rise slightly, culminating in their highest values on Saturdays and Sundays. This behaviour is

depicted in Figure 4-3a. Maximum hourly ozone values show a less discernible pattern, with only 2001 and 2002 data showing marginally higher values on the weekend.

The monthly trend of average hourly ozone concentration shows a definite maximum in May, with a steady decrease as the summer season progresses (Figure 4-4a). This pattern may suggest the effects of stratospheric ozone intrusion, since the tropopause is at its lowest during spring in western Canada (CEPA/FPAC WGAQOG 1999). In addition, solar radiation levels are highest in the spring, at the vernal equinox. Since ozone is a photochemical pollutant, it is expected that formation would be greatest when radiation levels are highest. No monthly patterns in maximum hourly ozone concentrations were identified. However, four exceedances of the AAQG occurred in July and one exceedance occurred in August.

Nitric oxide. NO concentrations averaged 0.008 ppm. NO concentrations peak daily between 7:00 and 8:00, levelling off and remaining steady for the rest of the day (Figure 4-2b). Levels are high during the week and tend to dip on weekends (Figure 4-3b), following standard urban traffic patterns. This observation is consistent from month to month, although peaks vary in their day of occurrence. Maximum hourly concentrations are also higher on weekdays than on weekends. Monthly, NO average hourly values are highest at the end of the summer (Figure 4-4b. These correspond well to lower ozone concentrations at this time of the year.

Nitrogen dioxide. NO_2 average hourly concentrations range from 0 to 0.068 ppm, with an average value of 0.013 ppm. NO_2 concentration peaks twice daily, at 7:00 and 22:00 (Figure 4-2c). Minimum values occur at 14:00. Day of the week NO_2 trends are similar to NO trends, exhibiting consistently lower averages and maxima on weekends (Figure 4-3c). The highest average hourly concentrations occur in May and September (Figure 4-4c).

Sulphur dioxide. Average hourly SO_2 daily trends show a single peak at 11:00 (Figure 4-2d), with steady values for the rest of the day. No real variations in the average hourly and maximum hourly concentrations occur during the week (Figure 4-3d). Monthly, no significant trends are apparent, with only slightly higher values in May and September

(Figure 4-4d). However, there is also a greater variability in the concentration values for these months from year to year.

Total hydrocarbons. Hourly THC concentrations average 2.4 ppm. Concentrations are generally steady all day, showing a slight dip in the afternoon between 13:00 and 15:00 (Figure 4-2e). There are no obvious THC trends with the day of the week or monthly plots (Figures 4-3e and 4-4e).

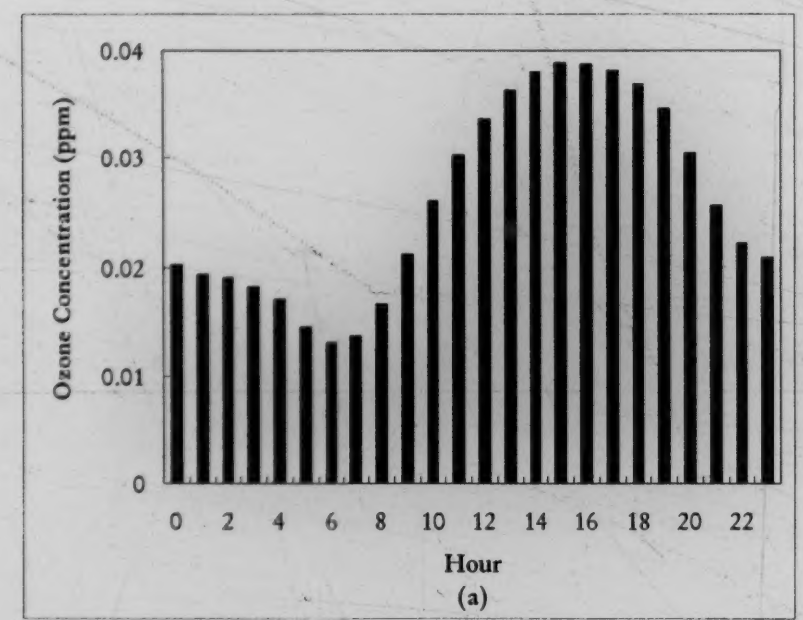

Figure 4-2. Edmonton East 1999-2002 diurnal hourly average concentration trends for: (a) ozone; (b) nitric oxide; (c) nitrogen dioxide; (d) sulphur dioxide; and (e) total hydrocarbons.

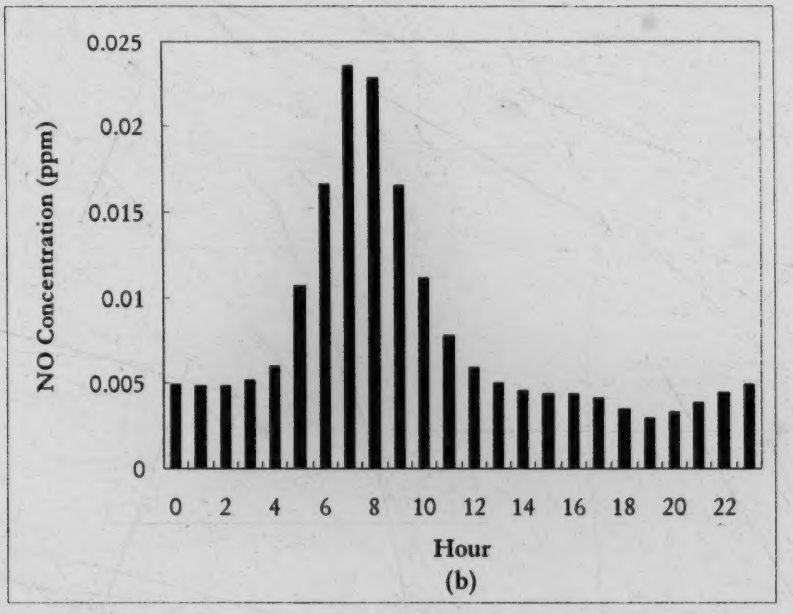

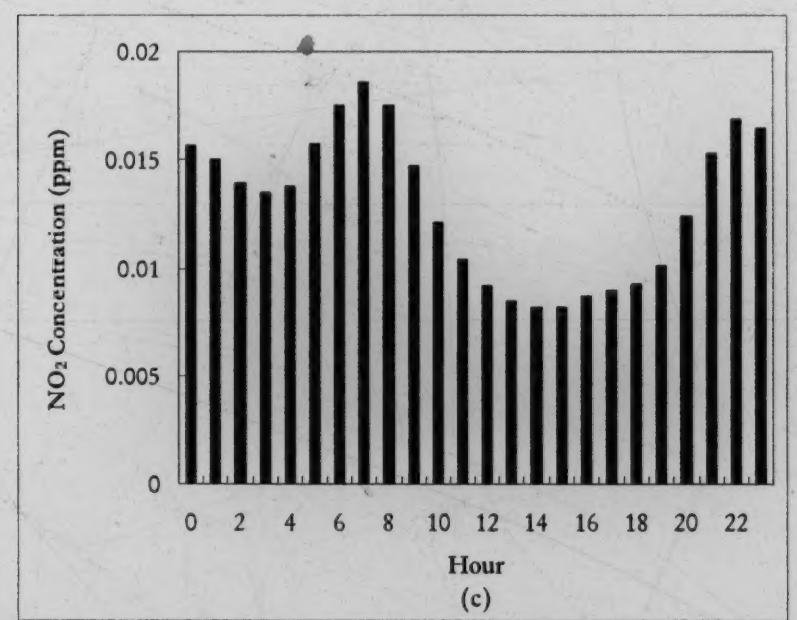

Figure 4-2 cont'd. Edmonton East 1999-2002 diurnal hourly average concentration trends for: (a) ozone; (b) nitric oxide; (c) nitrogen dioxide; (d) sulphur dioxide; and (e) total hydrocarbons.

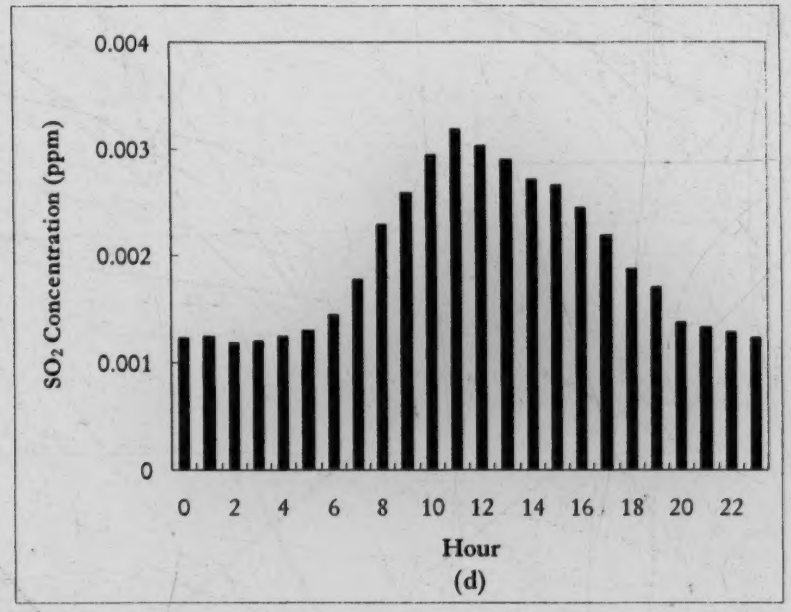

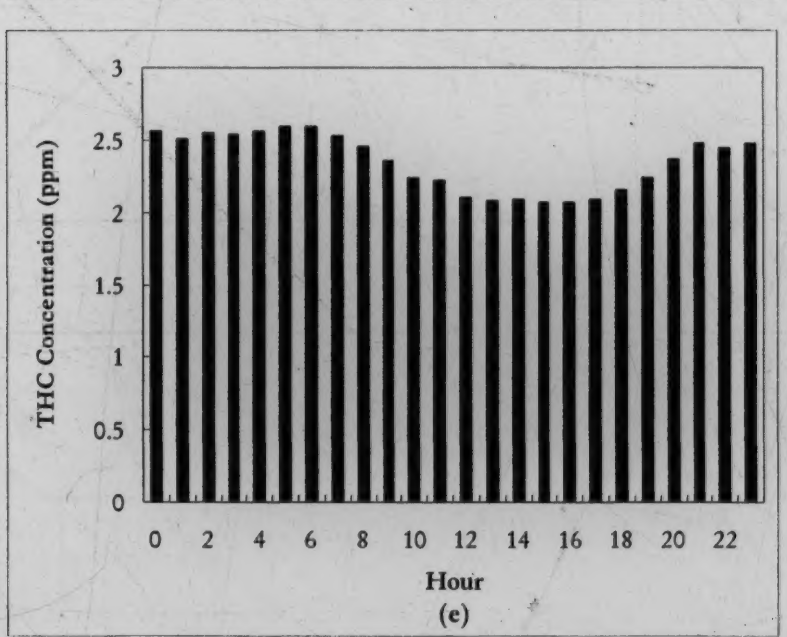

Figure 4-2 cont'd. Edmonton East 1999-2002 diurnal hourly average concentration trends for: (a) ozone; (b) nitric oxide; (c) nitrogen dioxide; (d) sulphur dioxide; and (e) total hydrocarbons.

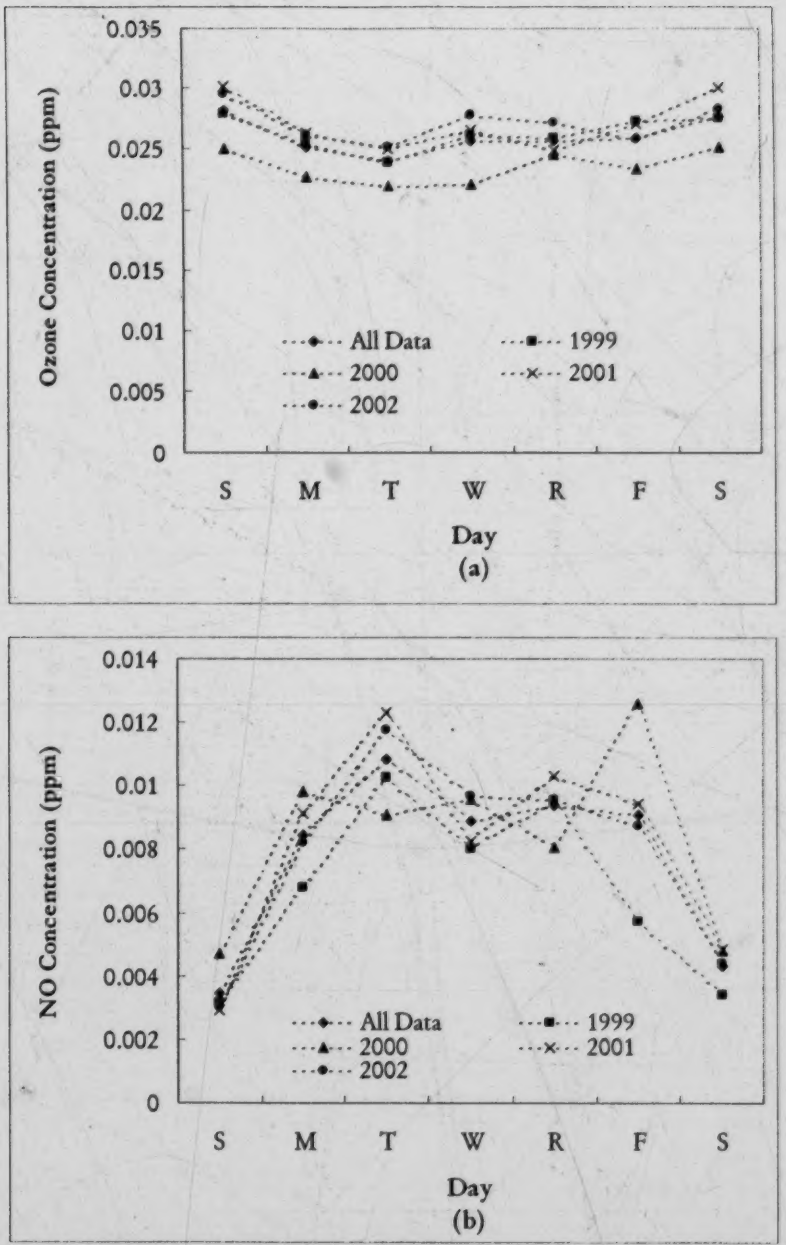

Figure 4-3. Edmonton 1999- 2002 day of the week trends in hourly average concentrations for: (a) ozone; (b) nitric oxide; (c) nitrogen dioxide; (d) sulphur dioxide; and (e) total hydrocarbons.

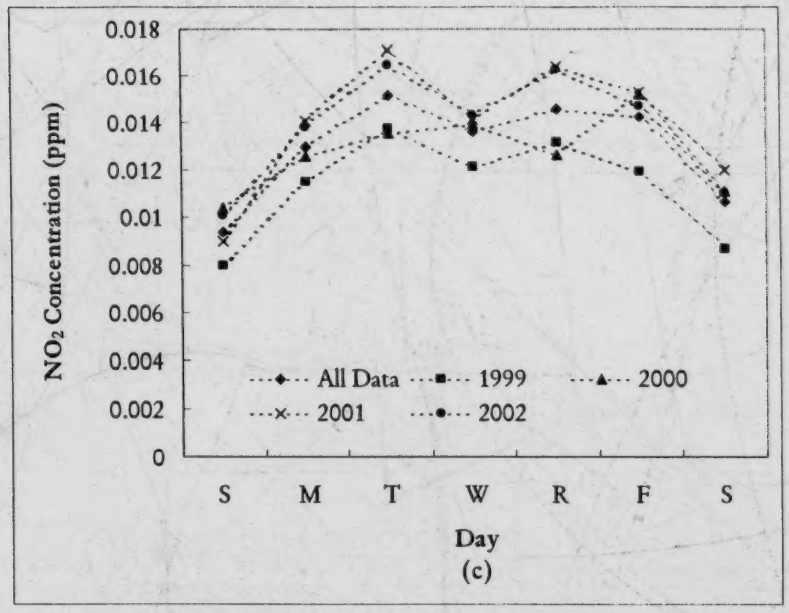

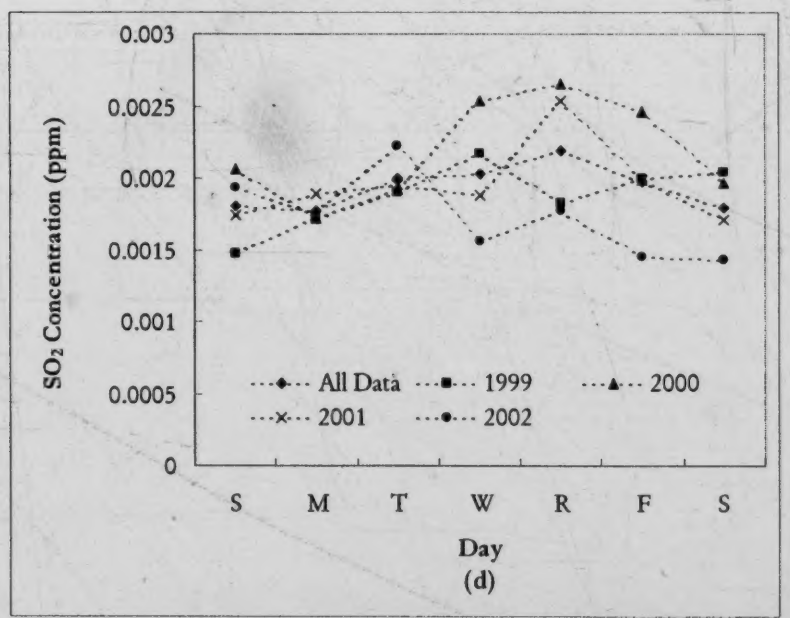

Figure 4-3 cont'd. **Edmonton 1999- 2002 day of the week trends in hourly average concentrations for: (a) ozone; (b) nitric oxide; (c) nitrogen dioxide; (d) sulphur dioxide; and (e) total hydrocarbons.**

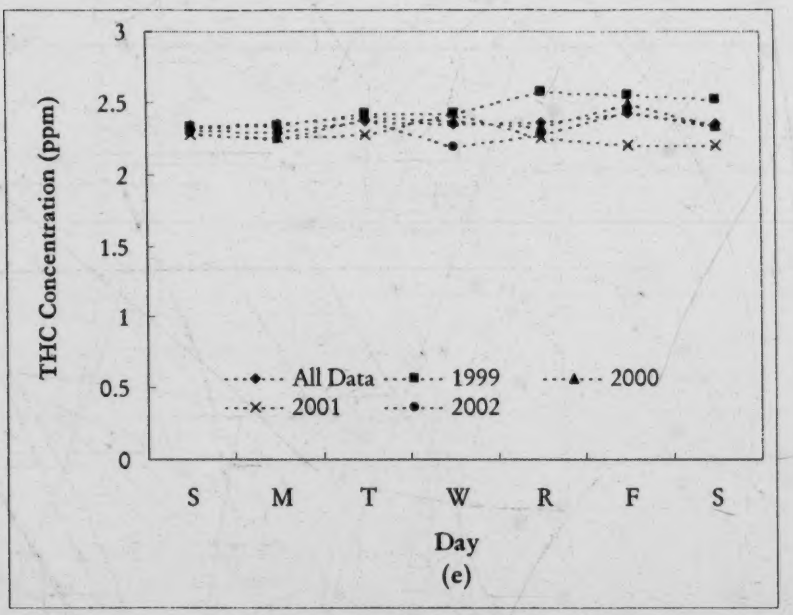

Figure 4-3 cont'd. Edmonton 1999- 2002 day of the week trends in hourly average concentrations for: (a) ozone; (b) nitric oxide; (c) nitrogen dioxide; (d) sulphur dioxide; and (e) total hydrocarbons.

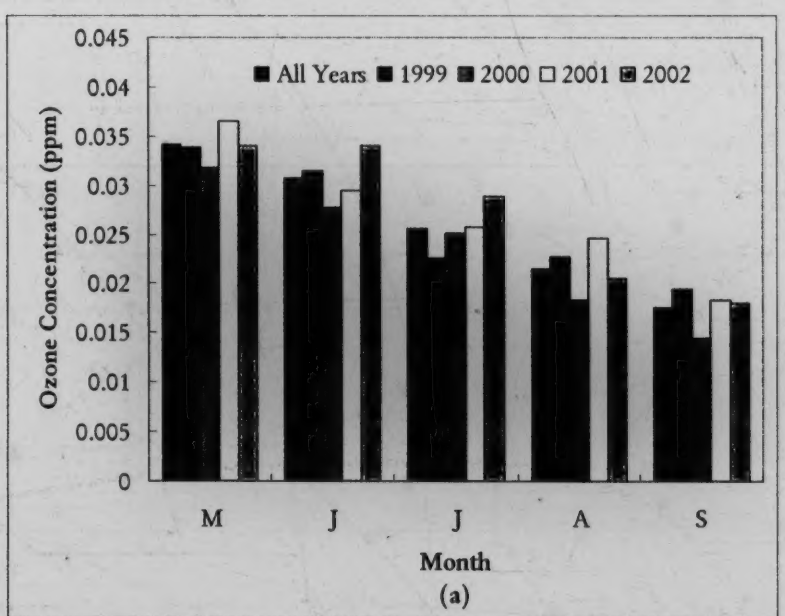

Figure 4-4. Edmonton 1999-2000 monthly patterns of average hourly concentrations for: (a) ozone; (b) nitric oxide; (c) nitrogen dioxide; (d) sulphur dioxide; and (e) total hydrocarbons.

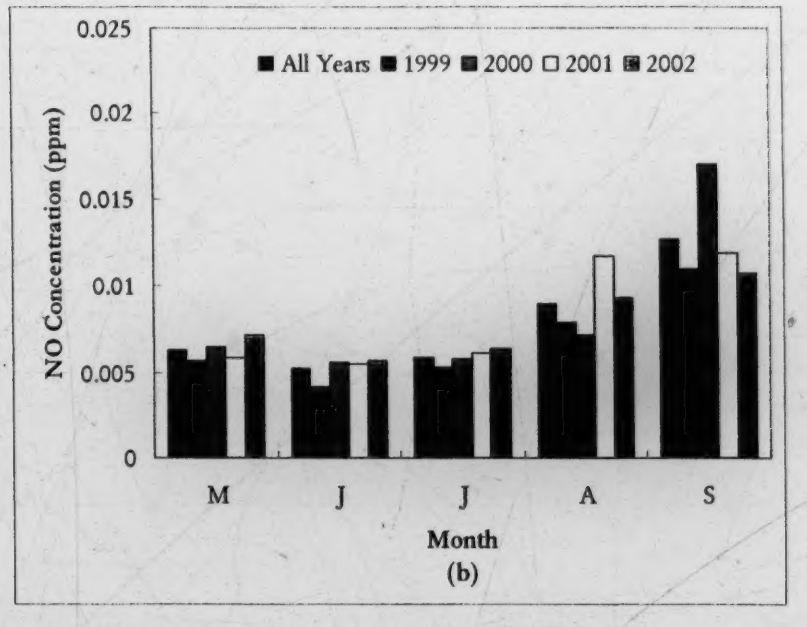

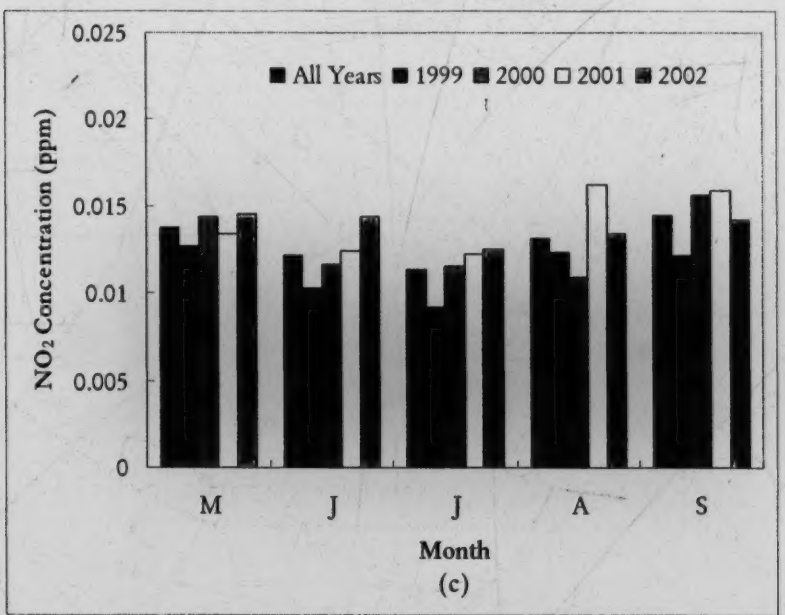

Figure 4-4 cont'd. **Edmonton 1999-2000 monthly patterns of average hourly concentrations for: (a) ozone; (b) nitric oxide; (c) nitrogen dioxide; (d) sulphur dioxide; and (e) total hydrocarbons.**

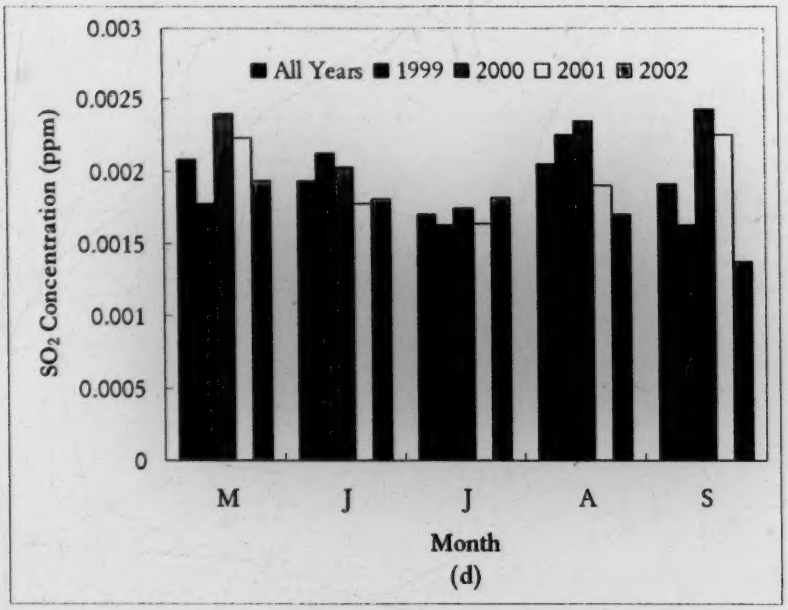

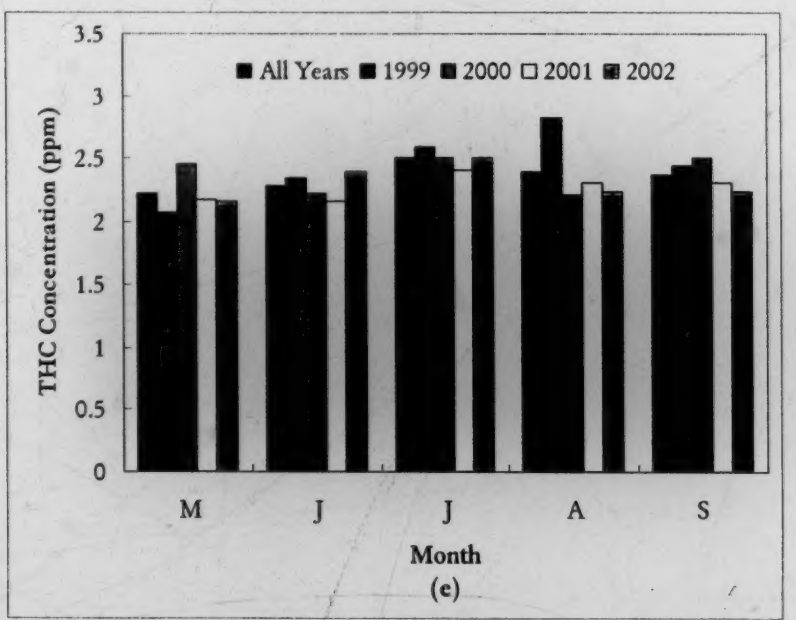

Figure 4-4 cont'd. **Edmonton 1999-2000 monthly patterns of average hourly concentrations for: (a) ozone; (b) nitric oxide; (c) nitrogen dioxide; (d) sulphur dioxide; and (e) total hydrocarbons.**

4.5.2 *Calgary East Data*

Ozone. Typical average hourly ozone measurements for the Calgary East station are depicted in Figure 4-5. The mean hourly average ozone concentration was slightly lower than in Edmonton at a value of 0.021 ppm. The diurnal ozone trend was the same, with a peak at 15:00 and a minimum at 6:00 (Figure 4-6a). Day of the week (Figure 4-7a) and monthly (Figure 4-8a) trends were also similar, with higher average hourly concentrations on weekends. Peak hourly average ozone concentrations declined steadily from May to September.

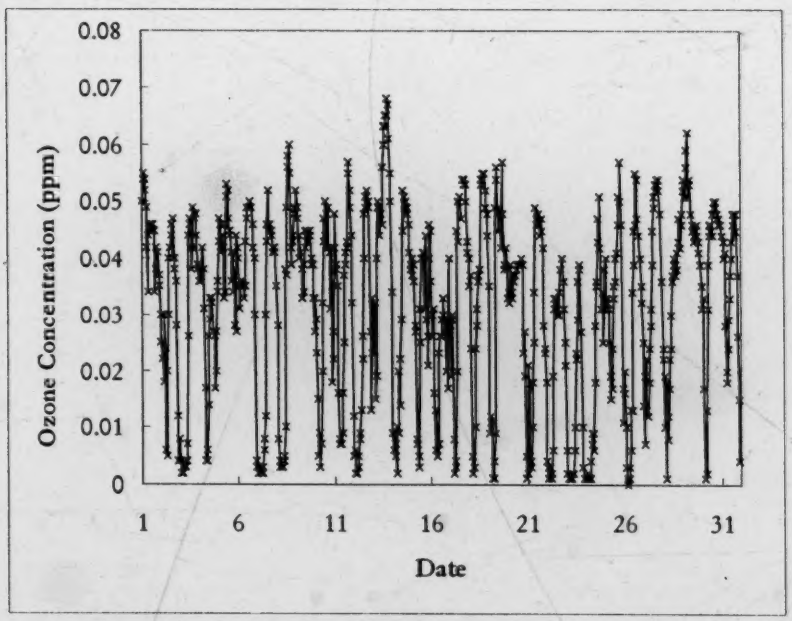

Figure 4-5 Calgary East typical hourly average ozone concentrations. Data for May 2001.

Nitric oxide. Mean NO in Calgary was higher than in Edmonton at 0.021 ppm. Concentrations peaked at 7:00, with another minor peak at about 23:00 (Figure 4-6b). As was the case in Edmonton, NO concentrations were slightly lower on weekends (Figure 4-7b). Both average and maximum hourly average concentrations were highest in September (Figure 4-8b).

Nitrogen dioxide. NO_2 hourly average concentrations were generally slightly higher than in Edmonton, with a mean of 0.019 ppm. As with Edmonton, two peaks are observable daily, at 7:00 and at 22:00, with a minimum average hourly concentration occurring between 13:00 and 14:00 (Figure 4-6c). NO_2 average hourly concentrations are lowest on weekends (Figure 4-7c), although the daily maximum appears to frequently occur on Thursday. Monthly, no trends were obvious in the average hourly concentrations (Figure 4-8c). The highest maximum hourly concentration occurred in September.

Sulphur dioxide. SO_2 concentrations are similar in Calgary and Edmonton. The mean average hourly SO_2 concentration in Calgary was 0.002 ppm. Average hourly concentrations peaked daily at 8:00 and again at 22:00 (Figure 4-6d). During the week, the average hourly concentrations experienced a dip on weekends (Figure 4-7d). No significant monthly trends were apparent (Figure 4-8d). For all the data, average hourly concentration values were slightly higher in September, but there was a greater spread in September concentrations through the years than with other months.

Total hydrocarbons. Average hourly THC in Calgary had a mean of 2.1 ppm, slightly lower than the mean for Edmonton. Average hourly THC values were steady, with a slight dip occurring at 15:00 (Figure 4-6e). No relationships with the day of the week or month of the year were apparent (Figures 4-7e and 4-8e).

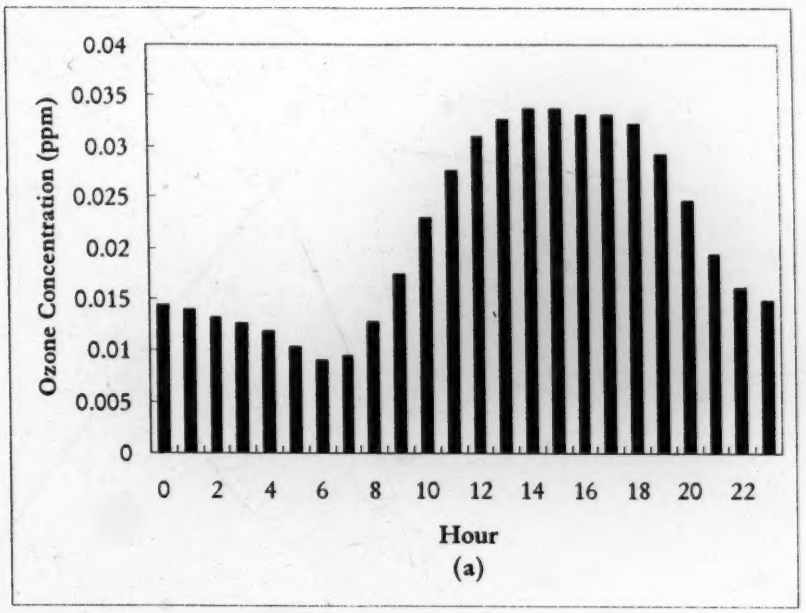

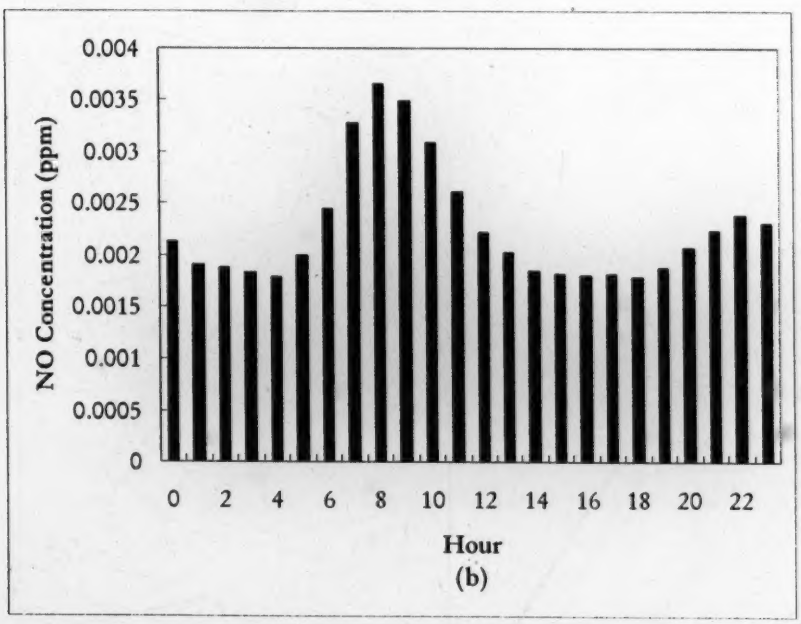

Figure 4-6 Calgary East diurnal hourly average concentration trends for: (a) ozone; (b) nitric oxide; (c) nitrogen dioxide; (d) sulphur dioxide; and (e) total hydrocarbons.

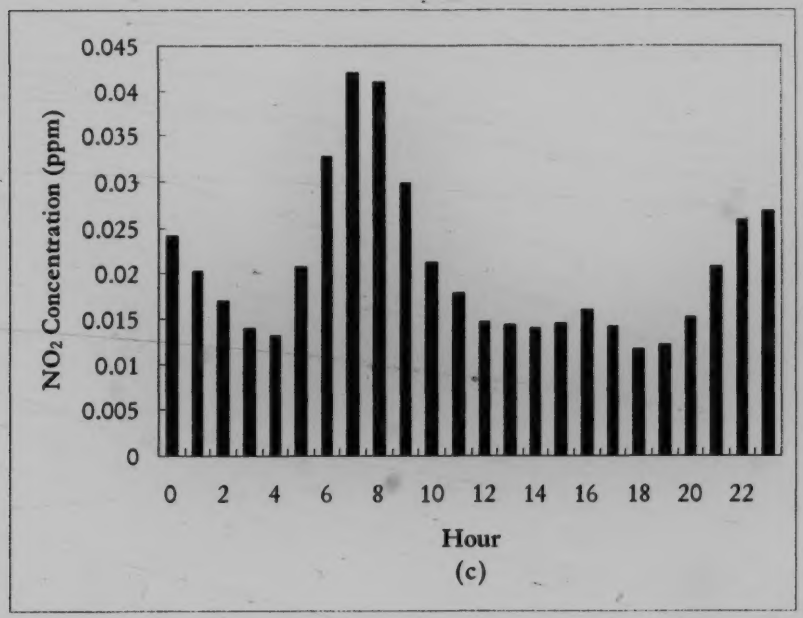

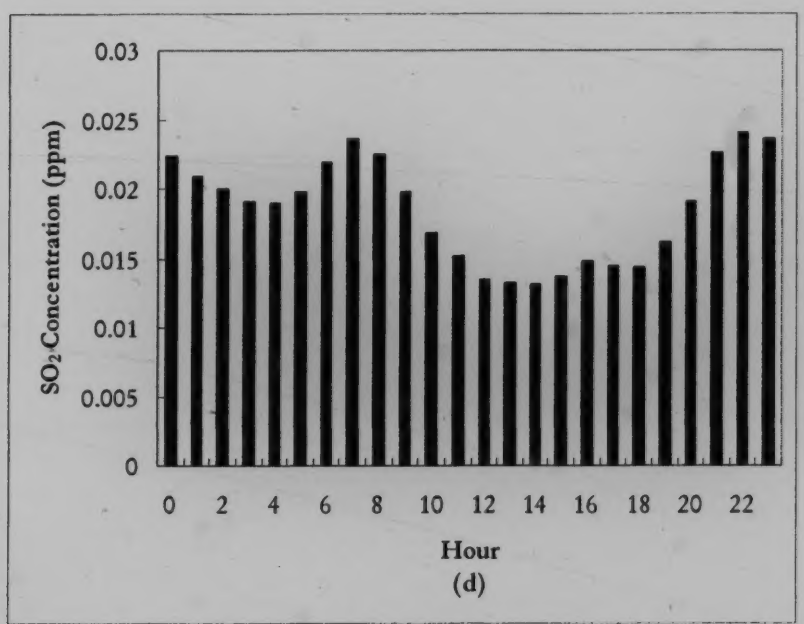

Figure 4-6 cont'd. Calgary East diurnal hourly average concentration trends for: (a) ozone; (b) nitric oxide; (c) nitrogen dioxide; (d) sulphur dioxide; and (e) total hydrocarbons.

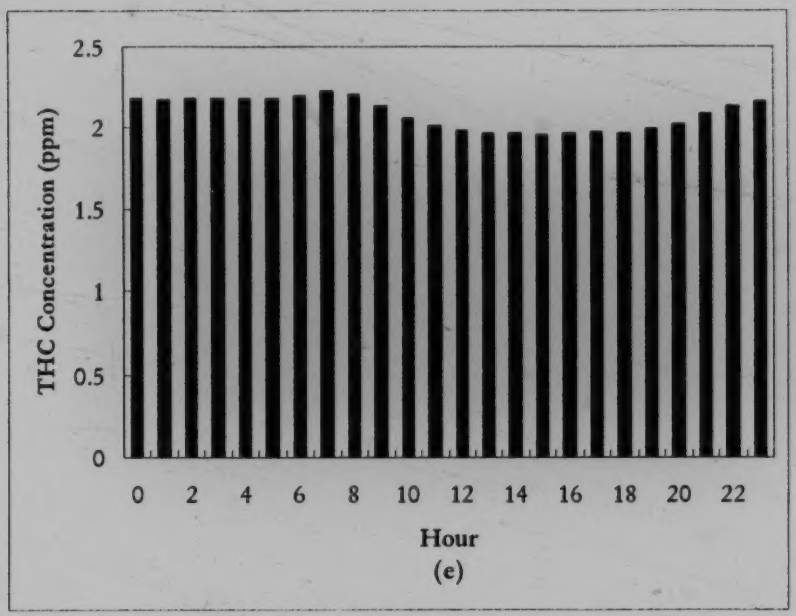

Figure 4-6 cont'd. Calgary East diurnal hourly average concentration trends for: (a) ozone; (b) nitric oxide; (c) nitrogen dioxide; (d) sulphur dioxide; and (e) total hydrocarbons.

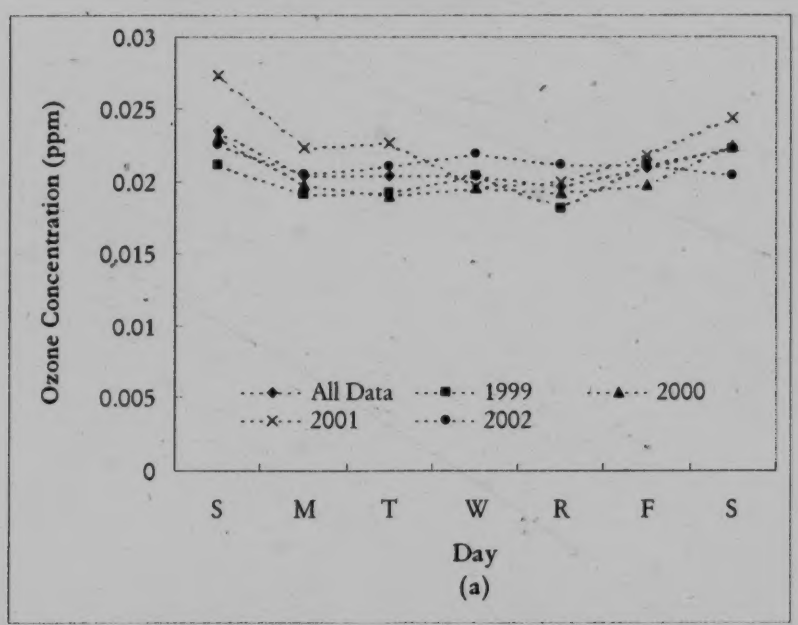

Figure 4-7 Calgary East day of the week variation in hourly average concentrations for: (a) ozone; (b) nitric oxide; (c) nitrogen dioxide; (d) sulphur dioxide; and (e) total hydrocarbons.

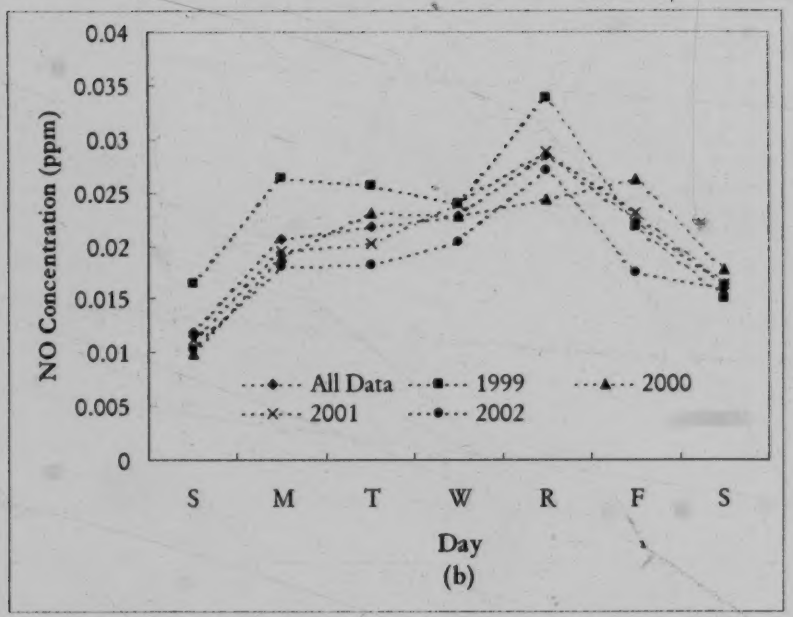

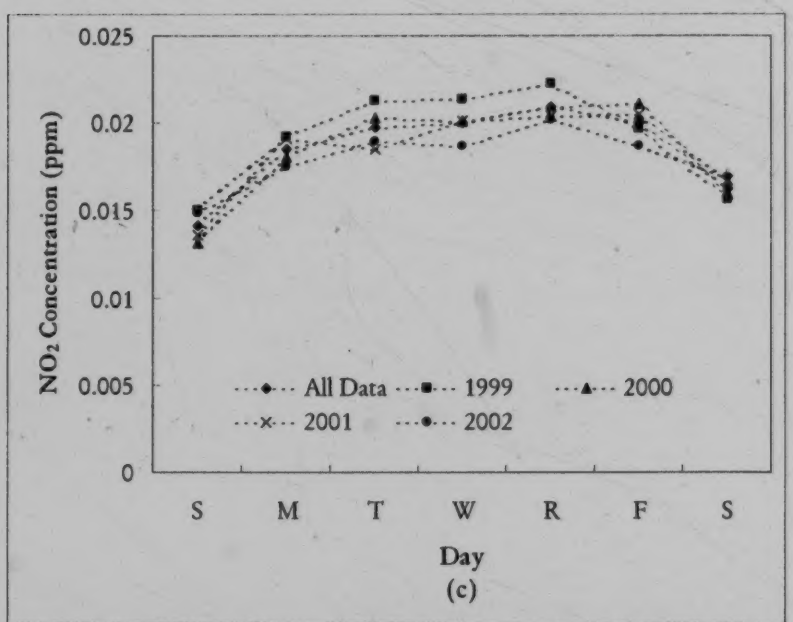

Figure 4-7 cont'd. **Calgary East day of the week variation in hourly average concentrations for: (a) ozone; (b) nitric oxide; (c) nitrogen dioxide; (d) sulphur dioxide; and (e) total hydrocarbons.**

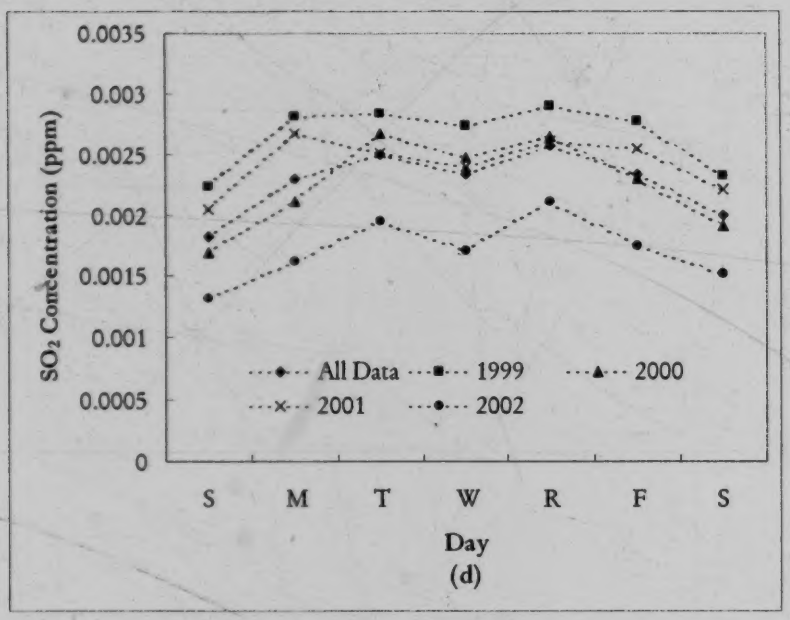

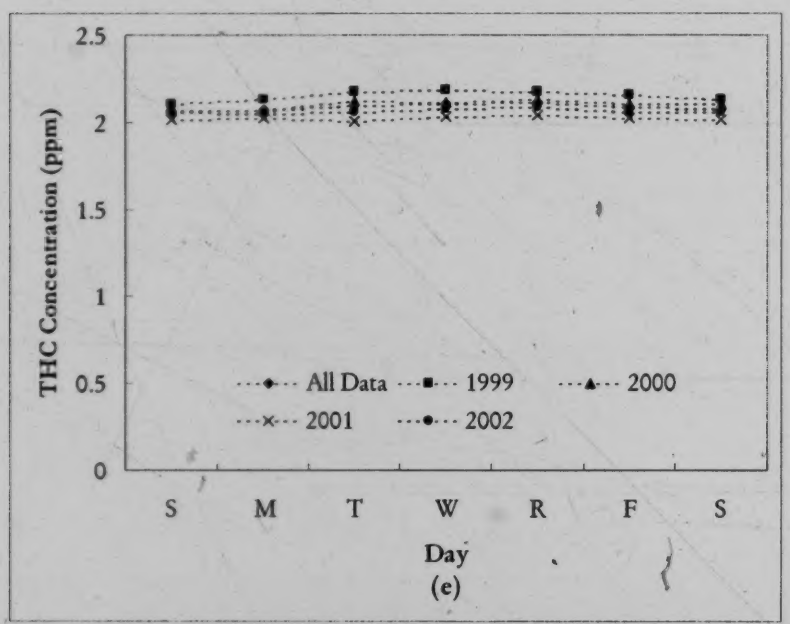

Figure 4-7 cont'd. **Calgary East day of the week variation in hourly average concentrations for: (a) ozone; (b) nitric oxide; (c) nitrogen dioxide; (d) sulphur dioxide; and (e) total hydrocarbons.**

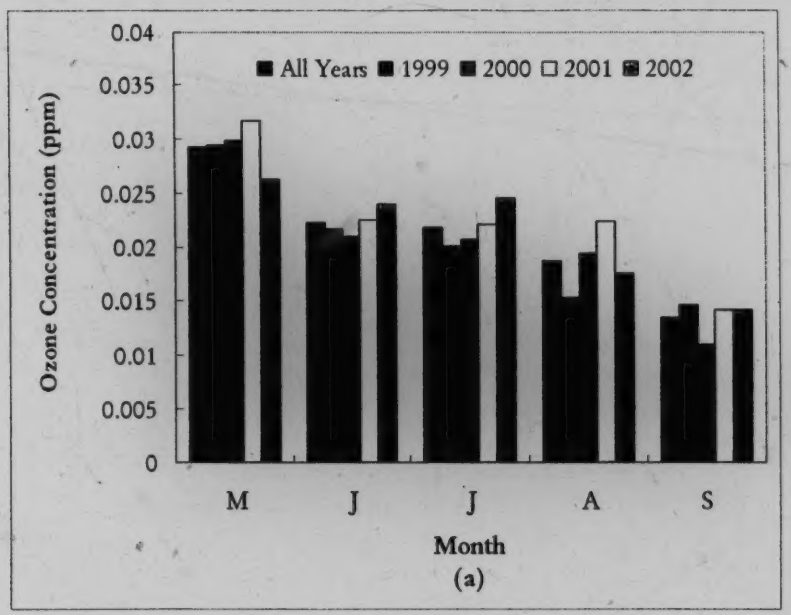

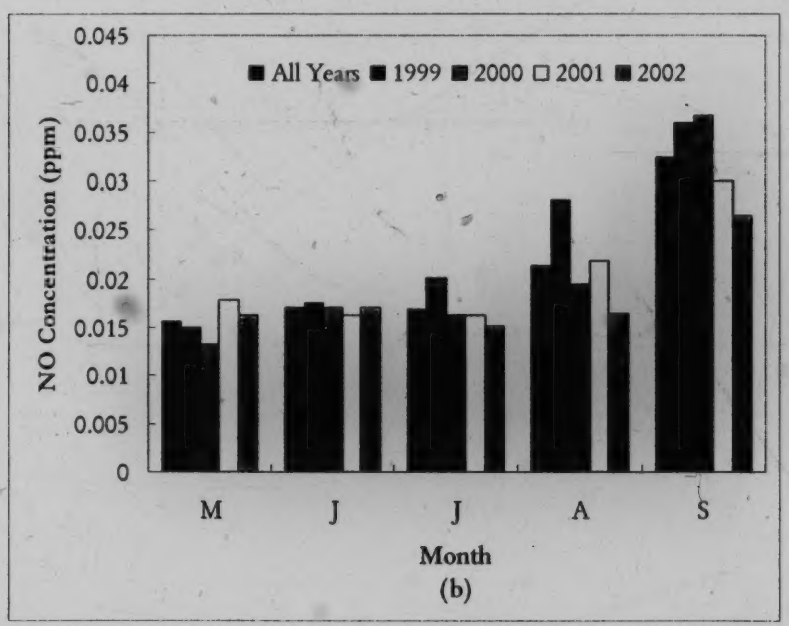

Figure 4-8 Calgary East monthly patterns of average hourly concentrations for: (a) ozone; (b) nitric oxide; (c) nitrogen dioxide; (d) sulphur dioxide; and (e) total hydrocarbons.

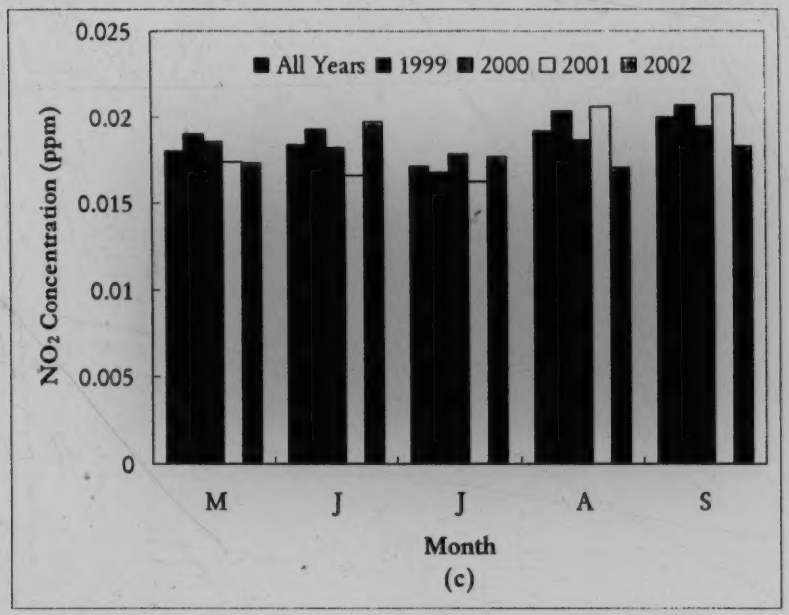

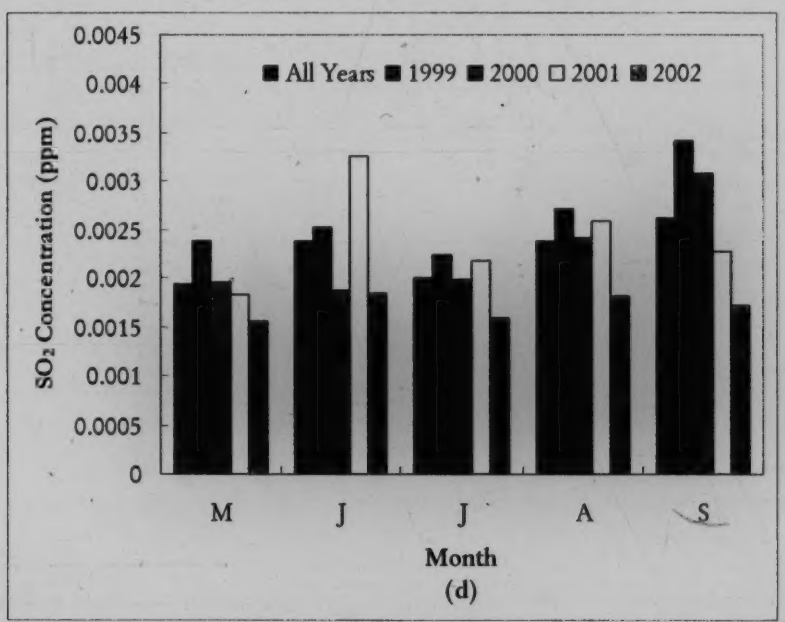

Figure 4-8 cont'd. **Calgary East monthly patterns of average hourly concentrations for: (a) ozone; (b) nitric oxide; (c) nitrogen dioxide; (d) sulphur dioxide; and (e) total hydrocarbons.**

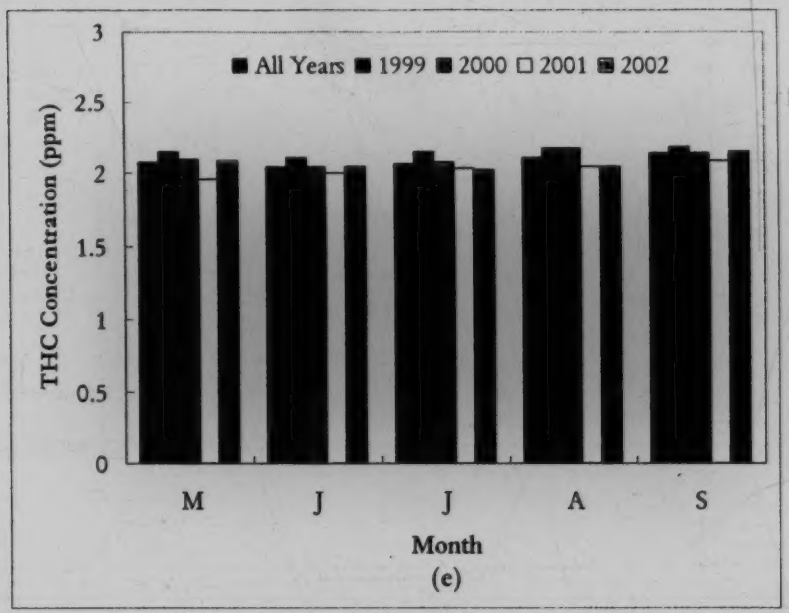

Figure 4-8 cont'd. **Calgary East monthly patterns of average hourly concentrations for: (a) ozone; (b) nitric oxide; (c) nitrogen dioxide; (d) sulphur dioxide; and (e) total hydrocarbons.**

4.5.3 Artificial Neural Networks Brief Description

Artificial neural networks (ANNs) are a form of artificial intelligence that attempts to exploit the pattern recognition capabilities of the human brain (Jain et al. 1996). The building blocks of ANNs are individual nodes called neurons that process inputs to the network. The most common type of network is the multilayer perceptron (MLP). In the MLP, an input layer of neurons receives input signals from the environment, with each neuron in the input layer representing an input variable. These signals are transformed and processed by one or more hidden layers of neurons that attempt to "fit" the inputs to the target output variable (Hadjiiski and Hopke 2000). The network is trained by feeding historical data with the corresponding output values into the network. The strength of the connections between neurons is adjusted during training as required to improve the fit of network predictions with the target output values (El-Din and Smith 2002a). In this manner, the network is able to "learn" the underlying trends in the data. The ANN approach is often termed a "black box" approach, because no equations describing the modelled process are required to

formulate the model, nor does the model produce any functions describing the relationships learned.

Since the ANN's ability to model is developed from historical data, it is critical that a comprehensive and representative database be available for "teaching" the network (Kao and Huang 2000). The extensive database of pollutant concentration and meteorological data available in Alberta are conducive to the application of ANNs.

4.5.4 Time Series Models Brief Description

Time series models are another example of the "black-box" modelling approach. Although time series models have been around for years, it was not until the 1960's when Box and Jenkins recognized the importance of the Auto-Regressive Moving Average (ARMA) models in the area of economic forecasting, that the well-known Box-Jenkins methodology for analysis of time series data was developed. The Box-Jenkins methodology for time series analysis is a stochastic modelling technique that is capable of describing complex environmental systems (Box and Jenkins 1976).

Two general approaches may be used when building a time series model: the "univariate" approach and the transfer function (also called the "multivariate") model approach. The univariate model approach is based on the idea that a time series in which successive values are highly dependent can be usefully regarded as generated from a series of uncorrelated independent "shocks" a_t, which are random drawings from a fixed distribution, usually assumed normal, and having a mean of zero and variance σ_a^2. Such a sequence of random variables $a_t, a_{t-1}, a_{t-2}, \ldots$ is called a "white noise process". A "linear filter" is a model that transforms the white noise process a_t to the process that generated the time series, z_t, and can be represented mathematically by the equation $z_t = \psi(B)a_t$. This transformation is accomplished through the operator:

$$\psi(B) = 1 + \psi_1 B + \psi_2 B^2 + \ldots = \sum_{j=0}^{\infty} \psi_j B^j \text{ with } \psi_0 = 1 \quad \textbf{...Equation 4-1}$$

where B is the backshift operator such that $B^j a_t = a_{t-j}$. In order to have a simpler representation of the stochastic process represented by Equation 4-1, it is usually advantageous to write

$$\psi(B) = \frac{\theta(B)}{\phi(B)} \quad \text{.....Equation 4-2}$$

where $\theta(B)$ is the moving average operator of the stochastic model, and is defined as $\theta(B) = 1 - \theta_1 B - \theta_2 B^2 - \ldots - \theta_q B^q$; $\phi(B)$ is the auto-regressive operator of the stochastic model, and is defined as $\phi(B) = 1 - \phi_1 B - \phi_2 B^2 - \ldots - \phi_p B^p$; and p and q are the orders of the stochastic model. The linear filter can represent any univariate time series model.

In contrast to ARMA models, which describe the behaviour of single time series in terms of a white noise, transfer function models can represent more complex systems in which the output is the stochastic response to one or more measured input series. The general form of a transfer-function noise model for the single input case is:

$$Y_t = \upsilon(B)X_{t-b} + N_t \quad \text{.....Equation 4-3}$$

where Y_t is the output series at time t; $\upsilon(B)$ is defined as $\upsilon(B) = (\upsilon_0 + \upsilon_1 B + \upsilon_2 B^2 + \cdots)$ and known as the impulse response function (it is the transfer function part of the model); X_{t-b} is the input series at time $t-b$, where b is a delay parameter; and N_t is a noise process at time t, defined by the linear filter $N_t = \psi(B)a_t$ and known as the stochastic model component (it is the noise part of the overall model). For the multiple input case, the model is:

$$Y_t = \upsilon_1(B)X_{1,t-b_1} + \upsilon_2(B)X_{2,t-b_2} + \cdots + N_t \quad \text{.....Equation 4-4}$$

Models represented by Equation 4-4 are usually called "combined transfer-function noise" models. The general approach for building models of this type consists of four main stages: identification, estimation (or fitting), forecasting, and diagnostic checking. The details of the

different stages involved in building time series models can be found elsewhere (Box and Jenkins 1976).

4.5.5 Implications of Pollutant Data Trends for the ANN and Time Series Models

The pollutant data show definite diurnal trends. However, the hour of the day is not expected to be a critical input if included as an independent variable in the ANN model. This is because the concentration fluctuations observed throughout the day are symptomatic of the effects of other parameters such as sunshine and human activities. These are time-related effects that more directly affect ozone chemistry and concentrations. These effects are inherently embedded in the combination of pollutant concentrations that result in high ozone events. Nevertheless, the hour of the day effects may be introduced into the ANN model by dedicating a few input neurons to represent an hour of the day index to the ANN model (El-Din and Smith 2002b).

The diurnal plots indicate a lag in ozone concentrations in response to high levels of precursors, so consideration of previous hours' values of precursors may help to improve predictions. This lagged effect also suggests that ozone concentrations can be successfully forecasted with previous hours' data, with peak precursor values providing clues to daily peak ozone concentrations. Since precursor peak concentrations appear to be strongly related to human activities like rush hour traffic, inclusion of a parameter representing human behaviour patterns as an input may be beneficial to the performance of the models. However, parameters such as traffic counts that are typically used in the literature (e.g. Hasham et al. 1998) are difficult to incorporate on an hourly basis and are not as readily available as real-time monitoring data. Incorporating traffic data into models requires delineation of the spatial boundaries of the traffic effects on the location modelled, to ensure identification of all potential sources. These sources and their effects would also be dependant on concurrent meteorological conditions, further complicating the process. In addition, the effects of traffic patterns are inherently represented in the historical data (i.e., the fluctuations observed in the historical ambient monitoring data are the result of traffic and other influences on the receptor).

Major fluctuations in pollutant concentrations tend to occur during daylight hours, so daytime data may be sufficient if the objective is to determine peak levels that could exceed guideline values. This would result in a more economical model with reduced training runtime requirements, but additional pre-processing time would be required to extract data for the hours of daylight in any given day. In Alberta, a northern zone, daylight hours can range anywhere from 7.5 hours in the winter to 17 hours in the summer (Sandhu 1999).

The day of the week effects are important to consider since many of the established precursors show different behaviours on weekends compared to weekdays. Ozone concentrations in urban environments are also prone to NO scavenging effects, and are related to NO concentrations in these areas. For the ANN modelling, the day of the week effect may be included either by presenting a day of the week index as input to the network or by simply developing two distinct ANN models, one operating for weekdays and the other for the weekend regime. However, weekend values of precursor compounds that are related to traffic patterns, like NO and NO_2, tend to be lower than weekdays, while ozone trends are reversed. This further suggests a relationship with traffic patterns, possible lagged effects, or persistence and accumulation of ozone levels, necessitating inclusion of either previous days' values of ozone or precursors as input.

Although this paper focuses on data from the summer months only, monthly trends within this season are readily apparent for ozone and some of its precursors. Neurons representing the month of the year would be useful for delineating summertime ozone trends, making these patterns more explicit for the ANN during training. As with day of the week considerations, a different network could be developed for each month of the season, although gains in prediction performance are offset by the increased effort and time required to develop additional networks.

The hour of the day and the day of the week effects could be introduced into the time series models by including higher order auto-regressive parameters into the structure of the ARMA model. However, the hour-to hour effects will probably be much stronger, and hence, may mask the hour of the day and day of the week effects. Since time series data have to be

continuous, a separate time series model would have to be developed for each summer season, and therefore, the monthly trends cannot be included in the time series model.

The similarity of pollutant concentration trends in Calgary and Edmonton, with differences in absolute magnitudes, suggests that human activities influencing pollutant concentrations in these cities are similar. Modelling can give clues as to which pollutants have the greatest influence on ozone levels in Edmonton and Calgary. However, different initial precursor concentrations and meteorological effects require the construction of specific models for each city. The advantage of the "black-box" approach proposed here is that no pre-existing knowledge of the relationships between ozone and its precursors are required. Black-box models can easily depict the complex relationships underlying the historical data that would otherwise require complex equations and terms in the traditional grid and trajectory models. No definitions of the regional terrain are required. In addition, the black-box modelling approach is economical because it makes use of the efforts already put into air quality monitoring. No further effort is required to obtain input data for the model.

Time series effects are important to consider, since there are lagged effects in the concentration of ozone relative to precursors. Development of the ANN requires investigation of the appropriate time window for incorporating this effect. Time series models will provide a benchmark to compare against when testing the performance of the ANN models that include time series components in their structures. Meteorological variables have also been shown to significantly contribute to ozone production and accumulation (CEPA/FPAC WGAQOG 1999), and can help to improve ANN predictions. For the practical application of the models, developers need to keep in mind that input data should be readily available. It should also be certain that regulatory bodies continue to monitor these inputs in the future.

4.6 Conclusion

Examination of historical air quality data shows that ozone and its precursors exhibit significant diurnal, weekly, and seasonal trends that must be considered and incorporated into air quality models. Diurnal patterns may be related to human activities such as traffic, or

may be influenced by meteorological considerations. Parameters representing these behaviours may be included in the model, but should be selected with care to ensure they are readily available for model application and economic to acquire. Similar pollutant trends in Calgary and Edmonton suggest that pollutant sources and activities affecting pollutant concentrations in these two cities are similar. Black-box models such as ANNs and time series models are promising tools for modelling ozone behaviour, as they are able to recognize temporal trends and non-linear patterns in the historical data. Lagged effects appear important, and their consideration in the ANN model may improve prediction performance.

4.7 References

Bates, D. 1991. The effects of ozone on plants and humans. Air & Waste Management Association Tropospheric Ozone and the Environment 3; Papers from an International Conference, Pittsburgh, PA, 15-22.

Bates, D.V., Baker-Anderson, M. and Sizto, R. 1990. Asthma attack periodicity: a study of hospital emergency visits in Vancouver. Environmental Research, 51: 51-70.

Box, G.E. and Jenkins, G.M. 1976. Time Series Analysis: Forecasting and Control. Holden-Day, Oakland, CA.

Burnett, R.T., Cakmak, S. and Brook, J.R. 1998. The effect of the urban ambient air pollution mix on daily mortality rates in 11 Canadian cities. Canadian Journal of Public Health, 89(3): 152-156.

CEPA/FPAC WGAQOG— Canadian Environmental Protection Act Federal/Provincial Working Group on Air Quality Objectives and Guidelines. 1999. National Ambient Air Quality Objectives for Ground-Level Ozone Science Assessment Document, Catalogue No. En42-17/702-1999E. Health Canada and Environment Canada, Downsview, ON and Ottawa, ON.

El-Din, A. and Smith, D.W. 2002a. Modeling a full-scale primary sedimentation tank using artificial neural networks. Environmental Technology, 23: 479-496.

El-Din, A. and Smith, D.W. 2002b. A neural network model to predict the wastewater inflow incorporating rainfall events. Water Research, 36(5): 1115-1126.

Hasham, F. A., Stanley, S. J., and Kindzierski, W. B. 1998. Modelling of urban air pollution in the Edmonton Strathcona Industrial Area using artificial neural networks. Transportation, Land Use, and Air Quality: Making the Connection Conference Proceedings, Portland, OR, pp. 246-255.

Hadjiiski, L. and Hopke, P. 2000. Application of artificial neural networks to modeling and prediction of ambient ozone concentrations. Journal of the Air & Waste Management Association, 50: 894-901.

Jain, A. K., Mao, J, and Mohiuddin, K.M. 1996. Artificial neural networks: a tutorial. Computer, 29: 31-44.

Kao, J. and Huang, S. 2000. Forecasts using neural network versus Box-Jenkins methodology for ambient air quality monitoring data. Journal of the Air & Waste Management Association, 50: 219-226.

Lipfert, F.W. and Hammerstrom, T. 1992. Temporal patterns in air pollution and hospital admissions. Environmental Research, 59: 374-399.

McDonnell, W.F., Abbey, D.E., Nishino, N. and Lebowitz, M.D. 1999. Long-term ambient ozone concentration and the incidence of asthma in non-smoking adults: the AHSMOG study. Environmental Research, Sec A, 80: 110-121.

Sandhu, H.S. 1999. Ground-Level Ozone in Alberta. Science and Technology Branch, Environmental Sciences Division, Alberta Environmental Protection, Edmonton, AB.

Thurston, G.D., Lippmann, M., Scott, M.B. and Fine, J.M. 1997. Summertime haze air pollution and children with asthma. American Journal of Respiratory and Critical Care Medicine, 155: 655-660.

USEPA— United States Environmental Protection Agency. 1996. Air Quality Criteria for Ozone and Related Photochemical Oxidants-Volume I, II & III EPA/600/P-93/004aF. Office of Research and Development, Washington, DC.

5.0 EDMONTON EAST OZONE ANN MODELS[2]

5.1 Introduction

With the growing population and urbanization of the world, air quality and the health effects associated with poor air quality are becoming increasingly important issues. Ground-level ozone is one of the pollutants currently under scrutiny for its role as an iniator and aggravator of respiratory illness. It is a secondary pollutant, formed in urban environments mainly from anthropogenic emissions of its precursor compounds, the oxides of nitrogen and volatile organic compounds. These ozone precursors are emitted from a variety of sources, both man-made and natural, including transportation, stationary source fuel combustion, industrial processes, vegetation, and solid waste disposal (CEPA/FPAC WGAQOG 1999; USEPA 1996). Health Canada and Environment Canada, and the United States Environmental Protection Agency (USEPA) have recently studied the atmospheric chemistry of ozone (CEPA/FPAC WGAQOG 1999; USEPA 1996). The commonly reported ground-level ozone formation process, in the presence of anthropogenic pollutants is illustrated in Figure 5-1.

Atmospheric ozone formation processes are non-linear and complex, challenging the success of traditional mechanistic modelling approaches. This, combined with the risk of adverse health effects associated with ozone exposure, has introduced the need for a reliable method for modelling ozone concentrations and predicting high ozone events. An approach that has recently piqued the interest of atmospheric scientists internationally is artificial neural networks (ANNs). ANNs are a form of artificial intelligence. They are patterned after the problem solving, trend recognition, and experiential learning abilities of the human brain (Baxter 2002). ANNs employ historical data to map out the relationships between a set of input variables and the output variable modelled. The networks consist of numerous individual processing units called neurons, commonly interconnected in a three layer structure (called a "three-layer multilayer perceptron"). These neurons are analogous to the neurons in the human brain that are responsible for information processing (Jain et al. 1996).

---

[2] A version of this chapter will be submitted to the Journal of the Air & Waste Management Association: Su, D., M. Gamal El-Din, A.G. El-Din, and A. Idriss. Artificial Neural Network Modeling of Ground-Level Ozone in Edmonton.

The neurons in the input layer receive input data, each neuron representing a single input parameter (Tupas 2000). The neurons in the hidden layer (hidden because they do not interact with any elements outside of the network) process the data and the neurons in the output layer report the results from the network (Tupas 2000).

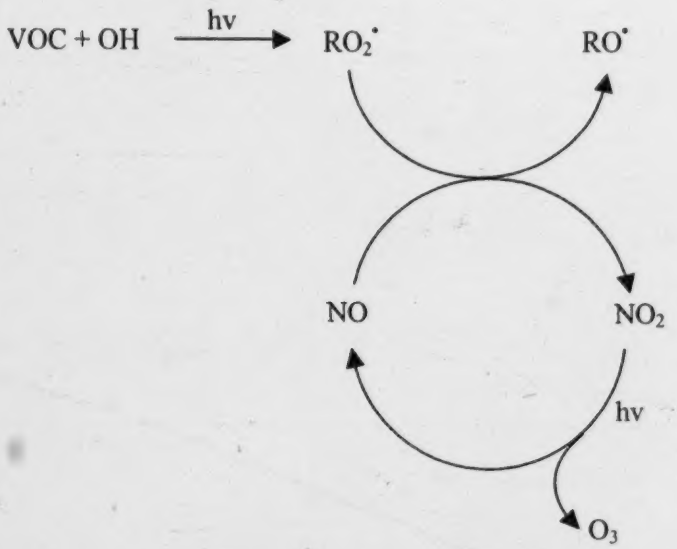

Figure 5-1. VOC contribution to ground-level ozone formation.
Adapted from USEPA (1996).

In the feedforward network, each neuron in a layer is connected to every neuron in the subsequent layer (Flood and Kartam 1997). These connections are akin to the limb-like dendrites and axons that connect and allow communication between neurons in the human brain. In the human brain, signals are transferred between neurons through these connections and across the synaptic gap, resulting in the release of chemicals that stimulate or inhibit the ability of neighbouring neurons to generate impulses (Jain et al. 1996). In the ANN, the "connection weight" between neurons represents this communication process. The sign and magnitude of connection weights describe the nature and strength of influence between the connected neurons (Garrett et al. 1997). The number of neurons in a network and how they are divided among the different layers, the connection weights, and the functions used in the neurons collectively describe the process modelled, and are specific to

this process. The features that best describe the process are determined during the development of the ANN.

Historical data that are representative of the process are introduced to the ANN during training. The data must be pre-processed to remove any noise, erroneous entries, and unexplained random variance, so the ANN is able to learn the true relationships underlying the data (Comrie 1997; Gardner and Dorling 2001). The historical data are typically segmented into three sets of data. The training data set is used to train the network. The validation set of data is used to determine the generalization ability of the network during the training phase of network development. Finally, the production data set is reserved as an independent set of data used to verify the network's predictive performance. Each subset of data should be representative of the entire data history for an accurate assessment of the network's performance. This can be done through statistical tests, or by swapping the data in the subsets, re-training the network with the swapped data, and comparing the results with the original network.

A learning rule dictates how the ANN responds to the training data (Jain et al. 1996). One of the most commonly used rules for training multilayer perceptron (MLP) networks is the backpropagation rule (Henseler 1995). In this approach, connection weights are initially set at small, random values. The training data are fed to the network to generate an output. The network output is compared to the actual value of the output, and the connection weights are adjusted accordingly. This process is repeated until a satisfactory level of accuracy is achieved. During training, care must be taken to avoid overtraining the network. Overtraining results in the network memorizing the data, including noise, rather than recognizing the underlying trends (Henseler 1995). The outcome is an acceptable performance during the training phase, but poor performance when the network is applied to an independent set of data (i.e., poor generalization ability).

The purpose of this project was to determine whether ANNs could be used as a modelling and forecasting tool for ground-level ozone concentrations in Edmonton. Specific goals were: (1) to develop ANN models to process real-time data and provide a corresponding ozone concentration; (2) to forecast future ozone concentrations using the current hour's

data and the maximum forecast window; (3) to evaluate ozone time series effects on model performance; (4) to use the ANN models to determine the parameters that contribute most to ozone formation; and (5) to determine the effectiveness of the systematic approach for ANN model development.

5.2 Background

Edmonton is a mid-sized city in the province of Alberta, Canada. It is situated around the North Saskatchewan River valley, and is home to over 900,000 people. Industries in the area include cement kilns, power plants, petroleum refineries, and chemical manufacturing facilities. Alberta Environment operates a network of ambient air monitoring stations in Edmonton. These monitoring stations continuously monitor ambient concentrations of pollutants, including carbon monoxide, nitric oxide, nitrogen dioxide, sulphur dioxide, total hydrocarbons, and ozone. Additional parameters measured at the ambient air monitoring stations are relative humidity, temperature, wind speed, wind direction, and wind direction deviation. Environment Canada monitors upper air data out of the Stony Plain station near Edmonton (approximately 45 km from the Edmonton East station), including mixing height (via balloon soundings) and cloud opacity. The data collected at these monitoring stations were used to train the ANN models developed in this project.

5.3 Methodology

Ward Systems Group, Inc.'s NeuroShell2 software package, along with its Batch Processor utility, was used to construct the ANN models. The systematic approach proposed by El-Din and Smith (2002) for a water treatment application is adapted for this project. The approach involves the methodical determination of the best network structure (number of neurons in the hidden layer and number of training epochs), the optimum inputs, the best combination of activation functions in the hidden and output layers, and the best prediction window for forecast models. The approach respects the principle of parsimony, in that for the final model, minimal resources are used to provide the best performance. The approach seeks to ensure that the final model is accurate, simple, and efficient.

The general steps of the systematic approach are:

1) Pre-process and characterize the historical data.
2) Format and sub-divide the data for entry into the model.
3) Find the best combination of hidden and output layer activation functions.
4) Determine the optimum inputs to the model.
5) Investigate time series effects on the modelled output.
6) Establish the optimum number of neurons in the hidden layer and number of training epochs.
7) Determine the maximum forecast window that meets the minimum acceptable performance requirements.
8) Complete a stability check, residuals analysis, and sensitivity analysis of the optimum model.

Each of the steps in the systematic approach used for this project is described in detail below.

Step 1: Data preprocessing and characterization

The input parameters considered in this project were based on the availability of historical data. Due to the dynamic nature of meteorology, the fast-paced growth of the City of Edmonton, and constant changes in lifestyle and habits of humans over time, this project uses only data from recent history, from June 1999 to August 2003. The parameters examined in this project were concentrations of carbon monoxide (CO), nitric oxide (NO), nitrogen dioxide (NO_2), sulphur dioxide (SO_2), and total hydrocarbons (THC), mixing height, opacity, relative humidity, temperature, wind direction, wind direction deviation, wind direction sector, wind speed, month, day of the week, and hour of the day. Each of these parameters is described further below. In the literature, indicators of human activities, such as traffic counts, were used as inputs. This project does not consider traffic counts because it is not the intent of this paper to build a complex source/receptor type of model. In addition, fluctuations in pollutant concentrations that may be caused by traffic patterns

are inherently embedded in the pollutant trends. Ozone concentration was the single output modelled.

The pollutant, relative humidity, temperature, and wind data for this project were obtained from Alberta Environment's Edmonton East ambient air monitoring station. This station was selected because the wind in Edmonton blows predominantly from the west in the summer months (Environment Canada 2003). Using the East station data ensures that urban effects can be captured in the model, without contamination of the data from the NO scavenging that occurs in the high volume idling traffic in the core of the city. All variables from the Alberta Environment station were measured as hourly averages. CO is measured using non-dispersive infrared photometry or by gas filter correlation. NO and NO_2 are measured using chemiluminescence. Ozone is measured with the UV-light process. SO_2 is measured through pulsed fluorescence. These methods are described in detail elsewhere (http://www.casadata.org/airquality/index.asp or at http://www3.gov.ab.ca/env/air/maml/mon_me.html).

Cloud opacity and mixing height data were obtained from the Environment Canada Stony Plain station. Environment Canada calculates mixing height data twice daily from balloon soundings. The twice a day mixing height data were converted to hourly values with linear interpolation to yield a mixing height value corresponding to every hour's pollutant concentration data. In addition, the Benkley and Schulman (1979) method was also applied to calculate hourly mixing height values from three hour centred average wind speed data. The Benkley and Schulman method applies when:

- The wind profile is logarithmic. This is generally true for only neutral atmospheric conditions (Kaimal and Finnigan 1994).
- The von Karman constant = 0.35.
- Coriolis parameter = 10^{-4}
- The roughness length is 5 cm.
- Mixing height is dominated by the mechanically driven value. The convective component is negligible. This usually does not apply during the daytime hours.

- The method is one-dimensional and does not apply to two-dimensional mesoscale features.

The linearly interpolated mixing heights calculated from the balloon soundings were compared to the mixing height calculated using the Benkley and Schulman method for the same hour. The lower mixing height from the two methods (the condition that would yield the highest ground-level pollutant concentration) was used in the ANN model.

In Edmonton, ozone concentrations are expected to be of greatest concern during the summer months, when photochemical activity and temperatures are greatest. For this reason, only the summer data were modelled in this project. The months considered in the project were May, June, July, August, and September.

To explicitly account for temporal variations, the month, day of the week, and hour of the day were added as distinct inputs. In the steps before determining the optimum inputs to the model, these variables were represented as indexed values, according to the assignments outlined in Table 5-1. Each parameter was represented with a single input neuron in the ANN model. During the determination of the optimum inputs step, the ANN identified the parameters most important for modelling ozone. After this step, any temporal parameters were represented with multiple input neurons representing each value of the parameter. For example, for the month of the year, May, June, July, August, and September each had their own input neurons. For a data pattern from July, the July input neuron was set to a value of 1 (or "on"). The input neurons for all other months were set to a value of 0 (or "off") for this data pattern. Representing each month, day of the week, and hour with multiple input neurons eliminates any biases associated with the magnitudes of the indexed inputs. This approach also allows the network to assign different connection weights to each month, day, or hour, depending on its importance to ground-level ozone concentrations.

The monitoring data express wind direction in degrees from north. With this convention, winds from the north have a value of either 0° or 360°, winds from the east have a value of 90°, etc. Wind speeds less than 1 km/h are referred to as calms. The current instrumentation is unable to accurately determine wind speeds and directions below this 1

km/h detection limit (McCullum 2003). To allow calms to be distinguished, all readings for winds from the north were assigned a value of 360°. Calms were represented with a wind speed of 0 and a corresponding wind direction of 0°.

Table 5-1 Values assigned to temporal variables in Edmonton East ozone models.

Index Value	Month	Day	Hour
0			Midnight
1		Sunday	01:00
2		Monday	02:00
3		Tuesday	03:00
4		Wednesday	04:00
5	May	Thursday	05:00
6	June	Friday	06:00
7	July	Saturday	07:00
8	August		08:00
9	September		09:00
10			10:00
11			11:00
12			Noon
13			13:00
14			14:00
15			15:00
16			16:00
17			17:00
18			18:00
19			19:00
20			20:00
21			21:00
22			22:00
23			23:00

An additional wind direction sector parameter was included as an input. Hasham (1998) expressed concern that the network may have difficulty recognizing the physical closeness of wind directions in the northeast quadrant with those in the northwest quadrant, because their degree values are significantly different in magnitude. For instance, a wind direction of 1° is physically near a wind direction of 359°, even though the difference in their magnitudes is great. To dispel any confusion to the network, Hasham recommended adding a parameter called wind direction sector that groups the wind direction data. For this project, the wind

direction data were classed into eight, equal-sized sectors corresponding to the major compass points. These sectors are described in Table 5-2.

Alberta Environment and Environment Canada removed erroneous values from the monitoring station data prior to making the data publicly available. However, the monitoring data still contained missing values, denoted with non-numeric values or blank cells. All non-numeric values were replaced with blank cells. Any patterns containing blank cells were removed from the historical data set. Each parameter in the historical data was plotted, and the graphs inspected to visually identify data trends and unusual values. To characterize the data, the mean, median, standard deviation, variance, minimum, maximum, and 1st, 5th, 25th, 75th, 95th, and 99th percentile values were calculated for each parameter.

Table 5-2 Wind direction sectors.

Sector	Bearing	Wind Direction (degrees from north)
0	N/A	Calms (wind speeds <1 km/h)
1	north	337.5-360; 0-22.5
2	northeast	22.5-67.5
3	east	67.5-112.5
4	southeast	112.5-157.5
5	south	157.5-202.5
6	southwest	202.5-247.5
7	west	247.5-292.5
8	northwest	292.5-337.5

Step 2: Data formatting

The data were formatted using Microsoft Excel. Headings (parameter names) were placed in the first row. The first column of each file contained the date and time of each record, serving as an identifier for each data pattern. The historical data were sub-divided into training, test, and production (validation) sets using a 3:1:1 ratio. To accomplish this, the historical data were first sorted according to the ozone concentration, with patterns containing the highest ozone concentrations listed first. Each pattern was then assigned a T (training), P (test), and V (production) classification. To maintain the 3:1:1 ratio and ensure that each sub-set was representative of the entire data set, the assignments were made in the

order: T, P, T, V, T. The subset assignments were listed in the second column of the Excel file. Once all patterns were assigned to a subset, the data were re-sorted temporally. The remaining columns of the Excel file contained the values of all the input parameters, with the final column containing the ozone concentration data.

Step 3: Activation function combinations

The three layer, feedforward multilayer perceptron (MLP) network configuration was preferred for this project because of its simplicity and proven adequacy in the ANN literature (Cobourn et al. 2000; Elkamel et al. 2001; Guardani et al. 1999; Kao and Huang 2000). However, prior to developing the network architecture, several preliminary runs were conducted to evaluate other network types. The default Ward network, a three-layer feedforward network, and a four-layer feedforward network were evaluated. Since these networks are inherently different, they could not be directly compared. The objective of the preliminary runs was to determine if any network configurations other than the MLP could produce a remarkable improvement in the network performance. There were no significant differences in the network performance with each of these configurations. For parsimony, all networks were developed using a three-layer feedforward configuration.

The best combinations of activation functions in the hidden and output layers of the network were evaluated for a network using all 16 inputs. For the hidden layer, the activation functions tested were the logistic, hyperbolic tangent (tanh), Gaussian, sine, hyperbolic tangent 1.5 (tanh15), Gaussian complement, and symmetric logistic functions. The output layer functions evaluated were the same as those tested in the hidden layer, with the addition of a linear function. In total, 56 (7x8) combinations were evaluated. Since the final network configuration was yet to be determined, all activation function combinations were tested at a low, middle, and high setting of number of hidden layer neurons and number of training epochs. These settings are defined in Table 5-3, and were chosen with the intent that their range would encompass the potential final network architecture. Testing each combination at the three settings ensures that the activation function combination selected for the final network is stable.

Table 5-3 **Settings for activation function combination testing.**

Setting	No. Hidden Layer Neurons	No. Training Epochs
Low	10	25
Middle	50	50
High	100	100

The best activation combination was the combination with the highest average coefficient of multiple determination (R^2) calculated for all three settings.

Step 4: Optimum input parameters

Once the best performing activation function combination was established, the relative contributions of each input parameter to the model were determined. A network was developed with all the available inputs to set a benchmark performance for comparison of the subsequent networks developed. With the number of training epochs arbitrarily set at 1000 and 5000 epochs, the number of neurons in the hidden layer that produced the best R^2 was determined. This network was deemed the benchmark network to be used for performance comparisons in the optimization of the input set of parameters. After determining this benchmark, a single parameter was removed from the network input. The network was then re-trained, and the effect of the removal of this parameter was assessed. The removed variable was then returned to the network inputs, and a second variable removed (i.e., the number of variables input to the network was constant throughout the test). This process was repeated for each of the input variables to evaluate the effect of each variable on the network performance. During the evaluation of the input parameters, the network architecture was fixed at the architecture of the benchmark network. The pertinent input parameters were those that, when excluded from the network's set of input variables, decreased the R^2 by 0.03 or greater.

Due to the potential for a variable's effects to be masked by another variable (because of some relationship between the two variables), the optimum variable test was repeated using a core set of inputs and evaluating the network's performance when additional variables were added to the core input set. For this step, any variables whose addition to the core input set

changed R^2 by less than 0.03 were removed from further consideration. The inputs assessed and their units are described in Table 5-4.

Table 5-4 Parameters available for input to the Edmonton East virtual monitor model.

Name	Description	Units
MTH	Numerical indicator of the month (May = 5, June = 6, July = 7, August = 8, September = 9)	unitless
DAY	Numerical indicator of day of the week (Sunday = 1, Monday = 2, Tuesday = 3, Wednesday = 4, Thursday = 5, Friday = 6, Saturday = 7)	unitless
HOUR	Numerical equivalent of the hour (midnight = 0, 01:00 = 1, 02:00 = 2, etc.)	unitless
CO	Carbon monoxide concentration, ambient hourly average	ppm
NO	Nitric oxide concentration, ambient hourly average	ppm
NO_2	Nitrogen dioxide concentration, ambient hourly average	ppm
SO_2	Sulphur dioxide concentration, ambient hourly average	ppm
THC	Total hydrocarbons concentration, ambient hourly average	ppm
MIX	Mixing height, lower of values calculated from linear interpolation of balloon sounding data and Benkley and Schulman method, hourly	m
OPA	Cloud opacity (amount of sky obscured by cloud), hourly	tenths of sky
RH	Relative humidity	%
TEMP	Temperature, ambient hourly average	°C
WDR	Wind direction, hourly average	° from North
DEV	Wind direction deviation, hourly average	°
SECT	Wind direction sector (North = 1, Northeast = 2, East = 3, etc.)	unitless
WSP	Wind speed at 10 m, hourly average	km/h

Step 5: Time series effects

The effects of adding previous hours' concentrations of ozone were investigated at the settings of the benchmark network. This process was similar to Step 4, except the benchmark network was modified to include only the optimum inputs determined in Step 4, and a baseline performance was established. Subsequent networks were built with consecutive inputs of previous hours' concentrations of ozone (i.e., for modelling ozone at time t, the first network included ozone concentration at t-1 as input, the second network

included ozone concentration at t-1 and at t-2, etc.). The changes in the network performance were then compared to the baseline performance.

Step 6: Number of hidden layer neurons and training epochs

In this step, a range of combinations of number of neurons in the hidden layer and number of training epochs was evaluated to find the combination most suitable for modelling ozone. The numbers of neurons in the hidden layer tested were 7, 8, 9, 10, 11, 12, 13, 14, 15, 16, 17, 18, 19, 20, and 25. The numbers of epochs used for training the network evaluated were 500, 1000, 1100, 1200, 1300, 1400, 1500, 2000, 3000, 4000, and 5000. The network performance was evaluated using the production set of data, to measure the network's ability to generalize. Starting with low numbers of epochs ensured the network was not overtrained.

Step 7: Maximum forecast window

The maximum prediction window that would yield an acceptable prediction performance was determined for the forecast models. In this project, the minimum performance standard adopted was a R^2 of 0.75. The maximum forecast window was determined by finding the best network architecture for increasingly large prediction windows, until the performance of the best network could no longer meet the minimum performance standard.

Step 8: Stability check, residuals analysis, and sensitivity analysis

The stability check confirms the network stability. The stability check was completed by swapping the patterns in the training set with those in the test and production data sets. To maintain the 3:1:1 ratio of patterns in each data set, only 2/3 of the training patterns were re-assigned to either the test or production data sets. The network was then re-trained using the revised training data set and its performance compared to the original network. With a stable network, the performance would not be compromised despite the data swap.

The residuals analysis detects whether correlations exist between the model residuals. In this step, possible correlations of residuals with time and with the modelled ozone concentration values were evaluated. This was done through visual examination of residual scatter plots, with time and modelled ozone concentrations on the independent axis.

The sensitivity analysis assesses the impacts on the model output when changes are made to a single input parameter while all other inputs are held constant. In this step, each input parameter was ranged from its minimum to maximum observed values while all other inputs were held at their observed median values. The resulting model output was noted and a plot against the changed input variable was generated.

5.3.1 Evaluation of network performance

Many methods of evaluating the ANN performance were possible, with each method offering different advantages and disadvantages. The statistic used most often in the literature, the coefficient of multiple determination (R^2), was adopted for this project. However, other performance statistics were also calculated for the final models to allow comparison with the models presented in the ANN literature. Each of these statistics is described briefly below.

Coefficient of multiple determination (R^2)

The coefficient of multiple determination indicates the fraction of the total variation of the modelled output that can be explained by the model (Walpole and Myers 1993). In NeuroShell2, this is calculated using the equation:

$$R^2 = 1 - \frac{\sum (x - y)^2}{\sum (x - \bar{x})^2} \quad \text{.....Equation 5-1}$$

where

x = actual output value (in this project, the ozone concentration from the ambient monitor historical data)

y = modelled output value (ozone concentration from the ANN)

$\bar{x}$ = mean of the actual output values

Pearson's product-moment correlation coefficient (r)

The Pearson's linear correlation coefficient is an estimate of the linear association between two variables, and ranges from –1 to +1 (Walpole and Myers 1993). The equation for Pearson's linear correlation coefficient used in NeuroShell2 is:

$$r = \frac{SS_{xy}}{\sqrt{SS_{xx} SS_{yy}}} \quad \text{.....Equation 5-2}$$

where

$$SS_{xy} = \sum xy - \frac{(\sum x)(\sum y)}{n} \quad \text{.....Equation 5-3}$$

$$SS_{xx} = \sum x^2 - \frac{(\sum x)^2}{n} \quad \text{.....Equation 5-4}$$

$$SS_{yy} = \sum y^2 - \frac{(\sum y)^2}{n} \quad \text{.....Equation 5-5}$$

x = actual output value (in this project, the ozone concentration from the ambient monitor historical data)

y = modelled output value (ozone concentration from the ANN)

n = number of data patterns

Mean squared error (MSE)

The mean squared error is the mean of the square of the residuals, or the mean of $(x-y)^2$.

Mean absolute error (MAE)

The mean absolute error is the mean of the absolute values of the residuals, or the mean of $|x-y|$.

Minimum absolute error

The minimum absolute error is the lowest value of the absolute value of the residuals.

Maximum absolute error

The maximum absolute error is the highest value of the absolute value of the residuals.

Fractional bias (FB)

The fractional bias is a dimensionless number that indicates whether a model is prone to overprediction or underprediction, proposed by Cox (1988) to be a good basic measure of operational performance. It is a symmetrical value that is bounded, ranging from -2.0 to +2.0. A FB of -2.0 indicates extreme overprediction while a value of +2.0 indicates extreme underprediction. A FB of ±0.67 indicates a factor of two over- or underprediction. Cox recommends applying the FB to the highest 25 observed values, using the equation:

$$FB = 2 \times \frac{(\bar{x}_{25} - \bar{y}_{25})}{(\bar{x}_{25} + \bar{y}_{25})} \quad \text{.....Equation 5-6}$$

where

$\bar{x}_{25}$ = average of the 25 highest observed values

$\bar{y}_{25}$ = average of the 25 predicted values corresponding to the 25 highest observed values

Wilmott index of agreement (d_1 and d_2)

Two versions of the Wilmott index of agreement can be found in the ANN literature. The Wilmott index of agreement measures the degree of agreement between actual and predicted values. It is dimensionless and ranges from 0 to 1, with 0 indicating no agreement and 1 indicating perfect agreement. The two forms of the index of agreement are calculated using (Comrie 1997):

$$d_1 = 1 - \left[\sum |y - x|\right]\left[\sum \left(|y - \bar{x}| + |x - \bar{x}|\right)\right]^{-1} \quad \text{.....Equation 5-7}$$

$$d_2 = 1 - \left[\sum |y - x|^2\right]\left[\sum \left(|y - \bar{x}| + |x - \bar{x}|\right)^2\right]^{-1} \quad \text{....Equation 5-8}$$

The distinction between d_1 and d_2 is that d_2 is based on squared differences (Comrie 1997).

In this paper, the performance of the ANNs is based on the R^2 value when the network is applied to the production data set. The network R^2 values when applied to the training and test data sets are also compared to the production set R^2 to ensure that the network is not overtrained. The R^2 values for all data sets should be comparable. A production set R^2 that is much lower than the training set R^2 is an indication the network's ability to generalize has been compromised. Conversely, a production set R^2 much higher than the training set R^2 may be a sign that the production data are not representative of the full spectrum of ozone concentrations that may be encountered in reality.

5.4 Results and Discussion

The preliminary statistics calculated for the available inputs are listed in Table 5-5. For some of the parameters, the maximum values were more than twice the 99th percentile values. However, since Alberta Environment and Environment Canada have already subjected the data to quality control procedures, these extreme values were not expected to be erroneous entries and were kept in the historical data set. Excursion events may be due to the influences of unusual situations such as nearby forest fires (Cheng et al. 1998) or a combination of meteorological events conducive to the formation or accumulation of ozone.

Figure 5-2 shows July 2002 data patterns that are typical of the Edmonton East ozone data. Diurnal trends are apparent in the plot, with ozone concentrations reaching their daily maximums between 15:00 and 16:00. Ozone concentrations were undetected (0 ppm) on some days. Minima generally occurred early in the morning, at about 6:00. From a regulatory standpoint and for the purposes of regulatory monitoring, it is most important for the ANN to accurately predict peaks in ozone concentrations such as that occurring on July 11, 2002.

Table 5-5 Edmonton East basic statistics for available inputs.

Statistic	CO	NO	NO_2	SO_2	THC	MIX	OPA	RH	TEMP	WDR	DEV	WSP	O_3
Mean	0.3	0.008	0.013	0.002	2.4	243.9	4	62	15.7	251	23	10.0	0.025
Median	0.3	0.004	0.011	0.001	2.2	222.2	4	62	15.2	201	17	9.2	0.024
Std. Dev.	0.2	0.014	0.009	0.003	0.9	200.6	4	23	6.7	101	20	5.8	0.016
Var.	0.0	0.000	0.000	0.000	0.8	40229	14	510	44.3	10257	404	33.9	0.000
Min.	0.0	0.000	0.000	0.000	1.5	0.0	0	10	-6.5	0	3	0.0	0.000
P(0.01)	0.1	0.000	0.002	0.000	1.7	0.0	0	19	0.6	0	6	0.0	0.000
P(0.05)	0.1	0.000	0.003	0.000	1.8	0.0	0	26	5.4	8	8	1.5	0.002
P(0.25)	0.2	0.001	0.006	0.001	2.0	85.7	0	43	11.0	135	13	6.0	0.013
P(0.75)	0.3	0.008	0.018	0.002	2.5	358.8	8	80	20.3	289	25	13.3	0.036
P(0.95)	0.6	0.033	0.031	0.007	3.5	604.1	10	97	27.1	343	64	20.9	0.052
P(0.99)	0.9	0.073	0.041	0.015	5.7	816.9	10	100	31.0	356	115	27.1	0.063
Max.	1.7	0.166	0.068	0.061	25.0	2261.5	10	100	38.0	360	170	42.7	0.101

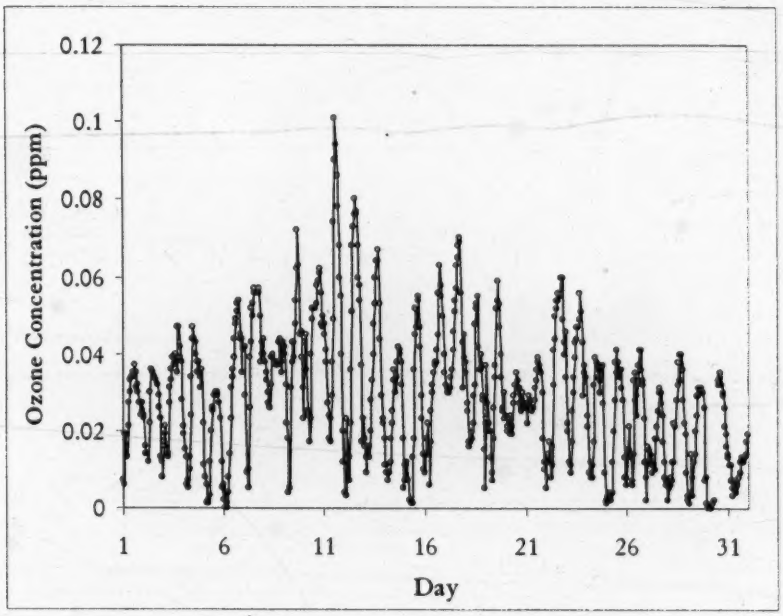

Figure 5-2 Typical Edmonton East ozone data (July 2002).

The activation function combination testing showed the combination of the Gaussian complement function in the hidden layer and the logistic function in the output layer provided the best overall R^2 for the three settings evaluated. The R^2 value for this combination was 0.80. The results of the activation function evaluation are listed in Table 5-

6. Considering that this project was the first ANN project for ozone in the City of Edmonton, the more common logistic-logistic combination was selected for further network development. This combination yielded a similar overall R^2 of 0.79, and should perform at a level similar to the less-proven Gaussian complement-logistic activation function combination.

Table 5-6 Activation function test results.

Setting	Hidden Layer Activation Function	Output Layer Activation Function	R^2 (prod)
Low	Gaussian complement	Logistic	0.78
Middle	Tanh15	Symmetric logistic	0.82
High	Sine	Symmetric logistic	0.83
	Gaussian complement	Symmetric logistic	0.83
Average	Gaussian complement	Logistic	0.80

Five core variables were identified as having the most impact on the network performance in the first step of the input variable analysis. These variables were MTH, NO, NO_2, OPA, and RH. For the network developed with these inputs, the R^2 was 0.73. The second step of the input variable analysis identified five additional key inputs: DAY, SO_2, THC, WDR, and WSP. The results of this step are shown in Table 5-7. The relative contribution factors of these variables for a network consisting of 4 neurons in the hidden layer and trained in 1000 epochs are shown in Figure 5-3. NO concentration was by far the largest contributor to the variability in ozone concentrations with a relative contribution of 0.49. THC and NO_2 concentrations were the next most relevant inputs. The order of importance of the remaining variables was RH/WSP, month, SO_2, opacity, day/WDR.

NeuroShell2 analyzes the weights of the network connections to determine the relative importance of input variables. While no details are given regarding the algorithm used in NeuroShell2 to process these connection weights, the software manual warns that the network can still find patterns among variables that are themselves not highly correlated to the output variable.

Table 5-7 Changes to R^2 with addition of inputs to core input set (R^2 for core input set = 0.73)

Added Input	Production Set R^2	Change in R^2
CO	0.73	0
DAY	0.77	0.04
HOUR	0.56	-0.17
MIX	0.75	0.02
SO_2	0.77	0.04
TEMP	0.73	0
THC	0.76	0.03
WDR	0.77	0.04
DEV	0.71	-0.02
SECT	0.74	0.01
WSP	0.76	0.03

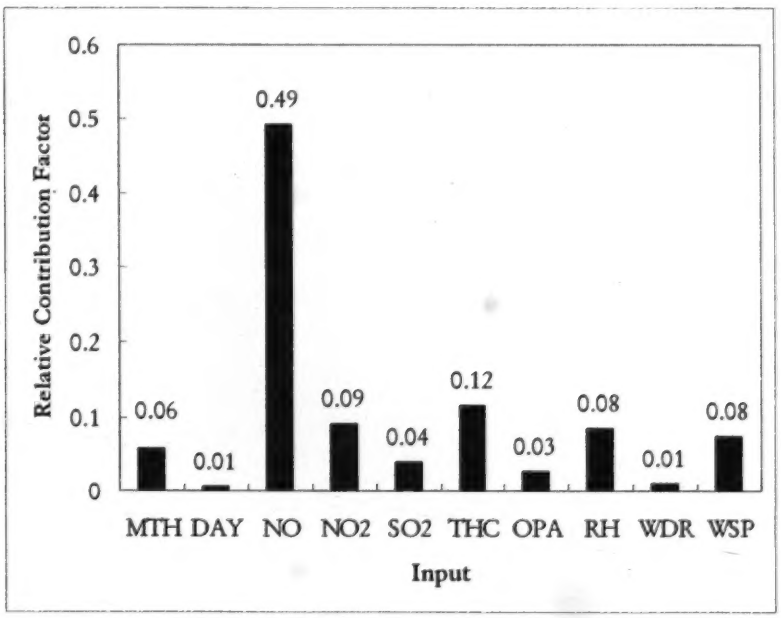

Figure 5-3 Relative contribution factors of the Edmonton East model using the best inputs, 4 hidden layer neurons, 1000 training epochs, logistic hidden and output layer activation functions.

The contribution factors calculated in NeuroShell2 are also related to the total number of input variables. The larger the number of input variables, the more similar the contribution factors of the variables will be. In this project, the contribution factors calculated by NeuroShell2 were also observed to change in relative importance when the network

structure (number of hidden layer neurons and training epochs) was changed. For example, in one network, the three highest contributing variables, in decreasing relative contribution factors, were NO, THC, and MTH. When the network structure was changed, the three highest contributing factors were TEMP, THC, and NO, despite the fact that the same inputs were used for both networks. The shift in relative importance is not surprising given that values of connection weights are expected to change when the network structure is altered. However, these relative contribution factor changes indicate a weakness in this method of determining the relative importance of a set of input variables for predicting a target output. It is possible that a variable excluded in the development of one network would become important in a network with a different architecture. This issue remains unresolved in the ANN literature. Garson (1991) proposed a calculation method for partitioning connection weights to determine the contribution "share" of each input variable, but this technique remains unproven. Abdul-Wahab and Al-Alawi (2002) applied the Garson method to determine the relative importance of input variables in their study, but did not evaluate the reliability of this method. Since no proven method is available for calculating relative contribution factors for the inputs, the NeuroShell2 default method was adopted for the entirety of this project. However, this means that the ozone model developed is simply the optimal network mapping for a particular set of input variables, and may not describe the general ozone formation process. This also highlights the importance of applying scientific knowledge of the process in developing the ANN model to ensure that the key variables identified in the science are included in the final model.

Although TEMP was not identified as a key input variable, it is recognized as a factor in the kinetics of atmospheric reactions. At the request of Alberta Environment and considering its importance in reaction kinetics, TEMP was included in the final set of inputs. Once TEMP was added as an input, the preliminary estimation of the optimum network structure indicated that a network with 7 neurons in the hidden layer performed best when trained in 1000 epochs. The effects of the ozone time series on network performance were evaluated at this setting.

The importance of NO, NO_2, and THC concentrations to the ozone model were not surprising, given that these compounds are involved in the natural and human-influenced

ozone cycles. MTH may be important because it indirectly represents solar radiation levels and hours of sunshine in the day. Spring months may be an indication of the likelihood for stratospheric ozone intrusion (CEPA/FPAC WGAQOG 1999), and summer months may reflect the conditions most conducive to forest fires. Average ambient temperatures are also related to the month of the year, and may explain why TEMP was not identified as a key input variable. The effects of TEMP may also have been reduced because only data from May to September were modelled. The temperature variation in this time period may be insignificant when compared to fluctuations in precursor concentrations or other stronger influences on ozone concentration. The importance of the day of the week hints at the influence of traffic volumes or other activity patterns that are human-related. The low relative contribution of this parameter shows that modelling ozone concentrations at the Edmonton East station indeed diminishes the influence of urban traffic, although these effects are not completely eliminated. OPA is related to the radiation levels necessary for the ozone photochemical reactions to occur. RH, as a surrogate parameter for precipitation, affects the ambient concentrations of ozone precursors and scavengers through wet deposition. SO_2 interacts with ozone in the atmosphere, and has been found to be important in previous ANN applications to ozone (Ruiz-Suarez et al. 1995; Abdul-Wahab and Al-Alawi 2002). The relative importance of wind direction suggests that either specific sources of precursors or scavengers or transport of ozone from other areas may contribute to ozone concentrations at the Edmonton East location, although their effects are weak when compared to other factors. Wind speed is an indicator of atmospheric stability that influences dispersion characteristics of ozone and its related compounds.

CO concentration, hour of the day, mixing height, wind direction deviation, and wind direction sector were relatively unimportant factors in the ground-level ozone concentrations at the Edmonton East station. CO is relatively inert in the atmosphere, and is sometimes used as an indicator of wind drift (Abdul-Wahab and Al-Alawi 2002). Its effects may be negligible in the presence of stronger indicators of atmospheric stability like wind speed. HOUR is an indicator of the strong diurnal patterns associated with urban ozone concentrations reported in the literature (CEPA/FPAC WGAQOG 1999; Chaikowsky 2001; Sandhu 1999). This parameter may not be important for this model because hour to hour fluctuations are inherently incorporated in the species concentrations input to the model.

The lack of importance of mixing height may be due to the limitations of the available methods used to determine hourly average values for mixing height. Linear interpolation of the balloon sounding data is invalid when mixing height does not vary linearly from hour to hour. The Benkeley and Schulman method is inappropriate when the basic assumptions of the method are not met. This method is very specific, limiting its applicability. In addition, sources of ozone precursors and the ambient monitoring station are near the ground, limiting the importance of mixing height as a model input. Wind direction deviation data may be unnecessary since there are other indicators of atmospheric stability in the model. Wind direction sector was also unimportant, suggesting that the ANN is not confused by the format used to present wind direction data.

When all the key variables were incorporated into the model, the resulting model performance was a R^2 of 0.78. At this point, the decision to use the logistic-logistic activation function combination was re-evaluated. To accomplish this, the Gaussian complement activation function was substituted for the logistic function in the hidden layer. The network generated a R^2 of 0.80, comparable to the model using a logistic-logistic activation function combination.

As part of the input variable optimization process, the effects of including ozone concentrations from successive previous hours was evaluated. The results of this evaluation (Figure 5-4) show that beyond inclusion of the ozone concentration from the previous hour, the gains in model performance are minimal. The baseline performance when no ozone concentrations from previous hours are included is slightly over a R^2 of 0.83. The inclusion of the ozone concentration at t-1 increases R^2 to 0.93. Beyond this point, R^2 stabilizes at approximately 0.94, with a dramatic dip when previous hours' ozone concentrations up to t-5 are included. Note that the network architecture was not yet optimized at this time for any of the networks. For a virtual monitor application, the preference is to avoid developing a model that is dependant on information from previous time periods. This is related to the scenarios where a virtual monitor model would be useful: when a "real" monitor is down for maintenance or repairs, or experiences problems that result in a prolonged shutdown. In these situations, previous hours' data may not be readily available. In addition, if the ANN model is in operation for an extended period, the use of modelled concentrations as input

would introduce additional error into the model prediction. It is advantageous to avoid using data from previous timeframes in these applications, in spite of the potential to improve the model's predictive ability. Data pre-processing of the training data are also more time consuming for the virtual monitor model with time series, since each data pattern must be supplemented with the appropriate concentration data from previous hours.

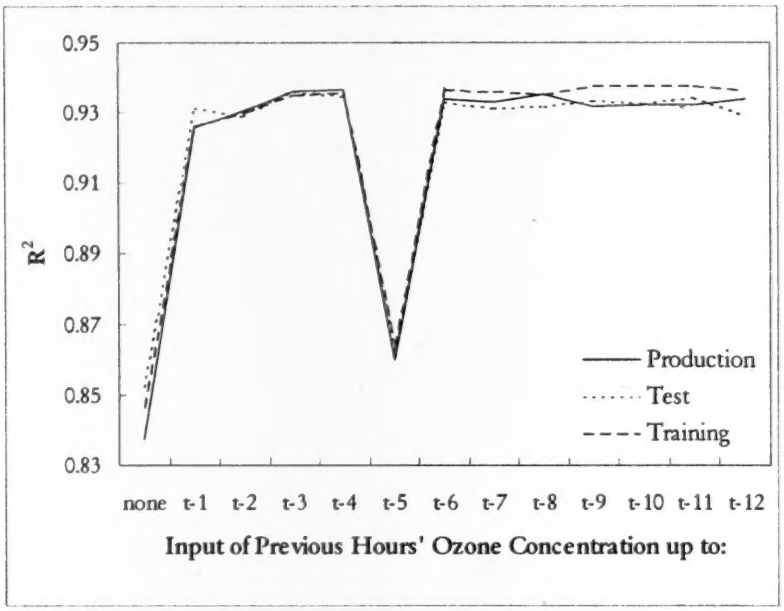

Figure 5-4 Edmonton East virtual monitor effects of ozone time series, fixed network architecture of 7 hidden layer neurons and 1000 training epochs.

Figure 5-5 shows the network architecture optimization results. The black areas on the surface plot indicate the best performing network architecture. Figure 5-5 shows the area with 19 to 25 hidden layer neurons and 3000 to 5000 training epochs (top right hand corner of plot) has the best performance. The region from 16 to 17 hidden layer neurons and 3000 to 5000 training epochs also performs well. Based on these results, the best performing and most economical network contains 17 neurons in the hidden layer and is trained in 3000 epochs, resulting in a R^2 of 0.87 for the production set of data.

An example of the model's performance for July 2002 data is shown in Figure 5-6. The July 2002 data contain the highest ozone concentrations in the production data set. In general, the ANN was able to predict the concentration trends well, and was able to accurately predict the highest peak in the production data. However, some over-prediction of peak concentrations can be seen, as well as some under-prediction of concentration minima. The fractional bias for the network was 0.084, indicating a slight underestimation of the highest 25 ozone concentrations. The Wilmott index of agreement was 0.83 for d_1 and 0.96 for d_2, indicating good agreement of modelled ozone values with measured values. The RMSE for this network was 0.006 ppm.

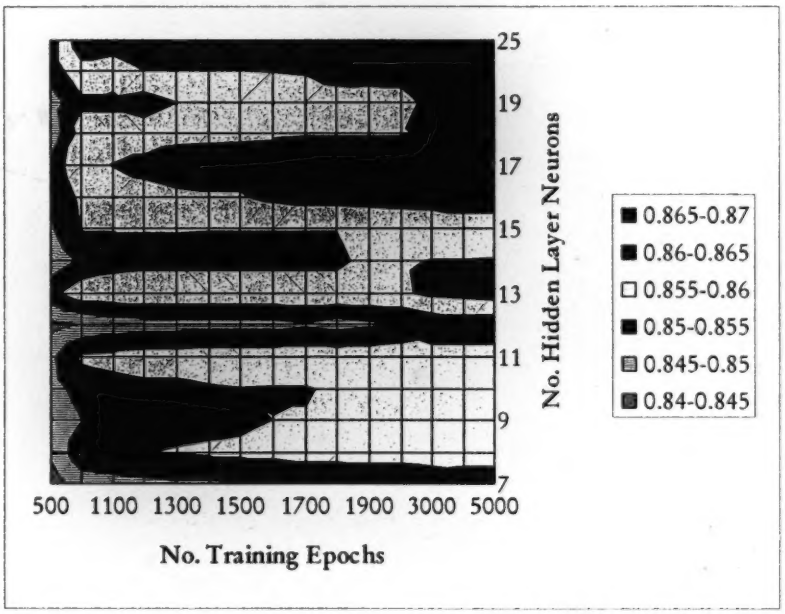

Figure 5-5 Edmonton East virtual monitor surface plot of network architecture testing.

Figure 5-7 shows a plot of the observed and modelled ozone concentrations. The solid line in this plot is the desired situation, representing perfect agreement between observed ozone concentrations and the model output. The results generally fall along this 45° line, confirming good agreement between the modelled and observed ozone concentrations. No indication of the slight tendency to under-predict high ozone concentrations is apparent from this figure.

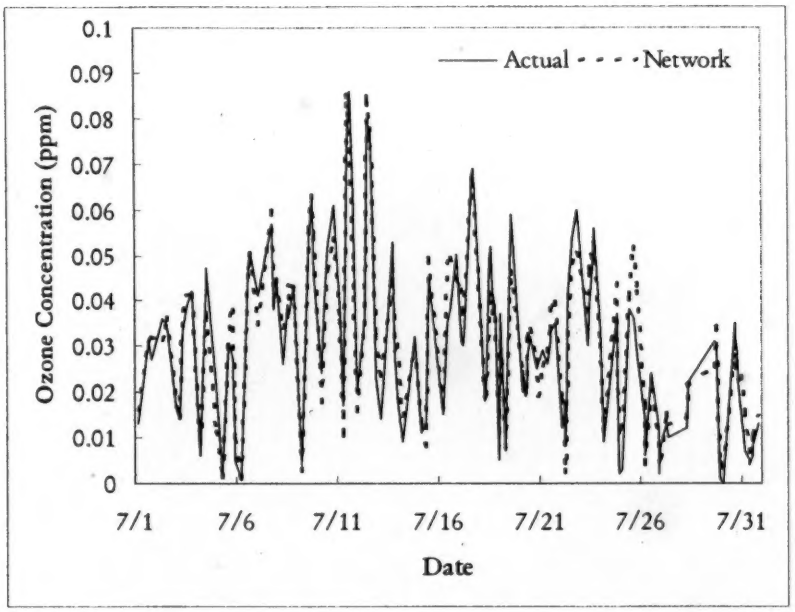

Figure 5-6 Edmonton East virtual monitor model results for July 2002 production set data, $R^2 = 0.87$.

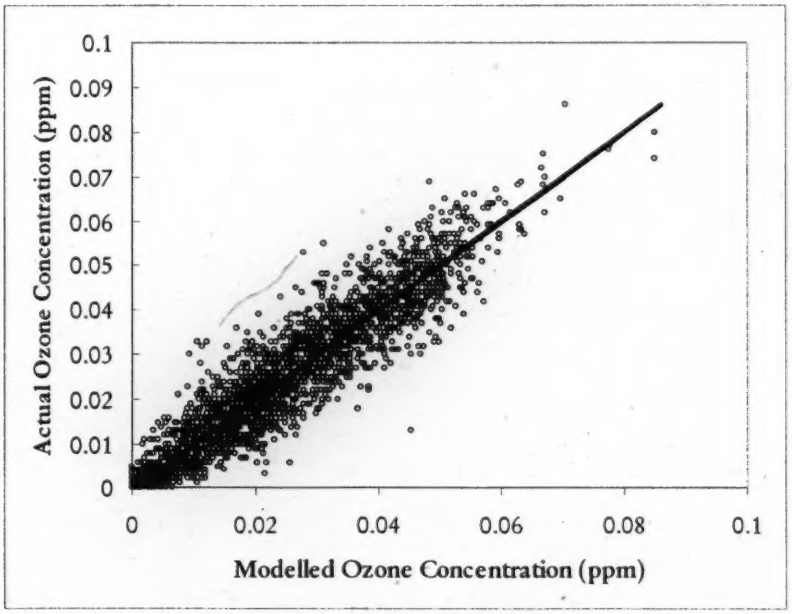

Figure 5-7 Edmonton East virtual monitor scatter plot of agreement between observed and modelled ozone concentrations.

Figures 5-8 and 5-9 show the residuals analysis of the virtual monitor model. Figure 5-8 is a sampling of the residuals plot for 2002. No trends are apparent for either the plot versus time or the plot versus the modelled ozone concentration. This suggests that introducing the training data to model in chronological order does not introduce a systematic error into the model.

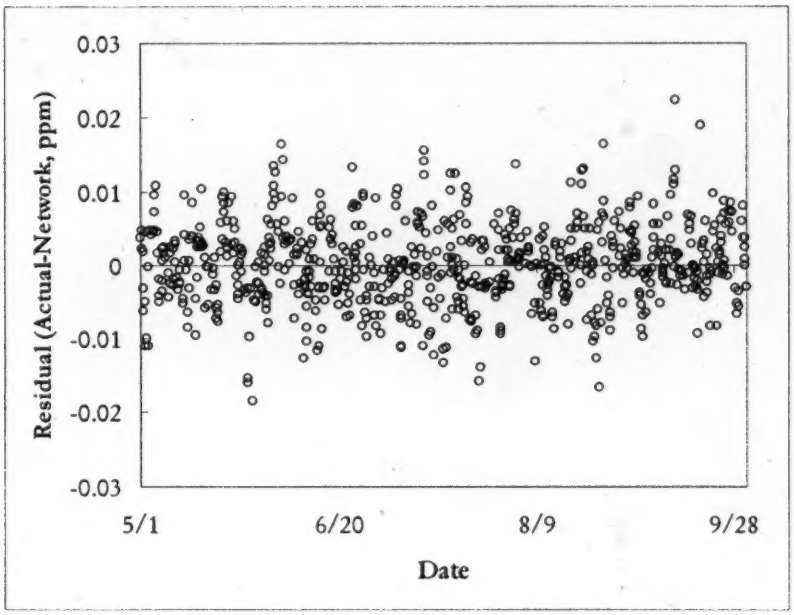

Figure 5-8 Edmonton East virtual monitor model residuals analysis: variance with time for 2002 production data.

The final Edmonton East virtual monitor ANN architecture indicates that the number of training epochs for the three settings used in the activation function testing were too low. However, the stability check of the model using swapped data verifies that the model is stable.

The network architecture for the Edmonton East virtual monitor model also provides guidance for the selection of settings for activation function testing in future studies.

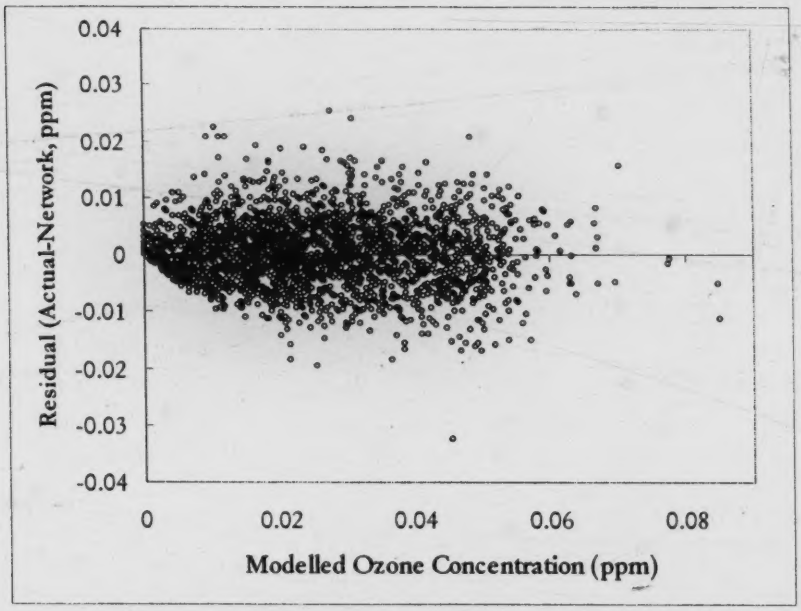

Figure 5-9 Edmonton East virtual monitor model residuals analysis: variance with modelled ozone concentration.

Once the virtual monitor model network structure was optimized, the effect of including the ozone time series into the model was re-evaluated, since the earlier evaluation compared unoptimized networks. As with the basic virtual monitor model, the best structure for the networks using ozone concentrations from up to two hours previous was determined and the performance compared. The results confirmed the results from the comparison of the unoptimized networks: no significant improvement to prediction performance was observed beyond the inclusion of ozone concentration from the previous hour (t-1). These results are depicted graphically in Figure 5-10. When the ozone concentration from the previous hour was included as an input to the model, the model R^2 increased from 0.87 to 0.94. Addition of the ozone concentration from two hours previous (i.e., ozone concentration at t-2) resulted in no change in R^2. Therefore, only the virtual monitor model with time series effects up to t-1 was further developed. The details of this model are discussed later in this chapter.

An analysis of the virtual monitor model's sensitivity to values of the model inputs was completed. A single input parameter was varied through its range of possible values while all

other inputs were fixed at their median values (refer to Table 5-5), and the model response recorded. For the day of the week and month inputs, the median values were assigned as Wednesday and July. The ozone sensitivity to month shows that with all other inputs held constant, ozone concentration tends to be highest in May, and decreases as the summer season progresses, levelling off in August and September (Figure 5-11a). This is consistent with previous observations for Edmonton (Chaikowsky 2001; Sandhu 1999).

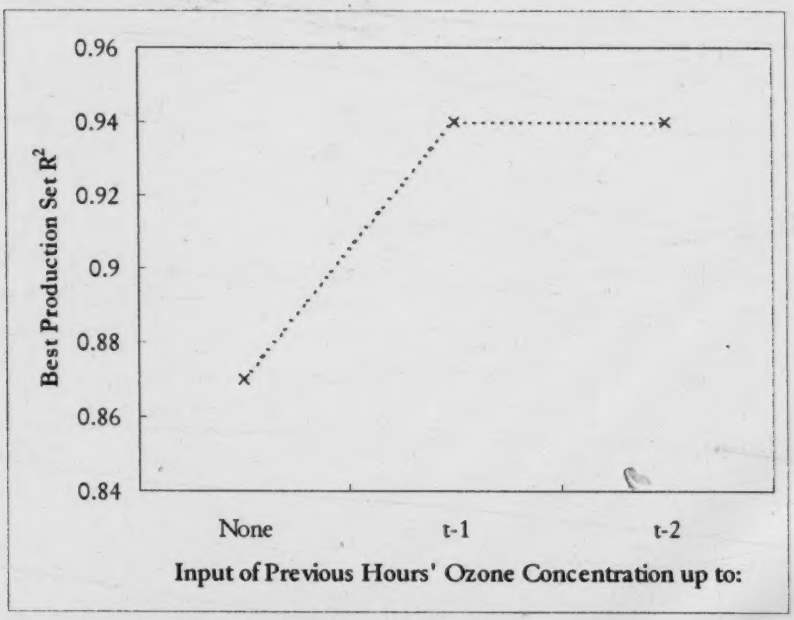

Figure 5-10 Edmonton East virtual monitor effects of adding previous hours' ozone concentrations as input with optimized network structure for each case.

When all other inputs are held constant, there is little fluctuation in ozone concentration with the day of the week (Figure 5-11b). Ozone concentration varies between 0.02 ppm and 0.03 ppm throughout the course of the week, with a slight dip in concentrations on the weekends. This is in agreement with the trends observed in Chapter 3, where average ozone concentrations for each day of the week in the historical data period were higher on weekdays than weekends.

The sensitivity of the ozone model to NO concentrations in Figure 5-12a shows the scavenging effects of NO, with a decay type of decrease in ozone concentrations when NO concentrations rise. Ozone concentration plateaus at NO concentrations greater than approximately 0.5 ppm. This suggests that at the conditions of the sensitivity analysis, NO scavenging of ozone becomes limited at this point.

Figure 5-12b shows the sensitivity of ozone concentration to NO_2 concentrations. The relationship shows an almost linear decrease in ozone concentrations with an increase in NO_2. This trend is contrary to the trend observed in USEPA (1996), where ozone concentrations increased with increases in the concentration ratio of NO_2 to NO. However, Konovalov (2002) reports that conflicting observations of ozone response to decreases in NO_x concentrations are common, with responses in ozone concentration dependent on the concentrations of VOCs and NO_x and on ambient conditions. Ozone concentrations level off at NO_2 concentrations greater than 0.04 ppm.

Ozone concentrations vary slightly with SO_2 concentrations (Figure 5-12c), from approximately 0.021 ppm to 0.027 ppm. This suggests a limited relationship between SO_2 and ozone concentrations when all other pollutants are held at constant concentrations and meteorology is unchanging. Ruiz-Suarez et al. (1995) suggest SO_2 is important only when wet aerosols or hydrogen peroxide are present. Otherwise, the role of SO_2 in ozone reactions is limited.

Figure 5-12d shows no definite pattern in the relationship between ozone and total hydrocarbon concentrations. At lower THC concentrations, ozone concentrations decrease with an increase in THC concentration. Beyond approximately 2.5 ppm, ozone concentrations increase with increasing THC.

Figure 5-13 shows the effects of changing meteorological conditions on ambient levels of ozone. Figure 5-13a indicates a minimal variation in concentrations of ozone with opacity, consistent with Figure 5-3, in which opacity has the lowest relative contribution factor of all the inputs. This suggests that changes in radiation levels have a minimal impact on ground-

level ozone concentrations compared to other variables present in the Edmonton urban environment.

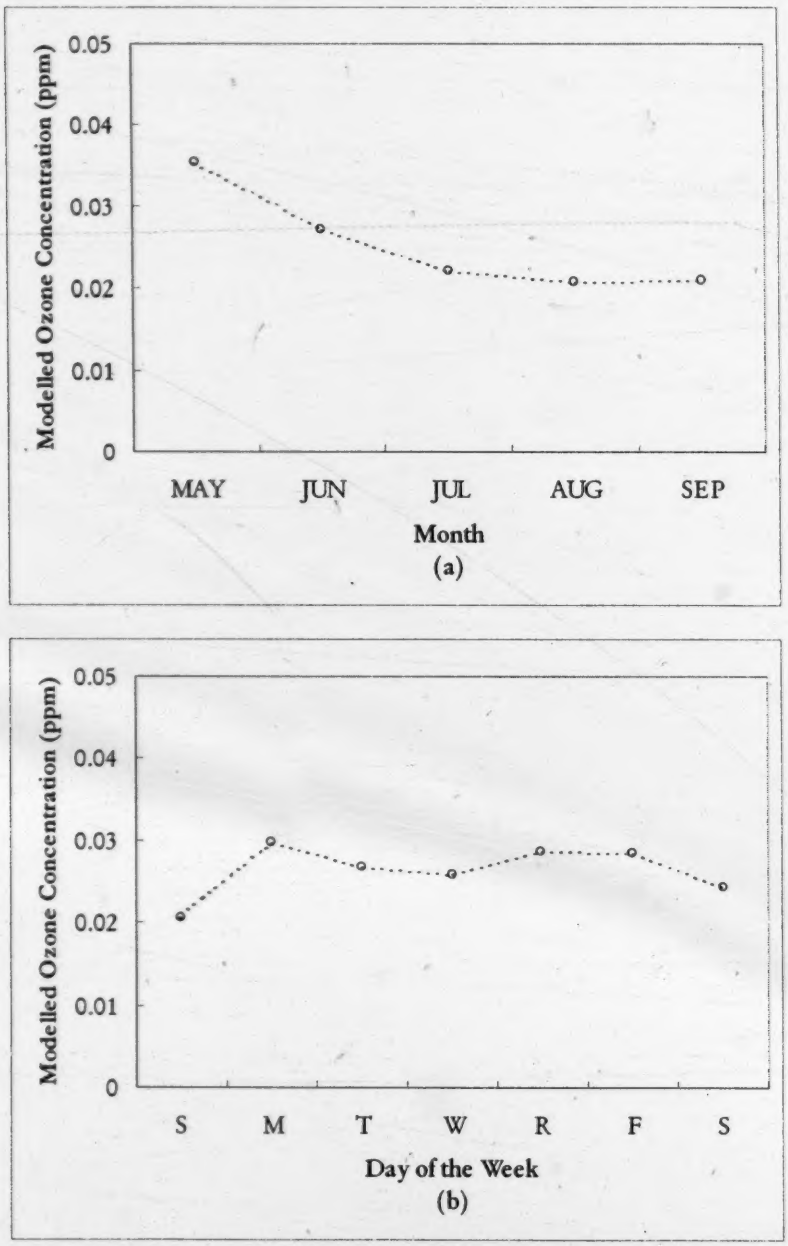

Figure 5-11 **Edmonton East virtual monitor modelled ozone concentration variation with temporal parameters: (a) month; and (b) day of the week.**

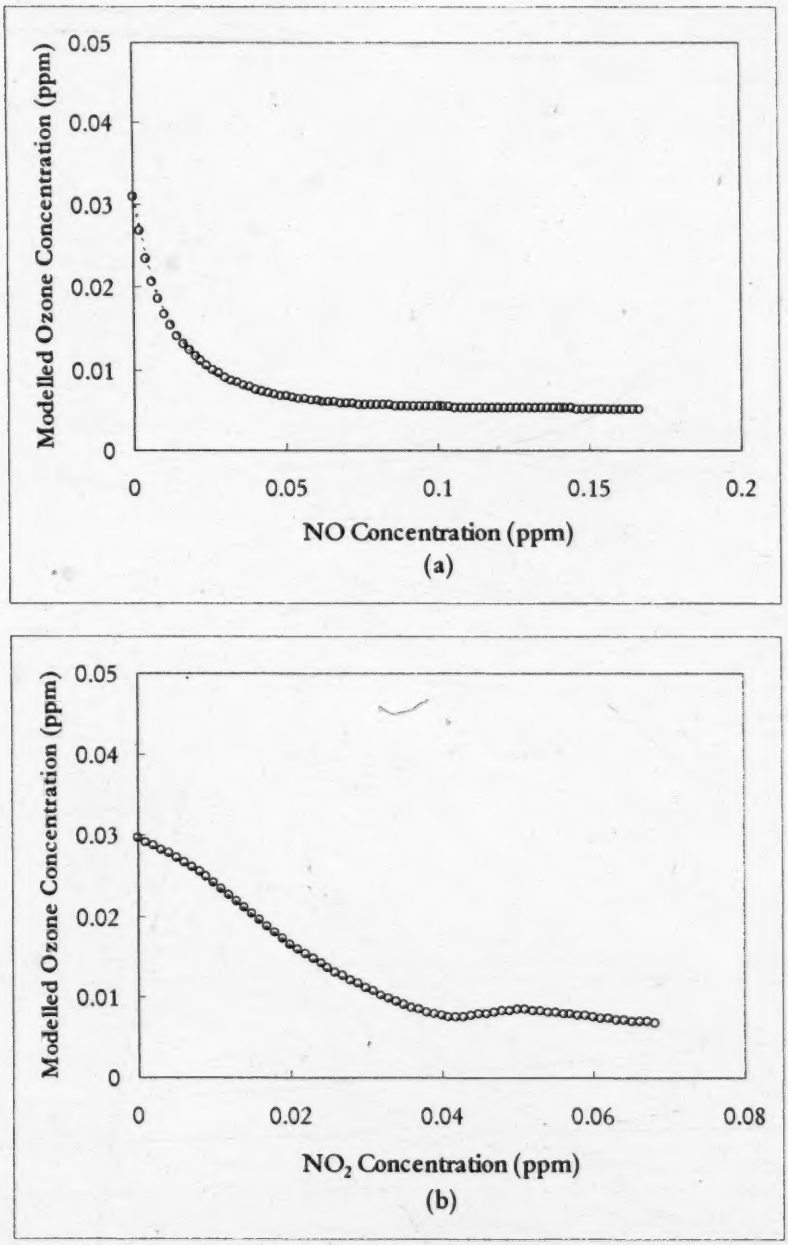

Figure 5-12 Edmonton East virtual monitor modelled ozone concentration variation with pollutant concentrations: (a) NO; (b) NO_2; (c) SO_2; and (d) THC.

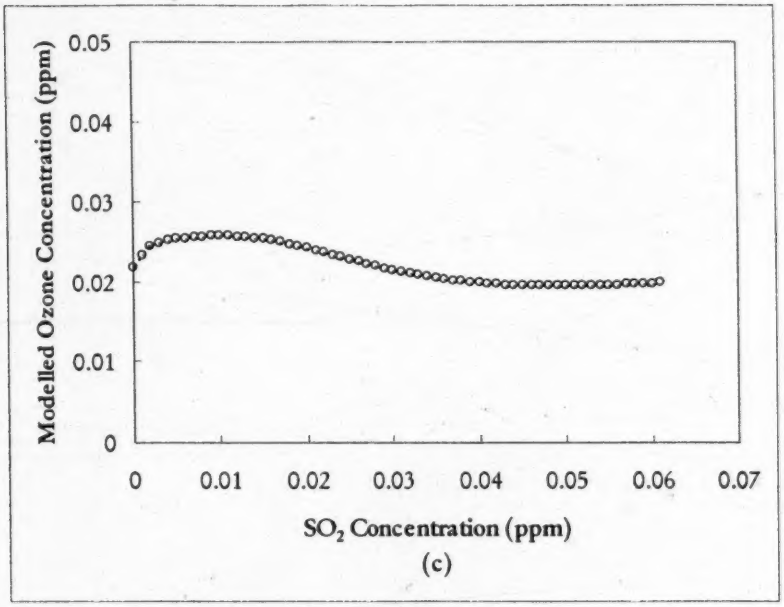

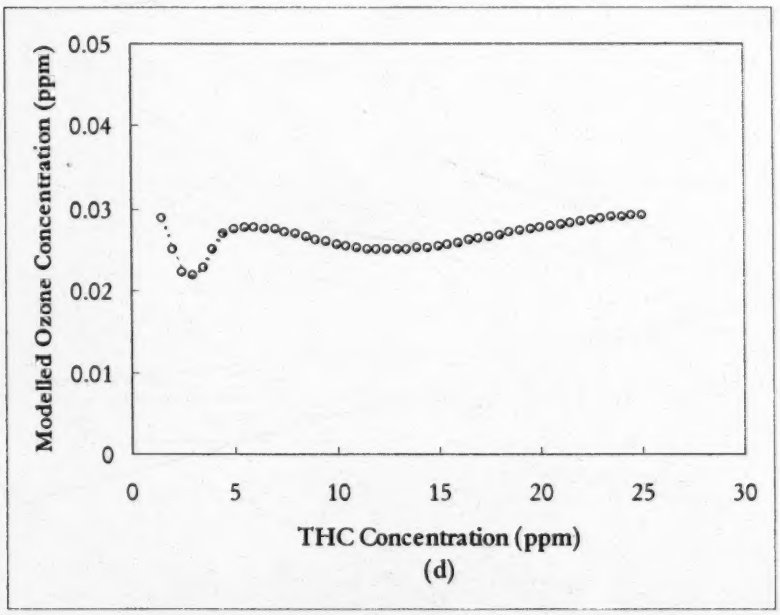

Figure 5-12 cont'd. Edmonton East virtual monitor modelled ozone concentration variation with pollutant concentrations: (a) NO; (b) NO_2; (c) SO_2; and (d) THC.

The sensitivity of ozone concentrations to relative humidity shows a definite trend, where an increase in relative humidity results in a decrease in ozone concentrations (Figure 5-13b). This may be related to the wet deposition of ozone and precursors from the atmosphere in

conditions of high humidity. Also, increased reactions between ozone and moisture in the air decrease concentrations of gaseous ozone.

Figure 5-13c shows a linear increase in ozone concentrations with increases in temperature up to 34°C. Beyond 34°C, ozone concentration rises more dramatically with an increase in temperature, indicated by a steeper slope. The large change in ozone concentration in the temperature range evaluated for the sensitivity analysis is consistent with the effects of temperature on reaction kinetics, but appears to disagree with the earlier input variable analysis, in which temperature was not a significant factor. This may be because in the sensitivity analysis, all other input variables are held constant at their median values. It is possible that fluctuations in the inputs found to be dominant in the input variable analysis have a greater impact on ozone concentrations than temperature fluctuation by itself.

According to Figure 5-13d, wind direction changes have a minimal effect on ozone concentrations. This is consistent with the analysis of input contribution factors in Figure 5-3, in which wind direction is relatively unimportant. There is approximately a 0.01 ppm change in ozone concentration over the 360° range of wind directions. Wind directions of 0°, or calms, resulted in the highest ozone concentrations. This is consistent with the fact that calm conditions allow pollutants to accumulate and persist, resulting in higher ambient concentrations. However, in this model, the changes in ozone concentrations with wind direction are negligible. At first glance, this would seem to suggest that no specific source of ozone or its precursors dominates ozone concentrations at this location. However, since all pollutant concentrations are held constant in the sensitivity analysis and only the wind direction is varied, the effects of any specific sources are hidden. Realistically, if a specific source of precursor compounds was present, there would be an accompanying increase in the pollutant concentration when winds were blowing from the source direction that would then affect ozone concentrations.

Figure 5-13e shows that when all variables are held constant, increases in wind speed result in increased ozone concentration. This is unexpected, considering that calms should produce the situations most conducive to ozone accumulation. The increase in ozone

concentrations when wind speeds are increased may be due to the selection of the East station for modelling. This station is located further away from high volume traffic sources. At higher wind speeds, the model may be detecting the influence of ozone transport from other locations further away from the monitoring station.

Although the sensitivity analysis gives an indication of how ozone concentrations respond to changes in pollutant concentrations and time, the best use of the ANN would be to model realistic scenarios, where inputs can simultaneously deviate from their median values. Since ozone formation is nonlinear and atmospheric conditions are dynamic, this would allow the model to account for the interplay between different species and conditions.

Since most of the variation in ozone concentration occurs during the day, the effect of using only daylight data to train the ANN was evaluated. Figure 5-14 shows a comparison of networks trained with 24 hour data and a network that uses only data from daylight hours for training. The months of May, June, July, and September had a slightly greater importance when only daylight data were used for training. August was the only month whose relative contribution factor decreased. With days of the week, no trends in the changes to the contribution factor were observed. NO remained the largest contributor, but showed an increased importance in the daytime only data. This may be due to the increase in vehicular traffic, and therefore greater scavenging effects, during the daytime. Increased solar radiation in the daytime also results in greater photochemical activity. NO_2, SO_2, and THC concentrations were less important to ozone prediction during the daytime. Opacity was also less important in the daytime model. Relative humidity, wind direction, and wind speed were slightly more important during the day, while the importance of temperature remained constant. Note that no effort was made to optimize the network structure for the daytime model. The relative contributions of the inputs to the daytime model would change if the network structure were changed.

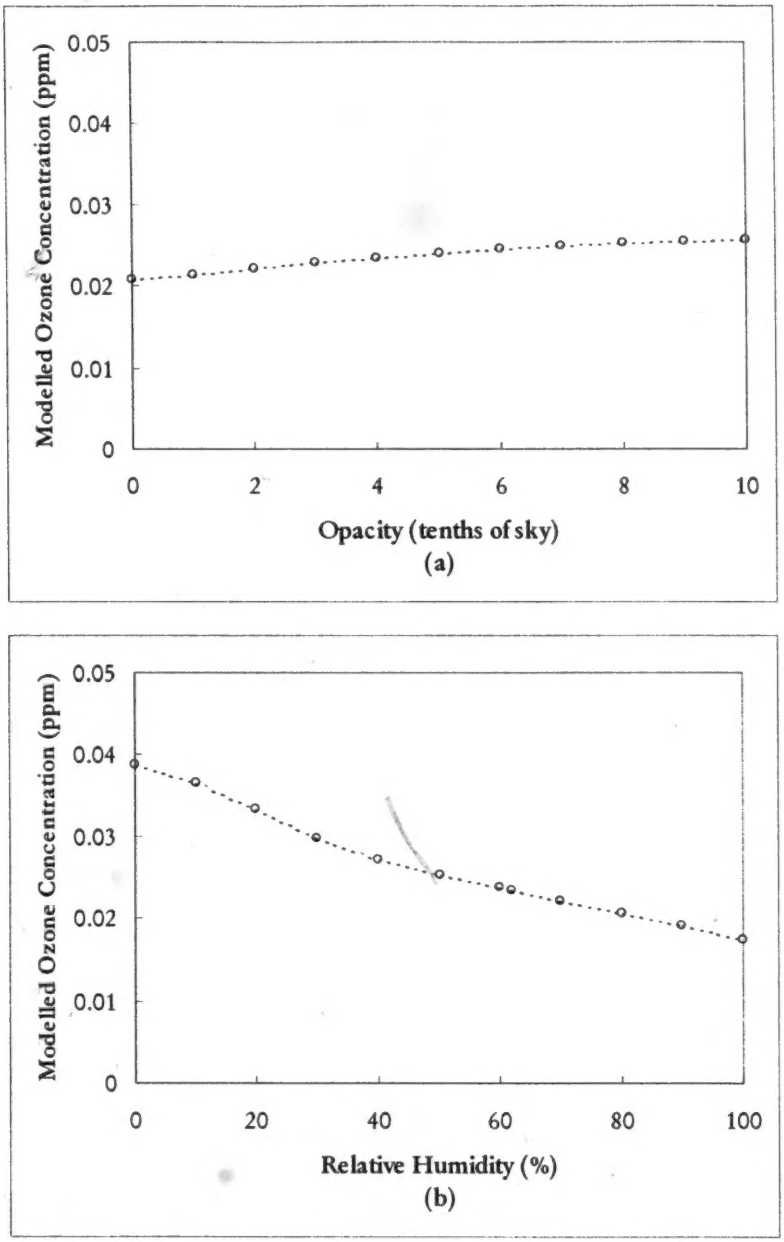

Figure 5-13 Edmonton East virtual monitor modelled ozone concentration variation with meteorological parameters: (a) opacity; (b) relative humidity; (c) temperature; (d) wind direction; and (e) wind speed.

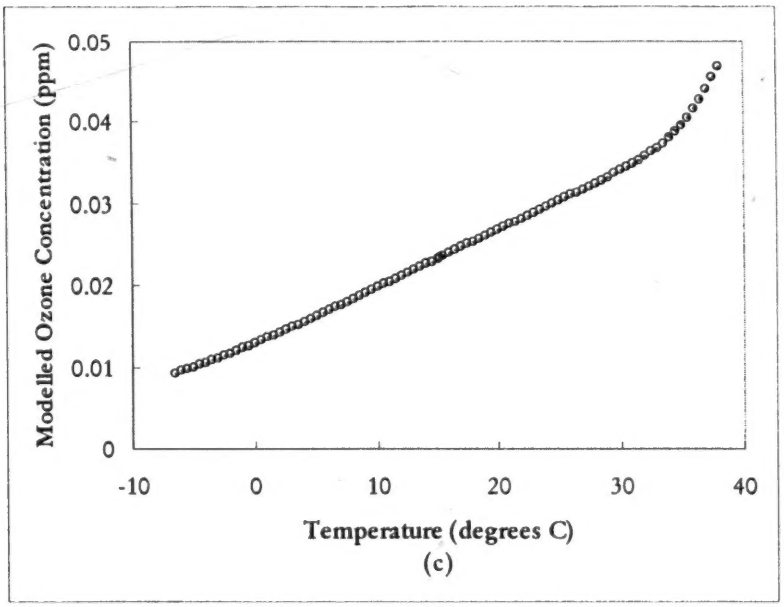

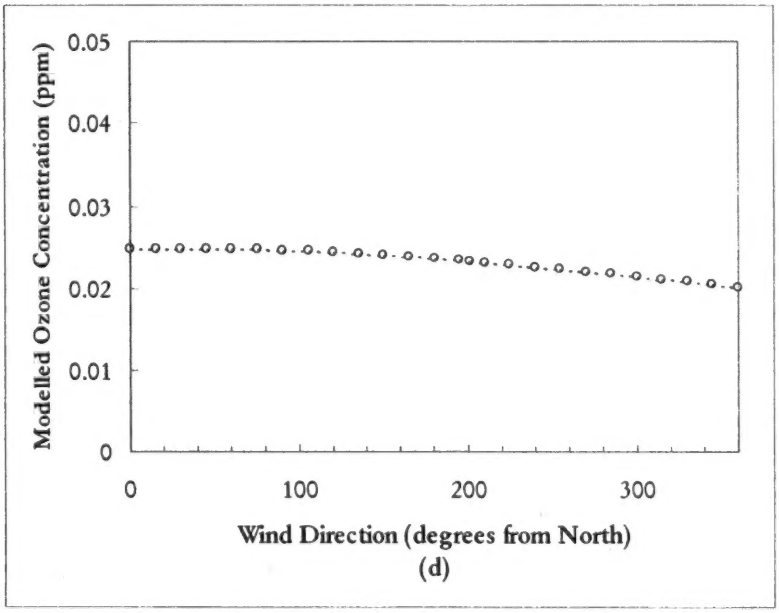

Figure 5-13 cont'd. **Edmonton East virtual monitor modelled ozone concentration variation with meteorological parameters: (a) opacity; (b) relative humidity; (c) temperature; (d) wind direction; and (e) wind speed.**

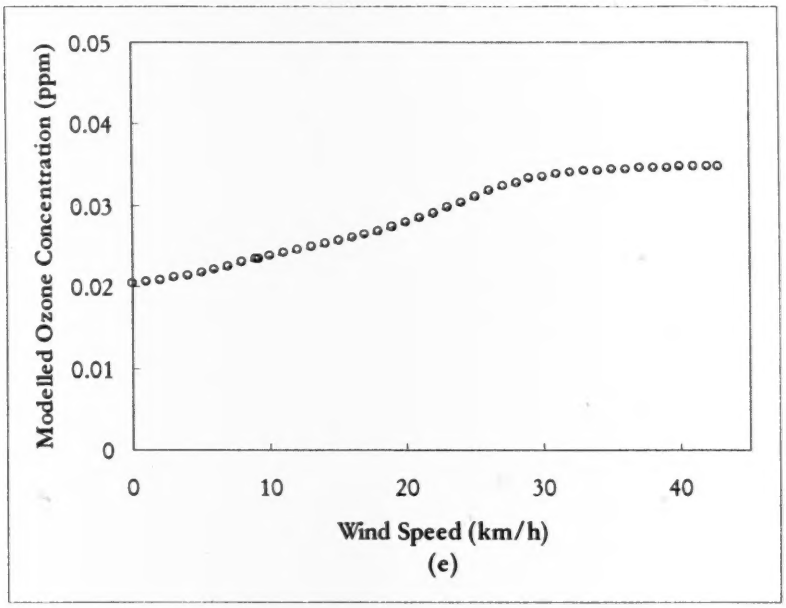

Figure 5-13 cont'd. **Edmonton East virtual monitor modelled ozone concentration variation with meteorological parameters: (a) opacity; (b) relative humidity; (c) temperature; (d) wind direction; and (e) wind speed.**

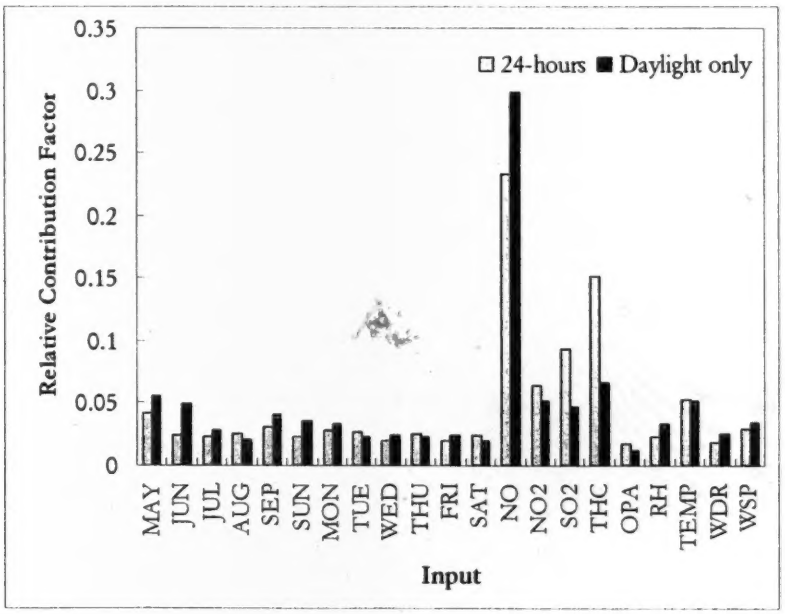

Figure 5-14 **Comparison of relative contribution factors for daylight only data and 24 hour data.**

The virtual monitor model including the ozone concentration from the previous hour was further developed. As discussed earlier, the disadvantage of the virtual monitor model is its reliance on the availability of ozone concentration from the previous hour. However, where the availability of these data is not a concern, the virtual monitor model with time series effects is able to more accurately predict ozone concentrations. Therefore, this model was optimized using the same process as for the virtual monitor without ozone time series effects.

Figure 5-15 is a surface plot showing the results of the network structure optimization. The best structure for the virtual monitor model with time series had 11 neurons in the hidden layer and was trained with 1100 epochs, resulting in a production set R^2 of 0.94. The model required a fewer number of hidden layer neurons and training epochs, despite the additional input parameter (ozone concentration at t-1).

The model performance for July 2002 production data, which contains the highest ozone concentration in the production data, is shown in Figure 5-16. The model is able to predict most peaks well. The fractional bias of the virtual monitor model is slightly higher, at 0.099, than the virtual monitor model, indicating a slight propensity to under-predict high values of ozone concentration. However, the Wilmott indices of agreement are better than the indices for the virtual monitor without time series effects, suggesting that this model has better predictive ability over the entire range of ozone concentrations than the model without ozone time series effects. Figure 5-17 shows the comparison between the modelled and actual ozone concentrations. Values of ozone concentration greater than 0.065 ppm reflect the tendency of the model to under-predict peaks, with the circles falling above the 45° line. Model predictions of concentration values below 0.065 ppm show good agreement and generally cluster around the 45° line. Figures 5-18 and 5-19 of the model residuals show no patterns with time or model predicted concentrations.

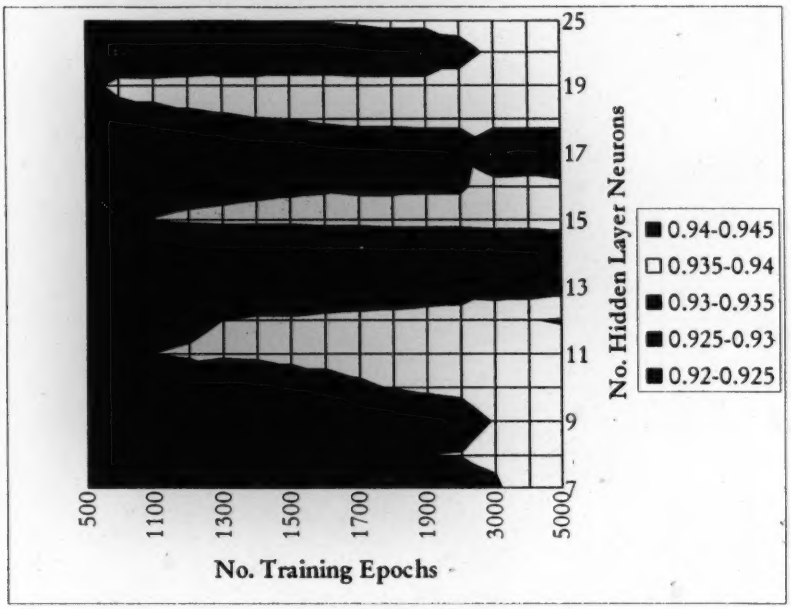

Figure 5-15 Edmonton East virtual monitor model with time series effects included: surface plot of architecture determination.

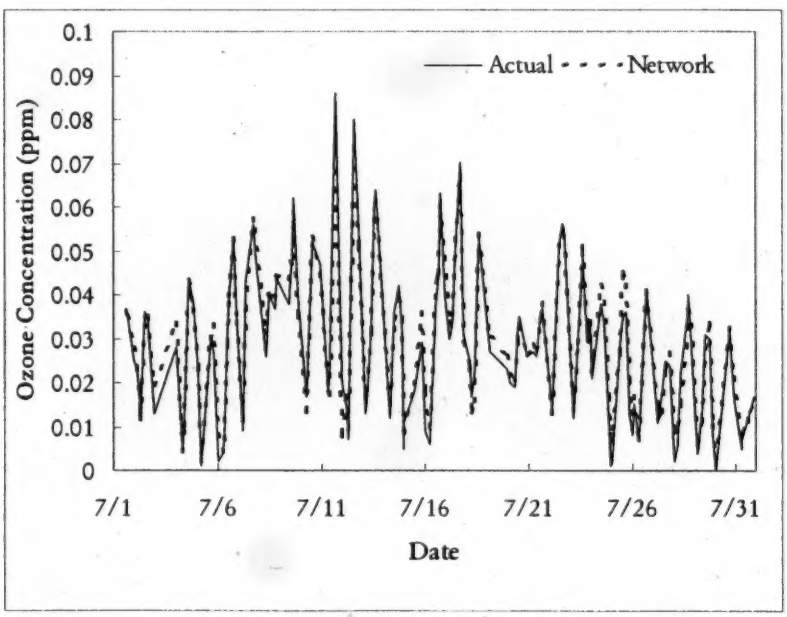

Figure 5-16 Edmonton East virtual monitor model with ozone time series: performance for July 2002 production data, $R^2 = 0.94$.

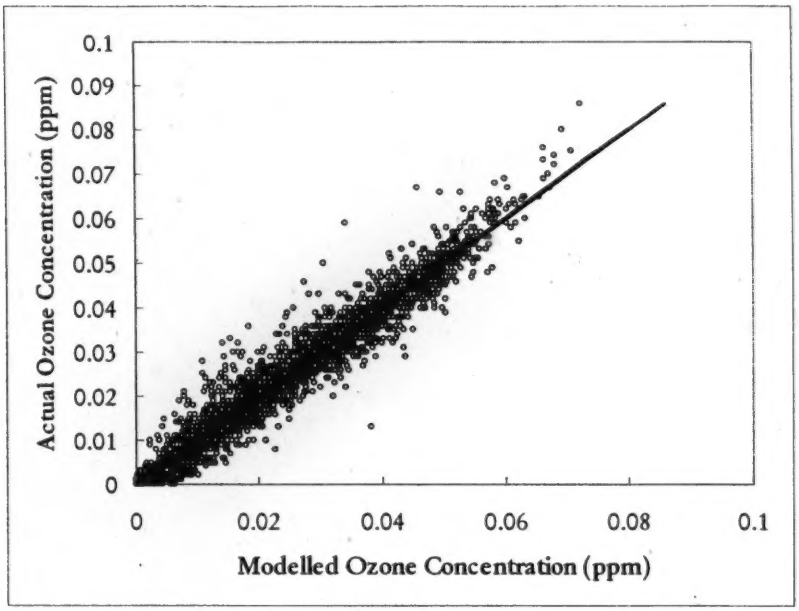

Figure 5-17 Edmonton East virtual monitor model with ozone time series: comparison of actual to modelled ozone concentrations.

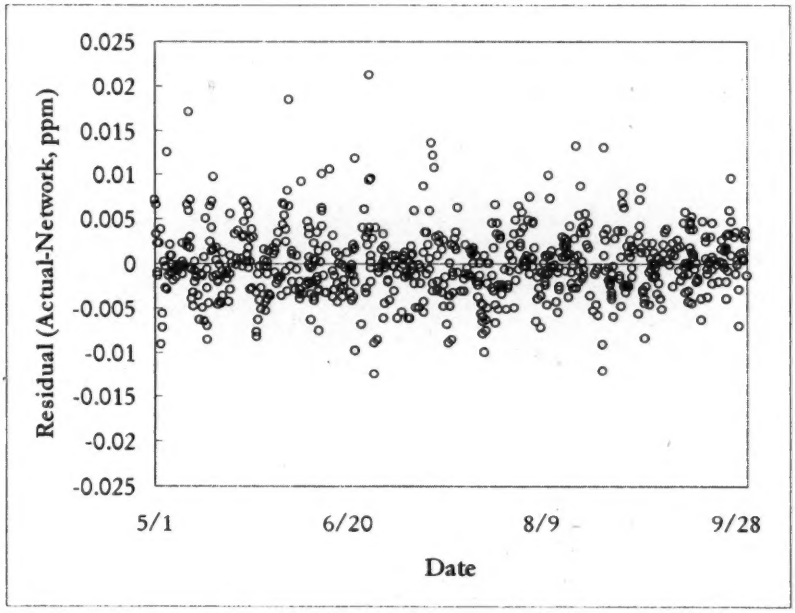

Figure 5-18 Edmonton East virtual monitor model with time series: variance of residuals with time for 2002 production set data.

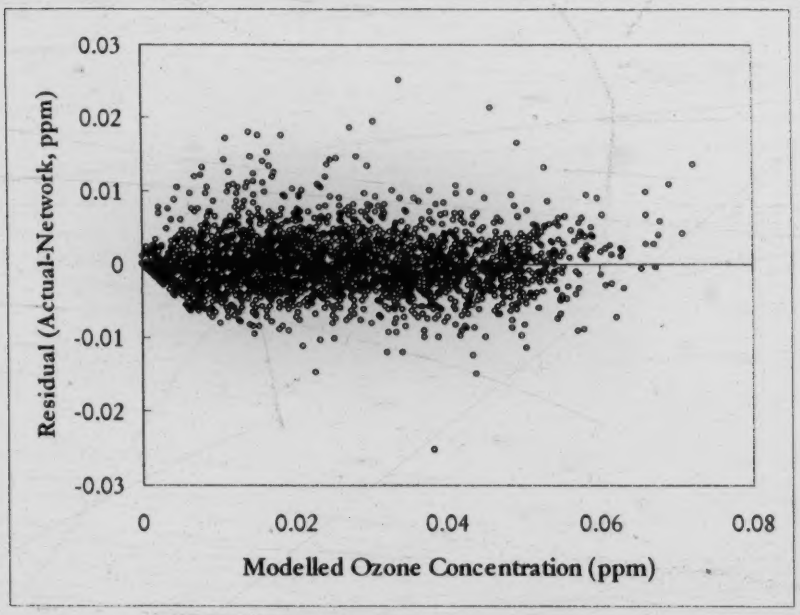

Figure 5-19 Edmonton East virtual monitor model with time series: variance of residuals with modelled ozone concentration.

Figure 5-20 shows a comparison of relative contribution factors between the model with ozone time series effects and the model excluding time series considerations. When ozone concentration from the previous hour is included in the virtual monitor model, the relative contribution factors of NO_2 and SO_2 increase, while contributions of NO and THC decrease. The contribution factors of all other inputs were fairly similar in the two models. The relative contribution factor of the ozone concentration from the previous hour was 0.129, indicating the importance of this variable for predicting ozone concentration.

Figure 5-21 shows the surface plot of the one hour in advance forecast structure determination. The best network consisted of 6 neurons in the hidden layer and required 2000 epochs to train. Note that for the forecast model, all parameters available at time t were used to predict the ozone concentration at t+1, including the ozone concentration at time t. This is somewhat equivalent to including ozone concentration at t-1 in the virtual monitor model, where the ozone concentration at t-1 accounted for greater than 12% of the ozone variability at t, since it acknowledges the serial correlation of ozone concentrations.

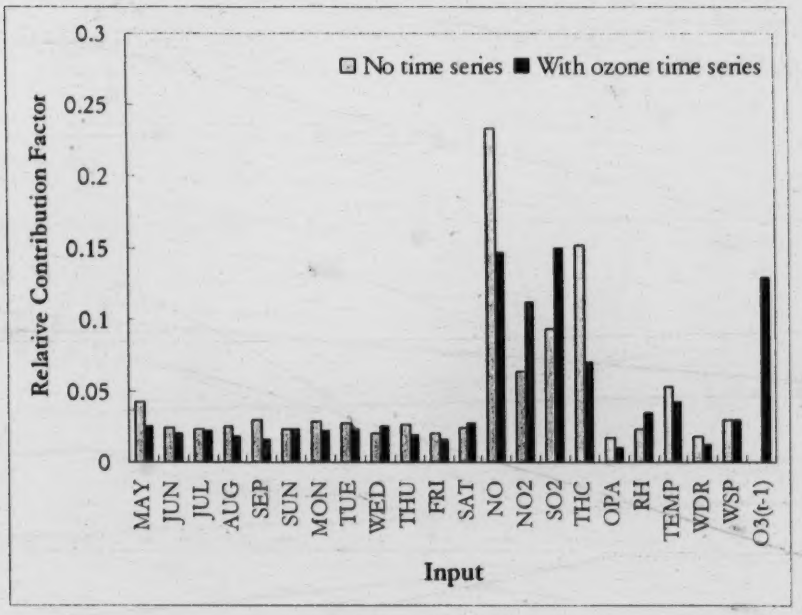

Figure 5-20 Edmonton East virtual monitor comparison of relative contribution factors for model with and without ozone time series effects.

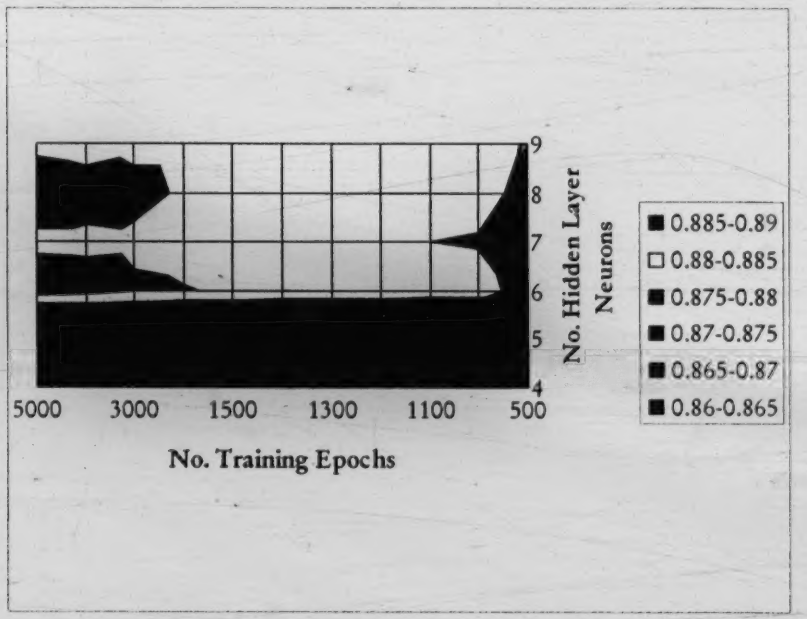

Figure 5-21 Edmonton East one hour in advance forecast model surface plot of architecture determination.

The one hour forecast model resulted in a R^2 of 0.89 for the production set of data. The performance of this model is shown in Figure 5-22, for July 2002 data. Surprisingly, the fractional bias of the one hour forecast model was less than the fractional bias of both the virtual monitor models. This indicates the forecast model is able to better predict the 25 highest concentrations without as much bias as the virtual monitor models (i.e., the forecast model under-predicted to a lesser degree). The Wilmott indices of agreement for the one hour forecast model are slightly better than the indices for the virtual monitor model, but slightly less than the indices calculated for the virtual monitor model with ozone time series effects.

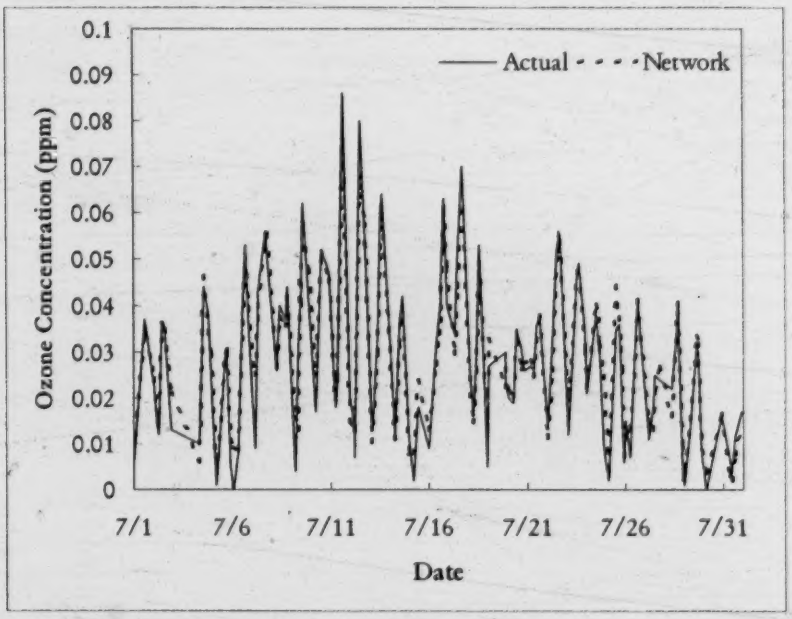

Figure 5-22 Edmonton East one hour forecast model performance for July 2002 production set data, $R^2 = 0.89$.

Figure 5-23, illustrating the actual versus modelled concentrations of ozone, shows that there may be a slight under-prediction of the highest 25 ozone concentrations, although a few of these peaks are over-predicted. In general, the plot falls along the 45° line, confirming good agreement between the modelled and actual ozone concentrations. As with the virtual monitor models, no trends are apparent in the residuals analysis (Figures 5-24 and 5-25).

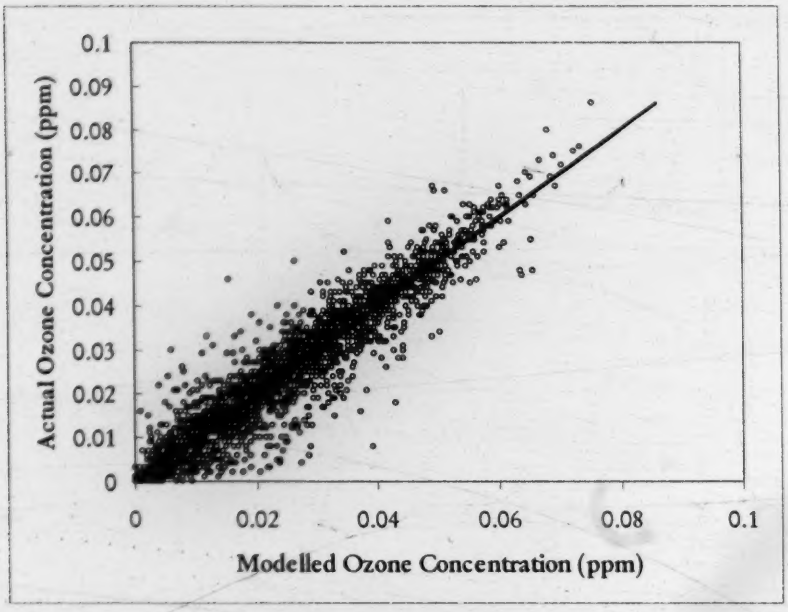

Figure 5-23 Edmonton East one hour forecast model comparison of actual and modelled ozone concentrations.

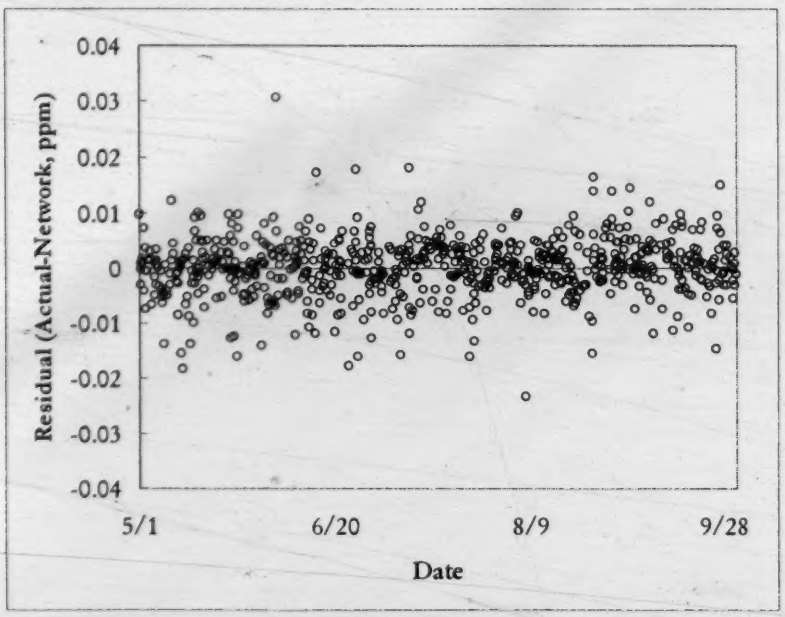

Figure 5-24 Edmonton East one hour forecast model residuals analysis: variance with time for 2002 production set data.

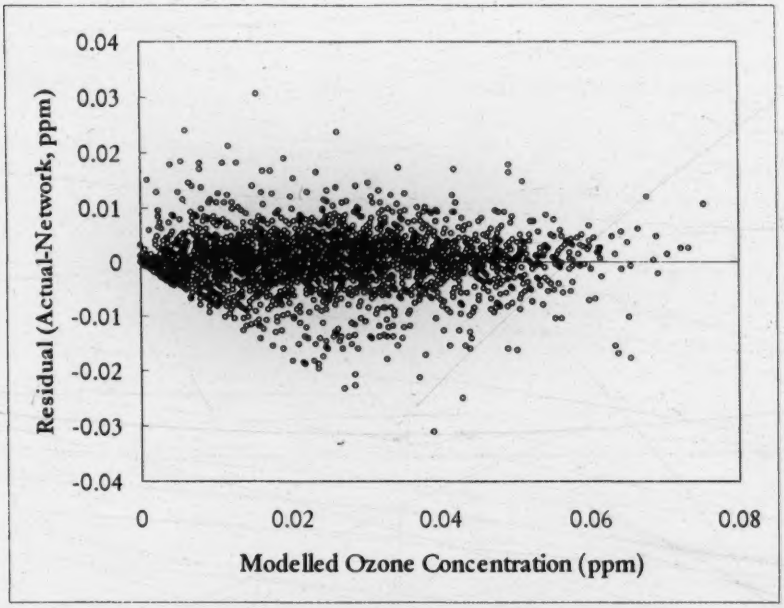

Figure 5-25 Edmonton East one hour forecast model scatter plot of residuals: variation with modelled ozone concentration.

To test the effects of the ozone time series in the forecast model, a one hour forecast network was developed including the ozone concentration at t-1. This model loosely parallels the virtual monitor model including ozone concentrations at both t-1 and t-2, since it incorporates ozone concentrations from the two time periods immediately preceding the time period of interest. Figure 5-26 shows the network performance on July 2002 production data. The best network for the one hour forecast including the ozone concentration at t-1 consists of 6 neurons in the hidden layer and 500 training epochs. The resulting production set R^2 was negligibly higher than that of the one hour forecast model, with a R^2 of 0.90. The fractional bias of the one hour forecast model with time series was slightly higher than the one hour forecast model, but the Wilmott indices were consistent. A one hour forecast model incorporating ozone time series concentrations to t-2 also showed no improvements with a production set R^2 of 0.89. Therefore, there are no advantages to having previous hours' concentrations of ozone in the forecast model. The results of the ANN models show that when modelling ozone, only concentrations from the hour

immediately preceding the hour of interest are useful for estimating the ozone concentration. The addition of further terms in the ozone time series does not benefit model performance.

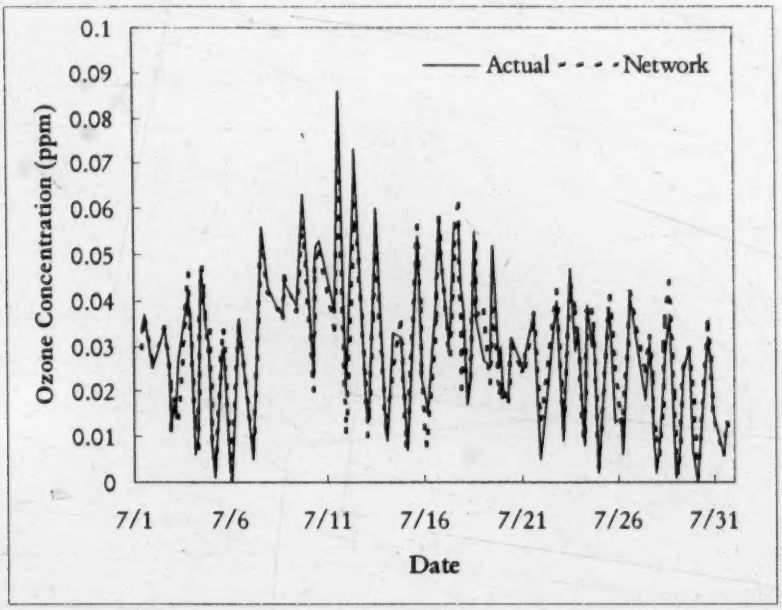

Figure 5-26 Edmonton East one hour in advance forecast with ozone time series effects: model performance for July 2002 production set data, $R^2 = 0.90$.

As expected, the ANN prediction performance declines for the two hour in advance forecast, barely meeting the minimum performance requirement with a R^2 of 0.75. The surface plot of the network structure evaluation is shown in Figure 5-27. The best network configuration has 15 neurons in the hidden layer and requires 1000 training epochs.

Figure 5-28 shows the performance of this model for July 2002 production data. Compared to the one hour forecast, there is an obvious decline in performance. The ANN struggled with pinpointing peaks in magnitude and in time, with time shifts in some of the peak predictions. There is a tendency for the ANN to under-predict the highest 25 concentrations, denoted with a fractional bias of 0.122. The Wilmott indices of agreement are 0.76 and 0.92 for d_1 and d_2, respectively.

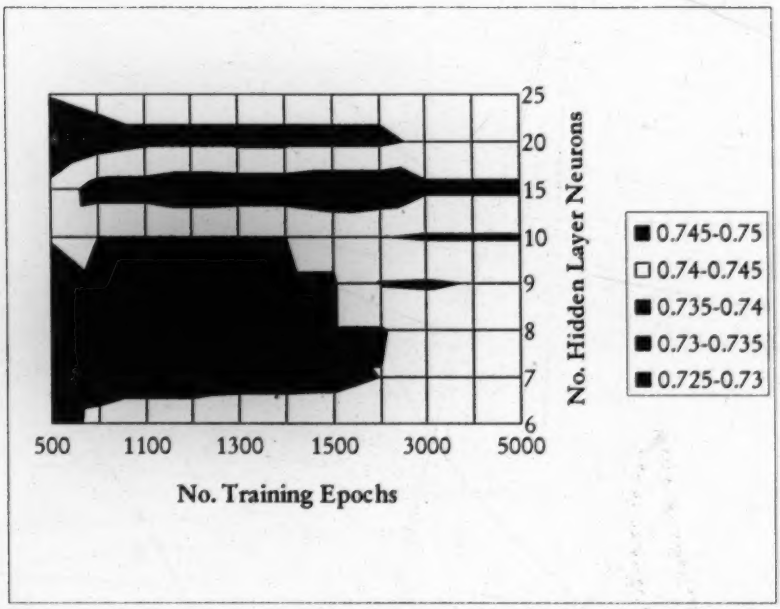

Figure 5-27 Edmonton East two hours in advance forecast model surface plot

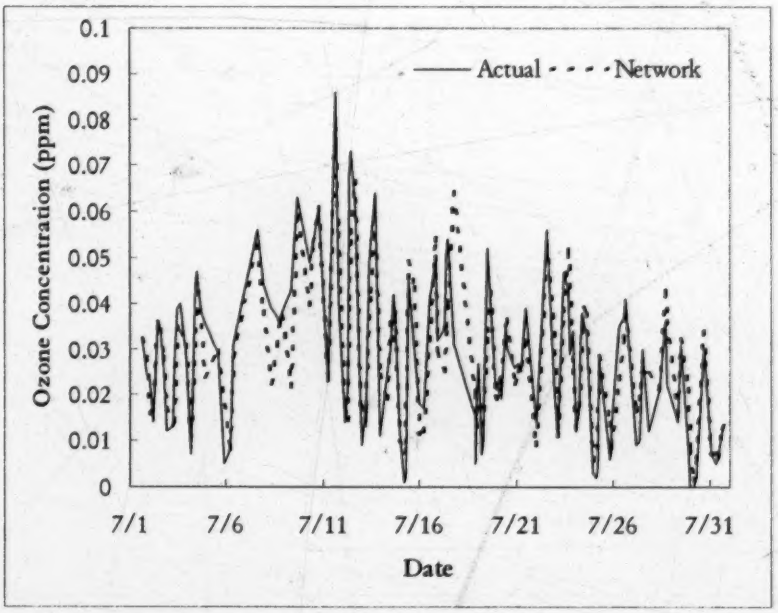

Figure 5-28 Edmonton East two hours in advance forecast model performance for July 2002 production set data, $R^2 = 0.75$.

The plot of actual to modelled ozone concentrations in Figure 5-29 confirms the model's tendency to under-predict at high end values of ozone concentration. The residuals analysis in Figures 5-30 and 5-31 show no trends in the model residuals.

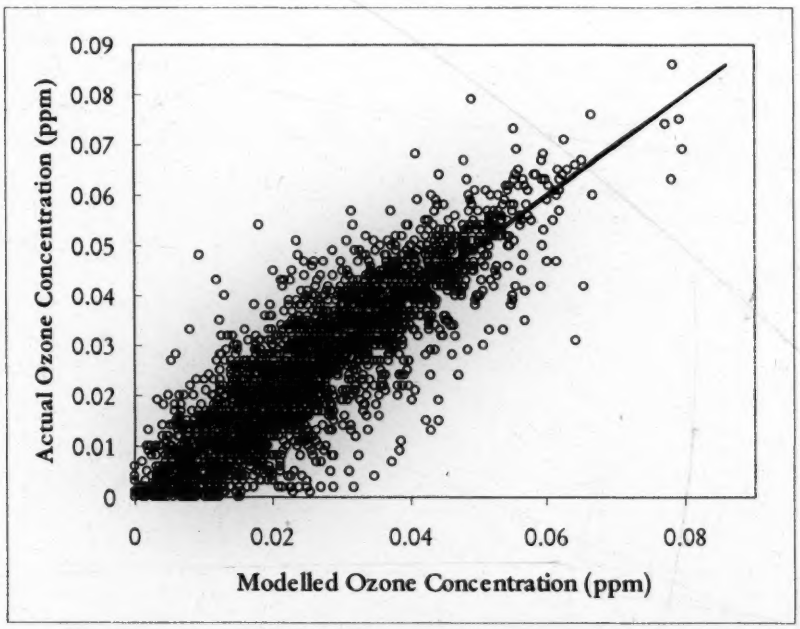

Figure 5-29 Edmonton East two hours in advance forecast model comparison of actual to modelled ozone concentration.

The two hour in advance forecast with ozone time series showed a slight improvement in predictive ability over the two hour forecast model without time series effects. The production set R^2 for this model was 0.78 (see Figure 5-32). The fractional bias of the two hour forecast with time series was slightly better as well, with a value of 0.081. This trend is opposite to that observed with the other models, where networks with time series effects had higher bias values. The Wilmott indices show a similar performance overall between the two hour forecast with and without ozone time series effects, with values of 0.77 and 0.93 for d_1 and d_2 for the model with ozone time series effects.

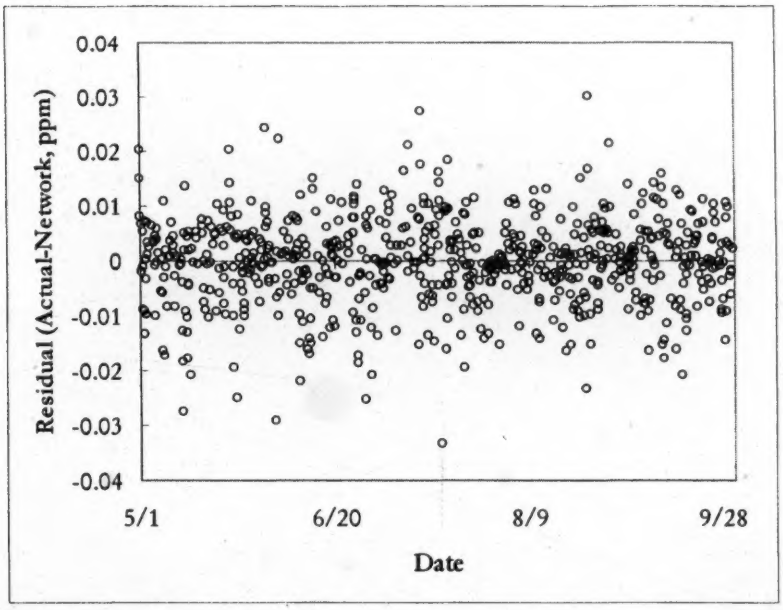

Figure 5-30 Edmonton East two hours in advance forecast model residuals variance with time.

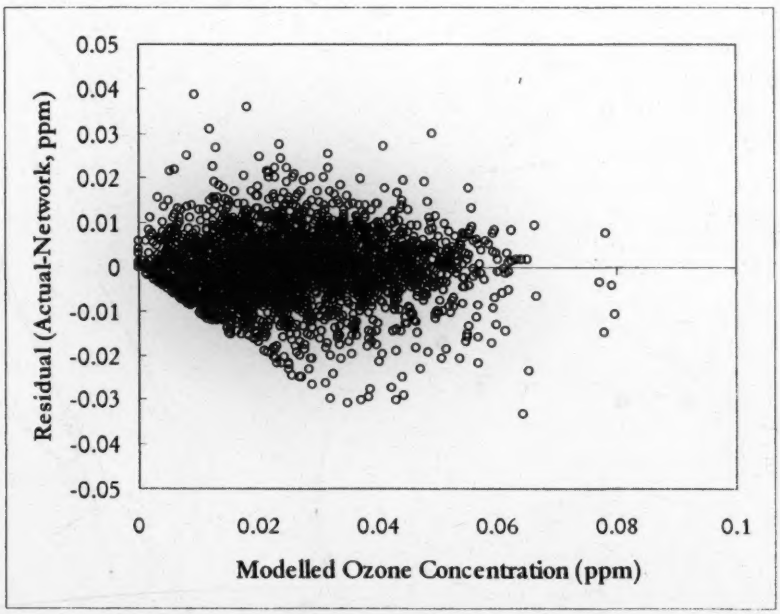

Figure 5-31 Edmonton East two hours in advance forecast model residuals variance with modelled ozone concentration.

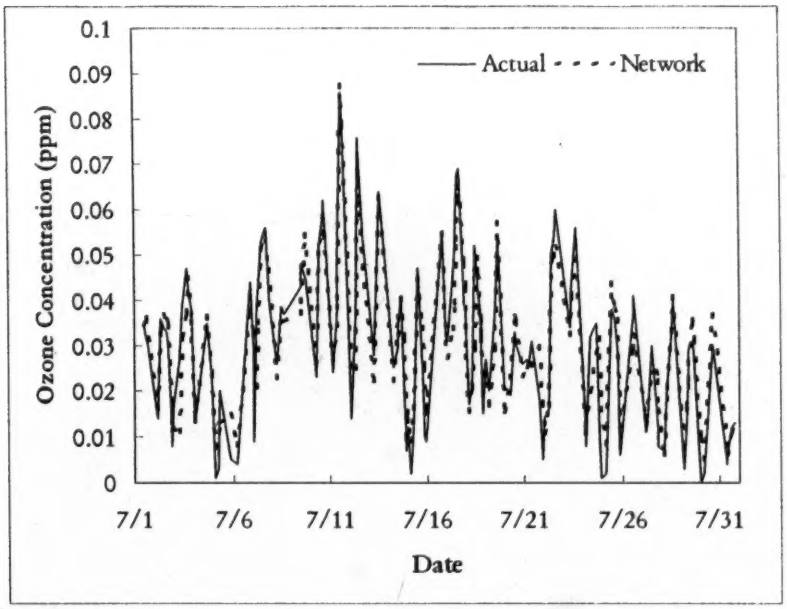

Figure 5-32 Edmonton East two hours in advance forecast with ozone time series: model performance on July 2002 production set data, $R^2 = 0.78$.

Comparison of the time series model with the no time series models, based on the Wilmott indices of agreement, indicates that models incorporating the ozone time series as input have an improved overall predictive ability.

Figure 5-33 shows the trend in model performance with increasing prediction window for models with and without ozone time series effects. Not surprisingly, increasing the prediction window results in a performance decline. This trend is observed for both models with and without ozone time series effects. The performance difference between models with and without time series effects also increases slightly as the prediction window increases. Based on the optimized models, the maximum forecast window that will meet a minimum R^2 value of 0.75 is two hours. This suggests that ANN models built to forecast greater than two hours in advance will likely exhibit poor prediction performance, because the ozone concentration at any given time t is correlated mainly with the concentration in the preceding hour t-1. The correlation with concentrations further removed than t-1 becomes progressively smaller, so that the larger the time window, the more difficulty the ANN has predicting the ozone concentration at t.

A possibility for overcoming this problem is predicting the hourly ozone concentration using conditions from the previous day (ozone concentration at t predicted with data from t-24). Since the ozone data consistently show strong diurnal patterns, the data from the same hour of the previous day may be a better indicator of the ozone concentration of the current day. This is an avenue for further exploration in future research, as there are many benefits in maximizing the prediction window. A day in advance warning of high ozone concentrations will allow regulatory bodies to better prepare their ozone management tactics and allow the public to develop a plan for exposure avoidance. Control strategies could also be implemented to avert the high ozone situation.

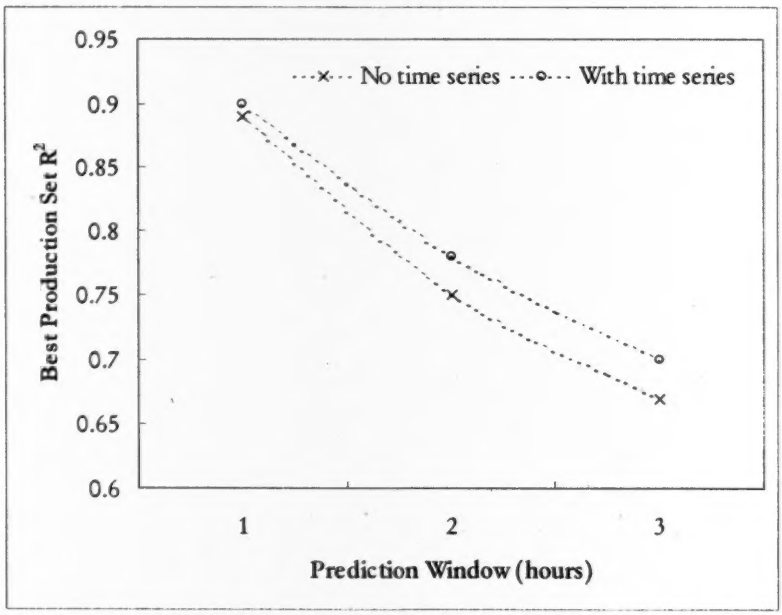

Figure 5-33 Edmonton East forecast model effects of increased prediction window and inclusion of time series inputs.

Table 5-8 is a summary of the features for the best Edmonton East ANN models. There were no relationships between the network structure and the type of model developed. Optimized forecast models did not necessarily have a more complex network architecture or require a greater number of epochs to train than the virtual monitor models. The time series

versions of the virtual monitor and one hour forecast models required fewer training epochs. However, this relationship was reversed in the two hour forecast model.

Table 5-8 Summary of network features for best Edmonton East ANN models.

Feature Description	VM	VMTS	FM_1	$FMTS_1$	FM_2	$FMTS_2$
Target output	$O_3(t)$	$O_3(t)$	$O_3(t+1)$	$O_3(t+1)$	$O_3(t+2)$	$O_3(t+2)$
Input layer						
No. inputs	21	22	22	23	22	23
Inputs at t	MAY JUN JUL AUG SEP SUN MON TUE WED THU FRI SAT NO NO_2 SO_2 THC OPA RH TEMP WDR WSP	MAY JUN JUL AUG SEP SUN MON TUE WED THU FRI SAT NO NO_2 SO_2 THC OPA RH TEMP WDR WSP $O_3(t-1)$	MAY JUN JUL AUG SEP SUN MON TUE WED THU FRI SAT NO NO_2 SO_2 THC OPA RH TEMP WDR WSP O_3	MAY JUN JUL AUG SEP SUN MON TUE WED THU FRI SAT NO NO_2 SO_2 THC OPA RH TEMP WDR WSP O_3 $O_3(t-1)$	MAY JUN JUL AUG SEP SUN MON TUE WED THU FRI SAT NO NO_2 SO_2 THC OPA RH TEMP WDR WSP O_3	MAY JUN JUL AUG SEP SUN MON TUE WED THU FRI SAT NO NO_2 SO_2 THC OPA RH TEMP WDR WSP O_3 $O_3(t-1)$
Hidden layer						
Activation function	logistic	logistic	logistic	logistic	logistic	logistic
No. neurons	17	11	6	6	15	9
Output layer activation function	logistic	logistic	logistic	logistic	logistic	logistic
No. training epochs	3,000	1,100	2,000	500	1,000	1,300
No. training patterns	7,754	7,682	7,681	7,612	7,647	7,547
No. test patterns	2,585	2,561	2,561	2,538	2,549	2,516
No. production set patterns	2,584	2.560	2,560	2,537	2,549	2,515

Key:
VM = Virtual monitor model
VMTS = Virtual monitor model with ozone time series effects
FM = Forecast model (subscript denotes prediction window in hours)
FMTS = Forecast model with ozone time series effects (subscript denotes prediction window in hours)

The corresponding performance statistics for the developed models are provided in Table 5-9. A range of performance statistics can be used for evaluating network performance. In general, the coefficient of multiple determination R^2 is a more conservative estimator of model performance than Pearson's product moment correlation coefficient r. The order of conservatism for the performance indicators, beginning with the most conservative, is: d_1, R^2, r, and d_2. The MSE of the time series models were slightly lower than the MSE of their corresponding models without time series effects. Time series models generally perform as well or better than the model without time series effects. As discussed earlier, the inclusion of time series inputs detracts from the versatility of the ANN model since the model then becomes dependant on the availability of data from previous hours. The connection weights between neurons in each of these networks are provided in Appendix A.

Table 5-9 Summary of performance statistics for best Edmonton East ANN models.

Statistic	VM	VMTS	FM_1	$FMTS_1$	FM_2	$FMTS_2$
Training set R^2	0.89	0.94	0.89	0.89	0.78	0.79
Test set R^2	0.87	0.94	0.89	0.89	0.77	0.77
Production set						
R^2	0.87	0.94	0.89	0.90	0.75	0.78
r	0.93	0.97	0.94	0.95	0.86	0.88
MSE (ppm^2x10^5)	3.27	1.59	2.80	2.53	6.17	5.48
RMSE (ppm)	0.006	0.004	0.005	0.005	0.008	0.007
MAE (ppm)	0.004	0.003	0.004	0.004	0.006	0.006
AE_{min} (ppm)	0	0	0	0	0	0
AE_{max} (ppm)	0.032	0.025	0.031	0.035	0.038	0.042
Bias(mean)	0.084	0.099	0.079	0.098	0.122	0.081
Wilmott d_1	0.83	0.89	0.85	0.86	0.76	0.77
Wilmott d_2	0.96	0.98	0.97	0.97	0.92	0.93

Although the systematic approach is somewhat labour intensive compared to an ad-hoc approach, it provides a standardized, methodical approach to developing ANN models that is currently lacking in the literature. There are areas of the approach that require further research for the atmospheric sciences field. During pre-processing, a better understanding of the causes of ozone excursions is required. Infrequent and relatively unpredictable incidences, such as forest fires and stratospheric intrusions, and their subsequent impacts on ground level ozone concentrations, are difficult to model. Methods for quantifying their

influences have been studied (e.g., Cheng et al. 1998 for forest fire effects), but are still poorly developed.

For each of the models developed for Edmonton East, several combinations of hidden and output layer activation functions and network architectures produced equivalent performance results. This finding reflects the black box nature of the ANN modelling tool, and suggests that the task of dissecting the network anatomy to build a general description of the modelled process would be challenging. This work also indicates that several network features are interrelated. The optimum inputs to the model are related to and influenced by the activation function combination chosen, the network structure, and the training requirements, in addition to the modelled process.

5.5 Conclusions

Ground level ozone modelling in Edmonton is complicated by the nonlinearity of the process and the variety of sources of precursor compounds. However, accurately predicting ground level ozone concentrations offers benefits such as the ability to provide advance warning of impending high levels and implementing control or exposure avoidance strategies. Artificial neural networks are a viable option for modelling ozone. The ANN virtual monitor model for Edmonton East performed at a R^2 level of 0.87, while the one hour forecast model produced a R^2 of 0.89. Including the ozone concentration from the previous hour in these models improved R^2 to 0.94 and 0.90, respectively. The variables most important to the model, in order of relative importance, were NO, DAY (combined contribution factor for all days), THC, MTH (combined for all months), SO_2, NO_2, TEMP, WSP, RH, WDR, and OPA. With a minimum acceptable performance level of R^2 equal to 0.75, the maximum forecast window was two hours.

The systematic approach provides a methodical strategy to develop an ANN model. However, the resulting model, although optimized for the network structure and inputs, is not unique to the process modelled, and several models may yield similar performance. For this reason, the task of interpreting the ANN to create a generalized description of the modelled process would be difficult. Therefore, developing an ANN model requires the

marriage of scientific knowledge of the process with the principles of the systematic approach.

5.6 References

Abdul-Wahab, S.A. and Al-Alawi, S.M. 2002. Assessment and prediction of tropospheric ozone concentration levels using artificial neural networks. Environmental Modelling & Software, 17: 219-228.

Baxter, C.W. 2002. Applications of Artificial Neural Networks in Drinking Water Treatment Process Modeling and Control, Ph.D. thesis. Department of Civil and Environmental Engineering, University of Alberta, Edmonton, AB.

Benkley, C.W. and Schulman, L.L. 1979. Estimating hourly mixing depths from historical meteorological data. Journal of Applied Meteorology, 6(18): 772-780.

CEPA/FPAC WGAQOG— Canadian Environmental Protection Act Federal/Provincial Working Group on Air Quality Objectives and Guidelines. 1999. National Ambient Air Quality Objectives for Ground-Level Ozone Science Assessment Document, Catalogue No. En42-17/702-1999E. Health Canada and Environment Canada, Downsview, ON and Ottawa, ON.

Chaikowsky, C.L.A. 2001. Overview of Ground-Level Ozone Observations in Alberta, 1986-1998. Science and Technology Branch, Environmental Sciences Division, Alberta Environmental Protection, Edmonton, AB.

Cheng, L., McDonald, K.M., Angle, R.P. and Sandhu, H.S. 1998. Forest fire enhanced photochemical air pollution. A case study. Atmospheric Environment Part A, 32(4): 673-681.

Cobourn, W.G., Dolcine, L., French, M., and Hubbard, M.C. 2000. A comparison of nonlinear regression and neural network models for ground-level ozone forecasting. Journal of the Air & Waste Management Association, 50: 1999-2009.

Comrie, A. C. 1997. Comparing neural networks and regression models for ozone forecasting. Journal of the Air & Waste Management Association, 47: 653-663.

Cox, William M. 1988. Protocol for Determining the Best Performing Model. United States Environmental Protection Agency Office of Air Quality Planning and Standards, Technical Support Division, Source Receptor Analysis Branch, Washington, DC.

El-Din, A. and Smith, D.W. 2002. A neural network model to predict the wastewater inflow incorporating rainfall events. Water Research, 36(5): 1115-1126.

Elkamel, A., Abdul-Wahab, S., Bouhamra, W., and Alper, E. 2001. Measurement and prediction of ozone levels around a heavily industrialized area: a neural network approach. Advances in Environmental Research, 5: 47-59.

Environment Canada. 2003. Canadian Climate Normals 1971-2000 for Edmonton City Centre Station. Environment Canada, Downsview, ON. Accessed via the Internet at http://www.climate.weatheroffice.ec.gc.ca/climate_normals/results_e.html on July 8, 2003.

Flood, I. and Kartam, N. 1997. Systems. In Artificial Neural Networks for Civil Engineer: Fundamentals and Applications, N. Kartam, I. Flood, and J.H. Garrett, Jr. Eds. American Society of Civil Engineers, New York, NY.

Gardner, M. and Dorling, S. 2001. Artificial neural network-derived trends in daily maximum surface ozone concentrations. Journal of the Air & Waste Management Association, 51: 1202-1210.

Garrett, J.H., Jr., Gunaratman, D.J. and Ivezic, N. 1997. Introduction. In Artificial Neural Networks for Civil Engineer: Fundamentals and Applications, N. Kartam, I. Flood, and J.H. Garrett, Jr. Eds. American Society of Civil Engineers, New York, NY.

Garson, G.D. 1991. Interpreting neural-network connection weights. AI Expert, 4: 47-51.

Guardani, R., Nascimento, C.A.O., Guardani, M.L.G., Martins, M.H.R.B., and Romano, J. 1999. Study of atmospheric ozone formation by means of a neural network-based model. Journal of the Air & Waste Management Association, 49: 316-323.

Hasham, Faizal A. 1998. Modelling of Urban Air Pollution in the Edmonton Strathcona Industrial Area Using Artificial Neural Networks, Master of Science thesis. Department of Civil and Environmental Engineering, University of Alberta, Edmonton, AB.

Henseler, J. 1995. Back propagation. In Artificial Neural Networks; An Introduction to ANN Theory and Practice, P.J. Braspenning, F. Thuijsman, and A.J.M.M. Weijters, Eds. Springer-Verlag Berlin Heidelberg, Germany, 37-66.

Jain, A.K., Mao, J., and Mohiuddin, K.M. 1996 Artificial neural networks: a tutorial. Computer, 3: 31-44.

Kao, J. and Huang, S. 2000. Forecasts using neural network versus Box-Jenkins methodology for ambient air quality monitoring data. Journal of the Air & Waste Management Association, 50: 219-226.

Konovalov, Igor B. 2002. Application of neural networks for studying nonlinear relationships between ozone and its precursors. Journal of Geophysical Research, 107(D11): 8.1-8.14.

McCullum, K. 2003. Environmental Engineer, Focus Corporation Ltd., Edmonton, AB. Personal communications, October 24, 2003.

Ruiz-Suarez, J.C., Mayora-Ibarra, O.A., Torres-Jimenez, J., and Ruiz-Suarez, L.G. 1995. Short-term ozone forecasting by artificial neural networks. Advances in Engineering Software, 23: 143-149.

Sandhu, H.S. 1999. Ground-Level Ozone in Alberta. Science and Technology Branch, Environmental Sciences Division, Alberta Environmental Protection, Edmonton, AB.

Tupas, R.T. 2000. Artificial Neural Network Modeling of Filtration Performance, Master of Science thesis. Department of Civil and Environmental Engineering, University of Alberta, Edmonton, AB.

USEPA--United States Environmental Protection Agency. 1996. Air Quality Criteria for Ozone and Related Photochemical Oxidants, National Center for Environmental Assessment— RTP Office of Research and Development U.S. Environmental Protection Agency, NTIS Distributor, Research Triangle Park, NC and Springfield, VA.

Walpole, Ronald E. and Myers, Raymond H. 1993. Probability and Statistics for Engineers and Scientists, 5th ed. Macmillan Publishing Company, New York, NY.

6.0 CALGARY EAST OZONE MODELS[3]

6.1 Introduction

In recent years, air quality issues in urban centres have become the focus of numerous research efforts. Ground level ozone, a secondary pollutant formed from oxides of nitrogen (NO_x) and volatile organic compounds (VOCs), is of particular concern due to its associations with respiratory illnesses (Bates 1991; Bates et al.1990; Burnett et al.1998; Delfino et al. 1997; Dockery et al. 1993, Last et al. 1998; Lipfert and Hammerstrom 1992; McDonnell et al.1999; and Thurston et al 1997). Ozone's role in causing poor public health has drawn the attention of regulators and researchers alike. With this renewed interest in ozone comes an awareness of the deficiencies of existing modelling approaches when applied to modelling ground level ozone. Ground level ozone is a secondary pollutant, formed through reactions between precursor compounds. Its chemistry in the atmosphere is photochemical, complex, and nonlinear, creating the need for a modelling approach capable of handling these traits. One approach that has recently garnered interest in the atmospheric sciences is artificial neural networks. In this paper, a systematic approach is followed to develop an artificial neural network model for Calgary, Alberta, Canada. The intent of this research is to evaluate the success of using an optimized, artificial neural network model for ground level ozone. The input variables and network features that provide the best prediction performance, and the largest forecast window with acceptable performance, are also investigated.

6.2 Background

Artificial neural networks are a form of artificial intelligence used to model nonlinear, complex, and poorly understood systems. They have spawned recent interest in the environmental sciences and engineering field. Their pattern recognition, data analysis, and experiential learning abilities have found contemporary application in water and wastewater treatment plant processes and control (Baxter 2002; El-Din and Smith 2002a and 2002b),

---

[3] A version of this chapter will be submitted to the Journal of Applied Meteorology, Application of ANN Models as Ground-Level Ozone Virtual Monitors and Forecast Tools.

modelling of atmospheric pollutants (Cappa et al. 2001; Sharma et al. 2003; Fernandez de Castro et al. 2003; Kolehmainen et al. 2000; Plochl 2001; and Viotti et al. 2002), and prediction of weather anomalies (Baawain et al. 2003).

The base unit of an artificial neural network is the neuron. Neurons are individual processing units configured in interconnected layers. The most common type of network is the three layer, multilayer perceptron shown in Figure 6-1 (Jain et al. 1996). This type of network consists of an input layer, one or more hidden layers, and an output layer (Tupas 2000). The input layer receives input from the outside environment and transfers the data to the neurons in the hidden layer. In the hidden layer, the data are processed to produce a value for the target output. The output layer is responsible for transmitting the network results to the outside environment. Each of the connections between neurons is weighted with a signed value (either positive, negative, or neutral) to reflect the influence between the interconnected neurons (Garrett et al. 1997). The modelled process is described by the specific functions used in the network, the number of neurons in each layer of the network, how they are connected, and the connection weights. These features are determined during the network development process.

In the training phase of network development, historical data are fed to the ANN. The historical data are pre-processed to remove erroneous data, noise, and any unexplained random variance (Comrie 1997; Gardner and Dorling 2001). During training, the ANN learns from the historical data, adjusting connection weights between neurons to map out the relationship between the set of inputs and the targeted output. How the ANN adjusts connection weights to fit the historical data is defined by a learning rule. Jain et al. (1996) describe several learning rules, the most common of which is backpropagation (Henseler 1995).

Like most modelling approaches, ANN performance is highly dependant on the quality of historical data. The historical data are typically divided into three subsets. The first subset is the largest, and is used to train the ANN. The second subset is the test set. This set is used in training to establish when training should stop, usually when the error has reached a pre-selected value. The final subset, the production set, is an independent data set used to

evaluate the generalization ability of the trained network. For proper development and evaluation of the network, each subset should be representative of the entire data set. This can be done with visual examination of the data subsets or calculation and comparison of key statistical features. The network stability is determined by swapping the data in the subsets, re-training the network, and comparing the performance of the re-trained network with the original network. The data swap should not compromise the network's performance.

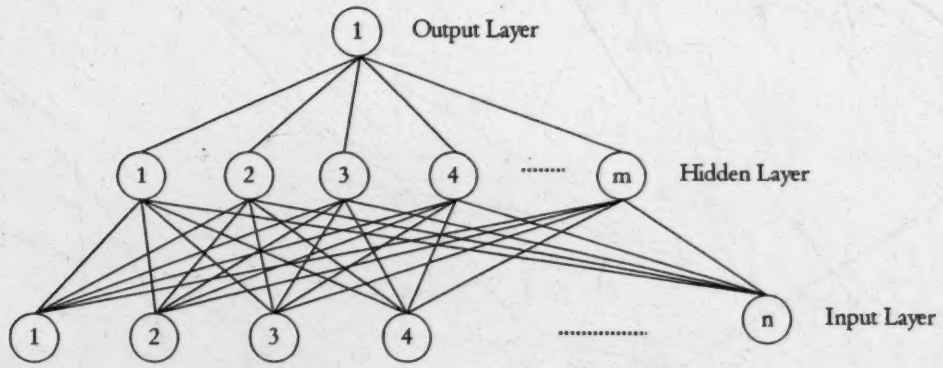

Figure 6-1 Schematic of a three layer perceptron network.
Adapted from Plochl (2001).

Several statistical parameters are commonly used in the ANN literature to evaluate the network's performance. The most commonly used statistic is the coefficient of multiple determination (R^2), defined as (Walpole and Myers 1993):

$$R^2 = 1 - \frac{\sum (x - y)^2}{\sum (x - \bar{x})^2} \quad \text{.....Equation 6-1}$$

where

x = actual output value (in this project, the ozone concentration from the ambient monitor historical data)

y = modelled output value (ozone concentration from the ANN)

$\bar{x}$ = mean of the actual output values

Other performance indicators that may be used include the mean squared error (MSE), mean absolute error (MAE), minimum absolute error, maximum absolute error, fractional bias (FB), and the Wilmott indices of agreement (d_1 and d_2), and are described in most basic statistics texts (e.g., Judd and McClelland 1989; Montgomery 2001; and Walpole and Myers 1993).

6.3 Methodology

Data for the Alberta Environment Calgary East ambient air monitoring station were collected for the period spanning June 2000 to September 2002. Since ozone concentrations are higher in the summer due to greater photochemical activity, only data from May through September of each year were used to develop the ANN. May 2000 relative humidity and temperature were unavailable, so this month was excluded from the data history. The hourly average data available from the Calgary East station were concentrations of carbon monoxide (CO), hydrogen sulphide (H_2S), nitric oxide (NO), nitrogen dioxide (NO_2), sulphur dioxide (SO_2), total hydrocarbons (THC), fine particulate matter ($PM_{2.5}$), and ozone (O_3), wind direction, wind direction deviation, and wind speed. All pollutant concentrations are measured in parts per million (ppm) by volume. Wind direction and wind direction deviation are measured as degrees from north, while wind speeds are in kilometres per hour (km/h). Relative humidity (%) and temperature (°C) data were only available at the Northwest station. These variables were also included in the project because minimal spatial variation of these parameters is expected throughout the city. These data were supplemented with upper air data from Environment Canada's Stony Plains station, located approximately 45 km west of the Edmonton East station. Parameters from this station included mixing height in metres (converted from balloon sounding data) and opacity (tenths of sky).

Alberta Environment processes the data to remove erroneous values prior to making the data publicly available, eliminating the need for quality control in this project. However, wind direction data for winds blowing from the north are recorded as both 0° and 360°. For consistency, all winds blowing from the north were assigned a value of 360°. Also, wind speeds less than 1 km/h are considered calms. Readings below this value are unreliable

because they exceed the sensitivity limits of the measuring instruments (McCullum 2003). Therefore, all wind speed readings less than 1 km/h were set to 0 km/h to represent calms, and their corresponding wind directions were assigned values of 0°. Although $PM_{2.5}$ concentration data are currently measured at the Calgary East station, the $PM_{2.5}$ history was considerably shorter than the history of the other pollutants and was therefore excluded from this project.

The balloon sounding data are measured twice daily at Stony Plain, Alberta. The sounding data were converted to hourly average mixing height values through linear interpolation between the two readings. Mixing heights were also calculated from three hour averaged wind speeds using the method proposed by Benkley and Schulman in 1979. The lower value of mixing height (i.e., the condition promoting higher ground level pollutant concentrations) was used for the model input.

In this paper, the systematic approach proposed by El-Din and Smith (2002a and 2002b) was adopted to develop two ANN models for ground level ozone in Calgary. The first ANN models hourly average ground level ozone concentrations. The second ANN is a forecast model that predicts future ground level ozone concentrations. In addition, variations of the models including ozone time series effects were developed. The systematic approach is a flexible methodology for determining the optimum ANN architecture. The steps in the systematic approach include determining the best combination of activation functions, input variables to describe the process modelled, number of neurons in the hidden layer, number of training epochs to avoid overtraining, and the largest forecast window for predictive models.

The hidden layer activation functions tested were the logistic, Gaussian, sine, tanh, tanh(15), Gaussian complement, and symmetric logistic functions. The output layer activation functions tested were the same as the function tested for the hidden layer, but also included the linear function. Various combinations of these functions were tested at three settings of hidden layer neurons and training epochs: low, middle, and high. The low setting consisted of 5 neurons in the hidden layer and 1000 training epochs. The middle setting contained 20 hidden layer neurons and 3000 training epochs, while the high setting contained 50 hidden

layer neurons and 6000 training epochs. Since this is the first step of the systematic approach and the optimum ANN architecture is still unknown, the low, middle, and high settings were assigned so that the expected (based on network architectures in previous studies— see Chapter 5) final network architecture was within these settings. This helped to ensure a stable final model.

The best set of input variables was determined using, as a starting point, the inputs found to be most important in previous ozone ANN models (see Chapter 5). The remaining variables were then added to the model in succession and the change in model performance was evaluated. A 0.03 increase in R^2 was arbitrarily set as the minimum improvement required to justify inclusion of a particular variable in the input set of the final network. In this step, temporal inputs such as month were represented by their numerical values and one input neuron (e.g., the input neuron has a value of 5 for May data, a value of 6 for June data, etc.), so that the relative contribution of month as an entire class could be determined. After this step, temporal inputs were represented with multiple input neurons set to either 0 (inactive) or 1 (active). This method avoids any biases, because all the temporal data have equal representation. For example, when a single input neuron is used to represent month, the neuron's value for September is 9, while the value for May is 5. When multiple input neurons are used, the input neuron representing May is set to 1 for data patterns from May, while the input neurons for June to September are inactivated. With this approach, an equal representation of the data is presented to the network and the network is given the freedom to establish the relevance of each individual month.

For determining the final architecture, the numbers of neurons in the hidden layer tested were 5, 6, 7, 8, 9, 10, 11, 12, 13, 14, 15, 20, and 25. The numbers of training epochs concurrently evaluated (i.e., every combination of hidden layer neurons and training epochs in these ranges were tested) were 100, 250, 500, 1000, 1500, 2000, 3000, 4000, and 5000. The most economic combination with the highest R^2 was selected for the final model. To ensure good generalization, the ANN must exhibit similar R^2 values for the training, test, and production data sets. The model's sensitivity to variability in each of the inputs was also evaluated. In this analysis, each of the variables was ranged from its minimum to maximum

value while all other variables were held at their median values, and the model response recorded.

The best forecast window was determined with a one hour forecast as the basic prediction window. The prediction window was increased in one hour increments and the optimized network's subsequent production set R^2 compared to the minimum acceptable performance standard. For this paper, the minimum performance standard was set at a R^2 of 0.75.

Ward Systems Group, Inc.'s NeuroShell2 software was used to develop all neural networks.

6.4 Results and Discussion

The basic statistics calculated for the parameters measured at the Calgary East air monitoring station, and for the relative humidity and temperature measurements from the Northwest station, are listed in Table 6-1. The mean ozone concentration measured was 0.021, similar to the median of 0.020 ppm. Ozone concentrations ranged from 0 to a maximum value of 0.068 ppm in the data period.

Table 6-1 Calgary East basic statistics of available inputs.

Statistic	CO	H_2S	NO	NO_2	SO_2	THC	MIX	OPA	RH*	TEMP*	WDR	DEV	WSP	O_3
Mean	0.5	0.001	0.020	0.018	0.002	2.1	188.2	4	59	14.4	316	19	7.5	0.021
Median	0.4	0.001	0.011	0.017	0.002	2	157.4	4	59	13.7	207	17	6.4	0.02
Std.Dev.	0.3	0.002	0.030	0.010	0.002	0.2	168.1	3	24	7.3	108	13	5.3	0.015
Var.	0.1	0.000	0.001	0.000	0.000	0.0	28248.7	12	577	53.9	11566	156	27.8	0.000
Min.	0.1	0	0	0.001	0	1.7	0	0	11	-7.2	0	1	0	0
P(0.01)	0.2	0	0	0.002	0	1.8	0	0	17	-2.1	0	3	0	0
P(0.05)	0.2	0	0	0.004	0	1.8	0	0	23	3	8	5	1.4	0.001
P(0.25)	0.3	0	0.003	0.011	0.001	1.9	60.9	1	37	9.2	131	11	3.5	0.007
P(0.75)	0.6	0.001	0.024	0.024	0.003	2.2	280.1	8	79	19.5	298	24	10.2	0.032
P(0.95)	1.1	0.003	0.077	0.038	0.006	2.4	505.8	10	98	27.4	346	39	17.6	0.045
P(0.99)	1.6	0.007	0.145	0.046	0.009	2.7	715.6	10	100	31.7	358	52	23.8	0.053
Max.	4.1	0.038	0.502	0.086	0.028	5.6	1094.9	10	100	37.5	360	174	107	0.068

Figure 6-2 shows typical ozone concentration data for Calgary East. Ozone concentrations follow the distinct diurnal pattern noted in several recent studies for Alberta (CEPA/FPAC

WGAQOG 1999; Chaikowsky 2001; and Sandhu 1999), with concentrations typically peaking daily in the late afternoon, between 16:00 and 17:00.

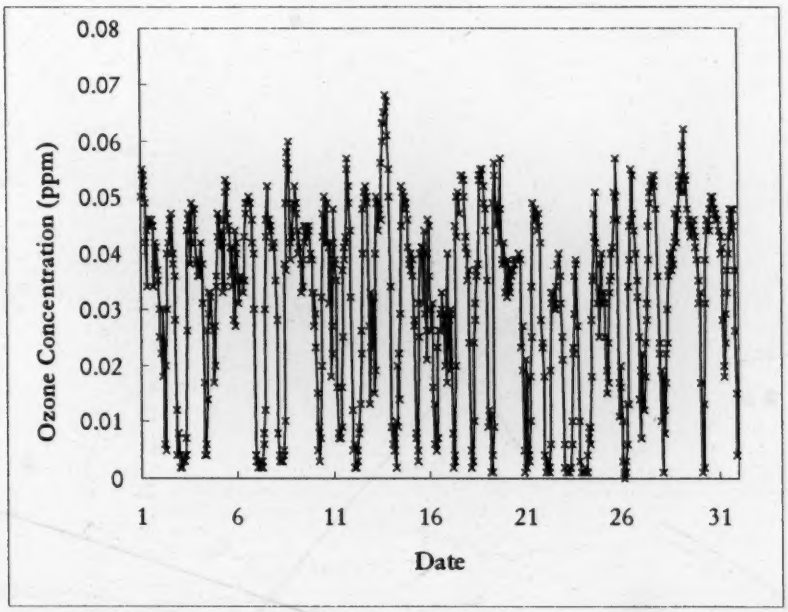

Figure 6-2 Calgary East typical hourly average ozone concentration data for May 2001.

Figure 6-3 shows the results of the activation function evaluation, averaged over the low, middle, and high settings of number of neurons in the hidden layer and training epochs. The best average function combination was the Gaussian function in the hidden layer and the linear function in the output layer. The logistic-Gaussian complement, tanh-Gaussian, and sine-Gaussian combinations produced negative R^2 results at the high setting and were excluded from further consideration. Initially, the ANN was developed with the Gaussian-linear activation function, but the resulting network occasionally (less than 2% occurrence) generated negative values for low concentrations. These negative values are the result of the inability of the linear function to account for rapid variability in the data. Therefore, the Gaussian-logistic combination was selected for further development. The average production set R^2 over the three settings was 0.87 for this function combination. Other function combinations that yielded similar outcomes were the Gaussian-sine and Gaussian-

tanh combinations. Another method used in the literature to avoid forecasting negative concentrations is to logarithmically transform the pollutant data (Schlink et al. 2003).

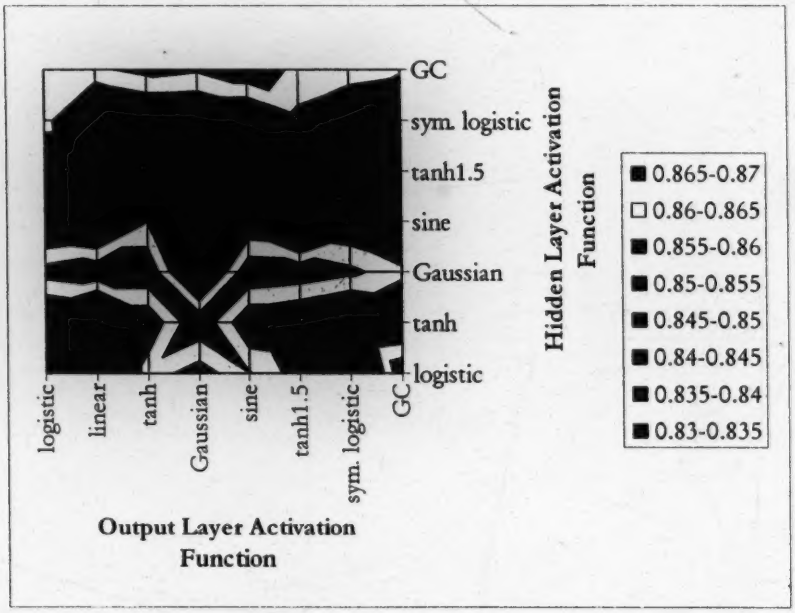

Figure 6-3 Calgary East function analysis results, average of three settings.

Based on the Edmonton East model results (see Chapter 5), the most important parameters for modelling ozone concentrations are nitric oxide (NO), month (MTH), nitrogen dioxide (NO_2), total hydrocarbons (THC), and sulphur dioxide (SO_2). The combined relative contribution factors of these inputs was 0.836 in the Edmonton East model. The benchmark network built with these five inputs generated a R^2 of 0.62 at the middle setting. The variable testing indicated that RH* and TEMP* improved R^2 much more than any of the other variables (changes in R^2 of 0.18 and 0.19 compared to 0.05 on average for other variables), so these were added to the core inputs. The model was re-run with the seven inputs to establish a new baseline, and the variable testing repeated. No other inputs were found to be relevant. The final optimum inputs to the model were NO, NO_2, SO_2, THC, RH*, and TEMP*.

Next, the runs to determine the best architecture for the virtual monitor model were completed. The results of these runs are shown in Figure 6-4. The best architecture for the ANN resides in the upper right hand corner of the plot, with the most economical architecture having 20 hidden layer neurons and 500 training epochs when the Gaussian-logistic activation function combination was used.

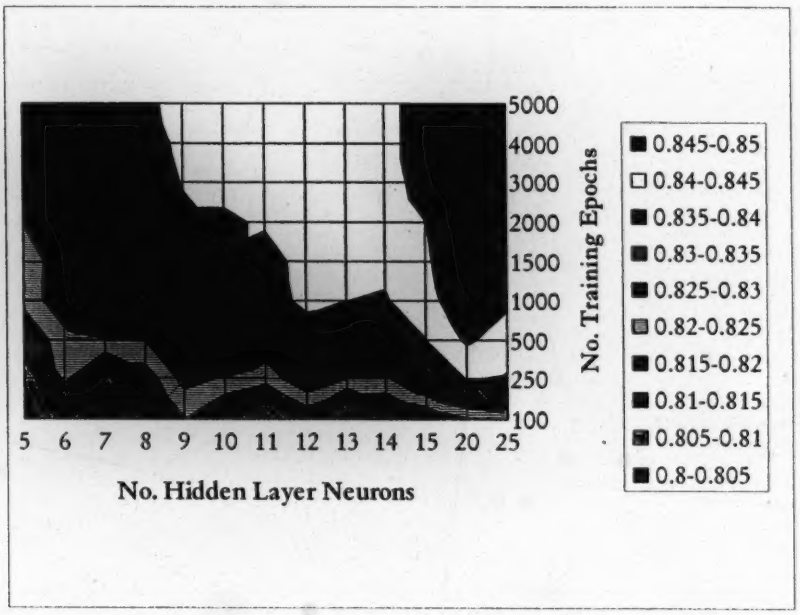

Figure 6-4 Calgary East virtual monitor model surface plot of architecture analysis.

Figure 6-5 shows the virtual monitor model's predictions for May 2001 production data. The R^2 was 0.85 for the production data set. The ANN appears to struggle with the highest peaks, but over-predicts some intermediate and smaller peaks. The fractional bias of the network was 0.196 for the 25 highest concentrations. This bias is still much lower than the 2 times factor recommended as the maximum allowable bias by Cox (1988).

The Wilmott indices of agreement show good agreement between the modelled and actual values at 0.82 and 0.96 for d_1 and d_2, respectively.

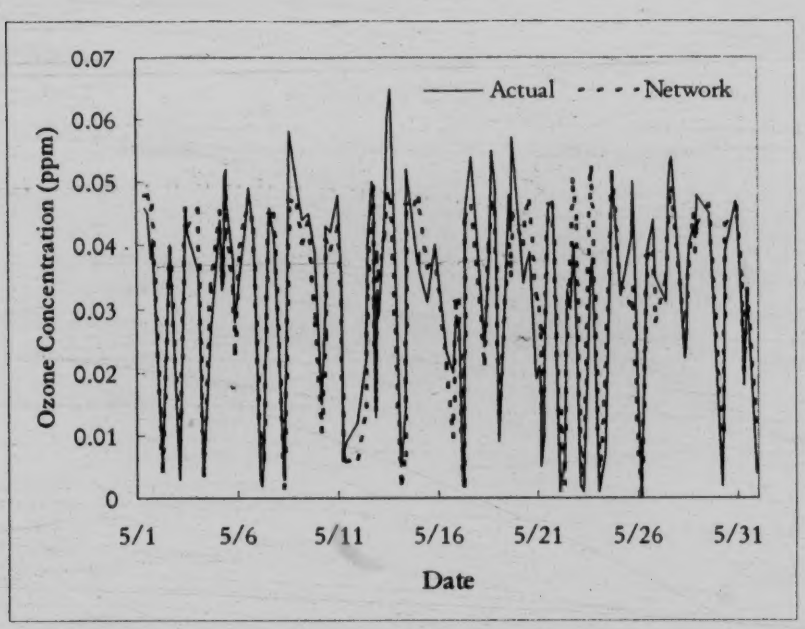

Figure 6-5 Calgary East virtual monitor model performance on May 2001 production set data, $R^2 = 0.85$.

The plot of the modelled versus actual ozone concentrations is shown in Figure 6-6. In this figure, the solid black line shows the ideal case, where the modelled concentrations are equal to the actual concentrations. The figure shows the model has a slight tendency to over-predict higher ozone concentrations, evidenced by the number of markers lying above the ideal case line. The model residuals shown in Figures 6-7 and 6-8 show no trends over time or the modelled values. The model stability check shows the model is stable when trained on swapped data, generating a R^2 of 0.84 when applied to the production set of data.

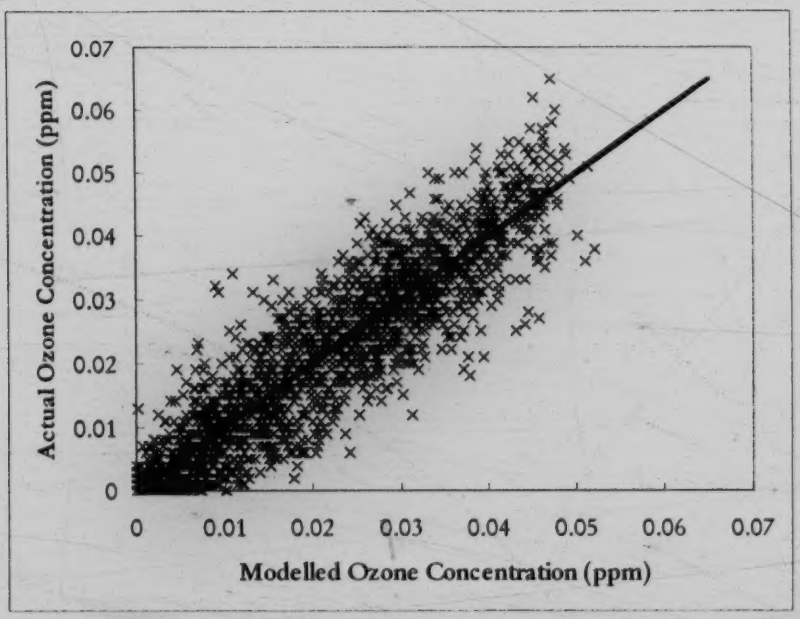

Figure 6-6 Calgary East virtual monitor model comparison of actual and modelled ozone concentrations.

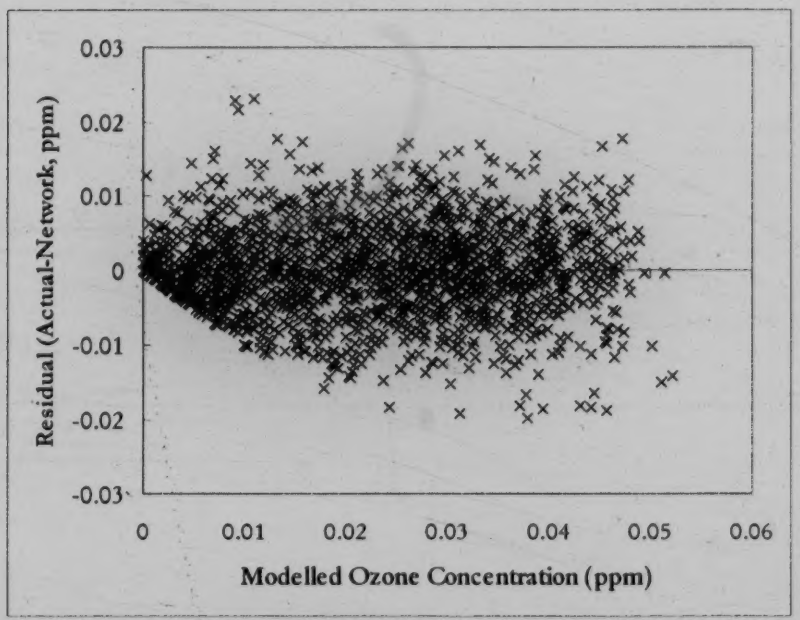

Figure 6-7 Calgary East virtual monitor model residuals analysis: variation with modelled ozone concentration.

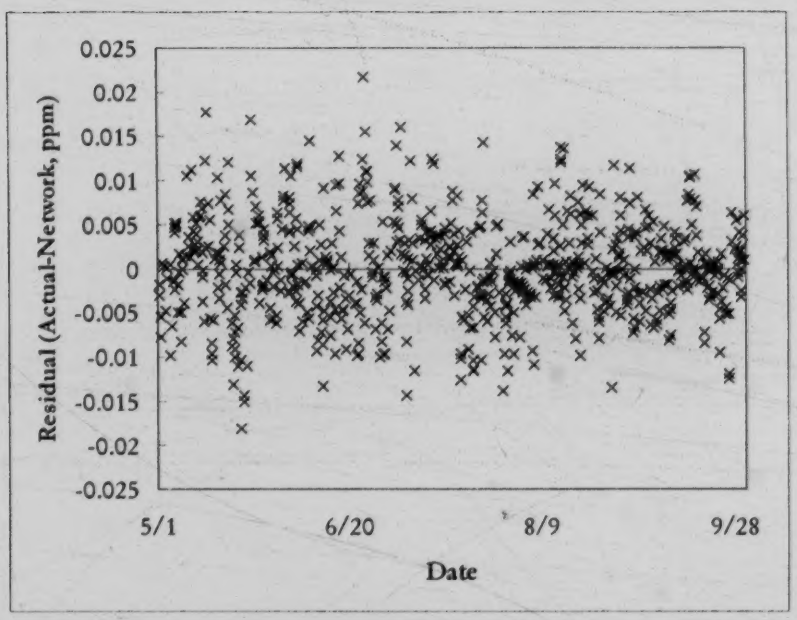

Figure 6-8 Calgary East virtual monitor model residuals variation with time.

Since ozone is a photochemical pollutant, the possibility of using only daylight data was evaluated by developing a model using only data from daylight hours to train the network. Daylight was arbitrarily assumed to be between the hours of 8:00 and 20:00 inclusive. The actual hours of daylight are expected to vary daily, and are dependant on the time of year. The model performance declined slightly, with a production set R^2 of 0.79. Figure 6-9 shows a comparison of the input variable relative contribution factors for the 24 hour and daylight only networks. NO became a larger contributor when only daylight data was used, as did TEMP*. The increased importance of NO may be due to the scavenging effects of NO emitted from daytime traffic. The importance of this effect is magnified in the daytime, when the variability of traffic volumes is greater with the morning and afternoon rush hours. The increased importance of TEMP* during the day is a reflection of the importance of photochemical activity. Since the relative importance of NO_2 decreases, this photochemical activity may pertain to reactions among other compounds. SO_2 and THC also decreased in importance.

The results of the sensitivity analysis are shown in Figures 6-10 through 6-12. Ozone concentration initially decreases as the summer progresses, levelling off in July and remaining fairly flat through to September (Figure 6-10). It has been shown in previous studies that on average, ozone levels are highest in the spring in Alberta (CEPA/FPAC WGAQOG 1999; Chaikowsky 2001). Figure 6-11 shows the sensitivity of ozone concentrations to concentrations of various pollutant species. In the sensitivity to NO (Figure 6-11a), ozone concentration decreases rapidly with an increase in NO concentration, for NO concentrations up to 0.1 ppm. Between 0.1 ppm and 0.3 ppm NO concentration, ozone concentration is unchanging at 0, but rises slightly at NO concentrations greater than 0.3 ppm. Three regions are distinguishable in the sensitivity to NO_2 concentrations (Figure 6-11b). Initially, at NO_2 concentrations less than 0.01 ppm, there is a small linear decrease in ozone concentration as NO_2 increases. In the region with NO_2 concentrations between 0.01 ppm and 0.025 ppm, ozone concentration decreases more rapidly than in the first region. At NO_2 concentrations greater than 0.025 ppm, ozone decays with an increase in NO_2 concentration, appearing to approach an asymptotic value of approximately 0.0014 ppm. The overall change in ozone concentration in response to SO_2 concentrations is small (Figure 6-11c). For SO_2 concentrations less than approximately 0.014 ppm, ozone decreases slightly as SO_2 concentration increases. This trend is reversed for SO_2 concentrations greater than 0.014 ppm, where ozone concentrations increase with increasing SO_2 concentrations. The changes in ozone concentration in response to THC concentrations are similar to those for SO_2, with the trend reversing at a critical concentration (Figure 6-11d). At THC concentrations less than 3 ppm, ozone concentration decreases with increasing THC concentrations. When THC concentration is greater than 3 ppm, ozone concentrations begin to rise as THC concentrations increase.

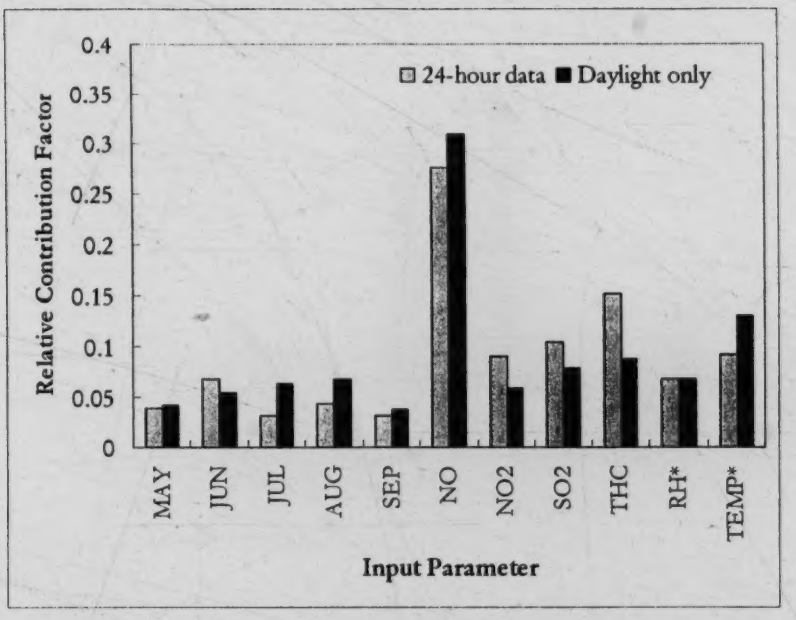

Figure 6-9 Calgary East comparison of input parameter relative importance for ozone modelling using 24-hour and daylight only data.

The sensitivity of ozone levels to meteorological parameters is shown in Figure 6-12. Not surprisingly, the RH* trend shows ozone concentrations decreasing with increasing RH* (Figure 6-12a). This is likely due to the wet deposition of pollutants when air moisture content is high. This effect stabilizes at RH* of 60%. The influence of temperature on ozone concentrations is shown in Figure 6-12b. The temperature influence shows two regions. In the first region where temperatures are less than 3°C, ozone concentrations decrease with increasing temperatures. At temperatures greater than 12°C, ozone concentrations increase with increasing temperature, with the region between 3°C and 12°C being a transition zone between the two regimes. The effects of temperature appear to begin levelling off at high temperatures.

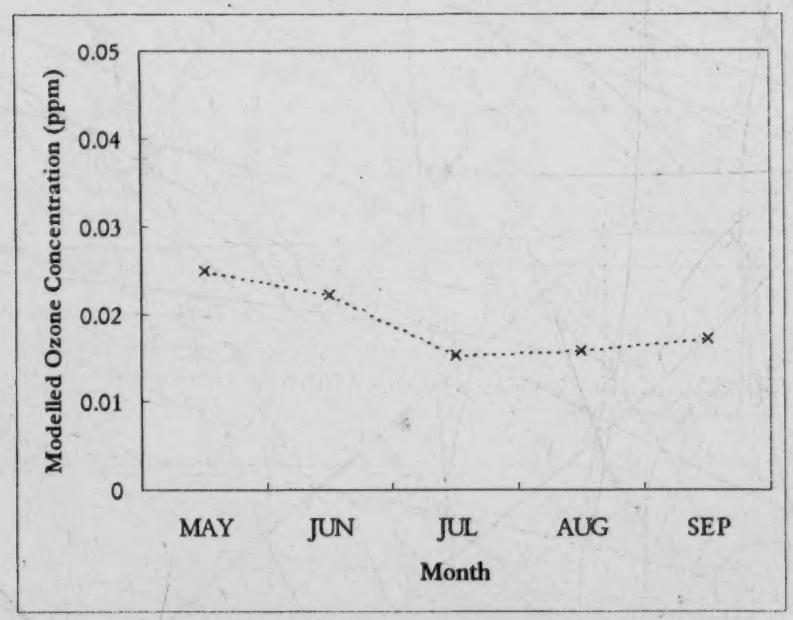

Figure 6-10 Calgary East variation of virtual monitor modelled ozone concentration with month.

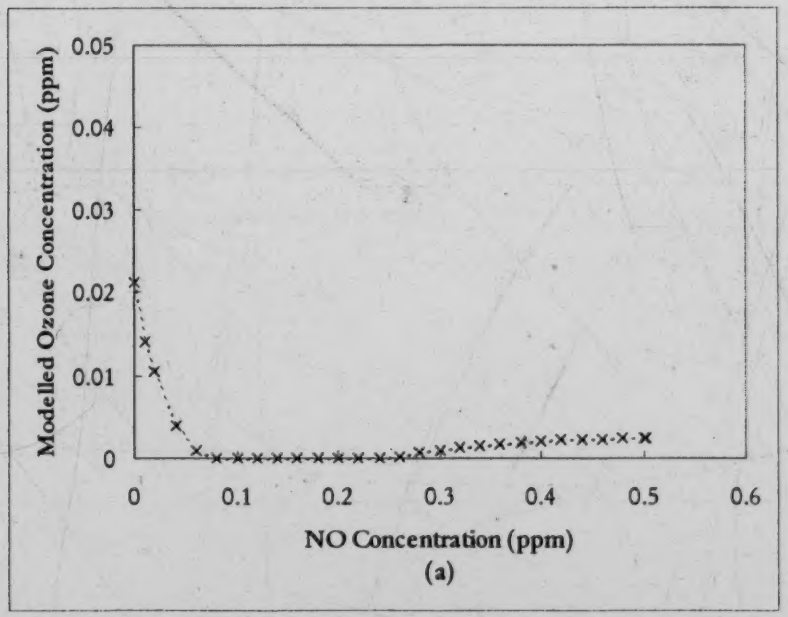

Figure 6-11 Calgary East sensitivity of virtual monitor modelled ozone concentration to pollutant concentrations: (a) NO; (b) NO_2; (c) SO_2; and (d) THC.

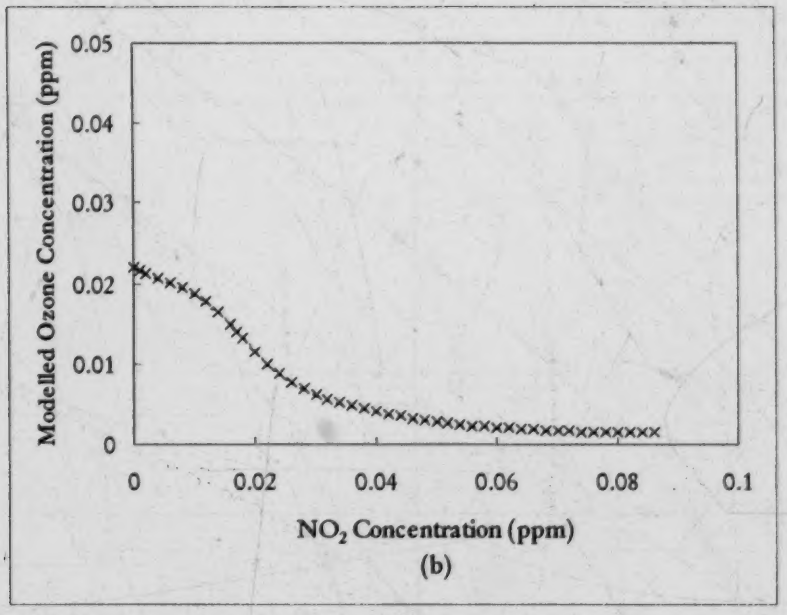

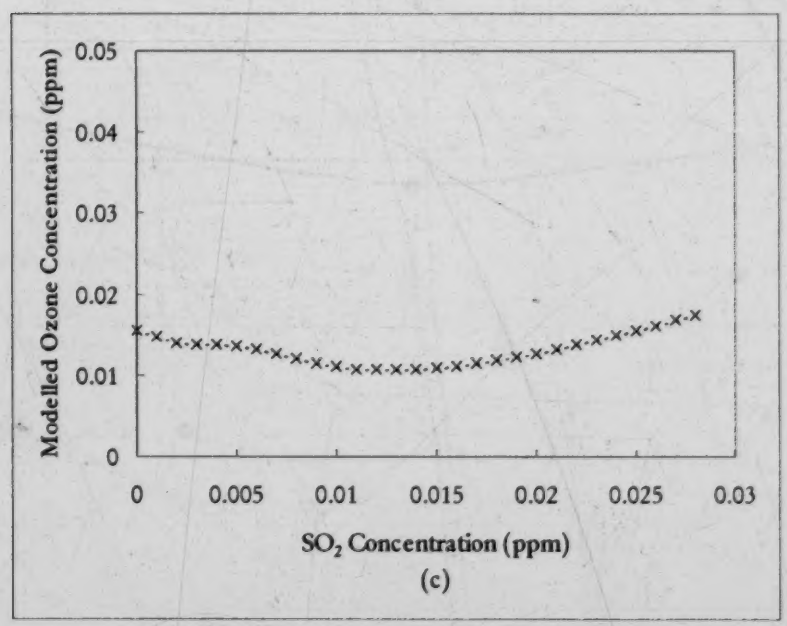

Figure 6-11 cont'd. Calgary East sensitivity of virtual monitor modelled ozone concentration to pollutant concentrations: (a) NO; (b) NO_2; (c) SO_2; and (d) THC.

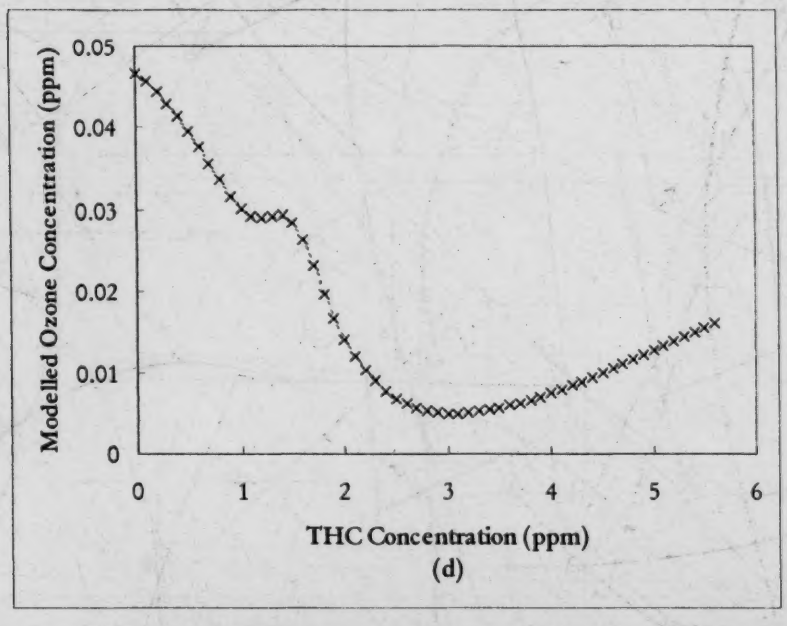

Figure 6-11 cont'd. Calgary East sensitivity of virtual monitor modelled ozone concentration to pollutant concentrations: (a) NO; (b) NO_2; (c) SO_2; and (d) THC.

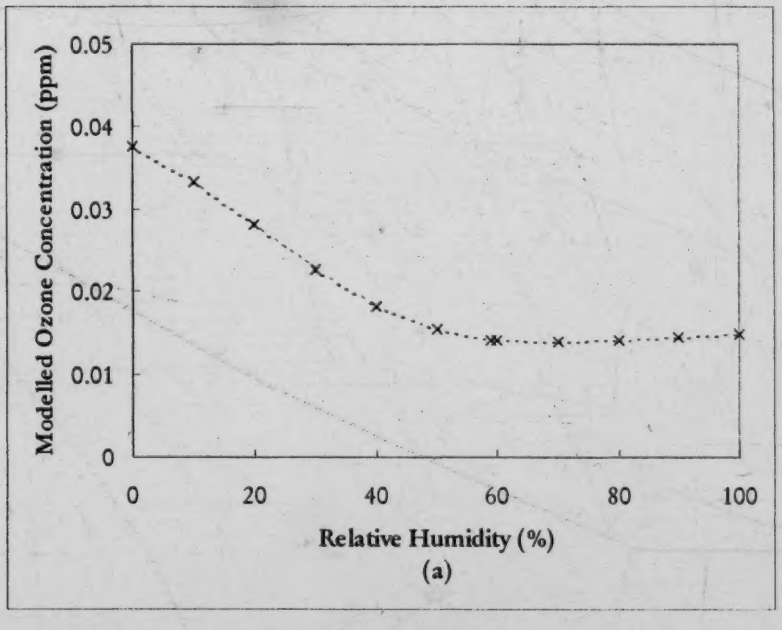

Figure 6-12 Calgary East sensitivity of virtual monitor modelled ozone concentration to meteorological parameters.

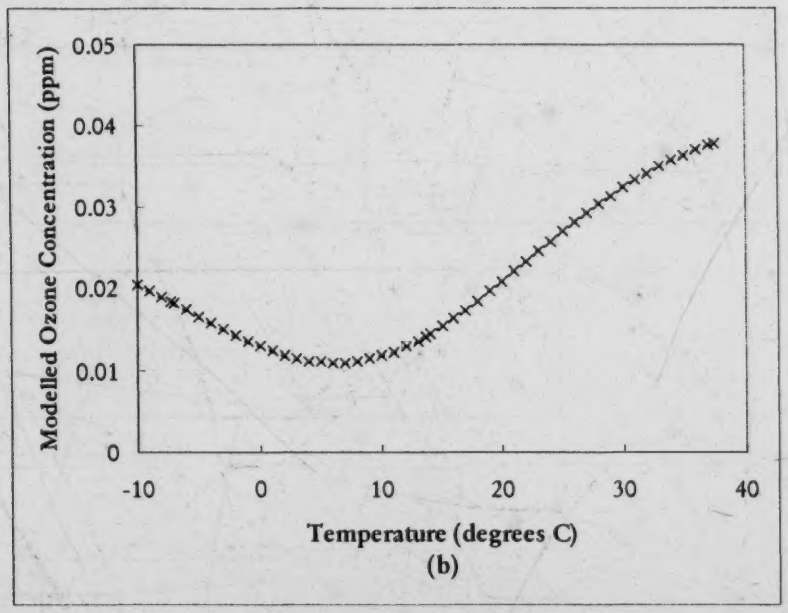

Figure 6-12 cont'd. Calgary East sensitivity of virtual monitor modelled ozone concentration to meteorological parameters.

Figure 6-13 shows the surface plot for the network architecture development for the virtual monitor model when ozone time series effects are incorporated in the model via inclusion of the ozone concentration from the previous hour in the input set of variables. The figure shows a large area where no variation in R^2 occurs, regardless of increased training epochs or an increased number of hidden layer neurons (dark areas on plot). Based on this exercise, the ANN structure that best balances performance with economy has 20 neurons in the hidden layer and 500 training epochs. Although performance is similar with lower numbers of hidden layer neurons, more training epochs are required for these structures. Increasing the number of training epochs results in greater increases in the network training time than incrementing the number of neurons in the hidden layer. The performance of this model is shown in Figure 6-14 for May 2001 production data. The ANN prediction performance increases to a R^2 of 0.92 for the production data set when the previous hour's concentration of ozone is included as an input parameter.

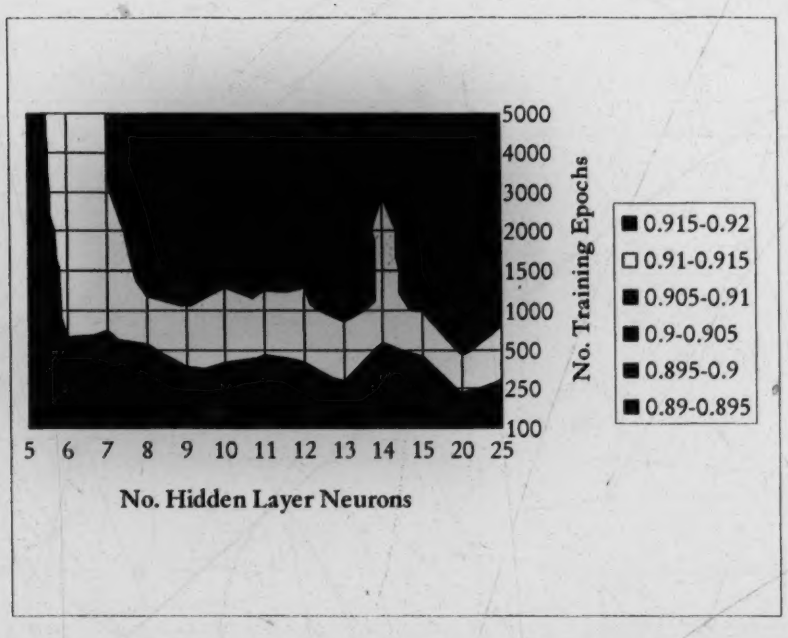

Figure 6-13 Calgary East virtual monitor model surface plot of network architecture evaluation when ozone concentration at t-1 included as input.

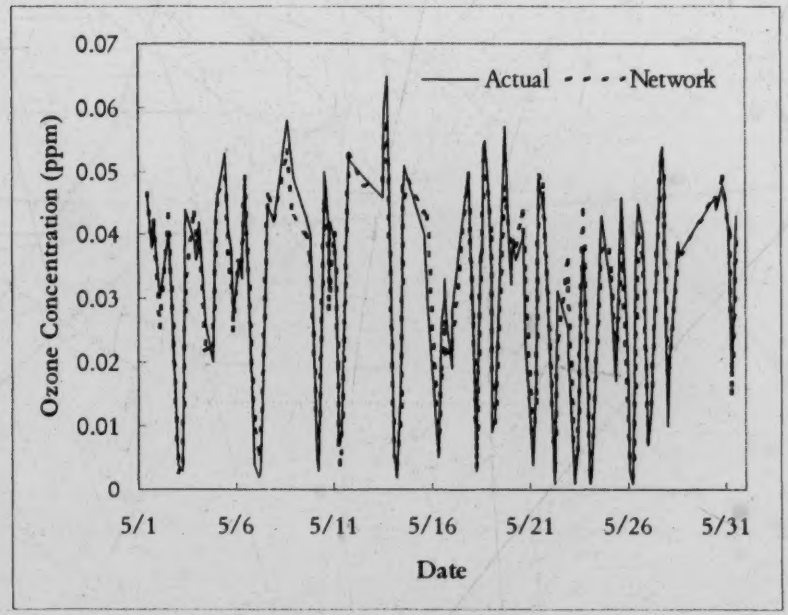

Figure 6-14 Calgary East virtual monitor model with ozone time series performance for May 2001 production set data, $R^2 = 0.92$.

The virtual monitor model with time series effects is slightly better at predicting the 25 highest ozone peaks than the virtual monitor model without time series effects, with a lower fractional bias of 0.096. This tendency to slightly under-predict high ozone peaks is also noticeable in Figure 6-15, where top values are above the ideal case line. The Wilmott indices of agreement are higher than the virtual monitor model without time series effects, at 0.87 and 0.98, indicating better overall predictive ability. No trends were identifiable in the residuals analyses shown in Figures 6-16 and 6-17.

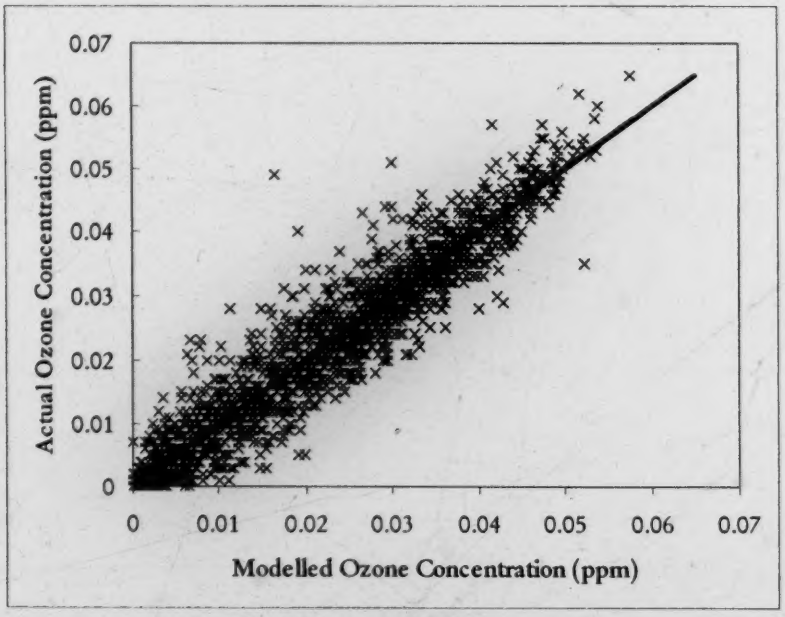

Figure 6-15 **Calgary East virtual monitor model with ozone time series: comparison of actual to modelled ozone concentration for production set data.**

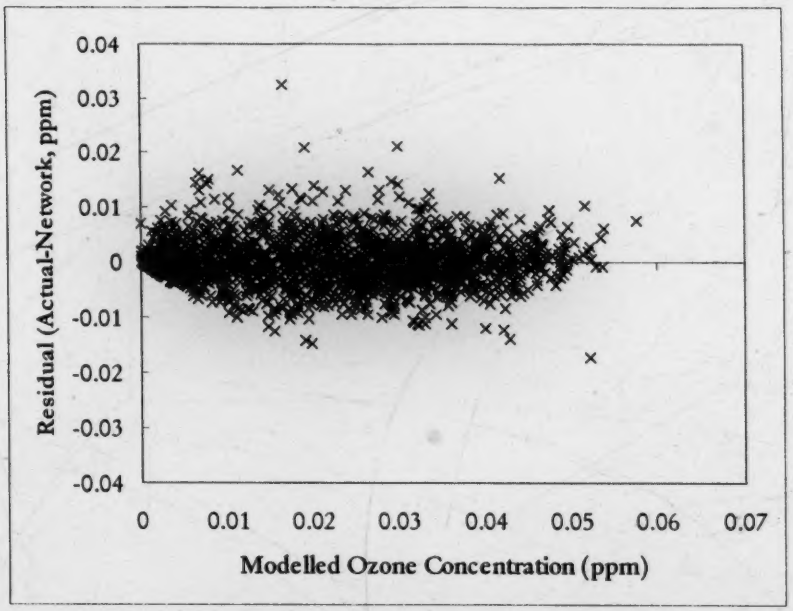

Figure 6-16 Calgary East virtual monitor model with ozone time series residuals analysis: variation with modelled ozone concentration for production set data.

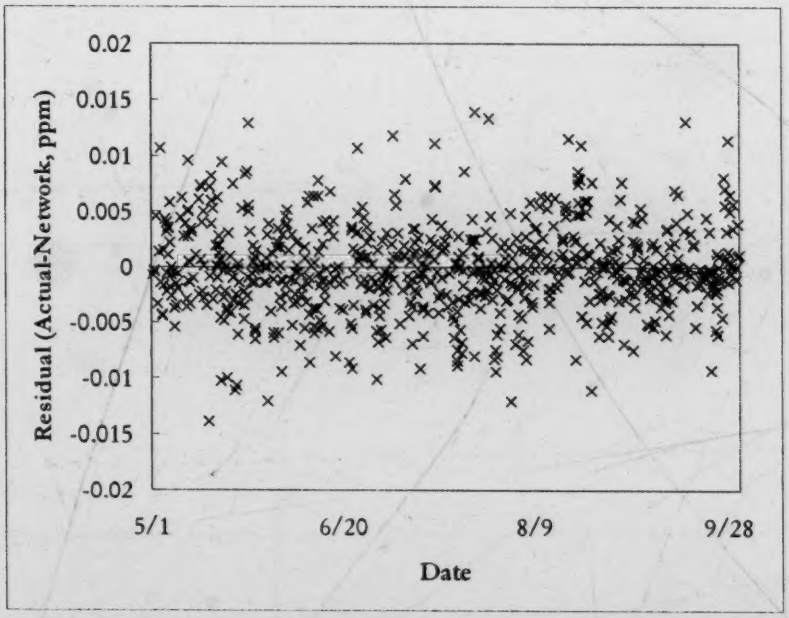

Figure 6-17 Calgary East virtual monitor model with ozone time series residuals analysis: variance with time for 2001 production set data.

Figure 6-18 shows the virtual model performance changes for structurally optimized networks when previous hours' concentrations of ozone were included in the virtual monitor model. The figure shows a dramatic increase in model performance when the previous hour's concentration of ozone is introduced to the model, but improvements are minimal after the first hour and appear to plateau. Therefore, there is no apparent advantage to including the ozone concentration from more than one hour previous. Figure 6-18 also suggests a limit to how many hours in advance ozone concentrations can be predicted. For good prediction success, the forecast window may be limited to a one hour prediction. Increasing the prediction window beyond this point may result in a performance decline. In such a case, the selected minimum acceptable performance requirement will fix the maximum forecast window.

Figure 6-19 shows the neural network structure development for the one hour in advance forecast of ozone concentration. Figure 6-19 indicates that numerous potential architectures yield similar performance (black areas). Of the best structures, the most economic is the network with 5 neurons in the hidden layer and 500 training epochs. The R^2 of this network is 0.86 for the production data, and runtime requirements are minimized. Figure 6-20 shows an example of the forecast model's performance on May 2001 data. The model has trouble predicting peak values, with a tendency to under-predict the highest peaks. Figure 6-21 of the actual versus modelled concentrations also shows this tendency to under-predict, with markers predominantly lying above the ideal case line for high ozone concentrations. This observation is verified by the fractional bias value of 0.166. The fractional bias of the forecast model is high compared to the virtual monitor models, but still below the factor of two performance standard recommended in the Cox (1988) paper. As with the other two models, no patterns are observable in the residuals analysis shown in Figures 6-22 and 6-23.

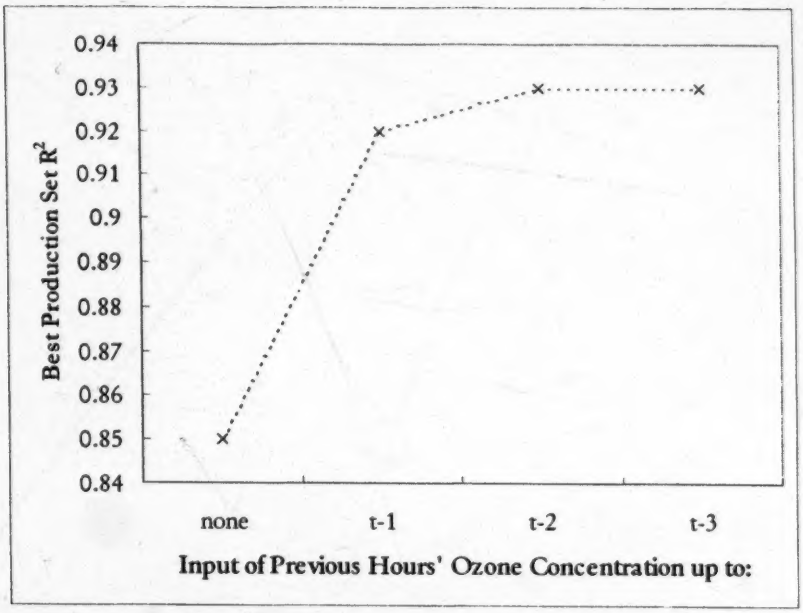

Figure 6-18 Calgary East virtual monitor model ozone time series effects

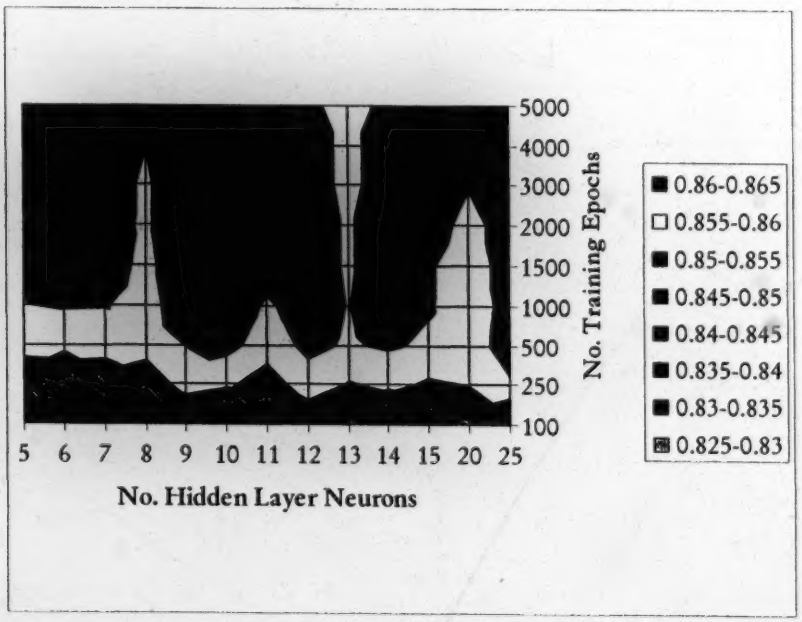

Figure 6-19 Calgary East one hour forecast surface plot of network architecture evaluation.

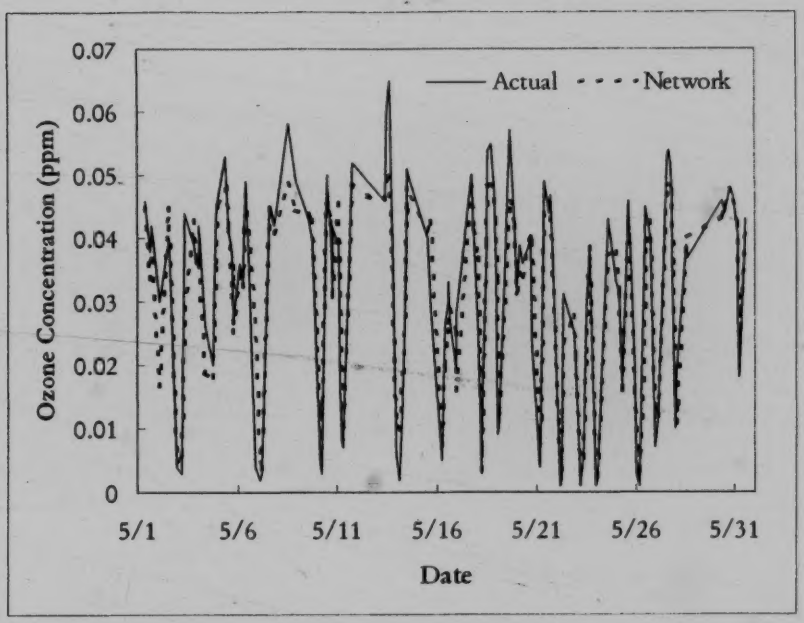

Figure 6-20 Calgary East one hour forecast model performance for May 2001 production set data, $R^2 = 0.86$.

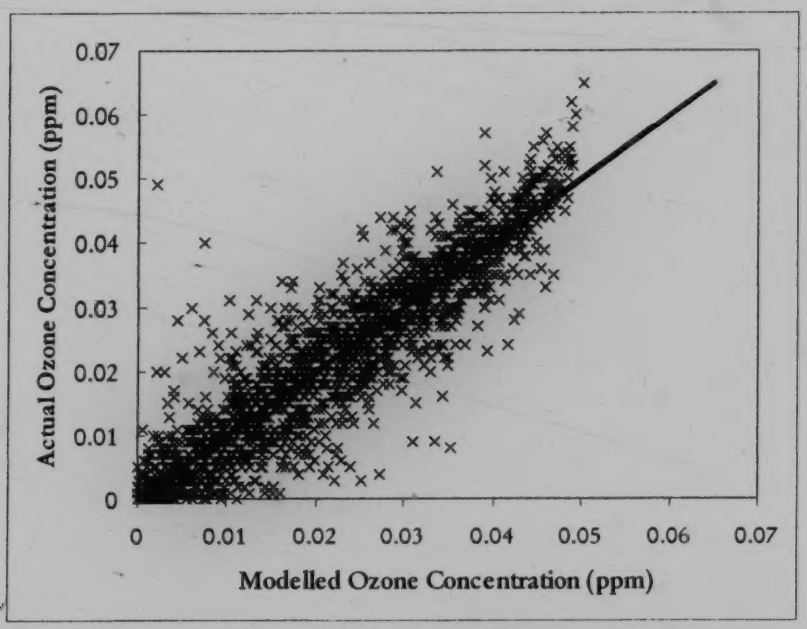

Figure 6-21 Calgary East one hour forecast model comparison of actual to modelled ozone concentration for production set data.

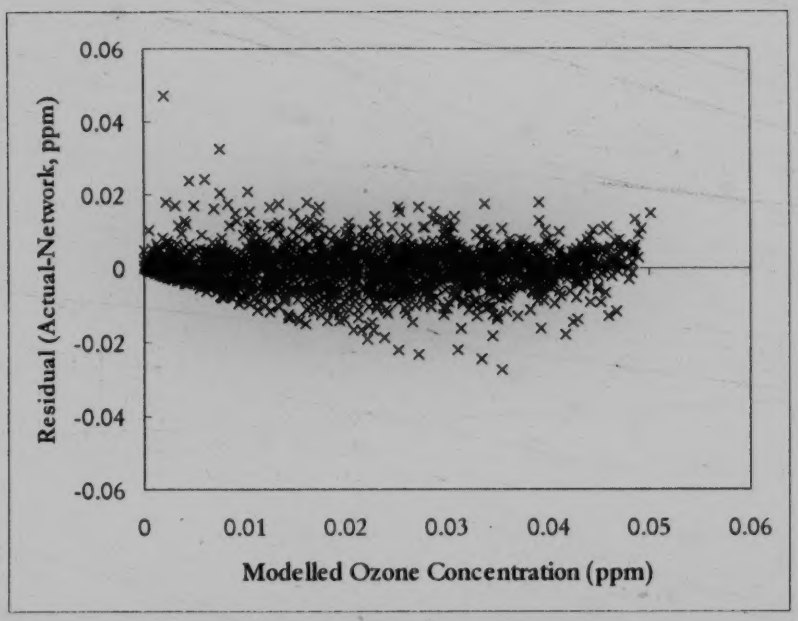

Figure 6-22 Calgary East one hour forecast model residuals analysis: variance with modelled ozone concentration for production set data.

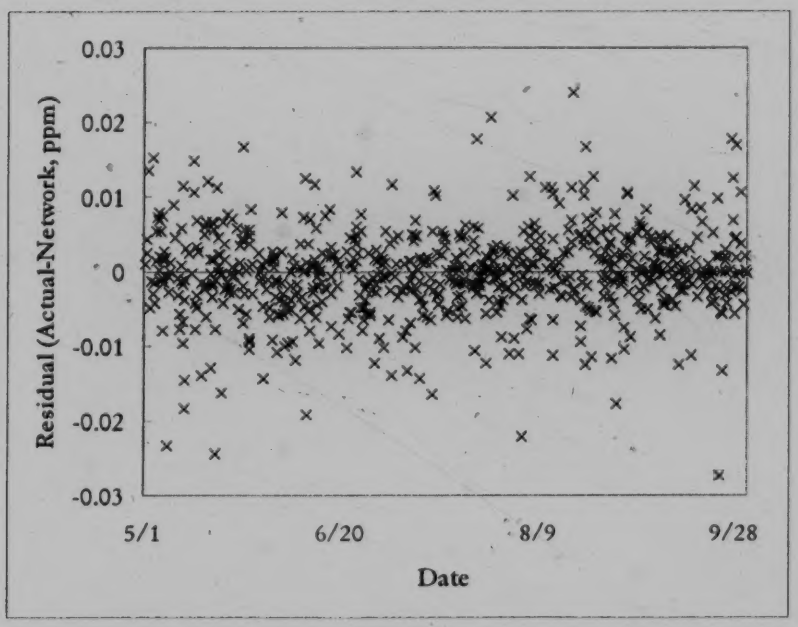

Figure 6-23 Calgary East one hour forecast model residuals analysis: variance with time for 2001 production set data.

The one hour forecast model is essentially another form of the models with ozone time series effects. In the one hour forecast, the model uses the ozone concentrations from the immediately preceding hour (ozone at time t) to determine the forecast ozone concentration (at t+1). Since performance gains were negligible when the time series effects were extended beyond the ozone concentration in the previous hour, it is unlikely that the addition of any more terms in the ozone time series would improve the network performance. However, for comparison purposes and to determine if improvements in peak predictions could be achieved, further ozone time series effects were incorporated into the one hour forecast model.

Figure 6-24 shows the network structure evaluation for the one hour forecast model with ozone time series effects (i.e., using ozone concentrations at t and t-1 to predict concentration at t+1). The most economical model has 12 neurons in the hidden layer and 250 training epochs, resulting in a production set R^2 of 0.87. As expected, this increase to R^2 is negligible compared to the one hour forecast without ozone time series effects.

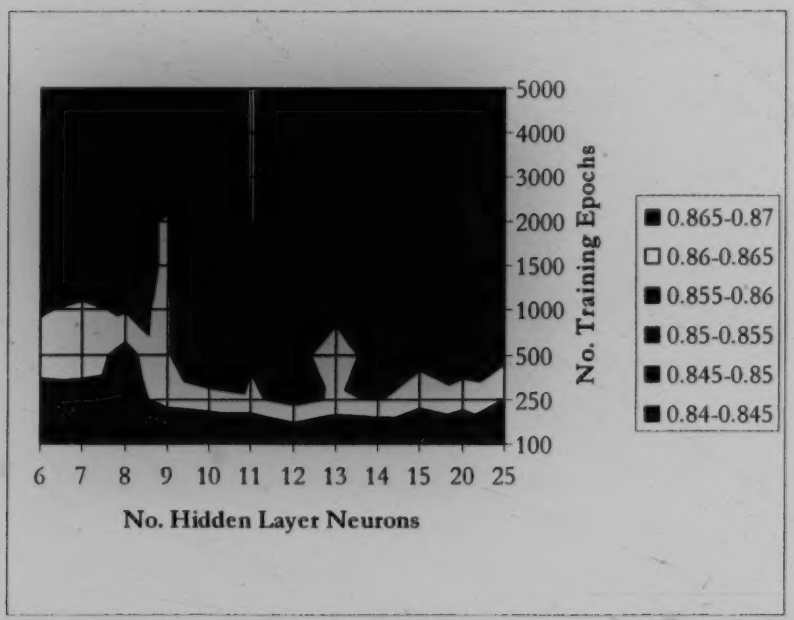

Figure 6-24 Calgary East one hour forecast with ozone time series surface plot of network architecture evaluation.

Figure 6-25 shows the model's prediction performance for May 2001 production set data. The time series forecast appears to have a slightly improved performance over the forecast model without ozone time series effects when predicting peaks. This is best illustrated in Figure 6-26, in which the markers are slightly above the ideal fit line. The fractional bias of the model at high ozone concentrations is slightly lower, at 0.155, than the model without time series effects. The Wilmott indices of agreement are the same for both the one hour forecast and the one hour forecast with ozone time series effects. This means that overall, the performance of the two models is equivalent. Like the one hour forecast, the ozone forecast with time series shows no discernible trends with either modelled ozone concentrations or time (Figures 6-27 and 6-28).

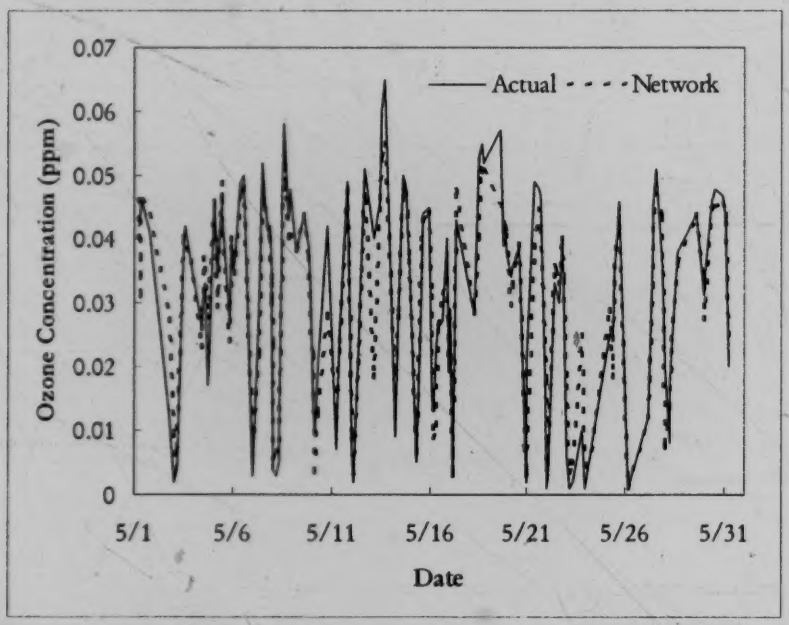

Figure 6-25 Calgary East one hour forecast with ozone time series performance for May 2001 production set data, $R^2 = 0.87$.

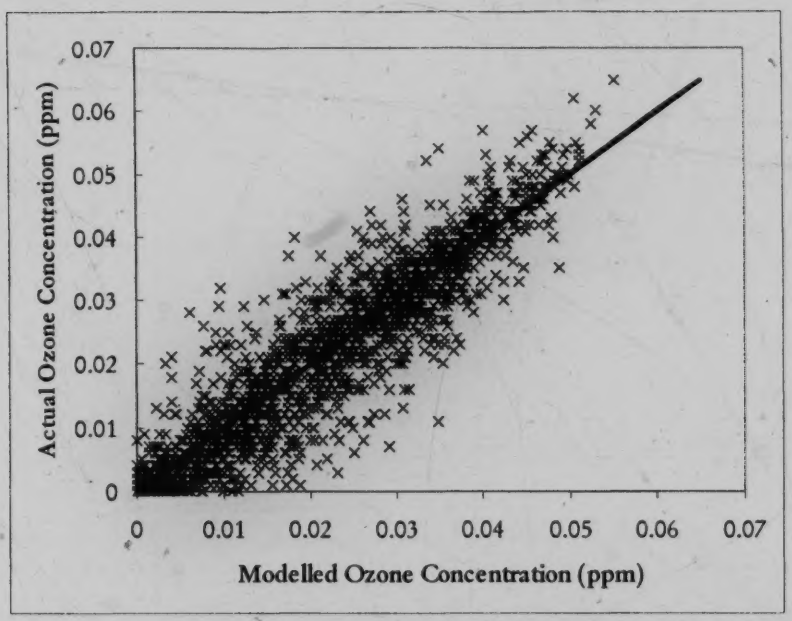

Figure 6-26 Calgary East one hour forecast with ozone time series comparison of actual to modelled ozone concentration for production set data.

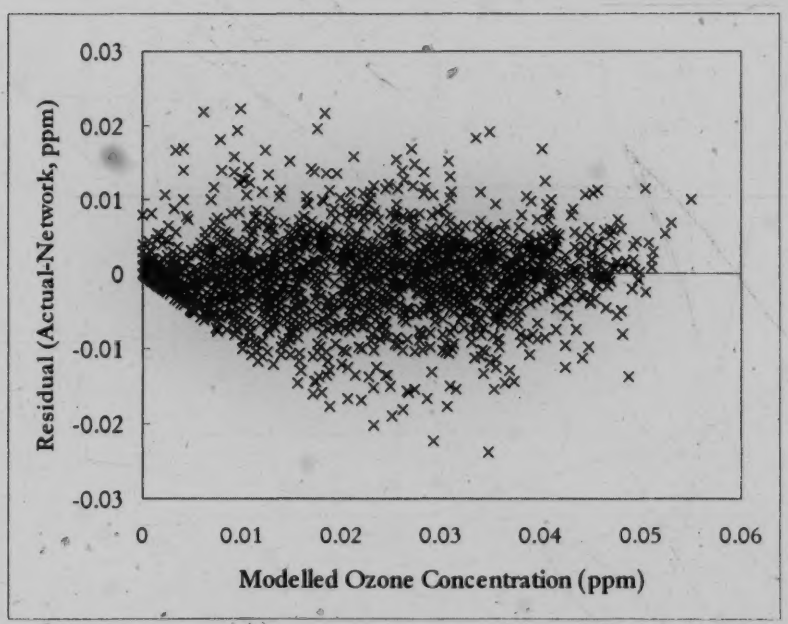

Figure 6-27 Calgary East one hour forecast model with ozone time series residuals variance with modelled ozone concentration for production set data.

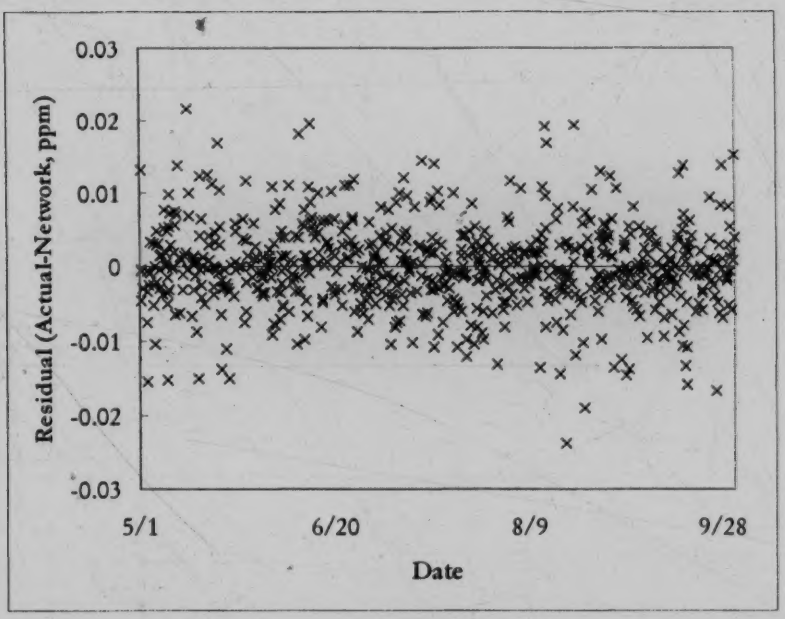

Figure 6-28 Calgary East one hour forecast model with ozone time series residuals analysis: variance with time for 2001 production set data.

As expected, the Calgary two hour forecast results were unable to meet the minimum performance standard of 0.75 for the R^2 value. Figure 6-29 shows the effects of an increased forecast window on the production set R^2 for the best network structures in each case. The time series cases are those networks that use two terms in the ozone time series as input (i.e. for the one hour forecast (ozone at t+1), inputs include ozone at t and at t-1, for the two hour forecast (ozone at t+2), inputs include ozone concentration at t and t-1, etc.). Figure 6-29 shows that increasing the forecast window results in a severe decrease in prediction performance. The difference in prediction performance between the time series and non-time series models also increases as the prediction window increases. Based on this plot, the maximum forecast window that can achieve the minimum performance requirement is one hour.

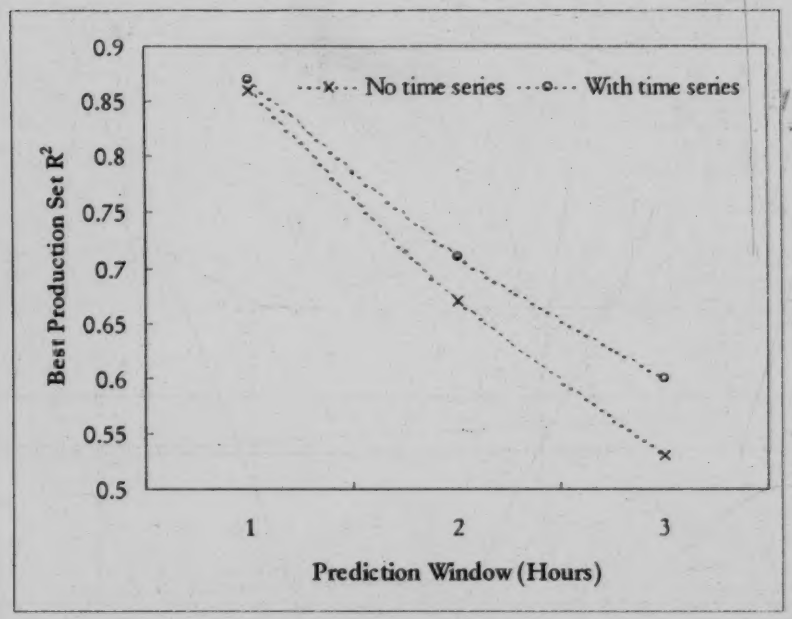

Figure 6-29 Calgary East forecast model effects of increasing prediction window and adding previous hours' ozone concentrations.

Table 6-2 summarizes the features of the best networks for each of the models, with corresponding statistics listed in Table 6-3. Connection weights for each of the Calgary East models are also tabulated in Appendix B. The performance statistics show that regardless of the performance measure used, the ANN models perform very well for modelling and one hour forecasting of ground level ozone concentrations. R^2 values for the models are all 0.85 or greater, with RMSE in the range from 4 ppb to 6 ppb. As with other ozone models in the ANN literature, the ANN models for Calgary all have a slight tendency to under-predict high ozone values, based on the highest 25 observed ozone concentrations. However, these fractional bias values are still significantly lower than the highest acceptable fractional bias recommended by Cox (1988).

Table 6-2 Summary of network features for best Calgary East ANN models.

Feature Description	VM	VMTS	FM_1	$FMTS_1$
Input layer				
No. inputs	11	12	12	13
Inputs	MAY JUN JUL AUG SEP NO NO_2 SO_2 THC RH* TEMP*	MAY JUN JUL AUG SEP NO NO_2 SO_2 THC RH* TEMP* O_3(t-1)	MAY JUN JUL AUG SEP NO NO_2 SO_2 THC RH* TEMP* O_3	MAY JUN JUL AUG SEP NO NO_2 SO_2 THC RH* TEMP* O_3 O_3(t-1)
Hidden layer				
Activation function	Gaussian	Gaussian	Gaussian	Gaussian
No. neurons	20	15	5	12
Output layer activation function	logistic	logistic	logistic	logistic
No. training epochs	500	500	500	250
No. training patterns	5,921	5,879	5,879	5,836
No. test patterns	1,974	1,960	1,960	1,946
No. production set patterns	1,974	1,959	1,959	1,945

Table 6-3 Summary of performance statistics for best Calgary East ANN models.

Statistic	VM	VMTS	FM_1	$FMTS_1$
Training set R^2	0.84	0.92	0.85	0.87
Test set R^2	0.84	0.92	0.85	0.87
Production set				
R^2	0.85	0.92	0.86	0.87
r	0.92	0.96	0.93	0.93
MSE (ppm^2x10^5)	3.29	1.80	3.06	2.85
RMSE (ppm)	0.006	0.004	0.006	0.005
MAE (ppm)	0.004	0.003	0.004	0.004
AE_{min} (ppm)	0	0	0	0
AE_{max} (ppm)	0.023	0.032	0.047	0.024
Bias(mean)	0.196	0.096	0.166	0.155
Wilmott d_1	0.82	0.87	0.84	0.84
Wilmott d_2	0.96	0.98	0.96	0.96

6.5 Conclusions

A systematic approach was applied to develop ANN models for modelling and predicting ground level ozone in Calgary, Canada, using ambient monitoring station data for input. The optimum architecture, most relevant inputs, time series effects, and largest forecast window meeting a minimum acceptable performance standard of R^2 equal to 0.75 were investigated.

The ANN modelling technique proved to be an effective modelling method for ground level ozone. The inputs most significant for quantifying ground level ozone were month of the year, concentrations of NO, NO_2, SO_2, and THC, relative humidity, and temperature. The ozone concentration from the previous hour also helped to improve the model's performance. The maximum forecast window able to meet a R^2 of 0.75 was one hour. Based on various performance statistics, the ANN modelling technique is a reliable and economic alternative to traditional mechanistic models for estimating ground level ozone concentrations.

6.6 References

Baawain, M.S., Nour, M.H., and Gamal El-Din, M. 2003. Applying artificial neural network models for ENSO prediction using SOI and NINO3 as onset indicators. In Proceedings of the 8th Environmental and Sustainable Engineering Specialty Conference of the Canadian Society for Civil Engineering, June 4-7. Canadian Society for Civil Engineering, Moncton, NB.

Bates, D. 1991. The effects of ozone on plants and humans. In the Air & Waste Management Association Tropospheric Ozone and the Environment 3; Papers from an International Conference. Air & Waste Management Association, Pennsylvania, held March 19-22, 1990 in Los Angeles, CA.

Bates, D.V., Baker-Anderson, M. and Sizto, R. 1990. Asthma attack periodicity: a study of hospital emergency visits in Vancouver. Environmental Research, 51: 51-70.

Baxter, C.W. 2002. Applications of Artificial Neural Networks in Drinking Water Treatment Process Modeling and Control, Ph.D. thesis. Department of Civil and Environmental Engineering, University of Alberta, Edmonton, AB.

Benkley, C.W. and Schulman, L.L. 1979. Estimating hourly mixing depths from historical meteorological data. Journal of Applied Meteorology, 6(18): 772-780.

Burnett, R.T., Cakmak, S. and Brook, J.R. 1998. The effect of the urban ambient air pollution mix on daily mortality rates in 11 Canadian cities. Canadian Journal of Public Health, 89(3): 152-156.

Cappa, C., Anfossi, D., Grosa, M.M., and Natale, P. 2001. Short-term prediction of urban NO_2 pollution by means of artificial neural networks. International Journal of Environment and Pollution, 15(5): 483-496.

CEPA/FPAC WGAQOG— Canadian Environmental Protection Act Federal/Provincial Working Group on Air Quality Objectives and Guidelines. 1999. National Ambient Air Quality Objectives for Ground-Level Ozone Science Assessment Document, Catalogue No. En42-17/702-1999E. Health Canada and Environment Canada, Downsview, ON and Ottawa, ON.

Chaikowsky, C.L.A. 2001. Overview of Ground-Level Ozone Observations in Alberta, 1986-1998. Science and Technology Branch, Environmental Sciences Division, Alberta Environmental Protection, Edmonton, AB.

Comrie, A. C. 1997. Comparing neural networks and regression models for ozone forecasting. Journal of the Air & Waste Management Association, 47: 653-663.

Cox, William M. 1988. Protocol for Determining the Best Performing Model. United States Environmental Protection Agency Office of Air Quality Planning and Standards, Technical Support Division, Source Receptor Analysis Branch, Washington, DC.

Delfino, R.J., Murphy-Moulton, A.M., Burnett, R.T., Brook, J.R., and Becklake, M.R. 1997. Effects of air pollution on emergency room visits for respiratory illnesses in Montreal, Quebec. American Journal of Respiratory and Critical Care Medicine, 155: 568-576.

Dockery, D.W., Pope, C.A., Xu, X., Spengler, J.D., Ware, J.H., Fay, M.E., Ferris, B.G. and Speizer, F.E. 1993. An association between air pollution and mortality in six U.S. cities. The New England Journal of Medicine, 329: 1753-1759.

El-Din, A. and Smith, D.W. 2002a. A neural network model to predict the wastewater inflow incorporating rainfall events. Water Research, 36: 1115-1126.

El-Din, A. and Smith, D.W. 2002b. Modelling a full-scale primary sedimentation tank using artificial neural networks. Environmental Technology, 23: 479-496.

Fernandez de Castro, B.M., Sanchez, J.M.P., Manteiga, W.G., Bande, M.F., Cela, J.L.B., and Fernandez, J.J.H. 2003. Prediction of SO2 levels using neural networks. Journal of the Air & Waste Management Association, 53: 532-539.

Gardner, M. and Dorling, S. 2001. Artificial neural network-derived trends in daily maximum surface ozone concentrations. Journal of the Air & Waste Management Association, 51: 1202-1210.

Garrett, J.H., Jr., Gunaratman, D.J. and Ivezic, N. 1997. Introduction. In Artificial Neural Networks for Civil Engineer: Fundamentals and Applications, N. Kartam, I. Flood, and J.H. Garrett, Jr. Eds. American Society of Civil Engineers, New York, NY.

Henseler, J. 1995. Back propagation. In Artificial Neural Networks; An Introduction to ANN Theory and Practice, P.J. Braspenning, F. Thuijsman, and A.J.M.M. Weijters, Eds. Springer-Verlag Berlin Heidelberg, Germany, 37-66.

Jain, A.K., Mao, J., and Mohiuddin, K.M. 1996. Artificial neural networks: a tutorial. Computer, 3: 31-44.

Judd, C.M. and McClelland, G.H. 1989. Data Analysis; A Model-Comparison Approach. Harcourt Brace Jovanovich, Inc., Orlando, FL.

Kolehmainen, M., Martikainen, H., Hiltunen, T., and Ruuskanen, J. 2000. Forecasting air quality parameters using hybrid neural network modelling. Environmental Monitoring and Assessment, 65: 277-286.

Last, J., Trouton, K. and Pengelly, D. 1998. Taking Our Breath Away: The Health Effects of Air Pollution and Climate Change. David Suzuki Foundation, Vancouver, BC.

Lipfert, F.W. and Hammerstrom, T. 1992. Temporal patterns in air pollution and hospital admissions. Environmental Research, 59: 374-399.

McCullum, K. 2003. Environmental Engineer, Focus Corporation Ltd., Edmonton, AB. Personal communications, October 24, 2003.

McDonnell, W.F., Abbey, D.E., Nishino, N. and Lebowitz, M.D. 1999. Long-term ambient ozone concentration and the incidence of asthma in non-smoking adults: the AHSMOG study. Environmental Research, Section A, 80: 110-121.

Montgomery, D.C. 2001. Design and Analysis of Experiments, 5th ed. John Wiley & Sons, Inc., New York, NY.

Plochl, M. 2001. Neural network approach for modelling ammonia emission after manure application on the field. Atmospheric Environment, 35: 5833-5841.

Sandhu, H.S. 1999. Ground-Level Ozone in Alberta. Science and Technology Branch, Environmental Sciences Division, Alberta Environmental Protection, Edmonton, AB.

Schlink, U., Dorling, S., Pelikan, E., Nunnari, G., Cawley, G., Junninen, H., Greig, A., Foxall, R., Eben, K., Chatterton, T., Vondracek, J., Richter, M., Dostal, M., Bertucco, L., Kolehmainen, M., and Doyle, M. 2003. A rigorous inter-comparison of ground-level ozone predictions. Atmospheric Environment, 37: 3237-3253.

Sharma, S., Barai, S.V., and Dikshit, A.K. 2003. Studies of air quality predictors based on neural networks. International Journal of Environment and Pollution, 19(5): 442-453.

Thurston, G.D., Lippmann, M., Scott, M.B. and Fine, J.M. 1997. Summertime haze air pollution and children with asthma. American Journal of Respiratory and Critical Care Medicine, 155: 655-660.

Tupas, R.T. 2000. Artificial Neural Network Modeling of Filtration Performance, Master of Science thesis. Department of Civil and Environmental Engineering, University of Alberta, Edmonton, AB.

Viotti, P., Liuti, G., and Di Genova, P. 2002. Atmospheric urban pollution: applications of an artificial neural network (ANN) to the city of Perugia. Ecological Modelling, 148: 27-46.

Walpole, Ronald E. and Myers, Raymond H. 1993. Probability and Statistics for Engineers and Scientists, 5th ed. Macmillan Publishing Company, New York, NY.

7.0 GENERAL DISCUSSION AND CONCLUSIONS

In this thesis, a systematic approach is used to develop four ground level ozone ANN models for each of Edmonton and Calgary, Canada. The first model developed is a virtual monitor model that uses a combination of meteorological and pollutant concentration inputs to model the corresponding ozone concentration. The second model is a forecast model that predicts ground level ozone concentrations up to two hours in advance. The final two models are variants of the first two, considering ozone time series effects. The data used to develop the models were obtained from the East monitoring stations in both cities. The Calgary model development was based on the knowledge obtained from the Edmonton East model development.

The systematic approach is a methodical strategy for developing ANN models. The systematic approach attempts to address the ad hoc nature of model development that is apparent in the ANN literature. With the systematic approach, the principle of parsimony is preferred, which limits the number of structures requiring evaluation, decreasing the time required to determine the optimum network architecture. The use of this approach for the Calgary and Edmonton East ANNs resulted in successful models compared to models presented in the literature. The systematic approach still requires judgements to be made in terms of trade offs in performance gains versus model simplicity and computation time. In addition, the model developer is required to set a minimum performance standard for the models, and a relative contribution cut-off when selecting the inputs to the model. These requirements highlight the importance of clearly delineating the modelling objectives and incorporating the current scientific knowledge of the process when making model development decisions.

The Edmonton East and Calgary East models performed comparably based on the coefficient of multiple determination (R^2) values. The Calgary East models eliminated the four least important inputs of day of the week, opacity, wind direction, and wind speed in the Edmonton East models. For the virtual monitor models, this resulted in fewer epochs required to train the model, but increased the number of neurons in the hidden layer. No similar trends were observed in the forecast models, but the maximum prediction window

yielding an acceptable prediction performance was lower for the Calgary models. The fractional bias of the Calgary East predictions was also slightly higher than for the Edmonton East models.

The order of importance of the input variables to the Edmonton and Calgary virtual monitor models were similar, based on the built-in NeuroShell2 method for establishing the relative contributions of input variables. For Edmonton, the most important inputs, in order of decreasing relative contribution, were NO, THC, SO_2, NO_2, temperature, and the month of May. This compares well to Calgary, whose most important inputs were NO, THC, SO_2, NO_2, temperature, relative humidity, and the month of June. These results suggest that the sources of precursor compounds and atmospheric influences in the two cities are similar. However, caution is required in interpreting relative contribution results, as no universally accepted method exists for establishing the relative importance of input variables. The work completed in this thesis also suggests that equivalent model performance may be derived from different ANN architectures, providing the ANN structure is optimized for the specific inputs. Therefore, incomplete knowledge about the relevant contributors to a process will not necessarily compromise the success of the ANN approach. Rather, it appears that some compensation in the model performance can be made through the network structuring.

The logistic activation function continues to be proven reliable in this work, and was the function selected for three out of four activation functions. In both the Edmonton and Calgary models, model performance improved with inclusion in the set of inputs of the ozone concentration from the previous hour. In both cases, performance gains from including the previous hour's ozone concentrations were higher when the forecast window was increased.

Compared with other virtual monitor type models in the literature, the Calgary and Edmonton East models developed in this thesis are top models (see Table 7-1). Based on R^2 values, only the models developed by Abdul-Wahab and Al-Alawi (2002) were better. However, Abdul-Wahab and Al-Alawi used 5 minute averaged monitoring data. This allowed a better incorporation of temporal trends and correlation information that is lost in the hourly averaged data used in this research. The Abdul-Wahab and Al-Alawi models were

also developed and tested using data collected over only one year. The ability of their models to handle year-to-year variations in meteorology and pollutant concentrations is therefore unknown. In addition, the time required to train the ANN on 5 minute averaged data for 5 years would be significantly longer than for hourly averaged data. For one year's data, Abdul-Wahab and Al-Alawi required more than 9 hours to train their neural network.

The third model of Narasimhan et. al. (2000), incorporating modelled upper air data, also produced a slightly better R^2 than for the Calgary and Edmonton East models. Similar upper air data were unavailable or unreliable for the Calgary and Edmonton East models, and were excluded from the model inputs. With R^2 values of 0.86 (and 0.92 with ozone time series effects included), it is clear that the ANN models generated in this project do not incorporate all the inputs that influence ozone concentrations in Edmonton and Calgary. The unaccounted remaining 8% of variability may be attributed to a number of parameters excluded from the models, including upper air information, vertical wind, temperature, and pressure profiles, precipitation data, and concentrations for specific volatile organic compounds (VOCs). However, in the interest of producing a model that can easily be used as a forecasting tool, only inputs that are publicly and freely available, and have a reasonable likelihood of being monitored in the future, were used in the Edmonton and Calgary models. Most of the important variables also appear to be captured by the current input data set, judging from the performance of the models.

Based on reported root mean squared error (RMSE), mean absolute error (MAE), and bias, the Edmonton and Calgary East virtual monitor model values were top performers.

For the forecast models, the R^2 values of the Edmonton East and Calgary East models were comparable to or better than literature values (Table 7-2). However, the forecast windows were smaller than some of the models presented in the literature. Again, the Abdul-Wahab and Al-Alawi (2002) model had a higher R^2 value, but the prediction window of their forecast was not provided. Consideration must also be given to the fact that some authors use actual values of meteorological inputs corresponding to the forecast time, so that these models are not true forecast models. RMSE and MAE values for the Calgary and Edmonton models were comparable or lower than values reported in the literature. Both

Wilmott indices of agreement and bias values for the Calgary East and Edmonton East models were also better than reported literature values. One method used in the literature for increasing the forecast window is using data from the same hour of the previous day for input to the model. This method would incorporate the diurnal patterns observed in the ozone concentrations of Edmonton and Calgary, and should be examined in future research. The features of literature models are summarized in Table 7-3.

ANNs have proven to be a viable modelling tool for Edmonton and Calgary. However, general acceptance and enthusiasm for this modelling approach is currently hindered by its black box image. A method is required for evaluating the contributions of individual input variables, and for amalgamating the information from connection weights, activation functions, and the network structure, to overcome this black box image. This would also increase the usefulness of the ANN model, because it could then be used to understand the mechanisms of the modelled process.

Operationally, the ANN models are potentially cost effective replacements for "real" ambient monitors. Models have been developed in the literature for SO_2 (Boznar et al. 1993; Mok and Tam 1998)), NO_2 (Cappa et al. 2001; Chelani and Hasan 2001), NO_x (Gardner and Dorling 1999), particulates (McKendry 2002; Perez et al. 2000), ammonia (Plochl 2001), and CO (Drozdowicz et al. 1997). With the monitoring practices in Alberta tending more and more towards airshed management approaches, ANNs can provide a means of obtaining greater quantities of pollutant information without prohibitive expense. With further research, ANNs may one day challenge the traditional mechanistic approaches in atmospheric modelling.

Table 7-1 Comparison of virtual monitor models to models reported in the literature.

Model	Year	Time Scale	R^2	r	MSE	RMSE	MAE	AE_{min}	AE_{max}	Bias	d_1	d_2
		hours			ppm^2x10^5	ppm	ppm	ppm	ppm			
Edmonton East	2004	1	0.87	0.93	3.27	0.006	0.004	0	0.032	0.084	0.83	0.96
Calgary East	2004	1	0.85	0.92	3.29	0.006	0.004	0	0.023	0.196	0.82	0.96
Abdul-Wahab	2001	5 min.	0.86									
Abdul-Wahab and Al-Alawi	2002	5 min.	0.94									
Cobourn et al.	2000	1				0.016	0.013			-1.9		
Gardner and Dorling (Cliffside)	2001	1	0.74									
Gardner and Dorling (Chicago)	2001	1	0.69									
Gardner and Dorling (Decatur)	2001	1	0.64									
Gardner and Dorling (Los Angeles)	2001	1	0.47									
Gardner and Dorling (Miami)	2001	1	0.32									
Gardner and Dorling (Washington)	2001	1	0.72									
Guardani et al. (station 2)	1999	1	0.86									
Guardani et al. (station 4)	1999	1	0.86									
Narasimhan et al. (model 1)	2000	1	0.77									
Narasimhan et al. (model 2)	2000	1	0.82									
Narasimhan et al. (model 3)	2000	1	0.88									
Soja and Soja	1999	1				0.052	0.039					

Table 7-2 Comparison of forecast models to models reported in the literature.

Model	Year	Forecast Window	R^2	r	MSE	RMSE	MAE	AE_{min}	AE_{max}	Bias	d_1	d_2
		hours			ppm^2x10^5	ppm	ppm	ppm	ppm			
Edmonton East	2004	1	0.89	0.94	2.80	0.005	0.004	0	0.031	0.079	0.85	0.97
Edmonton East	2004	2	0.75	0.86	6.17	0.008	0.006	0	0.038	0.122	0.76	0.92
Calgary East	2004	1	0.87	0.93	2.85	0.005	0.004	0	0.024	0.155	0.84	0.96
Abdul-Wahab and Al-Alawi	2002	n/a	0.93									
Balaguer Ballester et al. (Paterna)	2002	24		*0.88*		0.008	0.007				0.73	0.91
Balaguer Ballester et al. (Alcoi)	2002	24		*0.87*		0.009	0.007				0.69	0.88
Balaguer Ballester et al. (Carcaixent)	2002	24		*0.90*		0.010	0.008				0.78	0.93
Cannon and Lord (T1)[a]	2000	n/a	0.27			0.008	0.006					
Cannon and Lord (T7)[a]	2000	n/a	0.48			0.010	0.008					
Cannon and Lord (T9)[a]	2000	n/a	0.52			0.009	0.007					
Cannon and Lord (T12)[a]	2000	n/a	0.64			0.009	0.007					
Cannon and Lord (T15)[a]	2000	n/a	0.47			0.009	0.007					
Cannon and Lord (T17)[a]	2000	n/a	0.38			0.008	0.006					
Cannon and Lord (T21)[a]	2000	n/a	0.49			0.010	0.008					
Cannon and Lord (T27)[a]	2000	n/a	0.44			0.009	0.007					
Cannon and Lord (T28)[a]	2000	n/a	0.63			0.009	0.007					
Cannon and Lord (T29)[a]	2000	n/a	0.57			0.011	0.008					
Cobourn et al.	2000	n/a				0.014	0.012			-3.7		
Comrie (Seattle)[b]	1997	24	0.70			0.009	0.007				0.72	0.91
Comrie (Pittsburgh)[b]	1997	24	0.65			0.014	0.011				0.68	0.88
Comrie (Chicago)[b]	1997	24	0.61			0.012	0.009				0.65	0.86
Comrie (Atlanta)[b]	1997	24	0.59			0.016	0.012				0.64	0.85
Comrie (Charlotte)[b]	1997	24	0.56			0.014	0.011				0.63	0.84
Comrie (Boston)[b]	1997	24	0.47			0.015	0.012				0.57	0.78

Table 7-2 cont'd. Comparison of forecast models to models reported in the literature.

Model	Year	Forecast Window	R^2	r	MSE	RMSE	MAE	AE_{min}	AE_{max}	Bias	d_1	d_2
Comrie (Tucson) [b]	1997	24	0.27			0.010	0.008				0.45	0.66
Comrie (Phoenix) [b]	1997	24	0.24			0.015	0.012				0.42	0.62
Hadjiiski and Hopke	2000	1		*0.98*		0.004						
Hadjiiski and Hopke	2000	3				0.008						
Hadjiiski and Hopke	2000	5				0.011						
Jorquera et al. (station C, C6)	1998	24				0.017						0.79
Jorquera et al. (station C, C7)	1998	24				0.021						0.82
Jorquera et al. (station E, E6)	1998	24				0.022						0.89
Jorquera et al. (station E, E7)	1998	24				0.034						0.70
Melas et al.	2000	24		0.80		0.014		0.050	0.060			
Sohn et al.	2000	1				0.009						
Sohn et al.	2000	2				0.011						
Sohn et al.	2000	3				0.012						
Sohn et al.	2000	4				0.013						
Sohn et al.	2000	5				0.013						
Sohn et al.	2000	6				0.013						
Sohn et al.	2000	16				0.014						
Sohn et al.	2000	17				0.013						
Sohn et al.	2000	18				0.013						
Sohn et al.	2000	19				0.012						
Sohn et al.	2000	20				0.012						
Sohn et al.	2000	21				0.012						
Spellman (Central London)	1999	24		0.77		0.010	0.007					
Spellman (Harwell)	1999	24		0.72		0.012	0.009					
Spellman (Birmingham)	1999	24		0.54		0.010	0.007					
Spellman (Leeds)	1999	24		0.53		0.009	0.007					

Table 7-2 cont'd. Comparison of forecast models to models reported in the literature.

Model	Year	Forecast Window	R^2	r	MSE	RMSE	MAE	AE_{min}	AE_{max}	Bias	d_1	d_2
Spellman (Strath Vaich)	1999	24		0.68		0.007	0.005					
Wang et al. (Tsuen Wan)	2003	n/a					0.012	0	0.058			
Wang et al. (Kwai Chung)	2003	n/a					0.014	0	0.046			
Wang et al. (Kwun Tong)	2003	n/a					0.013	0	0.038			

a Performance for individual, converged models, since these models are most similar to the models developed in this research.
b Performance for models excluding maximum hourly ozone concentration from previous day. Note models use actual values from the forecast day as inputs, and are therefore not true forecast models.
Italics indicate values calculated based on information in the paper.

Table 7-3 Summary of literature models.

Source	Year	Environment	Model	No. Layers	No. Hidden Layer Neurons	No. Training Epochs	No. Training Patterns	No. Test Patterns	No. Production Patterns
Abdul-Wahab and Al-Alawi	2002	urban residential	24-hours	3		13427	4078		719
			daylight hours	3		19384	1386		244
			daily max O_3	3		1054327	16		3
Balaguer Ballester et al.	2002	urban (Paterna)	24-hr forecast	3	5 to 40	2 to 20	2880		
		urban (Alcoy)	24-hr forecast	3	5 to 40	2 to 20	2736		
		rural (Carcagente)	24-hr forecast	3	20	2 to 20	2448		
Cannon and Lord	2000	Lower Fraser Valley, BC	daily max O_3	3	50				
Comrie	1997	Atlanta, GA	daily max O_3	3	6		440		250
		Atlanta, GA	daily max O_3	3	7		440		250
		Boston, MA	daily max O_3	3	6		440		250

Table 7-3 cont'd. Summary of literature models.

Source	Year	Environment	Model	No. Layers	No. Hidden Layer Neurons	No. Training Epochs	No. Training Patterns	No. Test Patterns	No. Production Patterns
Comrie	1997	Boston, MA	daily max O_3	3	7		440		250
		Charlotte, NC	daily max O_3	3	6		440		250
		Charlotte, NC	daily max O_3	3	7		440		250
		Chicago, IL	daily max O_3	3	6		440		250
		Chicago, IL	daily max O_3	3	7		440		250
		Phoenix, AZ	daily max O_3	3	6		440		250
		Phoenix, AZ	daily max O_3	3	7		440		250
		Pittsburgh, PA	daily max O_3	3	6		440		250
		Pittsburgh, PA	daily max O_3	3	7		440		250
		Seattle, WA	daily max O_3	3	6		440		250
		Seattle, WA	daily max O_3	3	7		440		250
		Tucson, AZ	daily max O_3	3	6		440		250
		Tucson, AZ	daily max O_3	3	7		440		250
Coburn et al.	2000	Louisville, KY	forecast daily max O_3	3	10		(1993-1997)	(1998)	(1999)
		Louisville, KY	hindcast daily max O_3	3	10		(1993-1997)	(1998)	(1999)
Elkamel et al.	2001	Kuwait industrial	O_3 every 5 minutes	3	25		2372	226	
Gardner and Dorling	2001	Cliffside Park, NJ	daily max O_3	4	10/10				
		Washington, DC	daily max O_3	4	10/10				
		Decatur, GA	daily max O_3	4	10/10				
		Miami, FL	daily max O_3	4	10/10				
		Chicago, IL	daily max O_3	4	10/10				
		Los Angeles, CA	daily max O_3	4	10/10				

Table 7-3 cont'd. Summary of literature models.

Source	Year	Environment	Model	No. Layers	No. Hidden Layer Neurons	No. Training Epochs	No. Training Patterns	No. Test Patterns	No. Production Patterns
Guardani et al.	1999	Sao Paulo Metropolitan Area	hourly avg O_3	3	8		(Oct-Nov, 1996)	(Oct-Nov, 1997)	
Hadjiiski and Hopke	2000	Houston, TX	sensitivity, hourly avg O_3	3	3	200			
		Houston, TX	hourly avg O_3 at t+1	3	5	60000			
Jorquera et al.	1998	Santiago, Chile	Station C daily max O_3	3				63	
		Santiago, Chile	Station C daily max O_3	3				60	
		Santiago, Chile	Station E daily max O_3	3				235	
		Santiago, Chile	Station E daily max O_3	3				93	
Kao and Huang	2000	Taiwan	hourly avg O_3 at t+1	3	2 to 38				
Melas et al.	2000	Athens, Greece	daily max O_3	3	8		1172	327	
Narasimhan et al.	2000	Tulsa, OK	Basic hourly avg O_3	3					
		Tulsa, OK	Basic w/previous O_3 inputs	3					
Prybutok et al.	2000	Houston, TX	daily max O_3	3	4				
Sohn et al.	2000	Seoul, Korea	1-hour ahead hourly avg O_3	3	50		31		

Table 7-3 cont'd. Summary of literature models.

Source	Year	Environment	Model	No. Layers	No. Hidden Layer Neurons	No. Training Epochs	No. Training Patterns	No. Test Patterns	No. Production Patterns
Sohn et al.	2000	Seoul, Korea	2-hours ahead hourly avg O_3	3	50		31		
		Seoul, Korea	3-hours ahead hourly avg O_3	3	50		31		
		Seoul, Korea	4-hours ahead hourly avg O_3	3	50		31		
		Seoul, Korea	5-hours ahead hourly avg O_3	3	50		31		
		Seoul, Korea	6-hours ahead hourly avg O_3	3	50		31		
		Seoul, Korea	16-hours ahead hourly avg O_3	3	50		31		
		Seoul, Korea	17-hours ahead hourly avg O_3	3	50		31		
		Seoul, Korea	18-hours ahead hourly avg O_3	3	50		31		
		Seoul, Korea	19-hours ahead hourly avg O_3	3	50		31		
		Seoul, Korea	20-hours ahead hourly avg O_3	3	50		31		
		Seoul, Korea	21-hours ahead hourly avg O_3	3	50		31		
Soja and Soja	1999	rural Austria	daily integrated ozone dose	3	3				
Spellman	1999	London (urban)	daily max O_3	4	3/3		306	306	
		Harwell (rural)	daily max O_3	4	3/3		306	306	

Table 7-3 cont'd. Summary of literature models.

Source	Year	Environment	Model	No. Layers	No. Hidden Layer Neurons	No. Training Epochs	No. Training Patterns	No. Test Patterns	No. Production Patterns
Spellman	1999	Birmingham (urban)	daily max O_3	4	10/8		306	306	
		Leeds (urban)	daily max O_3	4	3/3		306	306	
		Strath Vaich (remote)	daily max O_3	4	6/9		306	306	
Yi & Prybutok	1996	Dallas-Ft. Worth	daily max O_3	3	4				

References

Abdul-Wahab, S.A. 2001. IER photochemical smog evaluation and forecasting of short-term ozone pollution levels with artificial neural networks. Process Safety and Environmental Protections: Transactions of the Institution of Chemical Engineers, Part B, 79(2): 117-128.

Abdul-Wahab, S.A. and Al-Alawi, S.M. 2002. Assessment and prediction of tropospheric ozone concentration levels using artificial neural networks. Environmental Modelling & Software, 17: 219-228.

Balaguer Ballester, E., Camps i Valls, G., Carrasco-Rodriguez, J.L., Soria Olivas, E., and del Valle-Tascon, S. 2002. Effective 1-day ahead prediction of hourly surface ozone concentrations in eastern Spain using linear models and neural networks. Ecological Modelling, 156: 27-41.

Boznar, M., Lesjak, M., and Mlakar, P. 1993. A neural network-based method for short-term predictions of ambient SO_2 concentrations in highly polluted industrial areas of complex terrain. Atmospheric Environment, 27B(2): 221-230.

Cannon, A.J. and Lord, E.R. 2000. Forecasting summertime surface-level ozone concentrations in the Lower Fraser Valley of British Columbia: an ensemble neural network approach. Journal of the Air & Waste Management Association, 50: 322-339.

Cappa, C., Anfossi, D., Grosa, M.M., and Natale, P. 2001. Short-term prediction of urban NO_2 pollution by means of artificial neural networks. International Journal of Environment and Pollution, 15(5): 483-496.

Chelani, A.B. and Hasan, M.Z. 2001. Forecasting nitrogen dioxide concentration in ambient air using artificial neural-networks. International Journal of Environmental Studies, 58: 487-499.

Cobourn, W.G., Dolcine, L., French, M., and Hubbard, M.C. 2000. A comparison of nonlinear regression and neural network models for ground-level ozone forecasting. Journal of the Air & Waste Management Association, 50: 1999-2009.

Comrie, A.C. 1997. Comparing neural networks and regression models for ozone forecasting. Journal of the Air & Waste Management Association, 47: 653-663.

Drozdowicz, B., Benz, S.J., Santa Cruz, A.S.M., and Scenna, N.J. 1997. A neural network based mdoel for the analysis of carbon monoxide contamination in the urban area of Rosario. In Proceedings of the 1997 5th International Conference on Air Pollution, Air Pollution V. Computational Mechanics Inc., Billerica, MA, 677-683.

Elkamel, A., Abdul-Wahab, S., Bouhamra, W., and Alper, E. 2001. Measurement and prediction of ozone levels around a heavily industrialized area: a neural network approach. Advances in Environmental Research, 5: 47-59.

Gardner, M.W. and Dorling, S.R. 1999. Neural network modelling and prediction of hourly NO_x and NO_2 concentrations in urban air in London. Atmospheric Environment, 33:709-719.

Gardner, M. and Dorling, S. 2001. Artificial neural network-derived trends in daily maximum surface ozone concentrations. Journal of the Air & Waste Management Association, 51: 1202-1210.

Guardani, R., Nascimento, C.A.O., Guardani, M.L.G., Martins, M.H.R.B., and Romano, J. 1999. Study of atmospheric ozone formation by means of a neural network-based model. Journal of the Air & Waste Management Association, 49: 316-323.

Hadjiiski, L. and Hopke, P. Application of artificial neural networks to modeling and prediction of ambient ozone concentrations. 2000. Journal of the Air & Waste Management Association, 50: 894-901.

Jorquera, H., Perez, R., Cipriano, A., Espejo, A., Letelier, M.V., and Acuna, G. 1998. Forecasting ozone daily maximum levels at Santiago, Chile. Atmospheric Environment, 32(20): 3415-3424.

Kao, J., and Huang, S. 2000. Forecasts using neural network versus Box-Jenkins methodology for ambient air quality monitoring data. Journal of the Air & Waste Management Association, 50: 219-226.

McKendry, I. 2002. Evaluation of artificial neural networks for fine particulate pollution (PM_{10} and $PM_{2.5}$) forecasting. Journal of the Air & Waste Management Association, 52: 1096-1110.

Melas, D., Kioutsioukis, I., and Ziomas, C. 2000. Neural network model for predicting peak photochemical pollutant levels. Journal of the Air & Waste Management Association, 50: 495-501.

Mok, K.M. and Tam, S.C. 1998. Short-term prediction of SO_2 concentrations in Macau with artificial neural networks. Energy and Buildings, 28: 279-286.

Narasimhan, R., Keller, J., Subramaniam, G., Raasch, E., Croley, B., Duncan, K., and Potter, W.T. 2000. Ozone modeling using neural networks. Journal of Applied Meteorology, 39: 291-296.

Perez, P., Trier, A., and Reyes, J. 2000. Prediction of $PM_{2.5}$ concentrations several hours in advance using neural networks in Santiago, Chile. Atmospheric Environment, 34: 1189-1196.

Plochl, M. 2001. Neural network approach for modelling ammonia emission after manure application on the field. Atmospheric Environment, 35: 5833-5841.

Prybutok, V.R., Yi, J., and Mitchell, D. 2000. Comparison of neural network models with ARIMA and regression models for prediction of Houston's daily maximum ozone concentrations. European Journal of Operational Research, 122: 31-40.

Sohn, S.H., Oh, S.C., Jo, B.W., and Yeo, Y. 2000. Prediction of ozone formation based on neural network. Journal of Environmental Engineering, 8: 688-696.

Soja, G. and Soja, A. 1999. Ozone indices based on simple meteorological parameters: potentials and limitations of regression and neural network models. Atmospheric Environment, 33: 4299-4307.

Spellman, G. 1999. An application of artificial neural networks to the prediction of surface ozone concentrations in the United Kingdom. Applied Geography, 19: 123-136.

Wang, W., Lu, W., Wang, X., and Leung, A.Y.T. 2003. Prediction of maximum daily ozone level using combined neural network and statistical characteristics. Environment International, 29: 555-562.

Yi, J. and Prybutok, V.R. 1996. A neural network model forecasting for prediction of daily maximum ozone concentration in an industrialized urban area. Environmental Pollution, 92(3): 349-357.

APPENDIX A: CONNECTION WEIGHTS OF EDMONTON EAST MODELS

Table A- 1 First layer of virtual monitor model.

To Hidden Layer Neuron	From Input Neuron												
	BIAS	MAY	JUN	JUL	AUG	SEP	SUN	MON	TUE	WED	THU	FRI	SAT
1	-2.07	-1.85	-0.70	0.27	-1.99	-0.18	-0.55	0.03	-2.43	23.63	-3.98	-2.65	-1.58
2	-0.56	-0.81	0.19	0.01	-0.46	-0.07	1.38	18.89	-2.77	-1.69	19.31	-0.44	-1.25
3	-34.69	-34.71	18.23	18.00	17.05	17.54	6.93	7.06	6.75	3.18	3.42	6.50	5.12
4	-0.86	-0.75	-0.05	0.59	2.85	2.56	-0.08	-1.57	-0.07	0.32	1.29	1.55	2.77
5	-1.48	-1.57	-1.28	26.43	-4.29	-5.53	8.50	4.67	-0.28	-2.44	-1.78	-4.07	-6.66
6	3.50	3.28	-0.80	-0.96	-2.02	-2.16	-0.78	-0.49	-1.50	-1.11	-0.34	-0.84	-2.34
7	-1.13	-1.33	-1.42	0.60	-0.72	1.57	1.53	-3.50	-1.88	-4.07	-1.08	-2.00	-2.92
8	0.21	-0.32	-0.19	0.30	0.60	1.14	-0.21	1.40	0.80	1.16	1.17	0.67	1.40
9	1.17	0.91	2.56	-0.82	1.26	-4.53	0.26	-1.52	0.55	-6.56	3.95	0.69	0.54
10	33.49	33.36	-1.24	-5.94	-1.47	-2.21	27.27	-2.88	-5.74	-4.87	-0.02	-4.92	-8.78
11	-0.89	-0.65	4.07	-1.11	0.35	-0.03	1.32	-0.66	24.29	-1.05	-0.83	-0.98	1.95
12	0.63	0.48	1.92	-0.14	-5.18	4.62	-0.66	-1.53	-1.44	-0.07	4.71	4.64	-0.60
13	27.49	27.43	17.29	0.68	-7.26	-5.07	-0.33	3.32	5.72	-0.46	-1.90	0.16	4.33
14	-0.22	-0.43	-3.61	6.70	-0.16	-1.79	-20.79	-11.07	-0.30	-0.09	4.06	-1.23	0.06
15	-0.45	-0.24	0.79	0.75	1.79	1.50	1.40	1.56	0.52	-0.85	2.68	1.50	1.84
16	0.20	0.47	0.98	-0.51	-0.19	-1.61	-0.78	-0.80	1.21	0.84	0.12	-2.11	0.85
17	-2.41	-2.26	0.42	-0.47	0.97	0.70	1.35	-0.57	0.81	0.39	1.14	0.11	1.25

Table A-1 cont'd. First layer of virtual monitor model.

To Hidden Layer Neuron	From Input Neuron								
	NO	NO_2	SO_2	THC	OPA	RH	TEMP	WDR	WSP
1	36.29	-8.81	22.86	150.69	0.51	-0.40	-3.88	1.58	1.40
2	1.00	1.11	0.71	32.17	2.21	0.91	-2.29	0.28	0.10
3	-166.60	25.54	22.79	-76.33	-3.64	-10.16	3.35	7.06	0.24
4	27.55	3.31	-10.00	-4.54	0.24	0.98	-1.40	-0.05	0.58
5	0.72	-3.88	13.30	2.41	-2.08	12.24	9.66	-0.91	-15.36
6	-0.22	1.80	-7.19	-9.78	-0.98	-2.13	3.11	-2.03	0.97
7	11.30	17.41	-64.17	-4.00	-1.72	-0.23	1.85	-0.64	-7.23
8	-12.01	8.67	-2.84	0.28	-0.24	1.56	-4.74	-3.10	-2.43
9	-7.44	2.75	-10.00	4.82	-4.85	1.77	-4.72	0.24	-0.31
10	30.78	-26.63	-4.41	15.79	-3.87	-6.31	-20.81	0.45	-8.27
11	50.80	1.74	-1.07	3.70	-2.86	1.23	-0.84	2.59	-4.88
12	-12.57	-0.40	-8.65	-22.06	-0.84	-1.33	2.16	0.14	0.08
13	-2.59	-9.18	5.74	-8.24	5.44	0.38	-30.21	-0.32	8.80
14	5.71	11.71	-4.50	-78.16	2.31	5.09	-7.45	4.33	16.09
15	-13.39	-5.64	-1.83	11.30	1.38	0.10	0.77	-0.01	0.62
16	-8.27	-0.98	5.02	4.76	-0.41	-0.95	2.34	-0.78	-0.51
17	-81.26	-2.93	-2.93	5.85	-0.69	0.54	4.28	0.50	-5.02

Table A- 2 Second layer of virtual monitor model.

To Output Neuron	From Hidden Layer Neuron																	
	BIAS	1	2	3	4	5	6	7	8	9	10	11	12	13	14	15	16	17
1	-0.10	-0.19	-0.24	0.91	-0.28	-0.21	0.55	-0.25	-0.52	-0.20	-0.24	-0.26	0.25	-0.33	-0.23	0.32	0.43	0.39

Table A- 3 First layer of virtual monitor model with time series.

To Hidden Layer Neuron	From Input Layer Neuron												
	BIAS	MAY	JUN	JUL	AUG	SEP	SUN	MON	TUE	WED	THU	FRI	SAT
1	-0.45	0.07	-0.49	-1.00	0.07	0.53	0.58	0.10	-0.21	0.35	-0.17	-0.09	-1.88
2	-0.51	-0.42	0.79	-0.44	-0.41	-0.26	-1.35	-1.66	-1.20	-0.49	0.30	-0.08	-0.61
3	-1.47	-1.28	0.00	-0.53	-0.25	-0.65	-1.03	-1.09	-1.17	-0.76	-1.24	-0.91	-0.42
4	-0.16	-0.46	0.98	1.31	0.89	0.57	0.48	0.97	0.30	0.94	0.44	0.38	1.27
5	-1.54	-1.88	-0.04	0.13	0.70	0.19	0.15	-0.09	0.15	0.26	-0.34	0.51	2.12
6	0.34	0.11	0.73	-0.18	-0.20	-0.09	0.64	0.46	0.52	0.72	1.03	0.98	0.62
7	0.50	0.51	0.08	-0.06	-0.08	-0.48	-0.26	-0.31	-0.14	0.23	-0.19	-0.42	-0.03
8	2.19	1.74	1.41	0.75	0.93	1.02	0.62	0.34	0.67	0.94	0.72	0.68	0.30
9	0.81	0.42	-0.28	0.09	0.31	-0.13	0.91	-0.05	0.69	-0.24	-0.22	-0.06	-0.03
10	-0.15	-0.01	0.18	0.72	0.59	0.23	-0.04	0.14	0.44	0.39	-0.26	-0.09	0.26
11	-0.40	-0.23	-0.56	0.54	0.29	-0.12	-0.08	0.37	-0.56	-2.15	0.38	-0.25	0.19

Table A-3 cont'd. **First layer of virtual monitor model with time series.**

To Hidden Layer Neuron	From Input Layer Neuron									
	NO	NO_2	SO_2	THC	OPA	RH	TEMP	WDR	WSP	O_3(t-1)
1	0.05	1.76	-1.68	-0.85	-0.23	1.33	0.18	0.29	-1.09	-3.10
2	2.04	2.01	-0.77	0.85	0.04	1.04	-0.39	-0.43	-0.04	-2.89
3	5.67	-0.09	3.99	-4.12	-0.59	-1.16	4.19	-0.57	-1.96	0.03
4	-1.04	2.41	-1.30	1.35	-0.14	0.21	0.60	0.07	0.98	-4.31
5	-0.60	1.87	0.11	0.47	-0.01	0.63	0.23	0.84	0.14	-2.81
6	-1.02	-9.40	11.30	2.33	0.51	-1.49	3.19	0.95	3.17	-0.82
7	-13.62	-0.77	2.01	0.97	-0.33	-0.40	0.58	-0.10	0.15	2.28
8	8.45	1.58	-0.41	6.23	-0.10	-1.84	-0.07	0.02	0.00	-7.23
9	0.10	1.96	-0.15	0.73	-0.23	0.45	0.01	0.10	-0.32	-3.37
10	3.60	-5.76	10.37	0.29	0.22	0.59	-1.31	0.20	-0.06	-4.59
11	-3.77	1.85	-8.78	1.25	-0.47	0.70	-0.10	-0.02	0.08	-2.46

Table A- 4 **Second layer of virtual monitor model with time series.**

To Output Neuron	From Hidden Layer Neuron											
	BIAS	1	2	3	4	5	6	7	8	9	10	11
1	-0.27	-0.27	-0.37	0.61	-0.45	-0.19	0.61	0.39	-0.57	-0.20	-0.72	-0.24

Table A- 5 First layer of one hour forecast model.

To Hidden Layer Neuron	From Input Layer Neuron												
	BIAS	MAY	JUN	JUL	AUG	SEP	SUN	MON	TUE	WED	THU	FRI	SAT
1	0.62	0.82	0.53	0.27	-0.32	0.93	0.36	0.77	0.54	0.25	0.93	0.66	0.50
2	1.94	2.14	1.61	2.05	2.13	32.18	1.69	2.05	1.51	1.69	2.64	2.06	1.48
3	-0.45	-0.08	-1.98	2.26	0.65	1.59	1.14	2.78	1.44	0.33	1.23	1.42	1.07
4	-0.75	-0.79	-0.71	-0.36	-0.42	0.30	-0.08	-0.05	-0.26	-0.39	-0.07	-0.16	0.02
5	1.55	1.30	1.23	0.88	0.51	0.51	0.92	0.60	0.96	1.12	0.64	0.81	0.97
6	-0.42	-0.19	1.06	0.34	2.11	0.82	0.55	0.50	0.78	0.86	0.85	0.70	0.53

Table A-5 cont'd. First layer of one hour forecast model.

To Hidden Layer Neuron	From Input Layer Neuron											
		SAT	NO	NO_2	SO_2	THC	OPA	RH	TEMP	WDR	WSP	O_3
1		0.50	-11.18	2.83	-16.20	4.42	-1.50	0.35	-0.36	-0.07	-4.03	-4.29
2		1.48	-33.24	0.26	-2.17	-6.15	0.73	-0.72	-1.12	-0.58	1.77	-7.94
3		1.07	-0.71	-0.61	-1.40	-0.26	0.07	0.20	-0.05	0.37	-0.98	-5.67
4		0.02	-5.49	1.76	-1.91	3.98	-0.01	0.61	0.58	0.31	-0.91	16.25
5		0.97	-5.22	1.85	-1.69	2.80	-0.16	-0.25	-0.26	0.06	-0.35	-6.53
6		0.53	0.44	-2.81	6.24	0.15	0.97	0.47	-0.50	0.39	1.17	-5.93

Table A- 6 Second layer of one hour forecast model.

To Output Neuron	From Hidden Layer Neuron						
	BIAS	1	2	3	4	5	6
1	-0.48	-0.60	-0.36	-0.26	1.43	-1.01	-0.62

Table A- 7 First layer of one hour forecast model with time series.

To Hidden Layer Neuron	From Input Layer Neuron												
	BIAS	MAY	JUN	JUL	AUG	SEP	SUN	MON	TUE	WED	THU	FRI	SAT
1	-0.36	-0.15	0.26	0.39	0.47	-0.04	0.25	0.63	0.36	1.07	0.22	0.44	0.99
2	-0.39	-0.19	-0.56	-0.66	-0.59	-0.60	-0.56	-0.20	-0.28	-0.45	-0.75	-0.51	-0.50
3	0.61	0.98	0.32	0.47	0.32	0.54	0.10	0.54	0.76	0.14	0.27	0.65	0.18
4	0.25	0.22	0.13	0.14	0.10	0.07	-0.17	-0.05	0.10	0.11	0.13	0.15	-0.18
5	0.81	0.56	0.24	-0.07	0.15	0.34	0.74	0.61	0.82	0.07	0.52	0.23	-0.02
6	0.02	0.24	0.39	0.11	0.50	0.57	0.50	0.80	0.44	0.76	0.38	0.31	0.34

Table A-7 cont'd. First layer of one hour forecast model with time series.

To Hidden Layer Neuron	From Input Layer Neuron										
	NO	NO_2	SO_2	THC	OPA	RH	TEMP	WDR	WSP	O_3(t-1)	O_3
1	-10.30	0.24	-0.12	-0.07	-0.17	0.70	-0.25	0.24	-0.20	3.27	-6.50
2	1.21	-0.36	2.36	-1.13	0.08	-0.42	0.35	0.01	0.10	-2.32	6.21
3	-1.54	-0.83	1.11	0.23	0.22	-0.13	0.12	-0.04	-0.29	0.69	-5.57
4	5.00	-1.79	2.80	-1.92	-0.14	0.19	-0.43	-0.50	0.56	-2.60	-19.72
5	-1.24	-0.76	1.75	-0.88	-0.03	-2.19	-0.53	0.00	-0.15	1.77	-5.65
6	-1.72	0.00	-0.04	0.29	-0.13	0.38	-0.07	0.26	-0.35	0.70	-4.87

Table A- 8 Second layer of one hour forecast model with time series.

To Output Neuron	From Hidden Layer Neuron						
	BIAS	1	2	3	4	5	6
1	-0.38	-0.49	1.29	-0.78	-1.18	-0.50	-0.54

Table A- 9 First layer of two hour forecast model.

To Hidden Layer Neuron	From Input Layer Neuron												
	BIAS	MAY	JUN	JUL	AUG	SEP	SUN	MON	TUE	WED	THU	FRI	SAT
1	-0.22	-0.21	-0.43	-0.23	0.65	0.95	0.01	0.39	0.33	0.38	-0.21	-0.46	0.34
2	-0.63	-0.91	-78.45	-1.43	0.34	1.00	-2.66	-1.07	-1.64	22.49	-0.90	-1.56	-5.73
3	0.12	0.23	0.08	-0.11	-0.08	-0.11	-0.26	-0.06	0.15	0.06	0.04	0.08	-0.29
4	-0.54	-0.94	-0.29	-0.43	-1.61	-1.11	-0.07	-0.19	-0.31	-0.98	-1.55	-1.60	-0.94
5	0.08	-0.18	-0.40	-0.30	-0.50	-0.98	-0.52	-0.02	-0.02	-0.16	-0.09	0.00	0.16
6	-5.29	-4.99	-4.47	-56.97	-3.99	-4.69	0.65	-52.73	1.40	0.78	-51.47	0.39	-0.59
7	-1.68	-1.62	-1.60	-0.57	-1.26	30.72	-0.02	0.37	-1.57	-1.14	-0.91	-0.71	-1.34
8	-0.72	-1.19	0.26	-2.60	-0.41	-1.11	0.44	-2.04	-0.77	-1.59	-1.15	-1.94	-0.13
9	0.30	-0.20	0.10	0.39	0.26	0.42	0.18	0.20	-0.03	-0.01	0.17	0.02	0.05
10	0.13	-0.32	0.48	0.70	1.42	0.31	0.52	-0.05	1.09	0.36	-0.19	-0.12	0.17
11	-2.41	-2.29	-1.06	-1.15	-1.13	-3.13	-1.49	-1.42	-1.68	-0.58	-2.41	-1.19	-0.65
12	-63.95	-64.14	14.14	13.78	2.98	-4.97	18.86	22.30	22.69	21.07	17.76	18.45	16.95
13	-0.17	-0.25	0.30	-0.53	0.22	0.18	0.58	-0.08	0.20	-0.16	0.29	0.66	0.15
14	0.04	0.09	1.19	1.21	0.09	2.23	0.24	1.99	0.29	2.15	0.21	0.36	-0.47
15	0.51	0.69	0.35	-0.03	0.36	0.52	0.11	0.25	0.58	0.66	0.76	0.35	0.06

Table A-9 cont'd. First layer of two hour forecast model.

To Hidden Layer Neuron	From Input Layer Neuron									
	NO	NO_2	SO_2	THC	OPA	RH	TEMP	WDR	WSP	O_3
1	0.63	-0.06	1.23	-0.65	0.19	0.36	-0.27	0.25	-0.07	-3.46
2	10.20	-5.99	5.96	-6.27	-2.49	4.25	-0.04	-0.34	3.40	4.20
3	4.52	-1.48	0.76	-0.93	-0.45	0.21	-0.86	-0.20	1.31	-15.92
4	10.22	-0.02	0.63	-0.48	-0.01	-0.49	1.50	0.04	-0.08	3.25
5	1.72	-0.49	0.65	-0.87	-0.06	-0.30	0.05	-0.10	-0.09	2.09
6	-21.07	12.71	-5.86	5.20	-1.28	1.26	0.53	0.97	3.48	5.08
7	146.51	-24.78	18.50	-2.50	1.57	-1.45	2.93	-1.11	-1.67	9.78
8	11.37	0.45	-5.90	-9.73	0.50	-0.43	1.25	-0.10	0.98	6.55
9	-1.31	0.25	-0.47	0.77	0.01	0.45	0.13	0.02	-0.05	-3.04
10	-5.20	-0.70	-1.53	-0.09	1.20	0.71	-0.21	0.00	-0.28	-3.58
11	76.24	-10.89	21.25	28.61	7.36	1.15	3.75	-1.60	5.58	3.65
12	20.12	30.92	4.14	12.11	-3.57	4.50	4.79	3.07	-1.07	41.12
13	-0.51	0.33	-0.24	0.87	0.21	-2.70	-0.53	0.31	0.10	-1.79
14	-2.89	-0.33	-0.43	0.86	0.08	0.09	-0.03	-0.09	0.46	-2.32
15	-8.01	0.47	-0.68	0.75	-0.11	0.41	0.01	0.19	0.01	-2.78

Table A- 10 Second layer of two hour forecast model.

To Output Neuron	From Hidden Layer Neuron															
	BIAS	1	2	3	4	5	6	7	8	9	10	11	12	13	14	15
1	-0.25	-0.41	0.18	-1.96	0.16	0.18	1.10	0.26	0.32	-0.45	-0.43	0.26	0.25	-0.75	-0.27	-0.46

Table A- 11 First layer of two hour forecast model with time series.

To Hidden Layer Neuron	From Input Layer Neuron												
	BIAS	MAY	JUN	JUL	AUG	SEP	SUN	MON	TUE	WED	THU	FRI	SAT
1	-1.33	-0.88	-1.86	-1.29	-1.70	-1.82	-0.89	-1.21	-1.10	-0.65	-0.84	-0.69	-0.66
2	0.30	0.07	0.92	0.73	0.42	0.92	-0.04	0.69	0.56	0.45	0.56	0.17	-0.07
3	3.69	4.09	1.08	0.36	2.55	11.62	0.87	-0.47	0.35	2.33	2.13	0.77	-0.25
4	-2.53	-2.59	-1.71	-0.80	-1.17	0.38	-0.96	0.56	-0.60	-0.75	-1.54	-1.59	-2.39
5	0.06	0.02	1.08	0.50	0.72	0.47	2.40	0.79	2.17	0.49	-0.37	0.74	0.83
6	-2.85	-2.96	-1.78	-2.35	-2.27	-1.47	-2.10	-1.87	-1.79	-1.25	-2.03	-1.84	-56.03
7	0.30	0.10	0.30	0.05	0.20	-0.16	0.07	0.03	0.22	0.13	0.16	0.21	0.14
8	0.39	-0.09	-1.13	0.62	1.80	2.83	-0.23	2.39	0.04	0.67	1.61	1.98	0.55
9	0.46	0.18	-1.20	-21.91	-0.32	-2.79	0.57	-2.44	-1.89	-64.27	-2.95	-1.16	11.54

Table A- 11 cont'd. First layer of two hour forecast model with time series.

To Hidden Layer Neuron	From Input Layer Neuron										
	NO	NO_2	SO_2	THC	OPA	RH	TEMP	WDR	WSP	O_3(t-1)	O_3
1	54.92	-3.68	2.73	-4.31	1.42	2.14	1.18	-1.19	3.84	-6.46	11.04
2	-16.98	3.62	-2.60	0.34	0.26	0.82	-0.70	-0.19	1.56	5.78	-8.37
3	-12.43	-6.63	1.98	-14.06	0.66	1.02	-0.79	0.16	1.64	-1.69	-8.26
4	-11.70	-3.03	-4.93	-11.67	-0.50	0.34	-0.02	-0.57	2.09	1.22	11.25
5	-8.46	3.84	1.55	0.13	0.38	0.60	-1.64	0.83	0.02	3.34	-4.78
6	-43.26	14.63	-0.57	-2.76	0.02	1.03	0.56	0.87	2.42	1.70	2.02
7	5.09	-1.98	2.08	-0.08	-0.12	-0.29	-0.83	-0.03	-0.30	0.30	-12.30
8	-8.09	-1.63	-1.21	3.85	-0.30	1.89	-0.30	-0.52	-0.78	0.13	-3.91
9	15.78	-12.41	12.35	-5.73	-0.30	4.81	-0.10	-0.22	0.25	2.33	3.77

Table A- 12 Second layer of two hour forecast model with time series.

To Output Neuron	From Hidden Layer Neuron									
	BIAS	1	2	3	4	5	6	7	8	9
1	0.21	0.52	-0.79	-0.34	0.37	-0.44	0.62	-2.37	-0.35	0.17

APPENDIX B: CONNECTION WEIGHTS OF CALGARY EAST MODELS

Table B- 1 First layer of virtual monitor model.

To Hidden Layer Neuron	From Input Layer Neuron											
	BIAS	MAY	JUN	JUL	AUG	SEP	NO	NO_2	SO_2	THC	RH	TEMP
1	-0.28	0.31	0.38	-0.32	-0.12	0.17	-4.56	-1.89	0.05	-1.02	-0.54	0.39
2	0.80	0.73	0.32	-1.24	-0.83	0.08	-6.95	-1.36	0.88	0.70	-2.02	-1.63
3	0.35	0.30	0.00	0.19	0.48	0.41	-5.58	-1.47	5.43	-6.46	-0.56	0.27
4	0.62	0.14	0.14	-0.14	-0.10	-0.07	-0.48	-0.51	0.39	-0.35	-0.01	0.10
5	0.76	0.42	0.26	-0.16	-0.34	-1.22	-0.24	0.05	0.99	1.67	-2.33	-0.14
6	-0.94	-1.00	1.11	0.85	0.77	1.23	-6.11	-4.40	-1.81	-3.31	-0.67	2.75
7	-0.17	-0.06	-10.66	-0.05	-9.92	0.40	-2.04	-0.91	-3.78	-11.82	0.33	-0.29
8	0.26	0.06	0.28	0.58	-0.01	-0.56	0.84	1.42	0.39	0.71	1.05	-0.92
9	0.71	0.58	0.28	0.30	-0.18	0.03	0.09	-0.12	0.02	-1.83	-0.08	-0.08
10	1.09	1.00	-1.24	-0.01	0.08	0.14	3.24	-1.20	0.59	1.29	-0.50	-2.92
11	-0.28	-0.29	0.16	0.36	0.46	0.13	0.00	-0.15	0.50	2.21	-0.73	1.11
12	-1.47	-1.59	1.41	1.31	1.29	1.72	40.34	-0.68	10.72	0.36	-0.46	2.86
13	0.12	-0.04	0.74	0.56	0.06	0.62	3.34	1.55	0.21	0.89	0.38	0.01
14	0.07	-0.03	10.66	-0.11	0.02	0.49	-0.81	2.94	0.52	1.01	0.55	-0.77
15	0.16	0.02	-0.11	0.14	-0.47	-0.39	-5.59	-0.85	-0.58	-0.79	-0.71	0.04
16	-0.27	0.09	-0.14	0.00	0.00	-0.32	-3.94	-1.29	0.46	-1.29	-0.31	0.25
17	-0.09	0.33	0.20	0.21	0.24	0.01	-0.59	-0.30	1.46	-0.03	-0.16	0.94
18	-0.02	0.24	-0.14	0.31	0.44	0.20	-27.92	8.91	-3.03	1.81	0.90	-2.13
19	-0.19	0.04	-0.06	0.05	-0.05	-0.51	-6.09	-1.01	0.67	-0.57	-0.48	0.13
20	-0.19	-0.11	-0.26	0.00	-0.07	-0.40	-26.64	-1.45	-0.38	0.30	-0.30	0.22

Table B- 2 Second layer of virtual monitor model.

To Output Neuron	From Hidden Layer Neuron																				
	BIAS	1	2	3	4	5	6	7	8	9	10	11	12	13	14	15	16	17	18	19	20
1	-0.05	0.28	0.37	0.30	-0.24	-0.45	0.23	0.35	0.15	-0.17	-0.61	-0.79	0.28	0.26	0.19	0.13	0.19	-0.63	0.24	0.23	0.27

Table B- 3 First layer of virtual monitor model with time series.

To Hidden Layer Neuron	From Input Layer Neuron												
	BIAS	MAY	JUN	JUL	AUG	SEP	NO	NO_2	SO_2	THC	RH	TEMP	O_3(t-1)
1	0.10	0.69	0.42	-1.69	0.59	0.37	-1.81	-3.95	-1.32	-9.62	-0.64	1.23	2.01
2	0.04	-0.03	-0.25	-0.62	-0.34	0.19	-3.63	-1.02	-0.26	-2.12	-0.83	-0.40	0.75
3	-0.20	-0.24	-0.11	-0.09	0.27	-0.05	0.45	0.65	-1.16	-0.26	-0.11	0.02	-0.97
4	-1.22	-1.71	1.73	0.59	0.82	12.31	10.14	4.77	1.74	-0.22	1.46	-1.68	-0.24
5	0.46	0.12	0.04	-0.36	0.31	0.46	-1.59	3.48	-1.48	1.85	0.42	-1.06	-0.25
6	0.14	0.08	0.08	0.22	0.09	0.05	0.23	-0.83	0.39	0.17	-0.09	0.40	0.73
7	0.26	0.36	0.54	-0.07	-0.01	0.16	5.80	-6.65	5.88	-1.78	0.40	1.59	-1.46
8	0.71	0.51	-0.13	-0.30	-0.31	-0.04	1.76	-0.06	-0.55	-0.72	0.20	-1.81	-0.10
9	0.30	0.17	-0.26	0.03	-0.21	-0.32	-0.41	0.39	-0.45	0.08	-0.26	-0.14	-1.14
10	-0.10	-0.18	-0.33	-0.05	-0.05	-0.07	1.24	0.15	-0.63	-0.39	-0.02	-0.16	-1.06
11	-0.20	-0.20	0.64	-0.20	-0.22	-0.23	-2.12	-0.96	-2.93	-0.49	-0.37	1.18	-0.23
12	0.25	0.14	0.27	0.46	0.49	0.55	1.60	1.22	-0.03	0.21	0.11	-0.06	-0.48
13	-0.25	-0.41	1.00	1.13	10.55	0.73	7.60	1.83	2.60	1.46	-0.39	0.67	-0.17
14	-0.16	-0.25	-0.09	-0.30	-0.26	-0.16	0.54	0.12	-0.48	0.16	0.08	-0.15	-0.84
15	0.11	-0.03	0.07	0.07	0.02	-0.03	-0.36	-0.54	0.58	-0.02	-0.01	0.42	0.98
16	-0.52	-0.17	-0.07	-0.17	-0.12	-0.14	-0.26	1.13	0.01	0.00	0.21	0.17	-0.86
17	-0.01	0.41	0.14	0.14	0.21	0.31	0.83	-0.20	0.88	0.12	0.05	0.29	1.15
18	-0.12	0.14	0.18	3.93	-0.85	-0.25	3.75	1.24	-7.41	0.77	0.92	0.99	-0.77
19	-0.27	-0.04	-0.01	-0.21	-0.09	-0.49	-3.10	-1.02	0.13	-0.66	-0.46	0.17	0.20
20	-1.92	-1.84	1.91	1.88	1.88	1.93	-3.99	-0.81	2.15	-1.51	-1.16	0.62	3.66

Table B- 4 Second layer of virtual monitor model with time series.

To Output Neuron	From Hidden Layer Neuron																				
	BIAS	1	2	3	4	5	6	7	8	9	10	11	12	13	14	15	16	17	18	19	20
1	0.35	0.17	0.21	-0.30	0.15	0.31	-0.18	0.23	-0.47	-0.29	-0.32	0.22	0.21	0.18	-0.28	-0.37	-0.33	-0.52	0.13	0.19	0.27

Table B- 5 First layer of one hour forecast model.

To Hidden Layer Neuron	From Input Layer Neuron												
	BIAS	MAY	JUN	JUL	AUG	SEP	NO	NO_2	SO_2	THC	RH	TEMP	O_3
1	-0.44	-0.15	-0.04	-0.08	-0.13	0.01	6.23	-0.36	1.50	0.05	0.74	-0.22	2.75
2	0.18	0.05	0.63	0.18	-0.28	-0.45	-2.02	0.68	-0.11	-0.03	0.07	-0.31	-2.12
3	-0.58	-0.16	-0.04	-0.07	-0.17	-0.21	2.19	-0.41	0.53	-0.11	-0.20	-0.35	-4.98
4	-0.56	-0.55	0.23	-0.93	-0.81	-0.27	2.54	-2.00	-0.30	-2.89	0.32	0.57	3.07
5	-0.27	-0.17	-0.16	-0.15	-0.28	-0.46	0.41	-0.32	-0.03	0.04	-0.53	-0.21	0.76

Table B- 6 Second layer of one hour forecast model.

To Output Neuron	From Hidden Layer Neuron					
	BIAS	1	2	3	4	5
1	-0.55	-0.94	-0.44	-1.98	-0.18	1.39

Table B- 7 First layer of one hour forecast model with time series.

To Hidden Layer Neuron	From Input Layer Neuron													
	BIAS	MAY	JUN	JUL	AUG	SEP	NO	NO_2	SO_2	THC	RH	TEMP	O_3(t-1)	O_3
1	-0.57	-0.15	0.00	0.01	0.15	-0.15	1.24	-0.65	0.45	0.55	0.29	-0.58	-0.59	-2.35
2	0.24	0.21	0.09	0.10	-0.07	-0.09	0.49	0.28	0.02	0.30	0.09	0.07	-0.62	1.88
3	0.09	0.16	0.09	-0.05	-0.10	-0.55	-2.96	0.26	0.20	-0.17	0.30	-0.05	-1.07	0.57
4	0.43	-0.05	0.04	0.04	0.15	-0.13	0.24	0.03	0.21	0.29	0.19	-0.04	-0.35	1.68
5	0.30	0.01	0.06	0.17	0.13	-0.25	0.57	0.08	-0.16	0.21	0.11	0.20	-0.51	1.76
6	-0.06	-0.12	-0.10	-0.02	0.05	0.01	-0.84	0.01	-1.19	-0.19	-0.02	0.05	0.25	-1.85
7	-0.03	-0.15	-0.50	0.10	0.06	-0.15	0.65	-0.69	0.06	-0.87	-0.37	-0.30	-0.60	1.12
8	0.54	0.11	0.09	0.23	0.12	0.00	0.16	-0.59	0.18	-0.17	0.01	-0.11	0.36	-0.98
9	0.00	0.10	0.45	0.46	0.40	0.60	-1.53	0.61	-1.45	-0.05	-0.10	0.33	-1.33	17.47
10	0.09	-0.09	-0.18	0.07	0.08	-0.09	-11.39	0.51	-0.90	0.03	-0.91	-0.24	0.30	-1.42
11	0.50	0.47	0.42	0.33	0.34	0.17	-1.13	1.52	0.15	0.74	1.12	0.50	0.21	-1.49
12	0.43	-0.08	0.06	-0.07	-0.05	0.05	0.05	0.24	-0.25	0.19	-0.07	-0.02	-0.94	2.24

Table B- 8 Second layer of one hour forecast model with time series.

To Output Neuron	From Hidden Layer Neuron												
	BIAS	1	2	3	4	5	6	7	8	9	10	11	12
1	-0.77	-0.39	-0.36	0.32	-0.47	-0.15	-0.55	0.46	0.60	-0.61	-0.58	0.75	-0.32